Air Quality Impact Assessment Independent Review

Version: E

NSW EPA

Cadia Mine
28 February 2025

Air Quality Impact Assessment Independent Review

Client name: NSW EPA

Project name: Cadia Mine

Version: E

Project manager: Tracy Freeman

Date: 28 February 2025

Prepared by: Tracy Freeman

Project no: IS473400

File name: Cadia Air Quality Impact Assessment Independent Review Master RevE

Document history and status

Version	Date	Description	Author	Reviewed	Approved
A	21 May 2024	Preliminary draft A for EPA comment	Tracy Freeman		
B	24 June 2024	Preliminary draft B	Tracy Freeman		
C	25 June 2024	Final draft C for EPA comment	Tracy Freeman		
D	4 November 2024	Final draft D	Tracy Freeman		
E	26 February 2025	Final rev E	Tracy Freeman		

Jacobs Group (Australia) Pty Ltd

Level 7, 177 Pacific Highway
North Sydney, NSW 2060
PO Box 632
North Sydney, NSW 2059
Australia

T +61 2 9928 2100
F +61 2 9928 2444
www.jacobs.com

Executive Summary

The Cadia Valley Operations (Cadia, or CVO) is located approximately 25 kilometres south-west of Orange, in the Central Tablelands of New South Wales (NSW). CVO comprises the Cadia East underground mine, which is one of the largest gold and copper deposits in the world. Cadia Holdings Pty Limited (CHPL) is the owner and operator of Cadia. CHPL is owned by Newmont Corporation (Australia), following the acquisition of Newcrest Mining Limited on 6 November 2023.

This report has been prepared for the NSW Environment Protection Authority (EPA). The purpose of this report is to provide an independent technical review of air quality impact assessments that have been prepared generally over the 2020-2023 period for CVO, and to prepare an independent atmospheric dispersion model for EPA that simulates the dispersion of particulate emissions from the mine.

Scope of Review

The primary scope of this review is the set-up of the atmospheric dispersion model for Cadia, which includes reviewing model inputs over three broad categories comprising emission rates from mining activities, meteorological model set up, and dispersion model set up. The review focuses on the prediction of concentrations of fine particulate (known as PM_{10} and $PM_{2.5}$) in ambient air outside of the Cadia boundary.

Todoroski Air Sciences (TAS) has been the principal author of air quality impact assessment (AQIA) reports involving dispersion modelling for CHPL since at least 2020. Two key reports prepared for CHPL by TAS have been included in this independent technical review:

- TAS (2020a) – AQIA for Modification application 14; full emission inventory and dispersion model.
- TAS (2023a) – AQIA for Cadia operations during the January 2022 to February 2023 period. Specific emission inventory for two periods – Jan-Dec 2022 and Jan-Feb 2023.

Emissions

Sources of dust emissions from CVO include a range of activities, such as surface stockpiles; ore processing and crushing; bulldozer and grader operations; loading and handling of ore, waste rock, and construction materials; vent emissions from underground mining; dust generated by the wheels of vehicles travelling on haul roads and unsealed surfaces (collectively referred to as ‘vehicle-tracked dust’); and wind erosion from Tailings Storage Facilities (TSFs) and other exposed surfaces including stockpiles and roads.

The dust sources at CVO and the emission factors relevant to each source are discussed in detail in the report, along with a review of the input variables adopted in TAS (2020a) and TAS (2023a). The report provides a sensitivity assessment for the emission factor variables for each source type. It was found that the model results are most sensitive to emission factor variables used to define the emission rates for loading and handling, vehicle-tracked dust, and wind erosion.

Several different approaches for defining emissions during wind erosion were tested, particularly for the TSFs. An approach called the “Threshold Friction Velocity Method” was found to have the potential to simulate the main dust lift-off events under high wind speeds that have been observed from the TSFs. However, the simulations cannot currently be calibrated to the CVO site because of the lack of available operational monitoring data close to the TSFs. Jacobs recommends that a new dust monitor be established downwind of the TSFs under northeasterly winds, that collects data that is appropriate to report externally to EPA and the public and can be used to demonstrate the effectiveness of the TSF mitigation plan and also calibrate the dispersion model under high wind speeds.

Meteorological modelling

Advanced dispersion models such as the CALPUFF model used for CVO allow meteorological conditions to vary across the modelling domain and up through the atmosphere. This is a complex situation that requires complex and realistic meteorological data inputs. Whilst CHPL operates two automatic weather stations known as 'Ridgeway' and 'Southern Lease Boundary (SLB)', meteorological observation sites do not provide the relevant data at every point in the modelling domain. A meteorological model called CALMET is used to predict and provide the meteorological variables at sites where information is not available. The CALPUFF dispersion model then uses this pre-processed meteorological data for analysis.

Jacobs applied similar values for most CALMET inputs compared to TAS, with the exception of a terrain weighting factor known as 'TERRAD'. Jacobs prepared preliminary CALMET models to compare CALMET outputs for these different TERRAD settings, and found that the model was slightly sensitive to the TERRAD settings, particularly in the south and southeast of the domain which is furthest from the observation sites.

The gap in local meteorological information in the southeast part of the modelling domain means that CALMET must make estimates of likely wind patterns in that part of the model domain, which are much more dependent on user settings for the radius of influence of observation sites than at locations closer to the Ridgeway and SLB automatic weather stations.

Confidence in future modelling results in this part of the domain could be increased if the meteorological modelling was supported by additional wind observations in the southeast part of the domain, somewhere in the area represented by the Triangle Flat and Meribah BAM locations. Jacobs recommends that an additional automatic weather station be installed in this area. The site would not need to host a full range of meteorological monitoring instruments, as the priority would be to collect wind speed and direction data.

The question of how 1-hour average wind directions are calculated from shorter term raw data is very important for atmospheric dispersion modelling. Jacobs found that there is a potential issue with the method of calculating 1-hour average wind directions in the meteorological data provided by CPHL, which can lead to errors such as a wind direction being recorded as southerly when it was in fact a northerly. This could be problematic if CPHL relies on this data (for example, comparing dates and times of complaint reports with wind direction records) or provides this data to external stakeholders. This issue appears to have been corrected in the modelling conducted by TAS (2023a). However, the problem may also be present in the 10-minute data averages provided by CPHL, which are also calculated values. The quality and methods of averaging all raw meteorological data collected by, or on behalf of CPHL should be reviewed.

Dispersion modelling methodology

In CALPUFF, sources can be generally characterised as point (such as from a stack), area (such as from an open exposed flat area of ground or water), or volume (such as a stirred-up cloud of dust from a building or vehicle). The TAS model uses volume sources to represent all emissions at CVO except for the vents which are modelled as point sources. Hypothetically, the open areas at CVO such as the TSFs should be modelled as area sources, however Jacobs tested the sensitivity of the dispersion model to this assumption and found that using the source split up into volume sources or area sources made very little difference to the model results. This is because of the long dispersion distances involved at CVO.

Another dispersion model input that is relevant to the CVO model is the use of dry deposition parameters. "Dry deposition" is an option in the CALPUFF model that simulates the settling of particles in the air as they travel downwind. The larger the aerodynamic diameter of the particles the faster they settle. CALPUFF requires user input for the size distribution of the particles that are being dispersed. TAS (2023a) indicates that dry deposition was used in the modelling, but does not state what size distribution settings were assumed. The model appears to be moderately sensitive to the use of deposition, with deposition causing the dispersion to occur more quickly with lower ground level concentrations predicted at sensitive receptors. Due to lack of information provided by TAS, Jacobs cannot review if dry deposition parameters were appropriately adopted in the TAS model.

Jacobs compiled a dispersion model using the closest possible replication of the TAS (2023a) emission inventory, and compared the model results from TAS (2023a) with the model results using Jacobs' CALMET and CALPUFF setup.

The PM_{10} and $PM_{2.5}$ results for the two models compared well in some parts of the domain for both the 24-hour and annual average periods, although there were some notable differences in the 24-hour average results in some parts of the domain. In most locations, the different concentrations predicted by the models were of low consequence for the "existing" 2022 emission inventory, because even with the addition of background concentrations the cumulative concentrations would not increase the existing number of sensitive receptors that are potentially exposed to concentrations that exceed the air quality objectives in Approved Methods.

However, there were some sensitive receptors, for example to the northwest of the Cadia boundary, where 24-hour average incremental concentrations were quite a lot higher in the Jacobs model than in the TAS model. Further analysis of cumulative concentration predictions was required to assess the risk of air quality exceeding the air quality objectives in Approved Methods at these locations (see next section).

The results for the Jacobs-replicate of the TAS (2023a) model were extracted for each hour at the locations of the four air quality monitoring stations (AQMS) operated by CHPL. Quantile-quantile (or Q-Q) plots comparing the statistical distribution of measured versus modelled concentrations were prepared. These showed that with the Jacobs model setup, the TAS (2023a) conclusion that at 2022 emission rates, PM_{10} emission rates from vent VR8 should be reduced by 90% and $PM_{2.5}$ emission rates by 50% to account for particle dropout in mud globules seems unrealistic because the modelled results with those assumed emission reduction factors were less than the measured concentrations.

The differences noticed between the Jacobs and TAS (2023a) models may be due to any or all the different approaches used to define the emission rates, how the dust is released from each emission source, and/or model setup. The differences between the models also could be relevant for future assessment of the effects of proposed development or mitigation scenarios.

Cumulative emissions model

Jacobs compared three options for the total cumulative emissions from current CVO operations (after VR8 controls installed) including background air quality, based on the review of emission factors and activity intensity data. The three options represented a 'lower bound' (lowest emission rate basis), 'upper bound' (highest emission rate basis) and 'moderate bound' (variant in-between the lower bound and upper bound models). The results for each of the models were extracted for each hour at the locations of the four AQMS operated by CHPL and compared in Q-Q plots. The plots showed that the statistical distribution of measured versus modelled concentrations for the moderate bound model was the most reasonable overall match with the monitoring data.

The 'moderate bound' model was adopted as Jacobs' recommended model. Based on the 2022 emission inventory, which is now historic as it included the VR8 emissions prior to installation of controls which have now been implemented, the recommended model indicated a risk of several privately-owned houses and CPHL-owned houses being exposed to 24-hour average cumulative PM_{10} or $PM_{2.5}$ concentrations approaching or exceeding the NSW EPA objectives.

It was also noted that the locations of the existing AQMS may not be suitable to capture the highest PM_{10} and $PM_{2.5}$ concentrations predicted by the model at residences.

Recommendations

Recommendations arising from the report focused on information that could improve external stakeholders' understanding of actual and potential air quality impacts due to operations at CVO. Recommendations included actions related to:

- Reporting in the Annual Environmental Monitoring Reports prepared by CHPL,
- Review of suitability of AQMS locations,
- Meteorological monitoring data location, availability and averaging,
- Representativeness of vent emission rates, and
- Detail on emission rate assumptions to be included in future air quality assessment reports.

The reviews conducted in this report have been more complex because of the lack of availability of model input files prepared by TAS on behalf of CPHL. The reasons for differences in model outputs between TAS (2023a) and Jacobs cannot be pinpointed and resolved without this information. Jacobs recommends that all model input files should be retained by the consultant or CPHL in future and be able to be provided to EPA if requested. Without this transparency, any model validation presented on behalf of Cadia cannot be fully independently reviewed.

Important note about this report

Contents

Appendices

Tables

Figures

Plates

Acronyms and abbreviations

ACARP	Australian Coal Association Research Program
AEMR	Annual Environmental Management Report
AMSL	Above Mean Sea Level
Am^3/s	Volumetric flow rate in cubic metres per second at operating temperature and moisture content.
ANSTO	Australian Nuclear Science and Technology Organisation
Approved Methods	*Approved Methods for Modelling and Assessment of Air Pollutants in New South Wales*, published by NSW EPA, August 2022
AP-42	USEPA Compilation of Air Pollutant Emissions Factors from Stationary Sources
AQIA	Air Quality Impact Assessment
AQMS	Air Quality Monitoring Station
AWS	Automatic Weather Station
BAM	Beta Attenuation Monitor
BOM	Bureau of Meteorology
Cadia	Cadia Valley Operations
CHPL	Cadia Holdings Pty Limited
COS	Crushed Ore Stockpile
CVO	Cadia Valley Operations
DDG	Dust Deposition Gauge
DEM	Digital Elevation Model
DHPI	Department of Planning, Infrastructure and Health
EF(s)	Emission Factor(s)
EPA	New South Wales Environment Protection Authority
EPL	Environment Protection Licence, number 5590 for Cadia operations
h/a	Hours per annum
ha	hectares

HAS	Holmes Air Sciences
HVAS	High Volume Air Sampler
IGF	Initial Guess Field (in meteorological model)
kg	Kilograms
km/h	Kilometres per hour
LVAS	Low Volume Air Sampler
mm	millimetres
µm	micrometres
MT/a	Million tonnes per annum
NEPM(AAQ)	National Environment Protection (Ambient Air Quality) Measure
NPI	National Pollutant Inventory
NTSF	Northern Tailings Storage Facility
NSW	New South Wales
PM_{10}	Particles with an equivalent aerodynamic diameter of 10 µm or less
$PM_{2.5}$	Particles with an equivalent aerodynamic diameter of 2.5 µm or less
PM_4	Particles with an equivalent aerodynamic diameter of 4 µm or less
POEO Act	*Protection of the Environment Operations Act 1997*
Project Approval	Project Approval No. 06_0295 for Cadia operations
Q-Q Plot	Quantile-Quantile statistical plot
Sm^3/s	Volumetric flow rate in cubic metres per second at standard conditions of dry gas, 0°C temperature and 1atm pressure.
SRTM	shuttle radar topography mission
STSF	Southern Tailings Storage Facility
T	Tonnes
T/a	Tonnes per annum
TAS	Todoroski Air Sciences
TAS Reports	Collective reference to AQIA reports prepared by TAS in 2020, 2021 and 2023.

TEOM	Tapered Element Oscillating Microbalance
TSFs	Tailings Storage Facilities
TSP	Total Suspended Particulate
USEPA	United States Environmental Protection Agency
VKT	Vehicle-kilometres travelled
VKT/a	Kilometres travelled by a vehicle or vehicle type per annum
WRAP	Western Region Air Partnership

1. Introduction

1.1 Report Purpose

The Cadia Valley Operations (Cadia, or CVO) is located approximately 25 kilometres south-west of Orange, in the Central Tablelands of New South Wales (NSW). CVO comprises the Cadia East underground mine, which is one of the largest gold and copper deposits in the world. Cadia East commenced commercial production in January 2013 and uses the large-scale mining method known as panel caving. The site also comprises the Cadia Hill Pit Tailings Storage Facility and the Ridgeway underground mine, which is currently in care and maintenance.

Cadia Holdings Pty Limited (CHPL) is the owner and operator of Cadia. CHPL is owned by Newmont Corporation (Australia), following the acquisition of Newcrest Mining Limited on 6 November 2023.

This report has been prepared for the NSW Environment Protection Authority (EPA). The purpose of this report is to provide an independent technical review of air quality impact assessments that have been prepared generally over the 2020-2023 period for CVO, and to prepare an independent atmospheric dispersion model for EPA that simulates the dispersion of particulate emissions from the mine.

1.2 Planning Approval

On 6 January 2010, the then Minister for Planning granted Project Approval No. 06_0295 to Cadia for the development described in the 2009 Environmental Assessment. The Project Approval is now taken to be a development consent for State significant development. The Project Approval was last modified on 13 December 2021.

1.3 Environment Protection Licence

CHPL holds an Environment Protection Licence (EPL-5590), issued in 2000 by EPA under the Protection of the Environment Operations Act 1997 (POEO Act). The EPL authorizes the carrying out of mining activities at the Cadia mine site. The EPL was last varied on 1 August 2023.

1.4 MOD15

In late 2023, CHPL applied to the Department of Planning, Infrastructure and Health (DPHI) seeking a modification to the Project Approval to place additional buttressing material on the outer slopes of the Northern and Southern Tailings Storage Facilities (NTSF and STSF) and therefore changes to the embankment footprints, the restart of the Ridgeway Underground Mine and other changes to related elements at Cadia. The modification is referred to as “MOD15”.

Except where stated, the review entailed in this report does not include:

- Consideration of any activities proposed in the modification,
- Any technical reports prepared for CPHL to support the modification application, or
- Any new information arising from those technical reports that was previously not available to NSW EPA.

1.5 Scope of Review

The primary scope of this review is the setup of the atmospheric dispersion model for Cadia, which includes reviewing model inputs over three broad categories:

1. Emission rates from mining activities,
2. Meteorological model set up, and
3. Dispersion model set up

In the course of completing this scope of work, Jacobs has also reviewed available ambient air quality and meteorological monitoring data, and underlying assumptions in the model set up including the sensitivity of the model to various changes in key inputs.

The review focuses on the prediction of concentrations of fine particulate (known as PM_{10} and $PM_{2.5}$) in ambient air outside of the Cadia boundary.

Todoroski Air Sciences (TAS) has been the principal author of air quality impact assessment (AQIA) reports involving dispersion modelling for CHPL since at least 2020. The following TAS reports prepared for CHPL have been included in this independent technical review:

- TAS (2020a) – AQIA for Modification application 14; full emission inventory and dispersion model.
- TAS (2021) – Focus on modelling of TSFs.
- TAS (2023a) – AQIA for Cadia operations during the January 2022 to February 2023 period. Specific emission inventory for two periods – Jan-Dec 2022 and Jan-Feb 2023.

Many of the methods used to develop the emission inventories and dispersion model are the same in all three of these reports prepared by TAS. Collectively, TAS (2020a), TAS (2021) and TAS (2023a) will be referred to as the TAS Reports.

The following reports have also been referred to where relevant, but have not been reviewed in the context of this report:

- Holmes Air Sciences (HAS) – 2009 report for original Cadia East Mine Environmental Assessment.
- Zephyr (2022) – Air Quality Audit report of dust mitigation practices commissioned by Cadia to satisfy condition 6A of the Project Approval which specifies that Cadia may process an additional 3 million tonnes of ore per calendar year subject to Cadia commissioning an independent air quality audit report to the satisfaction of the Secretary of the Department of Planning, Industry and Environment.

1.6 Data Relied On

Data sources relied on for this report include:

- Annual Environmental Management Reports (AEMRs) which CPHL must prepare annually as a requirement of the EPL (CPHL 2016, 2019, 2020, 2021, 2022, and 2023). These are published on the CVO website[1]. In this report, each AEMR is referred to with the financial year-ending that the report relates to – for example AEMR 2023 relates to the AEMR for the financial year ending June 2023.
- Georeferenced aerial map of CVO which was supplied by CPHL, herein referred to as the "Cadia aerial map".
- Air quality monitoring reports published on the CVO website[2].
- Cadia air quality and greenhouse gas management plan, 2018 and 2024 versions.

[1] https://www.cadiavalley.com.au/newcrest/cvo/environmental-management/reporting/annual-review

[2] https://www.cadiavalley.com.au/newcrest/cvo/environmental-management/monitoring/air-quality

- Human health and air quality assessments reported in Serinus (2021), SAGE (2023) and ANSTO (2023).
- Information included in Newcrest (2023b) and (2023c)
- Monitoring data from automatic weather stations and ambient monitoring sites, as referred to in relevant sections throughout this report.

1.7 Limitations and Assumptions

In addition to relevant notes provided above, the following limitations and assumptions apply to this report:

1. This report does not consider potential air quality-related effects on water quality or rainwater-derived drinking water quality.
2. This report does not provide independent review of the health impact reports prepared for CPHL (Serinus 2021, SAGE 2023 and ANSTO 2023).
3. It is assumed that all monitoring data was collected and analysed according to standard methods except where stated in published monitoring reports.
4. Technical difficulties with the measurement of particulate emission rates from vent VR8 have been the subject of rigorous investigation by both CVO and EPA, and are beyond the scope of this report.

1.8 Site Visit

Tracy Freeman from Jacobs conducted a site visit to Cadia on 4 September 2023. Several staff members from NSW EPA also attended the site visit. Visitors were escorted on-site by David Coe and Michael Dewar from Newcrest.

The site visit included the north and south tailings dams, although access to the edge of the dams was not permitted for safety reasons. The site visit also included vent VR8, a viewing point for the processing area, and the Ridgeway automatic weather station (AWS). The Southern Lease Boundary (SLB) AWS could not be visited due to the available CPHL staff not having access.

Where relevant, photographs taken by Jacobs from the site visit are provided in Appendix A and referred to throughout this report.

2. Background Information

2.1 Overview of Mine

2.1.1 Site Activities

The mine site comprises a range of activities associated with the current and historical mining operations. These include the processing area, waste rock dumps (both active and rehabilitated), stockpiles, tailings storage facilities, and access/haul roads. Photographs showing various activities at the mine, taken by Jacobs during the site visit, are provided in Appendix A.

The locations of these activities were supplied to Jacobs in the form of digital shape files, as shown in Figure 2-1.

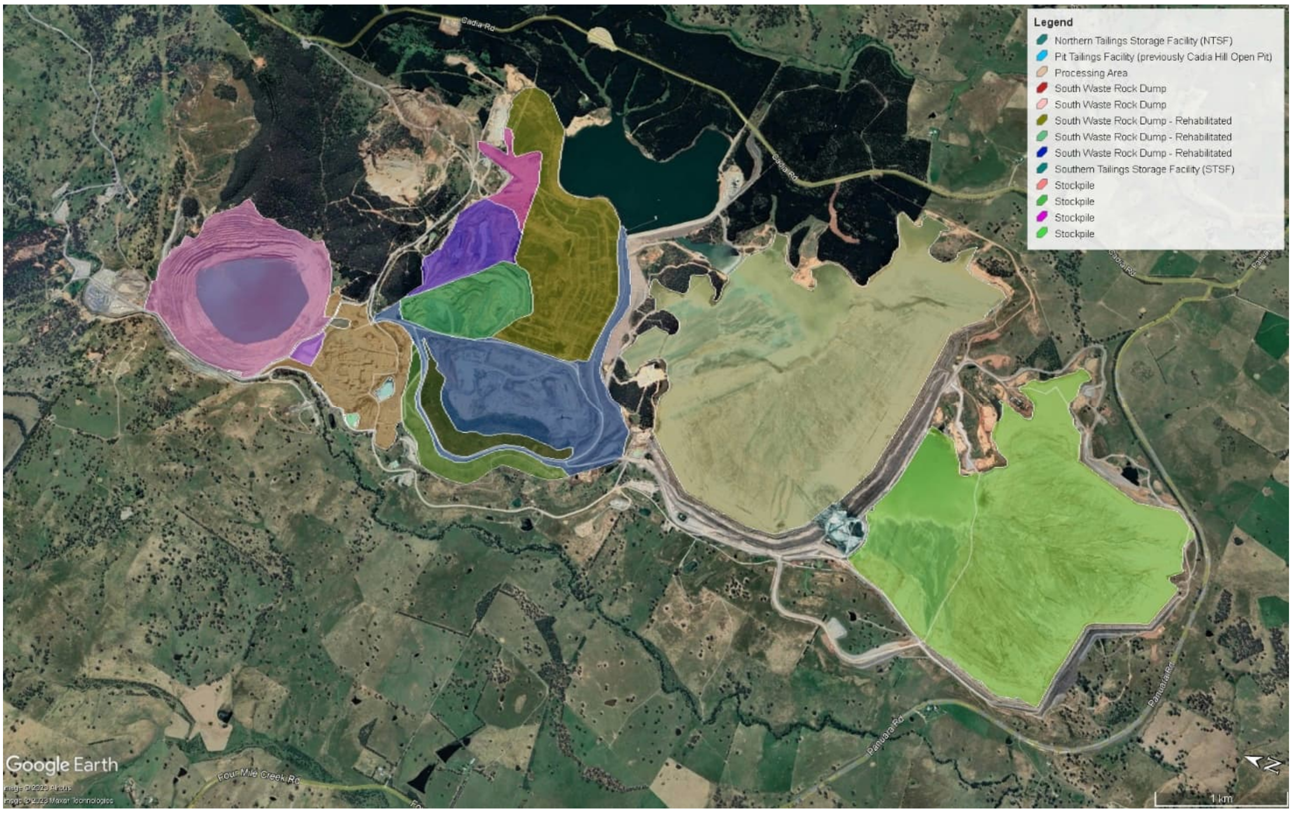

Figure 2-1. Location of various activities at Cadia mine.

2.1.2 Ore Processing Operations

The ore is crushed underground at Cadia East before being transported via a conveyor belt to a stockpile on the surface. From the stockpile, the ore is treated through one of two separate concentrators. Concentrator 1 plant uses High Pressure Grinding Rolls to crush the ore prior to milling. Semi-autogenous grinding mills use the crushed material inside the mill cylinder as the grinding medium with a small amount of steel balls. Ball mills are partially filled with steel balls to further grind the ore to a fine powder.

The mills in Concentrators 1 and 2 are used to reduce the ore to a fine powder (150 micron) suitable for flotation.

Part of the ground ore is then passed through gravity concentrators which recover around 25% of the gold and is smelted into gold doré[3]. The smelting process heats the ore to very high temperatures and is likely to involve some emissions of pollutants into air, such as particulates and metal fumes. However, potential air quality impacts from these emissions are likely to be very localized and not detectable beyond the site boundary due to the large separation distances from the processing site. Air emissions from the smelting process were not included in the reports reviewed for this study detailed in Section 1.6.

The doré bars are sent to the ABC Refinery in Sydney for refining into high purity gold bullions and other items. The remaining ore undergoes a flotation process, where copper and gold-bearing minerals are floated out to produce a rich copper-gold concentrate. The concentrate is thickened and then pumped to the CVO dewatering facility at Blayney, where the water is removed. The dry concentrate powder is then transported by rail to Port Kembla for export.

A Molybdenum Flotation Plant is also located on the mine site which commenced production in February 2020. The Plant is made up of a series of flotation cells, thickeners, a grinding mill, dryer, scrubber and bagging plant. Molybdenum is extracted from the copper concentrate stream prior to it being pumped to Blayney, producing a concentrate that is approximately 50% molybdenum in dry powder form. Due to the dust controls, the molybdenum plant is not considered to be a significant source of dust emissions.

2.1.3 Tailings Storage Facilities

Tailings are the resulting material from finely-ground processed ore-bearing rock that has been through several sizing, grinding, and processing steps. Tailings are discharged as dense slurry into containment areas known as tailings storage facilities (TSFs).

CVO has three TSF facilities:

- Cadia Hill open pit
- Northern Tailings Storage Facility (NTSF) and
- Southern Tailings Storage Facility (STSF).

The NTSF and STSF are shown in Picture A-1 in Appendix A. The NTSF and STSF are very large open areas in the southern part of the mine site. On 9 March 2018 part of the embankment wall around the NTSF slumped, releasing tailings which were captured in the abutting lower STSF. This meant that tailings could no longer be deposited into the NTSF. In October 2019, deposition of tailings in the STSF was also suspended as it was nearing capacity although tailings were later accepted again until 2021. All tailings are now deposited into the Cadia Hill open pit. Due to the suspension of tailings emplacement in the NTSF and STSF, the tailings surface dried, making it susceptible to wind generated dust lift-off.

The combination of no active deposition of tailings to either TSF and extreme drought conditions until early 2020 led to a significant increase of windblown dust emissions and an increase in community complaints.

Additional dust mitigation measures were implemented by CPHL to manage dust generation from the TSFs during wind conditions. These are summarized in TAS (2021). In mid-2019 a wood fibre hydro mulch was identified as the best performing product to manage windblown dust from the surface of the TSF and a plan was developed to cover the entire TSF surfaces, while applying polymer dust suppressant in the interim. According to TAS (2021), the hydro mulch was successfully applied over the entire NTSF by November 2020 and STSF by July 2021. However CPHL advised at the site visit that the vegetation growing from the hydro

[3] https://www.cadiavalley.com.au/newcrest/cvo/map, "Ore treatment" pop-up window.

mulch could not be sustained due to lack of water for irrigation of the TSF surfaces and did not establish an effective surface coverage.

CPHL also employ two polymer type dust suppression products to target specific areas of the TSF using Prinoth Panthers (Panthers) and crop duster aircraft. Figure 2-2 shows a picture of the Panther in operation. Polymer application was the main method of dust control for the TSFs at the time of the site visit. CPHL explained that the Panthers cannot work if the radars which detect movement in the TSF embankments are not functioning correctly, which was the case at the time of the site visit. However, application of the polymer via aircraft was observed during the site visit.

The polymer slowly degrades over time after application, and CPHL continue to reapply dust suppression on the TSFs as needed to maintain the existing covers. Jacobs understands that additional and more permanent options are being explored by CPHL.

Figure 2-2. Polymer application to NTSF (from AEMR 2021, Plate 6-1).

2.1.4 Venting

Underground mining operations are ventilated through the use of fans and ventilation rises which bring the exhaust air to the surface. The mine currently has four ventilation rises in operation, with the most significant for potential emissions to air being ventilation rise 8 (VR8). The other ventilation rises are known as VR3A, VR5 and VR7.

While VR8 had previously been operated using an underground axial fan to generate the necessary circulation, in December 2020 Cadia replaced this fan with three large centrifugal surface fans to help increase underground airflow and minimise the amount of dust and other air impurities that were settling underground. The surface form of VR8 now consists of three exhaust vents, as shown in Figure 2-3 and the site visit photographs in Picture A-2 (Appendix A).

Testing of emissions from the ventilation rises is conducted by Ektimo Pty Limited (Ektimo). Test results from sampling in November 2021 and February-March 2022 recorded concentrations of solid particles exceeding the standard of concentration prescribed by the *Protection of the Environment Operations (Clean Air) Regulation 2021*. The Zephyr (2022) independent air quality audit included an inspection of the mine site in April 2022, where it was noted that "*a site inspection of VR8 indicated that there were significant visible particulate emissions from this vent shaft. These emissions could be seen clearly from the molybdenum plant approximately 2 km to the south across the dam lake.*"

In April 2023, CVO installed two new dry air filtration scrubbers underground, directly into the exhaust ventilation ducts from the tipple being operated in primary crusher 2E. The purpose of these filtration scrubbers was to remove solid particles from the airstream before it was emitted into the atmosphere from VR8. These scrubbers commenced operation at the start of May 2023.

Measurement of particulate emissions from VR8 has been found to be problematic due to the duct design and moisture content of the ventilation air. Commentary on the validity of various test methods for this emission source is beyond the scope of this report, except to note that the measured concentrations are likely to overestimate the actual particulate emissions released into the atmosphere because some of the particles will be entrained in moisture droplets that fall to the ground as mud.

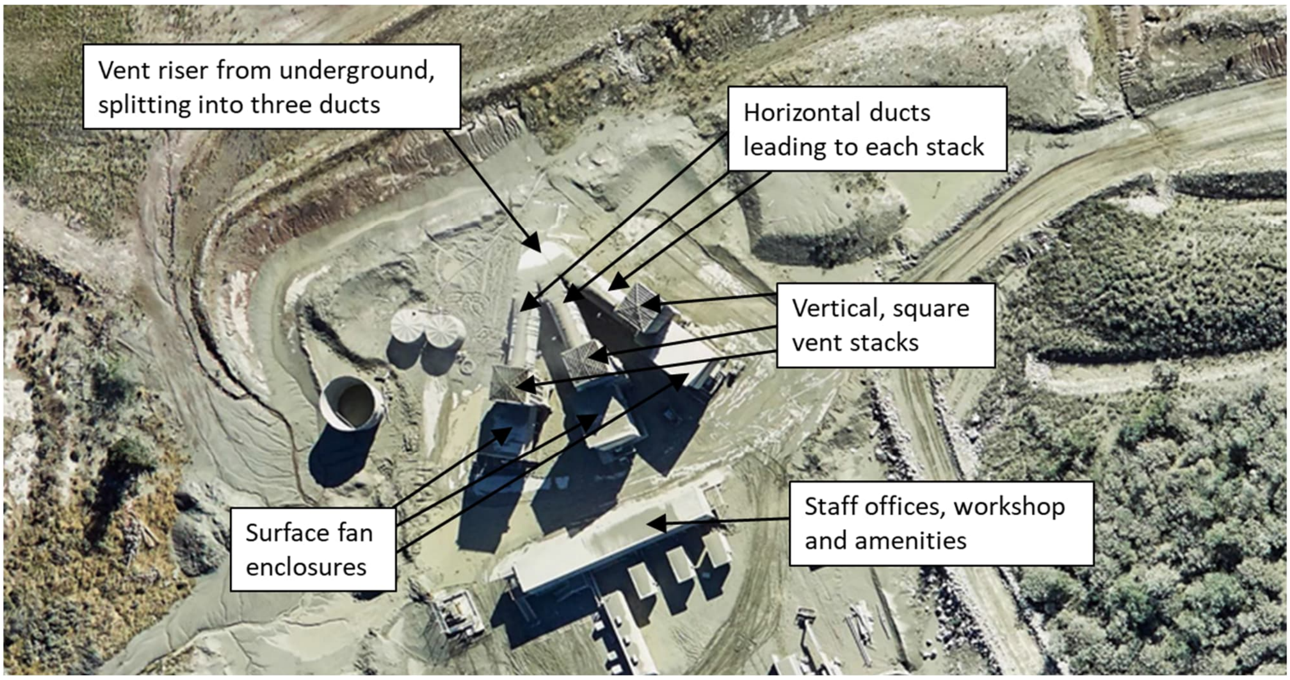

Figure 2-3. VR8 as shown in Cadia Aerial Map.

2.2 Dust Types

The main pollutant discharged to air from Cadia is particulate matter. Particles emitted into the air present a risk of causing a range of impacts to human health and the environment. Particles can impact human respiratory and cardiovascular health and ecosystem health. In addition, particles can cause nuisance and amenity issues through soiling of surfaces.

The health effects of particles are strongly influenced by the size of the particles. Particles are therefore classified according to their size. Two size categories for fine particles are recognised internationally as having the greatest potential to cause health problems due to their inhalation potential:

- PM_{10} (particles with an equivalent aerodynamic diameter of 10 micrometres (μm) or less). These particles are very small - 10 μm is 0.01 millimetres (mm). These particles are small enough to pass through the throat and nose and enter the lungs. Once inhaled, these particles can affect the heart and lungs; and
- $PM_{2.5}$ (particles with an equivalent aerodynamic diameter of 2.5 μm or less). These particles are even smaller than PM_{10}; so small they can get deep into the lungs and into the bloodstream. The PM_{10} category includes the $PM_{2.5}$ size range.

Airborne particulate matter produced by mining is generally associated with the larger size fraction ($PM_{10-2.5}$), due to its generation via mechanical processes, as opposed to the smaller size fraction ($PM_{2.5}$ and smaller) generally associated with combustion and high temperature processes (Serinus, 2021).

The total mass of all particles suspended in air is defined as Total Suspended Particulate matter (TSP). The upper size range for TSP is nominally taken to be 30 μm as in practice particles larger than 30 to 50 μm will settle out of the atmosphere too quickly to be regarded as air pollutants (TAS, 2020).

Particles larger than the PM_{10} size fraction do not have known concentration thresholds for health impact risk, but have the potential to cause nuisance and amenity issues such as settling of dust on surfaces.

The particles emitted from the various activities at the mine are composed of elements from the underground rock that is being crushed, and/or surface rock.

2.3 Relevant Air Quality Standards and Guidelines

2.3.1 National Environment Protection Measure

The key framework for ambient air quality in Australia is established by the National Environment Protection (Ambient Air Quality) Measure (NEPM(AAQ)). State jurisdictions enforce the key criteria (or standards) for ambient air quality set by the NEPM(AAQ) and are required to implement programs to measure air quality against the criteria. In terms of airborne dust, the NEPM(AAQ) only covers PM_{10}, $PM_{2.5}$ and lead.

2.3.2 Approved Methods

For air quality criteria not established by the NEPM(AAQ), each state sets its own standards or guidelines. In NSW, these criteria are provided in the *Approved Methods for Modelling and Assessment of Air Pollutants in New South Wales*, last updated in August 2022 (EPA, 2022). Herein, this document will be referred to as the **Approved Methods**. The air quality criteria for airborne particles in Approved Methods are the same as those in the NEPM(AAQ), and are provided in Table 2-1.

Approved Methods also provides impact assessment criteria for airborne toxic air pollutants such as heavy metals, all referenced to a 1-hour averaging period.

Approved Methods Section 7.1.2 defines the means of applying the impact assessment criteria, including:

- The criteria must be applied at the nearest existing or likely future off-site sensitive receptor.
- Background concentrations must be included (i.e. the assessment criteria apply to total or cumulative concentrations including both the incremental concentration from the pollutant source alone, plus background concentrations).

Table 2-1. Relevant objectives in Approved Methods for particles

Pollutant	Averaging period	Concentration	Deposition rate
$PM_{2.5}$	24 hours Annual	25 µg/m^3 8 µg/m^3	
PM_{10}	24 hours Annual	50 µg/m^3 25 µg/m^3	
TSP	Annual	90 µg/m^3	
Deposited dust	Annual		2 g/m^2/month (incremental) 4 g/m^2/month (cumulative)

3. Existing Conditions Review

3.1 Topography

CVO is in the Central Tablelands of NSW, approximately 23 km south-southwest of Orange and 52km west-southwest of Bathurst. A photograph showing the undulating terrain within and near to the mine site, taken by Jacobs during the site visit, is shown in Picture A-3 in Appendix A.

The topography of the Central Tablelands area is shown at broad scale in Figure 3-1, and closer scale in Figure 3-2. The elevation data used to construct these figures is sourced from Geoscience Australia DEM-1s[4] database. The mine is located on the southwestern edge of an elevated plateau, at an elevation of about 900m above mean sea level (AMSL) at the north end of the site, falling to about 650m AMSL at the south end of the site. The terrain elevation falls away to the south and west of the site towards Cowra, Forbes and Parkes, and is flanked to the north by Mount Canobolas, a mountain on a spur of the Great Dividing Range which reaches an elevation of 1390m AMSL.

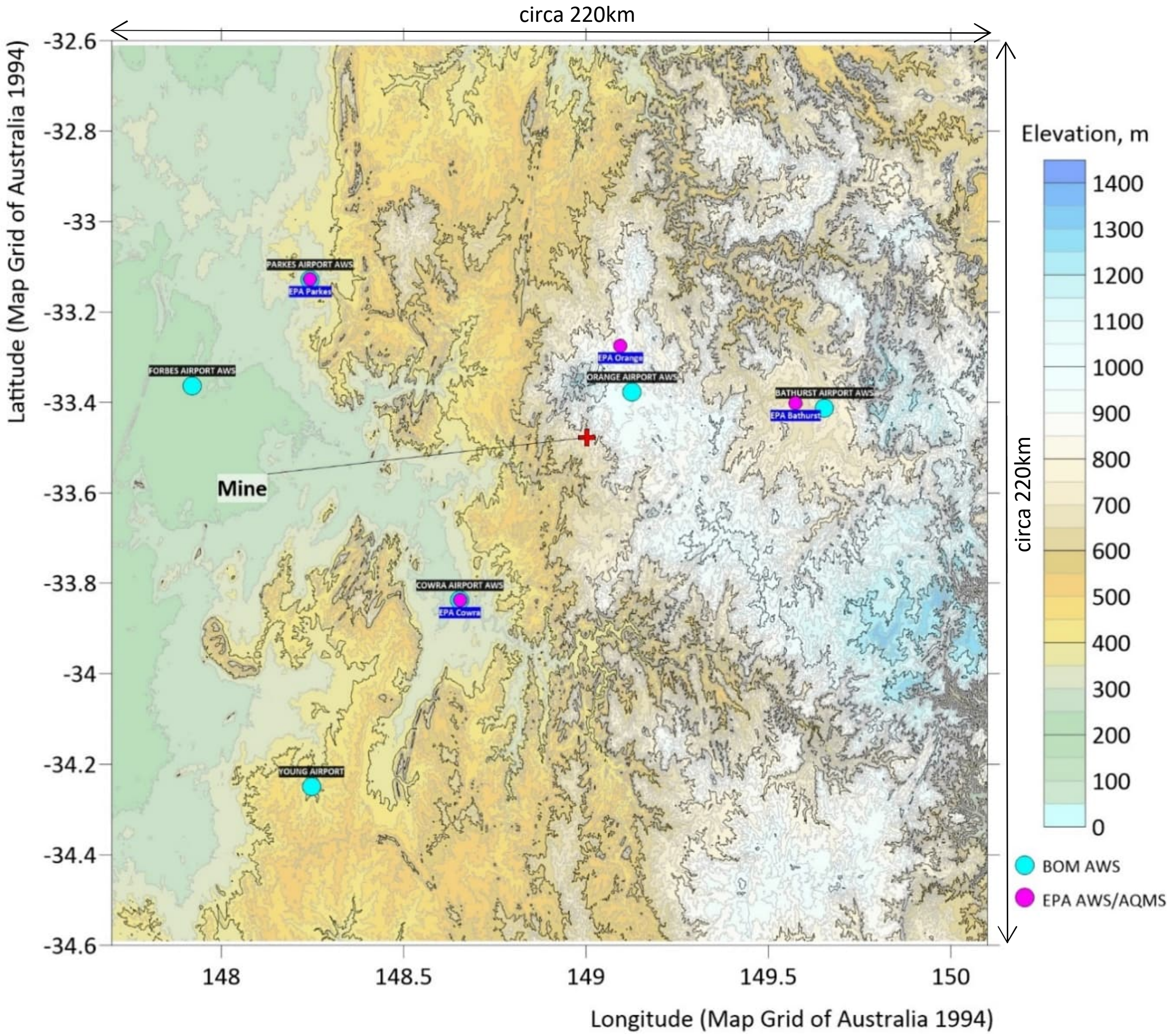

Figure 3-1. Broad scale topography of Central Tablelands region.

[4] Geoscience Australia, 1 second shuttle radar topography mission (SRTM) derived smoothed digital elevation model. https://pid.geoscience.gov.au/dataset/ga/72759

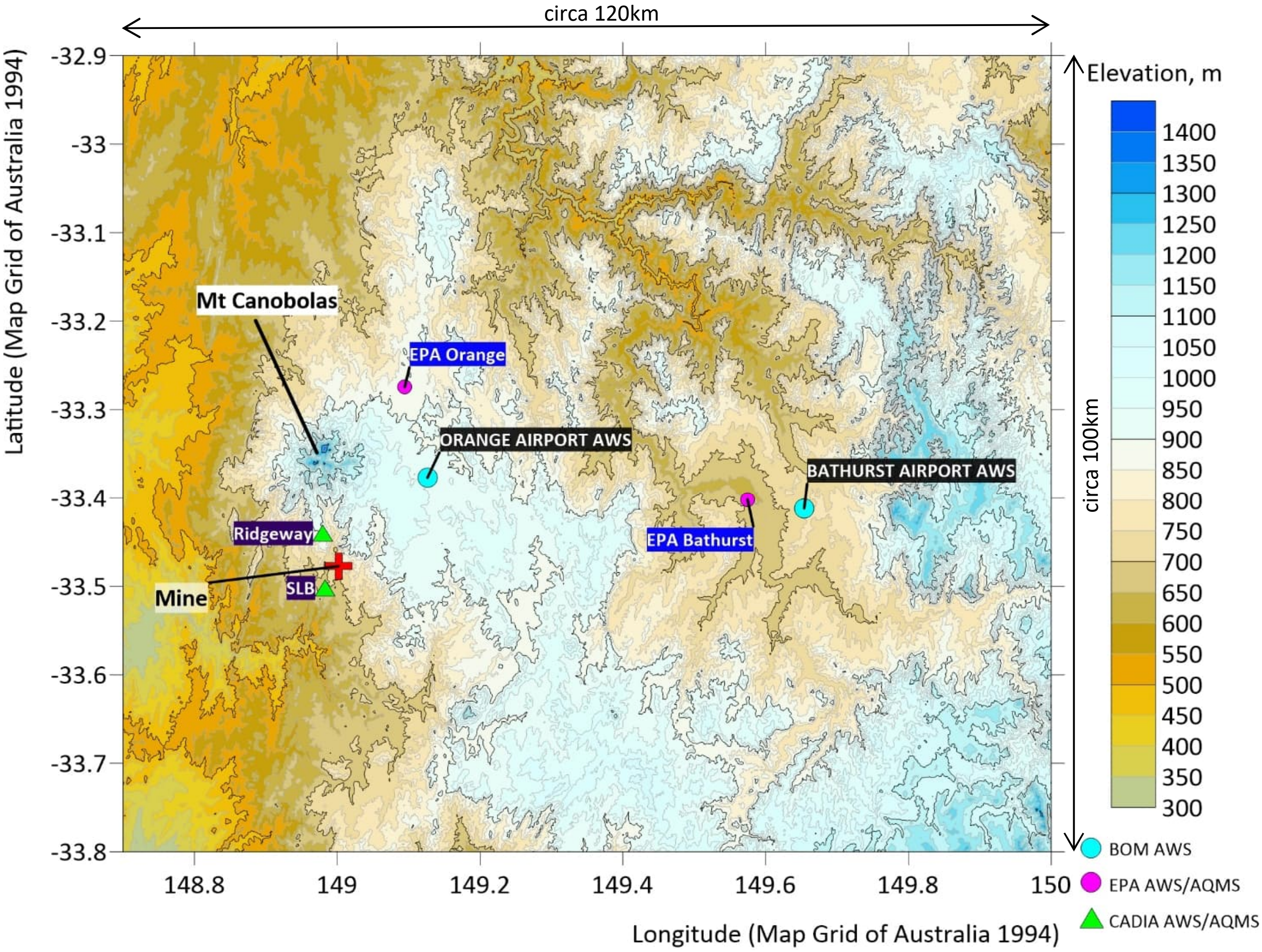

Figure 3-2. Closer scale topography of Central Tablelands region.

Figure 3-3 shows the mining lease boundary of the Cadia mine site and the locations of the Cadia air quality and meteorological monitoring sites, taken from Figure 3 of Newmont (2024).

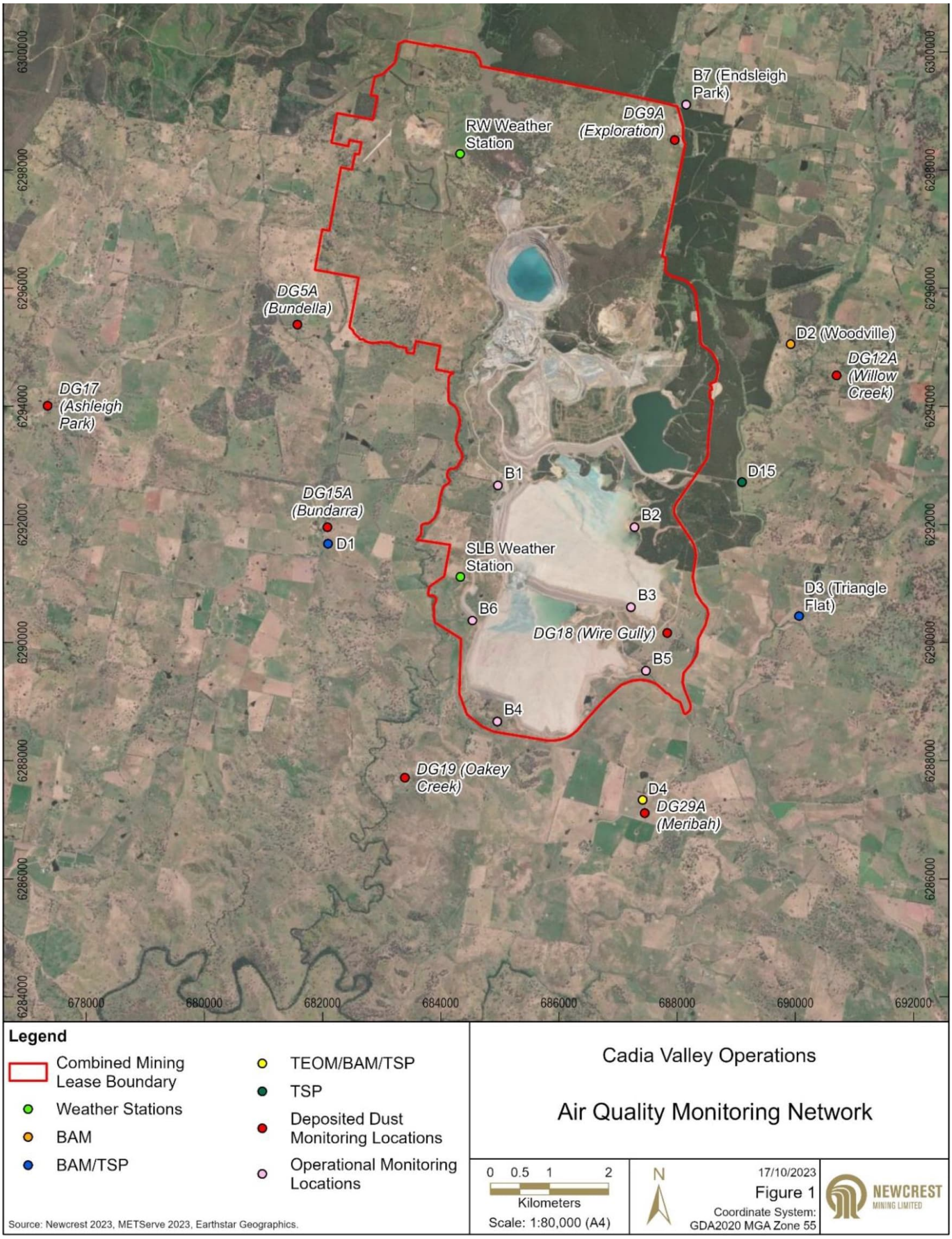

Figure 3-3. Cadia mining lease boundary and monitoring locations from Figure 3 of Newmont (2024).

3.2 Meteorology

3.2.1 The importance of meteorology

Meteorological data is one of the most important inputs into any air dispersion model because it directly influences how pollutants disperse in the atmosphere. Ground-level concentrations of contaminants are primarily controlled by two meteorological elements: wind direction and speed (for transport), and turbulence and mixing height of the lower boundary layer (for dispersion).

The atmospheric dispersion model that is used for dispersion simulations at CVO is called CALPUFF. CALPUFF relies on a separate meteorological model called CALMET which is run first to process all the meteorological and topographical inputs ready for use by CALPUFF.

CALMET takes meteorological inputs from local surface observations, supplemented with data from a meteorological grid model if needed, and predicts the behaviour of wind across the extent of area to be modelled (called the model domain). This wind behaviour can vary across the domain depending on local terrain fluctuations.

Therefore, the quality of meteorological observations that is available used in the CALMET model is extremely important. In this section, the availability and quality of these observations for the CVO location is reviewed.

3.2.2 CVO data

3.2.2.1 Data availability

CVO operates two automatic weather stations (AWS) for meteorological monitoring. The two sites are named Ridgeway and SLB (Southern Lease Boundary), and their locations are shown in Figure 3-3. The Ridgeway AWS was visited during the site visit and is shown in Picture A-4 in Appendix A. The SLB AWS could not be visited during the site visit, but a photo of the AWS is shown in Figure 5-5 of Zephyr (2022) and is provided in Picture A-5 of Appendix A. The two AWS are at markedly different elevations, with the Ridgeway AWS at approximately 886 m above mean sea level (AMSL), and the SLB AWS at approximately 695 m AMSL.

Both sites are understood to have a sensor height of 10 m above ground for wind and temperature, as well as measuring pressure, relative humidity, solar radiation, rainfall, and temperature at 2 m above ground.

From the photos in Appendix A, it is seen that the wind speed and direction at both AWS is measured with a propellor-and-vane mechanical sensor. The make and model of wind sensor is not stated in the CVO air quality monitoring plans (Newcrest, 2018 and Newmont, 2024), nor in the monthly monitoring reports on the Cadia website[5], but from the photos the sensors appear to be an RM Young anemometer (Figure 3-4). Therefore, the stall speed of the wind speed sensor is likely to be either 0.4 m/s or 1.0 m/s, depending on what anemometer model is installed.

The Australian/New Zealand Standard for meteorological monitoring for ambient air quality monitoring applications[6] requires a minimum starting threshold of ≤0.4 m/s for wind speed sensors, and ≤0.5 m/s for wind direction sensors. The permitted accuracy for wind speed in the Standard is ±0.2 m/s or 3% (whichever is greater), and for wind direction is ±3 degrees. Some of the RM Young anemometer models do not meet this specification.

5 https://www.cadiavalley.com.au/newcrest/cvo/environmental-management/monitoring/meteorology

6 AS/NZS 3580.14:2014 Methods for sampling and analysis of ambient air – Meteorological monitoring for ambient air quality monitoring applications.

Figure 3-4. Typical RM Young wind sensor.

Data from the two AWS that was provided to Jacobs by CPHL includes:

1. From Ridgeway AWS:
   a. Hourly-average wind speed and direction, wind direction standard deviation, station-level atmospheric pressure, relative humidity, solar radiation, temperature (2m and 10m height) for the period 1/1/17 – 31/5/23.
   b. Hourly rainfall for the period 1/1/17 to 3/7/23.
   c. 10-minute average wind speed and direction, temperature at 2m and 10m, and pressure for the period 1/1/15 to 26/9/23.
   d. Wind gust speed data at 10 minute intervals for the period 21/2/22 to 28/9/23. The definition of gust provided by CPHL is "*The maximum wind velocity is calculated by the program reviewing at each 1 second scan in a 10-minute recording period and recording the highest velocity (m/s) within those 600 scans, the program then logs the maximum wind velocity for the 10-minute recording period*". CPHL also advised that collection of gust data only started in February 2022, hence the short period of data available.
2. From SLB AWS:
   a. Hourly-average wind speed and direction, wind direction standard deviation, station-level atmospheric pressure, relative humidity, solar radiation, temperature (2m and 10m height) for the period 1/1/17 – 31/5/23.
   b. Hourly rainfall for the period 1/1/17 to 3/7/23.

3.2.2.2 Wind speed and direction averaging

Wind sensors send a continuous signal to a datalogger, which samples the signal at very short intervals (such as every second, or every few seconds), calculates an average based on the user's setting using standard scalar and/or vector averaging techniques, and then records the data as an observation. Averaging intervals are commonly in the range of 1 minute to 10 minutes, with 10 minutes being the maximum permitted in AS/NZS 3580.14:2014.

If the wind speed drops below the manufacturer's specified wind speed threshold with a mechanical sensor, the datalogger should register the wind speed as "calm", with both speed and direction written to zero or some other calm indicator. It is important that the direction is also registered as calm. Calculating and understanding average wind speeds when the wind speed is around the sensor threshold is a particular challenge. However, as low or near-calm wind speeds do not appear to be common in the measurements at Ridgeway and SLB, this is not likely to be an important issue for the Cadia modelling.

The question of how wind direction averages are calculated is very important for atmospheric dispersion modelling. Raw data should be converted to 10-minute and 1-hour average wind directions using the methods recommended in USEPA (2000) with wind direction computed as a vector averages. For example, if one has a series of direction readings under northerly winds, these might fluctuate between, say, 350 degrees and 10 degrees over the course of an hour. If an arithmetic, or scalar average of these readings is calculated, the resulting wind vector might be from about 180 degrees (southerly) which is not representative of the real situation. USEPA (2000) provides recommendations for calculating the average that take account of the discontinuity in wind direction that occurs between 360 degrees and 0 degrees.

Jacobs used the 10-minute average data provided by CPHL for Ridgeway to compute the 1-hour average wind speed and direction using the methods in USEPA (2000). For wind speed, this is simply a scalar arithmetic average. For wind direction, this requires a vector computation of the east-west and north-south components of the direction, which are multiplied by the wind speed and then converted back into a vector using a trigonometry function to yield the final average direction.

The 1-hour average wind speed calculated from the 10-minute average data was found to be the same as the 1-hour as-received data from CPHL. However, some notable differences were found in the computed average directions. Figure 3-5 shows the windrose for Ridgeway for 1-hour average wind speed and direction, comparing the 1-hour averages as-received from CPHL, with the 1-hour averages calculated by Jacobs from the 10-minute data using the vector averaging method in USEPA (2000). The windrose for Ridgeway in TAS (2023a) is also shown for comparison.

The windrose calculated from 10-minute average data shows a much higher frequency of winds from the northerly direction, higher frequencies from the north-northwest and north-northeast directions, and lower frequencies from the south. The windrose also matches well with the windrose data for Ridgeway displayed in TAS (2023a). This is an indication that there is a potential issue with the method of calculating 1-hour average wind directions in the data provided by CPHL, although this issue was corrected by TAS in the modelling in TAS (2023a). The issue with the 1-hour averages could be problematic if CPHL relies on this data for operational management (for example, comparing dates and times of complaint reports with wind direction records). This issue may also be present in the 10-minute data averages provided by CPHL, which are also calculated values. Jacobs used the Ridgeway 1-hour average wind directions computed from the 10-minute data in the meteorological model setup described in Section 5.3 of this report.

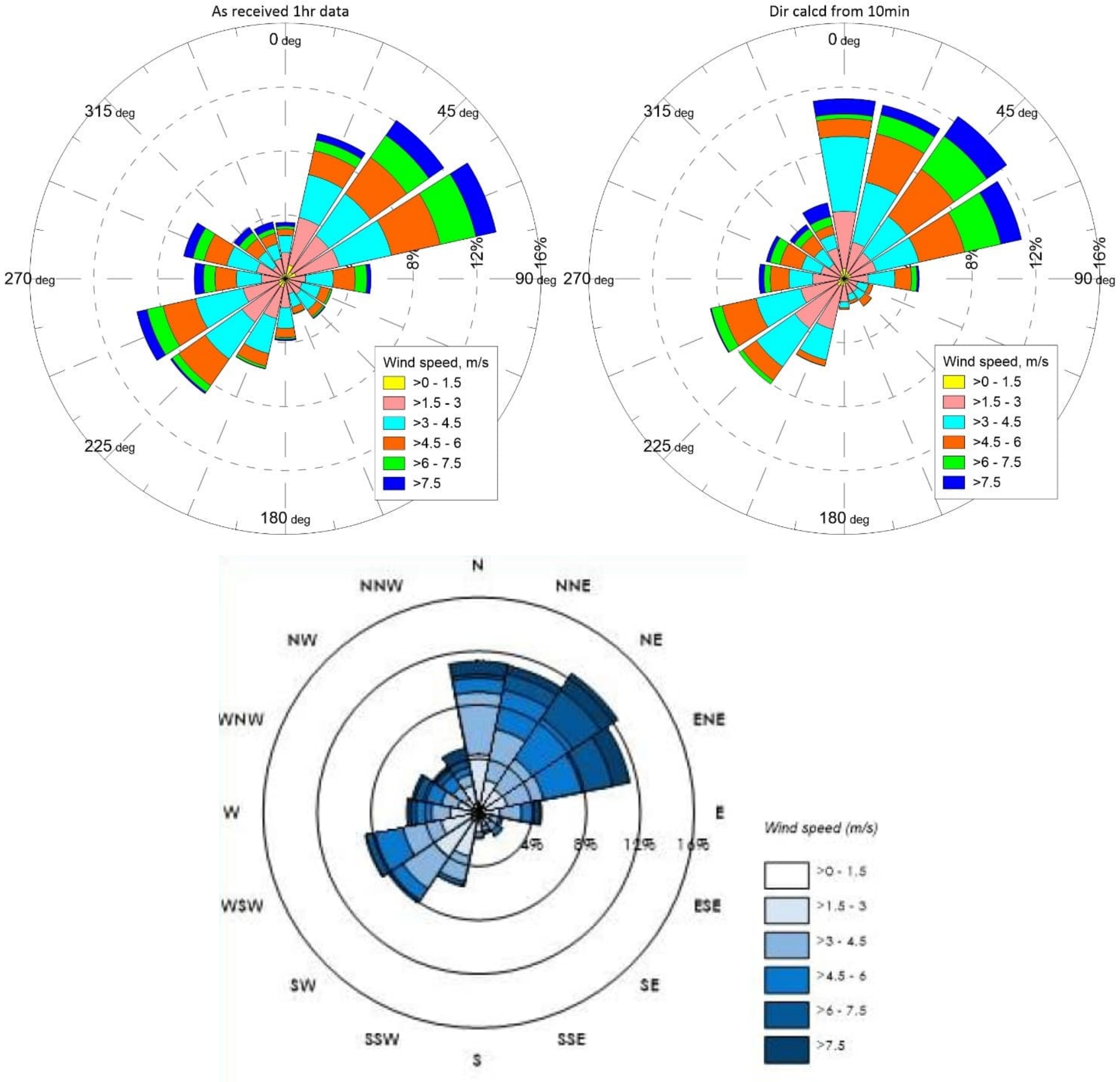

Figure 3-5. Windroses comparing 1-hour average wind speed and direction for January 2022 – February 2023 at Ridgeway, comparing as-received data from CPHL (top left), with computed vector averages based on the 10-minute data (top right). Bottom: Windrose for Ridgeway for same period in TAS (2023a).

Jacobs did not have access to the 10-minute data for SLB, and relied on the 1-hour as-received data from CPHL for the meteorological model setup. Examination of the 1-hour data for SLB showed that similar issues in the method of averaging were present as found in the Ridgeway data. Jacobs reviewed the entire 2022 SLB meteorological data to remove or amend obvious outliers arising from this issue before using the data in CALMET, however it would be preferable to access the 10-minute dataset from SLB. Figure 3-6 shows the windrose for SLB comparing 1-hour averages as-received from CPHL, with the 1-hour averages amended by Jacobs and also the windrose provided in TAS (2023a). The windroses in the data used by Jacobs, even after amending for obvious outliers, have a lower frequency of northerly winds than the data used by TAS. The model is potentially sensitive to this data difference, particularly in the southern part of the model domain.

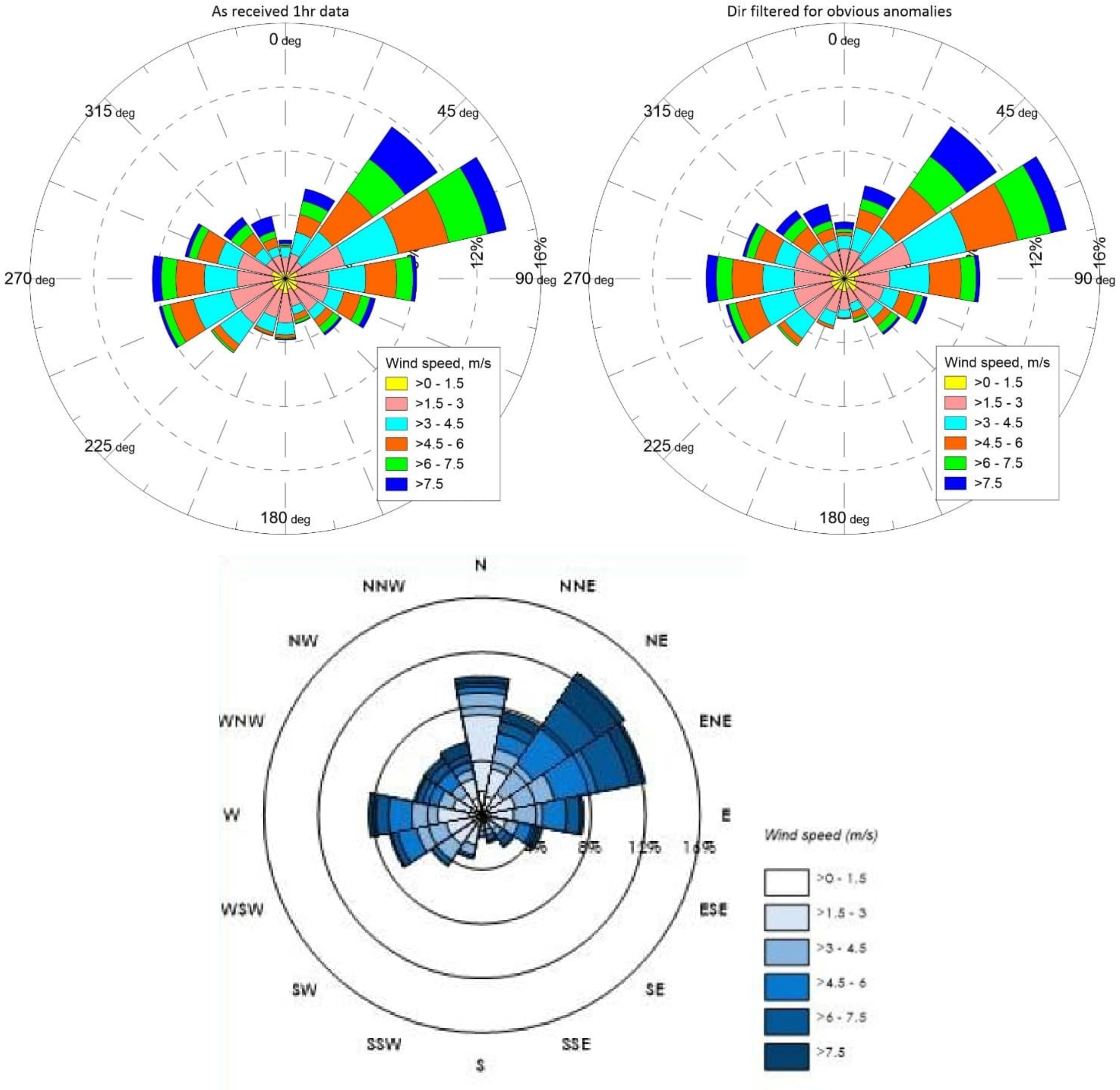

Figure 3-6. Windroses comparing 1-hour average wind speed and direction for 2022 at SLB, comparing as-received data from CPHL (top left), with computed vector averages based on the 10-minute data (top right), and the windrose for SLB for same period in TAS (2023a).

3.2.3 BOM data

3.2.3.1 Data availability

The Bureau of Meteorology (BOM) operates several meteorological monitoring sites in the Central Tablelands region. The sites are shown on Figure 3-1 and include Orange Airport, Bathurst Airport, Parkes and Cowra. However, only the Orange Airport AWS is relevant to the Cadia mine location, with all of the other sites being too far away and influenced by topographical charactistics that are not relevant to the simulation of dispersion of pollutants from Cadia.

Jacobs purchased data from BOM for the Orange Airport location, and also from the Bathurst Airport location in case data from that site was needed to supplement periods of missing data from Orange Airport (such as cloud cover data).

The data from the Orange Airport and Bathurst Airport AWS that was provided to Jacobs by BOM includes:

1. From both Orange Airport and Bathurst Airport AWS:
   a. Hourly-average wind speed and direction, wind gust, wind direction standard deviation, relative humidity, temperature, rainfall, atmospheric pressure and cloud cover for the period 01/01/15 – 1/07/23.
   b. 1-minute average wind speed and direction, and wind direction standard deviation for the period 01/01/15 – 1/07/23.

3.2.3.2 Data analysis

Figure 3-8 shows a windrose constructed from the as-received 1-hour average wind speed and direction data for the Orange Airport AWS. The windrose shows similar wind speed frequencies compared to Ridgeway and SLB, and reasonably similar wind direction distributions notwithstanding a greater frequency of northwesterly winds. Orange Airport located in a different topographical context with respect to the location of Mount Canobolas compared to Ridgeway and SLB, so some differences in wind direction frequencies may be expected.

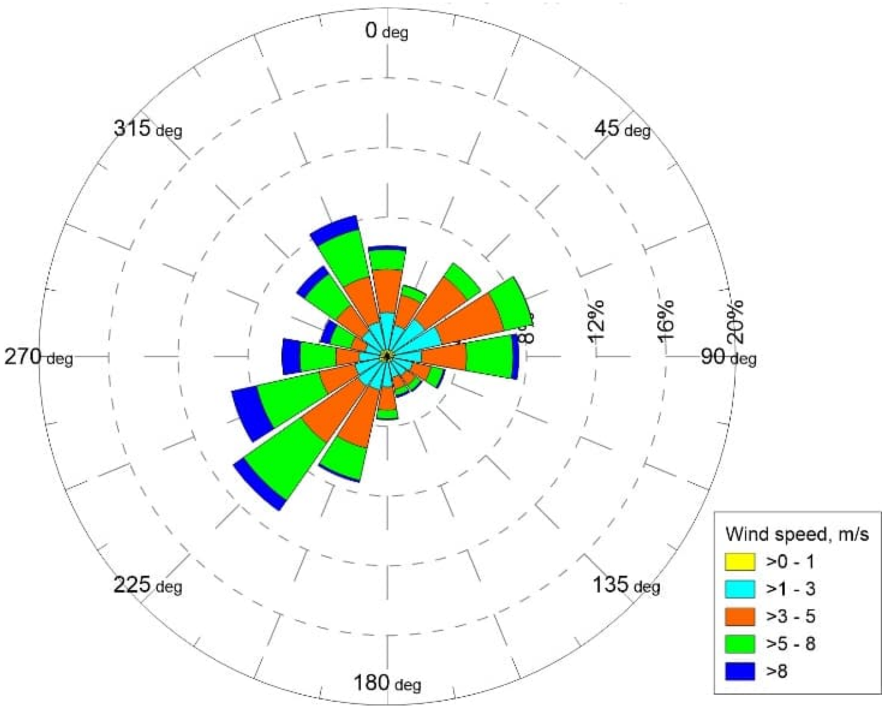

Figure 3-7. Windrose displaying 1-hour average wind speed and direction as received from BOM for Orange Airport AWS, January 2015 – June 2023.

Jacobs calculated 1-hour average wind speeds and directions for Orange Airport using the as-received 1-minute data and following the recommendations in USEPA (2000), to compare with the as-received 1-hour average data. The following similarities and discrepancies were found:

- Jacobs' scalar-averaged 1-hour wind speeds matched the BOM 1-hour average wind speeds.
- The BOM as-received 1-hour average wind directions matched most, but not all, of the calculated vector-averaged wind directions. The resultant windrose from the calculated wind speed and direction was very similar to Figure 3-8.
- The greatest inconsistencies in wind direction occurred in hours where there are lots of calm winds and/or the wind changes during the hour.
- Jacobs therefore revised the 1-hour average dataset so that hours with a significant proportion of calm winds were designated as "calm", rather than being assigned a wind speed and direction.

3.2.4 EPA data

3.2.4.1 Data availability

NSW Government operates two automatic weather stations (AWS) for meteorological monitoring in Orange[7] and Bathurst[8]. Both AWS were visited during the site visit and are shown in Pictures A-6 and A-7 in Appendix A. Jacobs was advised by EPA that both sites have a sensor height of 10m above ground for wind monitoring. The wind sensors are ultrasonic type, capable of measuring very low wind speeds. Jacobs was also provided with sub-hourly data from the Orange AWS in the form of 1-minute averages.

Data from the two AWS that was provided to Jacobs by the EPA includes:

1. From Orange AWS:
   a. Hourly-average wind speed and direction, wind direction standard deviation, relative humidity, temperature, rainfall for the period 18/01/19 – 1/01/23.
   b. 1-minute average wind speed and direction, wind direction standard deviation, relative humidity, temperature for the period 18/01/19 – 19/09/23.
2. From Bathurst AWS:
   a. Hourly-average wind speed and direction, wind direction standard deviation, relative humidity, temperature for the period 1/01/15 – 1/01/23.

3.2.4.2 Data analysis

Figure 3-8 shows windroses constructed from the as-received 1-hour average wind speed and direction data for the Orange and Bathurst AWS. The two sites show quite dissimilar wind patterns to each other and to the Ridgeway, SLB and Orange Airport windroses shown in Figure 3-5, Figure 3-6 and Figure 3-7. These differences are apparent in both the prevailing wind directions and the frequency of the various wind speed categories, with wind speeds generally being lower than at Ridgeway, SLB and Orange Airport.

The wind speed differences are most likely due to the Orange and Bathurst township locations being more sheltered in the urban setting compared to the rural sites of Ridgeway, SLG and Orange Airport.

[7] Located at Jaeger Reserve, 149 Hill Street, Orange.

[8] Located at Bathurst Sewage Treatment Plant, off Morrisset Street, Bathurst

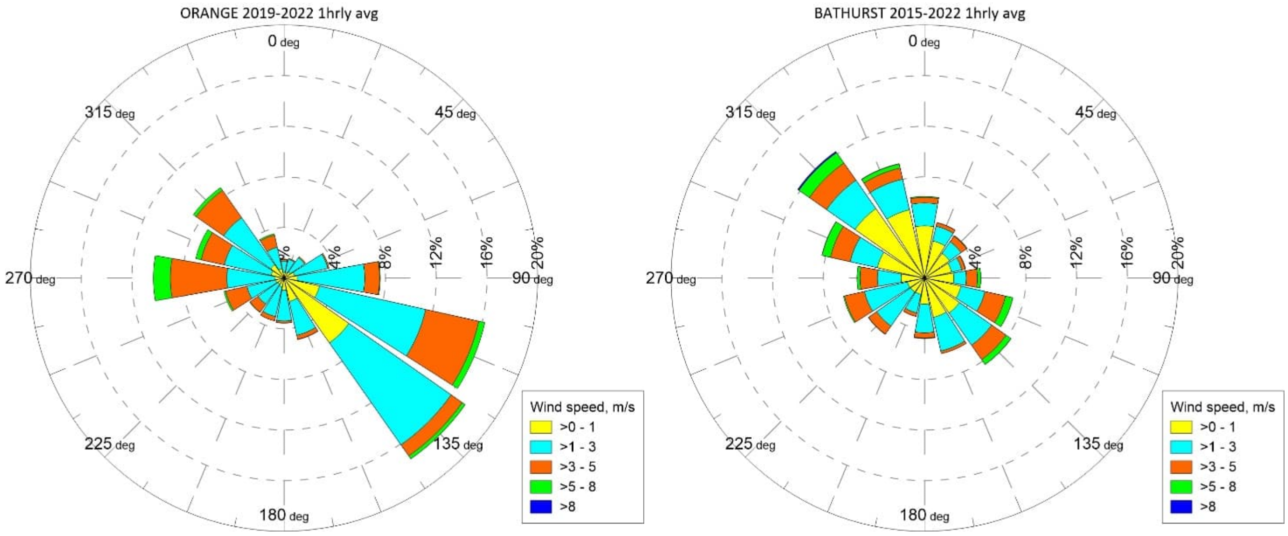

Figure 3-8. Windroses comparing 1-hour average wind speed and direction as received from EPA, for Orange and Bathurst AWS.

Jacobs investigated the Orange AWS dataset for any data-averaging issues that may explain the differences in directions between the windrose for Orange compared to Ridgeway and SLB. One-hour vector averages of wind direction were calculated from the 1-minute raw data by following the recommendations of USEPA (2000). The resultant 1-hour average data set was the same as the as-received data set, indicating no anomalies in the calculation of the 1-hour average data provided by EPA.

In addition, Jacobs reviewed the patterns of wind directions under high wind speeds measured at the Orange AWS compared to the data for the same time period from the Orange Airport AWS, as it was expected that the directions would be similar under high wind speeds. An example of this comparison is shown in Figure 3-9. The directions appear to be consistent, indicating that there is unlikely to be some direction calibration error at the Orange AWS. On the graph in Figure 3-9, there are a lot less data points in the Orange dataset than for the Orange Airport dataset; this is because contemporaneous wind speeds at Orange are typically lower than at the airport site.

From Jacobs' investigations, there is no evidence that there are any issues with the quality of the Orange AWS data, and the data is therefore assumed to be representative of that location even though it has a very different pattern to the Ridgeway and SLB AWS windroses. As shown in Figure 3-1 and Figure 3-2, the Orange AWS is located in a different topographic setting to the Cadia AWS's, with higher terrain to the south and southwest and terrain falling away to the north and east. Therefore, Jacobs does not consider data from the Orange AWS to be representative of the Cadia location.

The Bathurst AWS windrose also shows significant differences compared to Ridgeway and SLB, as well as compared to Orange. The Bathurst AWS is located at the Bathurst Sewage Treatment Plant close to the Wambuul/Macquarie River in a valley that follows the river in a northwest/southeast orientation consistent with the prevailing wind directions shown in the windrose. This valley system can be seen in Figure 3-2. Therefore, the wind speeds and directions at this AWS are likely to be influenced by local topographical features. Jacobs does not consider data from this AWS to be representative of the Cadia location.

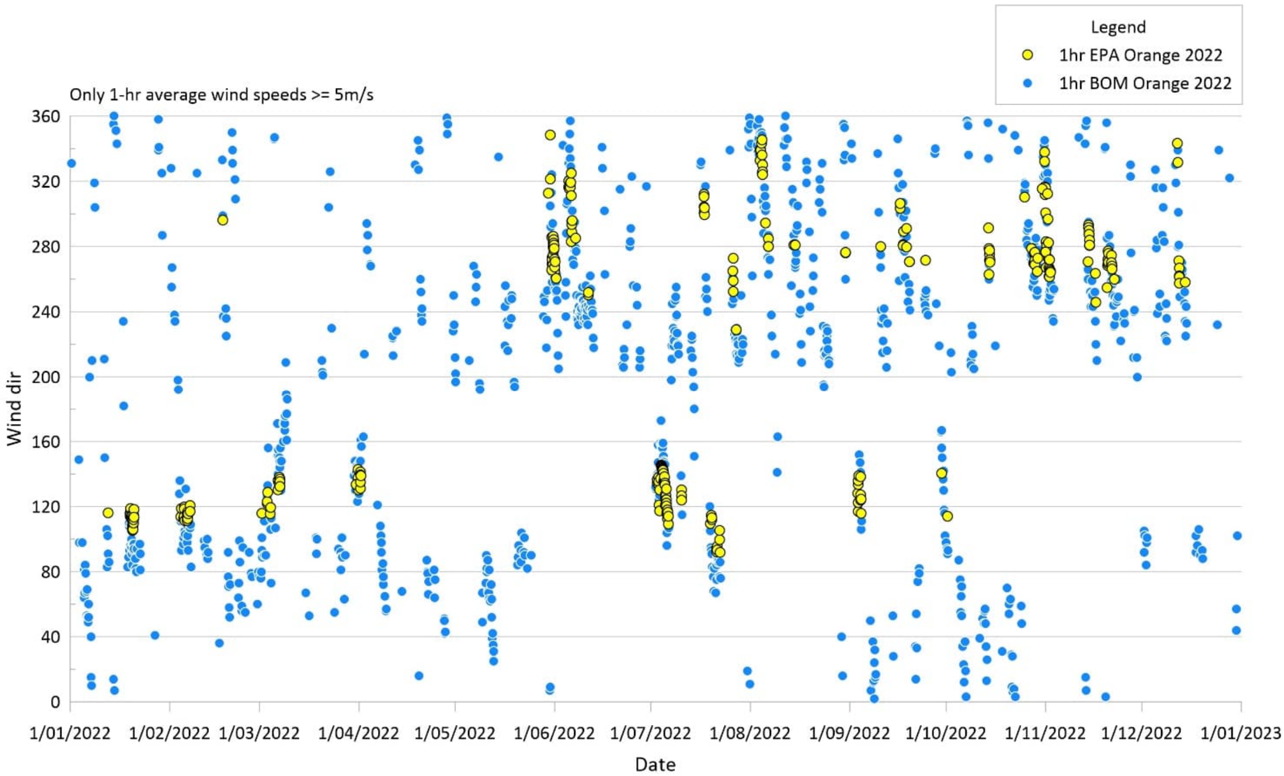

Figure 3-9. Comparison of wind directions at Orange and Orange Airport for hours when the 1-hour average wind speed exceeded 5 m/s, for 2022.

3.3 Local Air Quality

3.3.1 Data sources and pollutants measured

A range of data sources are available to quantify local air quality around the Cadia mine. These sources include the following continuous monitoring sites:

- Concentrations of PM_{10} and $PM_{2.5}$ measured continuously on an ongoing basis by CVO by Beta Attenuation Monitor (BAM) technology at four locations outside the mine site.
- Historical PM_{10} concentration data measured continuously by CVO by Tapered Element Oscillating Microbalance (TEOM) instrumentation at four locations outside the mine site (now discontinued at all but one site).
- Dust Deposition Gauges (DDGs) which are located at eleven sites around the Cadia District and the Cadia Dewatering Plant at Blayney. The DDGs are analysed monthly on an ongoing basis for metals and total dissolved and insoluble solids.

The locations of these sites are shown in Figure 3-3.

In addition, data is available from the following intermittent or short-term monitoring campaigns:

- 24-hour average PM_{10} and metals concentrations measured approximately fortnightly by CVO by High Volume Air Sampler (HVAS) methodology over the 2020 year at four locations outside the mine site (reported in Serinus (2021)). See Section 3.3.5.1 for further discussion of HVAS data.
- Limited number of 24-hour average $PM_{2.5}$ concentrations measured by CVO by Low Volume Air Sampler (LVAS) methodology over July – December 2020 at two locations outside the mine site (reported in Serinus (2021)). See Section 3.3.5.2 for further discussion of LVAS data.

- $PM_{2.5}$ monitoring campaign conducted by the Australian Nuclear Science and Technology Organisation (ANSTO, 2023) a 12-month period in February 2022 to February 2023. Monitoring was conducted at four sampling sites with a 24-hour average sample collected each Sunday and Wednesday. After the sampling was completed, the samples were analysed for $PM_{2.5}$ mass, and 23 other chemical species.

PM_{10} and $PM_{2.5}$ is also monitored continuously by NSW Government in Orange and Bathurst.

AEMR 2023 and Newmont (2024) (replicated in Figure 3-3) show six monitoring locations designated as "operational monitoring sites" around the TSFs and one other at the northeast of the mining lease boundary. The seven locations are labelled B1 to B7. These locations were not shown on the corresponding map in previous AEMRs. Newcrest (2023a) states that the operational monitoring comprises "*a network of real-time dust and weather monitors to inform dust management in operational areas such as the TSFs. Operational monitoring aims to identify emerging or 'at risk' dust and meteorological conditions, and provide CVO with the opportunity to implement proactive and reactive mitigative measures. Operational monitoring is not intended to be used for compliance purposes, with its primary objective to inform proactive and reactive dust management at the TSFs.*"

Newcrest (2023a) also states that the operational dust and weather monitors were commissioned in 2022 and are linked to real-time alarms that notify CVO personnel if pre-set dust thresholds are exceeded so that reactive actions are triggered. In addition, the meteorological data collected by these monitors informs predictive software to forecast the likelihood of conditions which may increase TSF dust emissions.

No information is available to Jacobs regarding the monitoring method used at these operational monitoring sites, nor the data that is collected.

TSP is not measured directly by CVO. Cadia (2018) states that *"TSP concentrations can be inferred from the PM_{10} monitoring data, by assuming that 40% of the TSP is PM_{10}. These measurements have been derived from data collected by co-located TSP and PM_{10} monitoring operated in the Hunter Valley (NSW Minerals Council, 2000)"*.

However, the final version of that report (NSW Minerals Council, 2001) states that:

> The **NSW SPCC (now EPA) (1986)** undertook a series of measurements on the particle size distributions in dust from operations on open cut coalmines in the Hunter Valley. The average of approximately 120 samples analysed indicated that 39.1% of TSP was in the PM_{10} size range and 4.68% of TSP was in the $PM_{2.5}$ size range. This means that about 12% of PM_{10} particles are in the $PM_{2.5}$ size range for these sources and 88% are in the range 2.5 to 10 μm. Note these measurements were all made within approximately 15 to 150 m of the source of dust. The ratios would be expected to change as the distance from the source to the measurement point increased. A finding of the SPCC study was that the particle size distribution depended strongly on the size distributions in the material being handled.

This implies that PM_{10} might be more than 39.1% of the TSP at downwind distances of greater than 150 m due to settling of the heavier particles. This means that concentrations of TSP determined from the PM_{10} concentrations will be greater than are likely in reality, so the 40% assumption is conservative and likely to overestimate TSP concentrations for monitoring around the Cadia site.

The corollary to this is that if any TSP concentrations are measured, that data should not be used to estimate PM_{10} and $PM_{2.5}$ concentrations using the same 40% ratio. However, Jacobs is not aware of any relevant air quality monitoring data conducted for the Cadia site that uses this approach.

3.3.2 Continuous PM_{10} and $PM_{2.5}$ monitoring at CVO sites

3.3.2.1 Locations, methods and data availability

Historically, continuous PM_{10} monitoring at Cadia has been undertaken using TEOM instrumentation. TEOM monitoring was carried out at four air quality monitoring sites (AQMS) known as Meribah, Triangle Flat, and Bundarra as shown on Figure 3-3 and another location known as Flyers Creek which was midway between D2 and D15 on Figure 3-3. Following consultation with regulatory and community stakeholders through 2021, Cadia committed to replace the TEOM instruments with the alternative BAM technology. Transition to the BAM technology sought to address (Advitech 2023):

- Ongoing issues relating to operability of the air quality monitoring network and availability of data:
  - these issues were driven by reliability of mains power supply in rural monitoring environments,
  - the BAM instruments have a lower power demand than TEOMs, making mains power with battery backup a feasible solution to this problem.
- Emerging expectation amongst regulatory and community stakeholders that the monitoring network should include provision for both PM_{10} and $PM_{2.5}$ monitoring.

In addition to instrumentation upgrades, commitment was also made to relocate the AQMS at Flyers Creek to a new site at 'Woodville' as shown in Figure 3-3. Following consultation with the EPA, transition from TEOM to BAM monitoring systems at the Bundarra, Triangle Flat and Meribah monitoring locations occurred on 1 April, 2022. Transition from Flyers Creek to the new Woodville monitoring location was delayed due to commissioning issues with BAM instrumentation at that site; monitoring commenced at that location on 1 June, 2022.

The location of the new Woodville site is reported as being at coordinates (690694, 6294520) in Newmont (2024) but is shown at a different location in Figure 3-3 and TAS (2023a) although the exact location is difficult to interpret from the scale of the maps. The exact location of the Woodville BAM should be confirmed with CVO. For this report, it is assumed to be at a CPHL-owned house at the location inferred from Figure 3-3 of approximately (690013, 6294996).

Validated data from the TEOMs and BAMs was provided to Jacobs for the periods summarized in Table 3-1.

Table 3-1. BAM and TEOM data availability

Site name	Type of monitor	Parameters measured	Validated data
Bundarra	TEOM	PM_{10}	24-hour average 1/01/2020 – 14/07/2022 1-hour average 1/01/2015 – 14/07/2022^
	BAM	PM_{10} and $PM_{2.5}$	24-hour average 1/04/2022 - 24/09/2023 1-hour average 1/04/2022 - 24/09/2023*
Flyers Creek Weir	TEOM	PM_{10}	24-hour average 1/01/2020 – 14/07/2022 1-hour average 1/01/2015 - 14/07/2022^
Triangle Flat	TEOM	PM_{10}	24-hour average 1/01/2020 – 14/07/2022 1-hour average 1/01/2015 - 14/07/2022^
	BAM	PM_{10} and $PM_{2.5}$	24-hour average 1/04/2022 - 24/09/2023 1-hour average 1/04/2022 - 24/09/2023*
Meribah	TEOM	PM_{10}	24-hour average 1/01/2020 – 14/07/2022 1-hour average 1/01/2015 - 24/09/2023^

	BAM	PM_{10} and $PM_{2.5}$	24-hour average 1/04/2022 - 24/09/2023 1-hour average 1/04/2022 - 14/07/2022*
Woodville	BAM	PM_{10} and $PM_{2.5}$	24-hour average 21/05/2022 - 24/09/2023 1-hour average 21/05/2022 - 24/09/2023*

^ 15-minute frequency data was also provided for the TEOMs, however the data was described as "raw" and Jacobs instead relied on the validated 1-hour and 24-hour average data that was supplied.

* 15-minute frequency records were also provided for the BAM, however each 15-minute record within an hour were duplicates.

Advitech (2023) and Cadia (2018) note that the locations of the Flyers Creek Weir TEOM and Meribah TEOM/BAM do not meet all of the criteria associated with Australian Standard /New Zealand Standard AS-NZS 3580.1.1.2007[9] for the location of monitoring equipment. It is not stated whether this means that these sites have the potential to understate or overstate deposition rates.

3.3.2.2 Data analysis

3.3.2.2.1 Data averaging

Jacobs conducted some preliminary analysis of the data provided in Table 3-1 to check for data and averaging anomalies, including calculating 24-hour averages (midnight to midnight)[10] from the supplied 1-hour data. The following findings were noted:

- For the TEOM data, the "Validated" 24-hour data concentrations provided by Cadia often did not match the arithmetic average of the validated 1-hour data concentrations as calculated by Jacobs – for example see Figure 3-10 which compares the 24-hour average concentrations for the 2020 year at Meribah. The figure shows that some of the as-received 24-hour averages were slightly lower (or occasionally slightly higher) than the calculated averages. However, these discrepancies are relatively small, and unlikely to have materially affected analysis of ambient air quality data in previous TAS reports.
- For the BAM data, the "validated" 24-hour data concentrations provided by Cadia compared well with the arithmetic averages calculated by Jacobs.

[9] This standard was updated in 2016.

[10] Calculated following the guidelines in AS 3580.19:2020 Methods for sampling and analysis of ambient air, Method 19: Ambient air quality data validation and reporting.

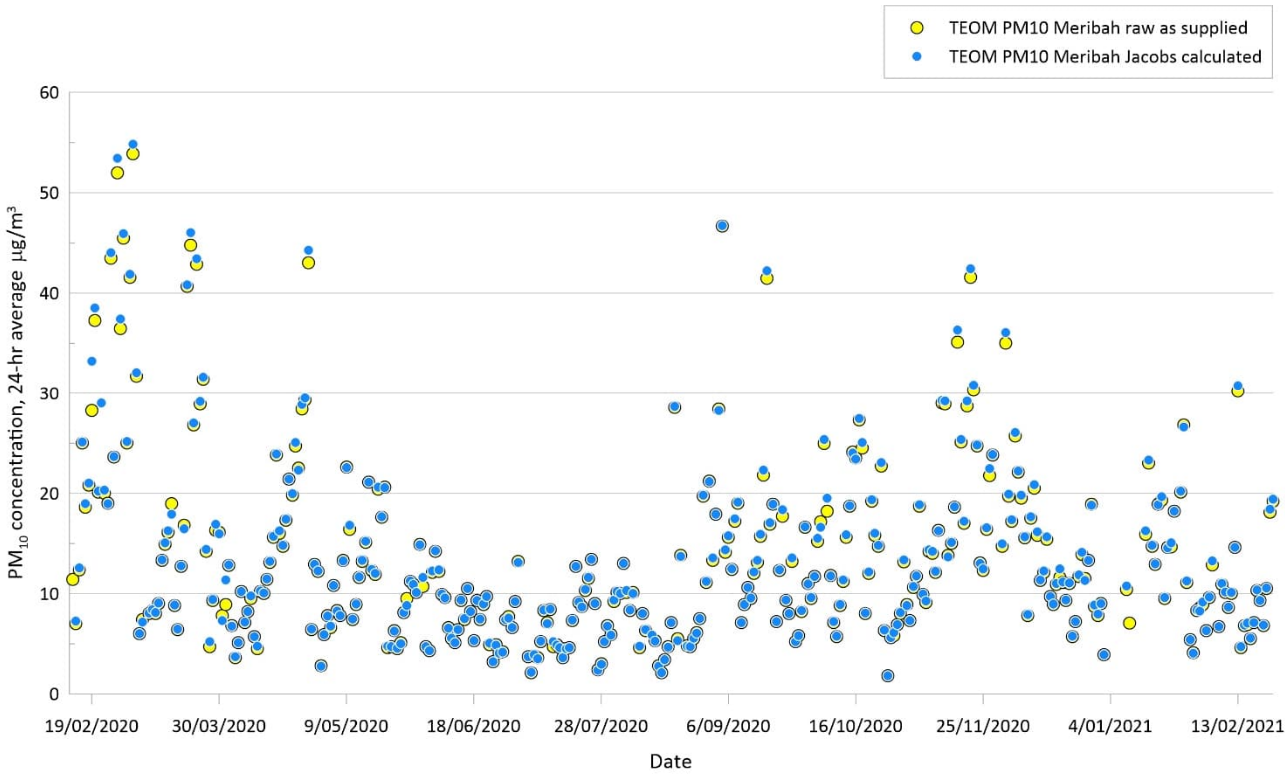

Figure 3-10. Comparison of 24-hour average PM_{10} concentrations at Meribah for 2020, for "validated" concentrations supplied by CVO versus calculated by Jacobs from 1-hour data.

3.3.2.2.2 TEOM vs BAM

The co-location of both TEOM and BAM equipment at the Meribah site allows comparison of the PM_{10} concentrations measured by the different technologies. Eighteen months of data was available to Jacobs for this comparison. Figure 3-11(a)-(c) show a comparison of 24-hour averages measured at Meribah with the TEOM and with the BAM from 20 March 2022 to 20 September 2023. The TEOM tends to report slightly higher concentrations than with the BAM. However, as the Meribah location is flagged by CVO as a site that does not comply with AS-NZS 3580.1.1.2007 for siting of air quality monitoring equipment, it is possible that the location issues have influenced concentrations measured at one or both monitoring stations.

3.3.2.2.3 24-hour average data

PM_{10} and $PM_{2.5}$ concentrations measured at the four AQMS sites by BAM method from 20 March 2022 to 20 September 2023 are shown in Figure 3-12 and Figure 3-13. The graphs show that the Approved Methods PM_{10} concentration of 50 µg/m^3 was not exceeded during this time except on one occasion at Woodville where a concentration of 59.1 µg/m^3 was measured on 8 March 2023. The AEMR (2023) acknowledges this data point but notes that "*Detailed analysis of this event was undertaken by third party specialists (Advitech Pty Ltd) who determined the exceedance was likely due to another dust source off-site. This conclusion came from the assessed west-southwest light winds averaging 2.9 m/s during the time of the exceedance, as well as no visible dust lift off events and the Bundarra dust monitor upwind recording 15 µg/m^3. The detailed analysis confirmed that the contribution of dust emissions from the Cadia operation was less than 50 µg/m^3 at this time.*"

Review of the analysis by Advitech (2023) for the measurement at Woodville on 8 March 2023 offers an alternative interpretation from that day. The CVO contribution to the measured concentration at Woodville was estimated in the range 40 to 45 µg/m^3, and it was the cumulative addition of the background concentration of 15 µg/m^3 that caused the measured exceedance. Whilst the explanation provided in AEMR 2023 is not incorrect, it downplays the likely contribution from CVO to the measured concentration on that day.

Cumulative frequency plots of the data from 20 March 2022 to 20 September 2023 are provided in Figure 3-14 and Figure 3-15. It is apparent that concentrations of PM_{10} and $PM_{2.5}$ measured at the Woodville site tend to be a little higher than at the other sites. However, from this analysis alone it is not possible to conclude whether this is due to dust emissions from CVO, or other background interferences.

TAS (2023) analyses the PM_{10} concentrations from the TEOM and BAM monitoring for January 2022 – February 2023 and concluded that:

- Air quality during the period is good with all recorded 24-hour average PM_{10} levels below the criterion of 50 µg/m^3.
- Overall, there appears to be a seasonal trend with PM_{10} levels generally decreasing during the winter.
- Regional dust events can be seen with elevated levels being recorded at all monitors at the same time.
- The Woodville monitor appears to record on occasion slightly more elevated 24-hour average levels in comparison to the other monitors at CVO, which may be due to the location relative to local emission sources.

Jacobs agrees with these conclusions, except to note that the reason the Woodville monitor records more elevated 24-hour averages than at the other sites could also be due to mine emissions.

Potential background interferences at the Woodville site are discussed further in TAS (2023a), Section 5.5.1. The report states that *"The Woodville monitor is located amongst several mine-owned dwellings which would generate wood smoke during cold periods. The monitor is also relatively close to large stands of trees/ plantations, and CVO staff indicate observing pollen from the trees. The monitor is located within approximately 50m of a dirt road between the site and the CVO. All of these are potential sources of $PM_{2.5}$, that are not included in the modelling with perhaps more significant $PM_{2.5}$ effects from the woodsmoke and pollens."*

According to Advitech (2023), the Woodville location was selected because this site would *"improve the representation of air quality monitoring in receiving airsheds to the northeast of the mine"*, but the local interferences mean that the reliability of this site is diminished because doubt can be raised about the validity and cause of any elevated PM_{10} (or $PM_{2.5}$) results at that site.

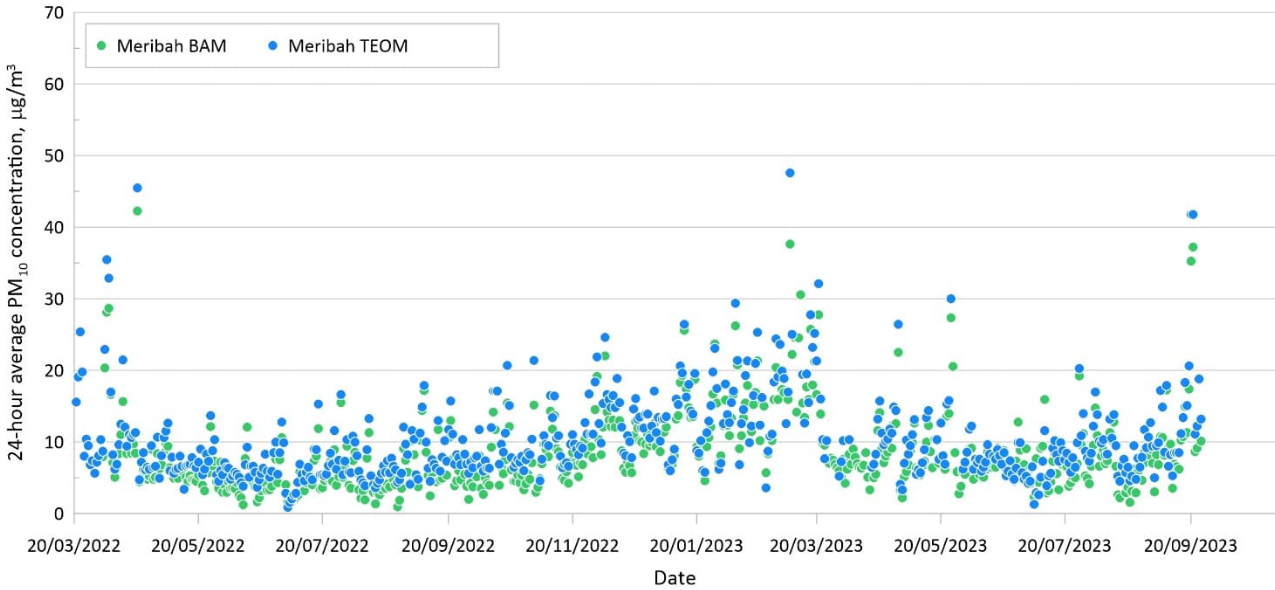

(a) Timeseries comparison

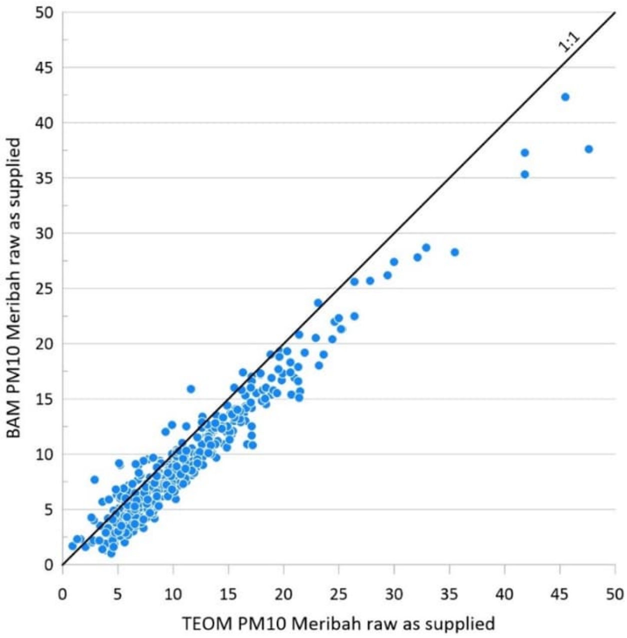

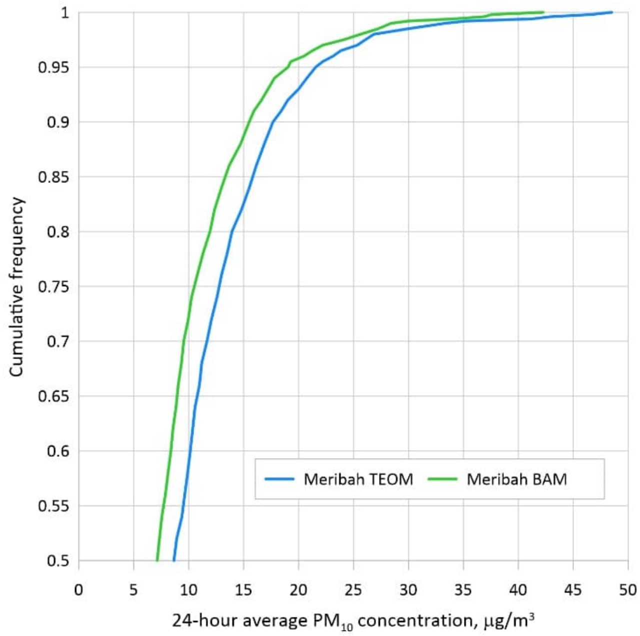

(b) Scatter plot comparing contemporaneous concentrations

(c) Cumulative frequency of measured concentrations.

Figure 3-11. Comparison of 24-hour average PM_{10} measured with BAM and TEOM methods at Meribah from 20 March 2022 to 20 September 2023.

Figure 3-12. 24-hour average PM_{10} measured with BAM at Bundarra, Triangle Flat, Meribah and Woodville AQMS from 20 March 2022 to 20 September 2023. Top – all stations combined; middle and bottom – individual stations.

Figure 3-13. 24-hour average $PM_{2.5}$ measured with BAM at Bundarra, Triangle Flat, Meribah and Woodville AQMS from 20 March 2022 to 20 September 2023. Top – all stations combined; middle and bottom – individual stations.

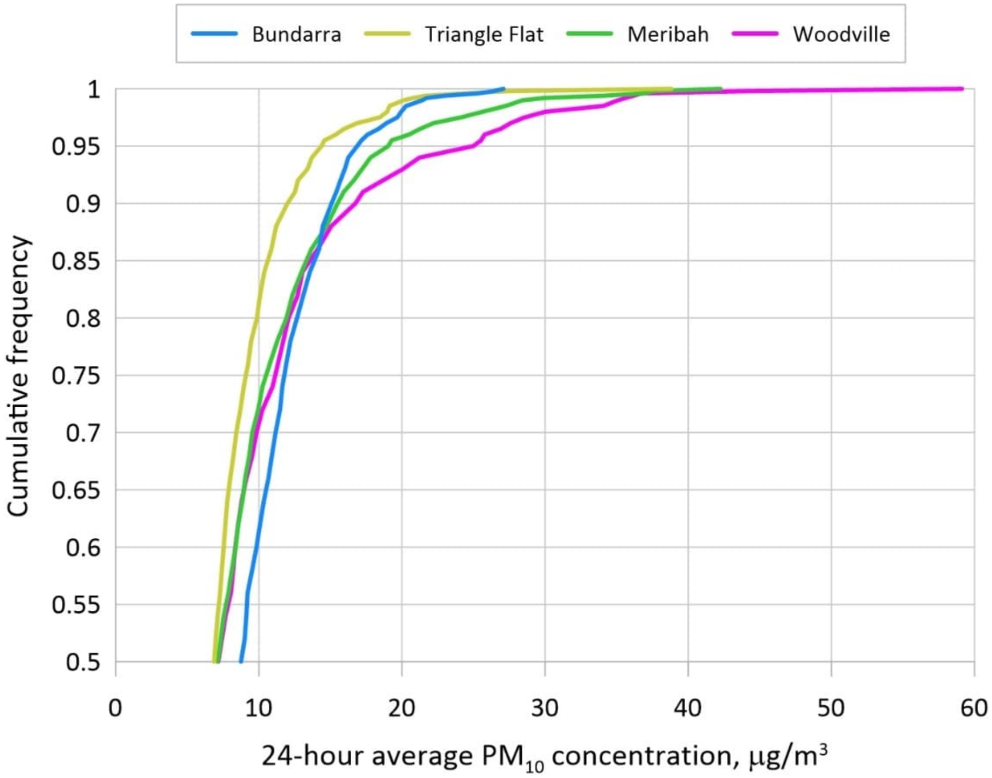

Figure 3-14. Cumulative frequency of 24-hour average PM_{10} measured with BAM at Bundarra, Triangle Flat, Meribah and Woodville AQMS from 20 March 2022 to 20 September 2023.

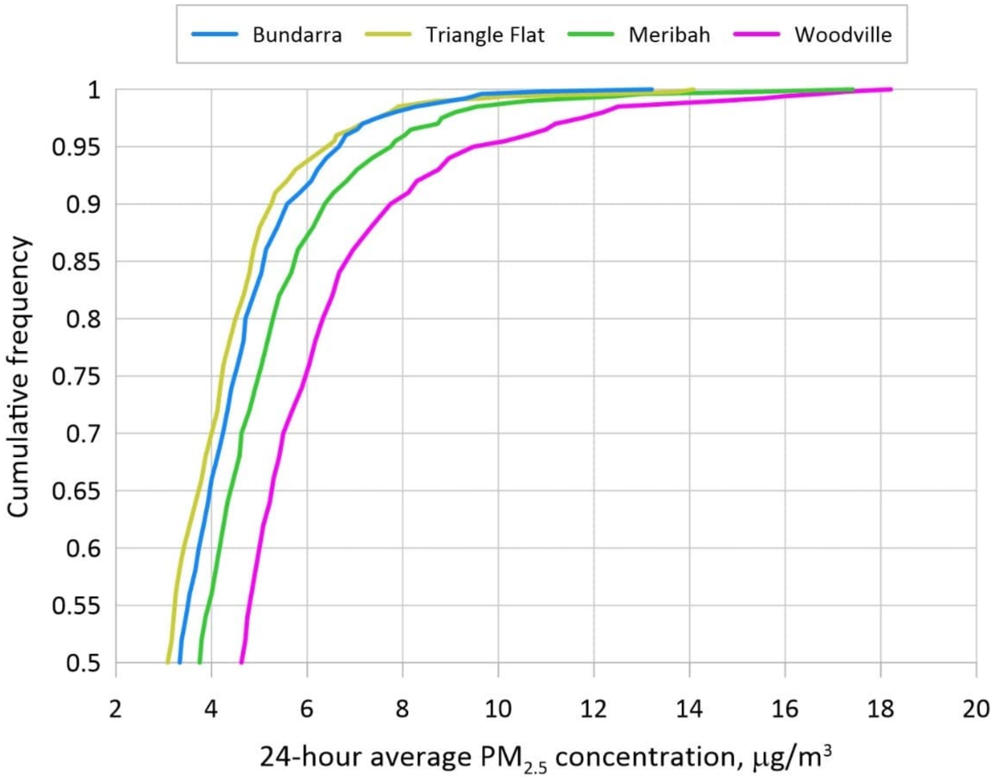

Figure 3-15. Cumulative frequency of 24-hour average $PM_{2.5}$ measured with BAM at Bundarra, Triangle Flat, Meribah and Woodville AQMS from 20 March 2022 to 20 September 2023.

3.3.2.2.4 Annual average

Annual averages are often reported as calendar year (January-December) averages, as defined in NEPM(AAQ). However, CVO adopts the convention of reporting the annual average by financial year (July-June).

As summer tends to be the season when higher PM_{10} and $PM_{2.5}$ 24-hour averages are recorded, it would be appropriate to report the annual average against the financial year so a full summer season is included in each annual average period.

Jacobs calculated both the calendar year (January-December) and financial year (July-June) annual average PM_{10} concentrations measured at the CVO AQMS sites by TEOM or BAM method from the supplied 24-hour average concentration data. For the 2022 years, where monitoring was changed from TEOM to BAM part way through the year, monitoring from both methods was combined to calculate the annual average, with BAM data preferred over TEOM if there was data available with both methods.

PM_{10}

The annual average PM_{10} concentrations calculated by Jacobs are shown in Figure 3-16 for the calendar years 2015-2022, and Figure 3-17 for the financial years 2016-2023.

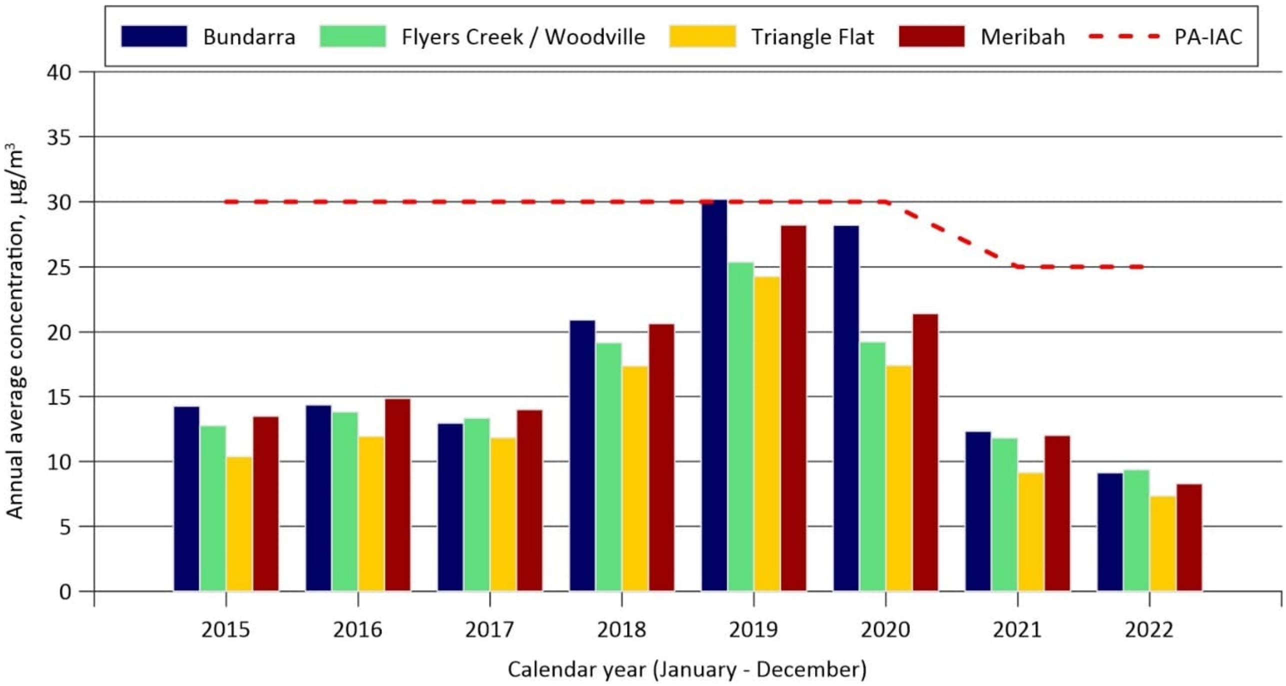

Figure 3-16. Annual average PM_{10} concentrations calculated by Jacobs, calendar year basis.

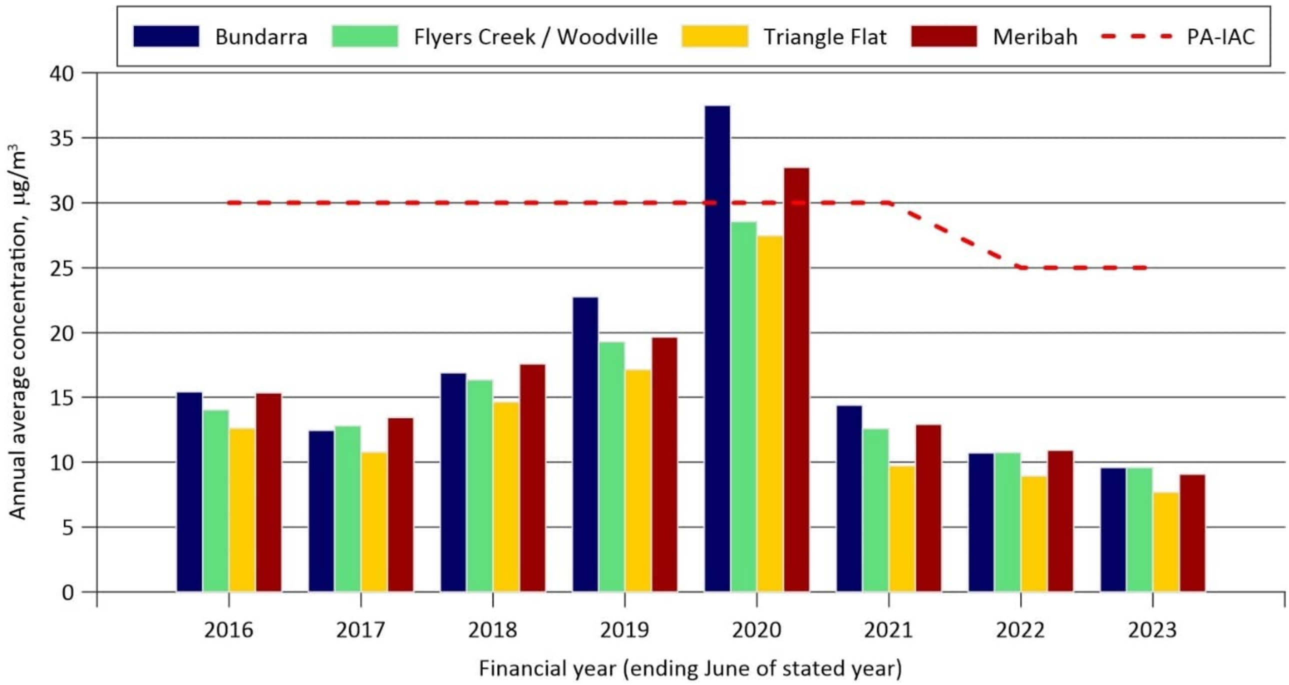

Figure 3-17. Annual average PM_{10} concentrations calculated by Jacobs, financial year basis.

The financial year annual averages for PM_{10} are also presented as graphs and tabulated values in the AEMRs. Figure 3-17 can be compared to Figure 8-5 of AEMR 2023 which is reproduced in Plate 3-1. It is apparent that the averages calculated by Jacobs are the same or very similar for the years ending June 2016, 2017, 2018, 2019, 2021 and 2023. However, the averages do not match for the years ending June 2020 and 2022, with the averages calculated by Jacobs being higher than the averages shown in the AEMR.

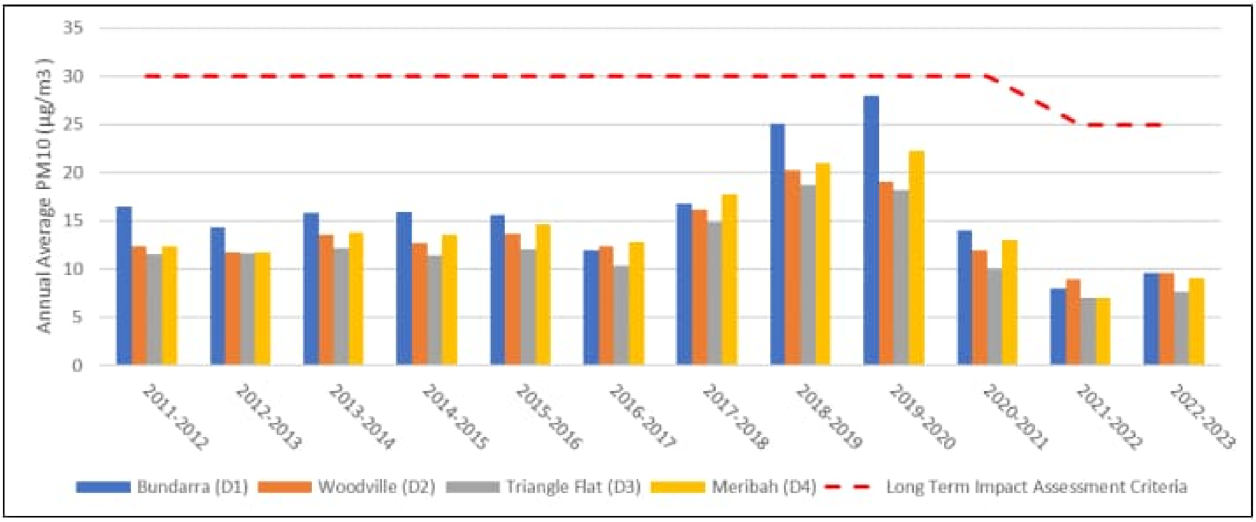

Plate 3-1. Annual average PM_{10} concentrations reported in AEMR 2023 Figure 8-5.

AEMR 2023 states that elevated annual averages for the 2018-19 and 2019-20 reporting period were a result of unprecedented bushfire seasons, regional dust storms, severe drought conditions and emissions from Cadia following the cessation of deposition into the NTSF and STSF. In the AEMRs for 2020 and 2021, the annual average concentrations presented were labelled as “after correction for bushfires/dust storms” although the means of filtering bushfire or dust storm-affected data was not explained. This is likely to explain the difference in 2020 between the annual average calculated by Jacobs versus that shown in Plate 3-1.

For transparency in data handling and reporting, it is recommended that each AEMR should clearly state that such events have been removed from the dataset, including an explanation for and list of the dates that were excluded.

For the year ending June 2022, the annual averages are low overall however the values calculated by Jacobs are higher than those in the AEMRs. It is not apparent whether any adjustments for extraordinary events were deemed necessary for this year, or whether the difference arises from the way the change in monitoring method during the year was handling in the calculation of annual average.

$PM_{2.5}$

$PM_{2.5}$ annual averages could only be calculated for the financial year ending June 2023 because $PM_{2.5}$ concentrations only started to be recorded in April 2022, meaning insufficient data was available to calculate any calendar year annual averages. Jacobs' calculated annual average $PM_{2.5}$ concentrations for 2023 agree with those published in AEMR 2023 and are shown in Figure 3-18.

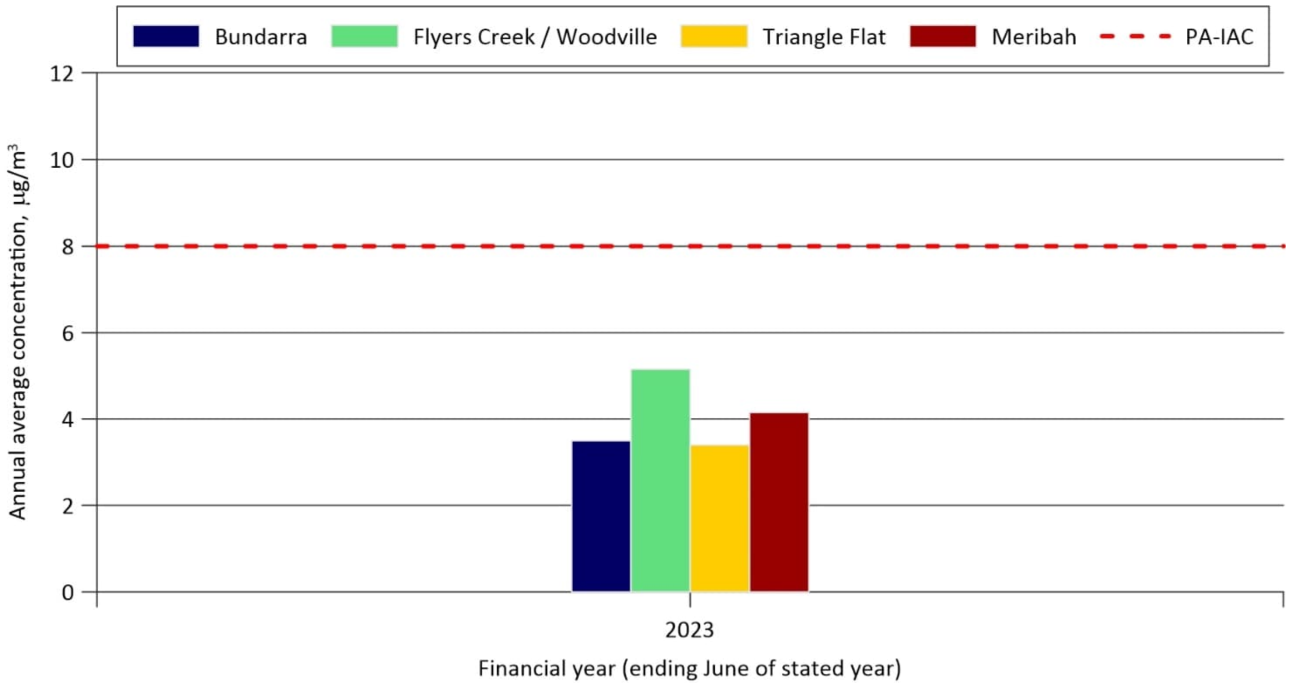

Figure 3-18. Annual average $PM_{2.5}$ concentrations calculated by Jacobs, financial year basis.

3.3.3 NSW Government monitoring

The NEPM(AAQ) requires the NSW Government to report annually on compliance with the national standards and goals for air quality measured at designated monitoring stations, to assess the exposure of the general population to air pollution. NSW Government monitors ambient air quality in Orange and Bathurst as part of its compliance monitoring network. Both sites comply with the siting and exposure criteria specified in the NEPM(AAQ) (NSW Government, 2023).

The NSW NEPM(AAQ) Compliance Monitoring Network is designed to measure air quality experienced by the general population and to capture pollution events which impact population centres. This means that the location of monitoring stations in each region is selected to optimise both population coverage and representation of the occurrences of higher pollutant concentrations. NSW Government (2023) notes that these stations represent the air quality considered typical for the urban areas of Orange and Bathurst, and not necessarily the broader air quality region.

The two monitoring stations are located at the same place as the meteorological monitoring sites introduced in Section 3.2.4. Air quality in these urban locations is expected to record higher concentrations of PM_{10} and $PM_{2.5}$ than in rural areas due to the surrounding density of homes with fuel-burning home heating and vehicle emissions from local roads, particularly in winter months.

Whilst these two sites are not expected to provide reliable background air quality data for the rural area around Cadia, they can be used to indicate when large-scale air quality events such as dust storms or forest fire smoke occur.

Hourly-averaged PM_{10} and $PM_{2.5}$ concentration data from the Orange and Bathurst AQMS was downloaded from the NSW Government data portal[11]. PM_{10} monitoring has been conducted at Bathurst for more than ten years, with $PM_{2.5}$ monitoring added from April 2016. At Orange, both PM_{10} and $PM_{2.5}$ have been monitored since January 2019.

Figure 3-19 shows 24-hour average concentrations of PM_{10} measured at Bathurst and Orange from 18 January 2019 to 31 December 2022, and Figure 3-20 shows the $PM_{2.5}$ concentrations. The influence of drought conditions and bushfires in the summer of 2019-2020 is clearly evident from the high concentrations measured over that period. The early months of 2019 also exhibit higher than normal ambient air quality concentrations. Mid-winter elevated concentrations of PM_{10} and $PM_{2.5}$ are also a feature of the winter months, particularly in Orange.

[11] https://www.dpie.nsw.gov.au/air-quality/air-quality-data-services/data-download-facility

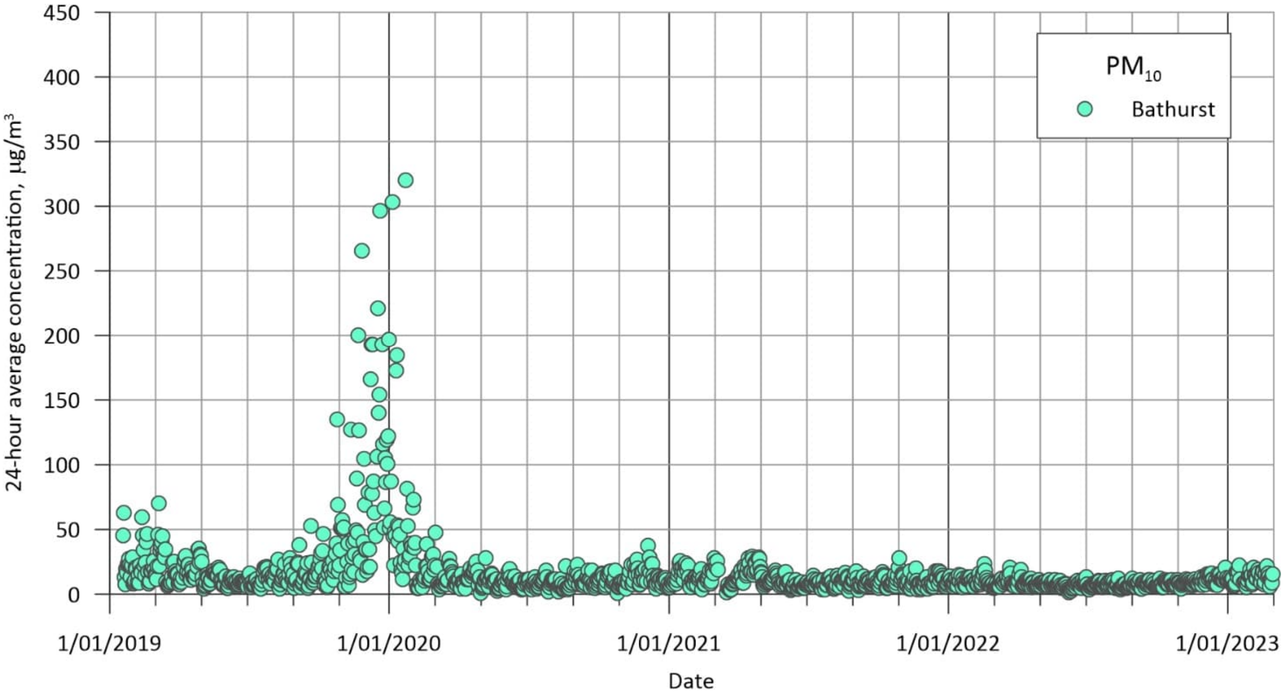

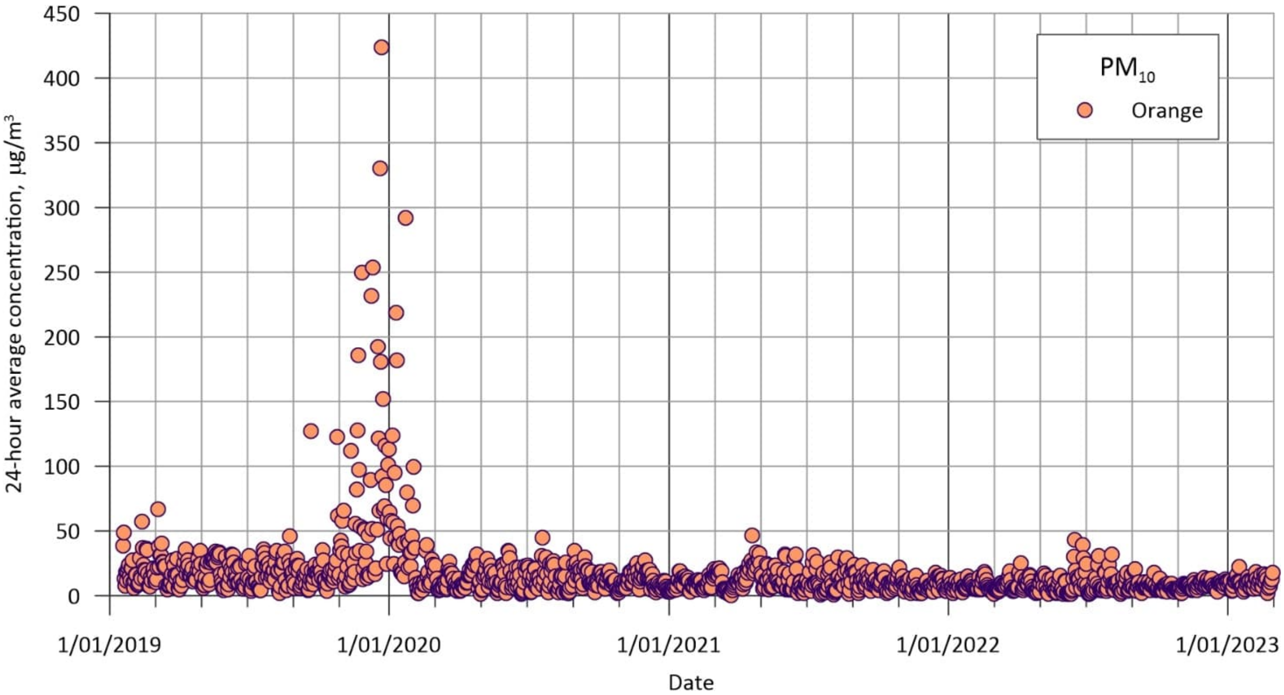

Figure 3-19. 24-hour average concentrations of PM_{10} measured at Bathurst (top) and Orange (bottom) by NSW Government.

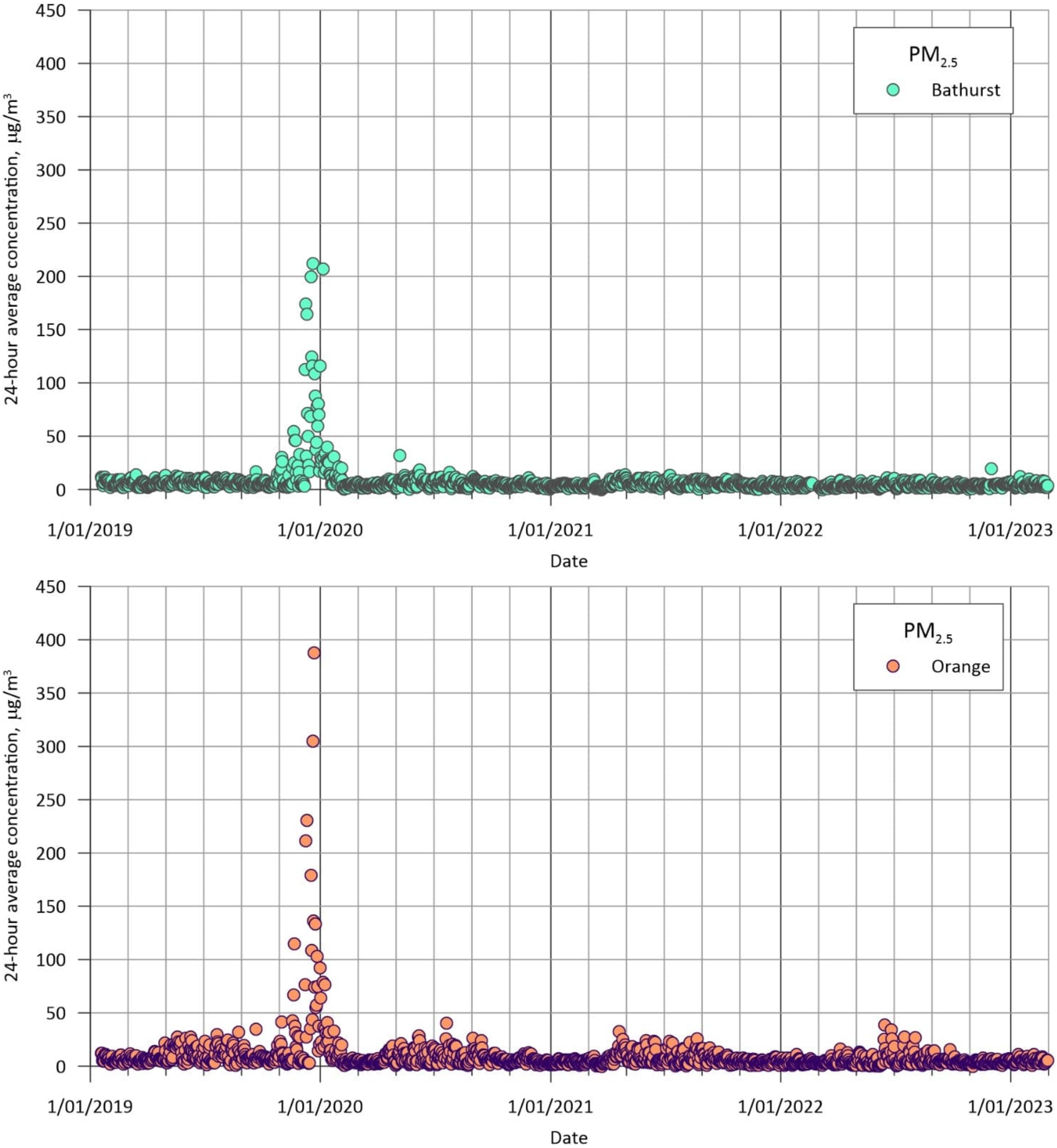

Figure 3-20. 24-hour average concentrations of $PM_{2.5}$ measured at Bathurst (top) and Orange (bottom) by NSW Government.

3.3.4 Dust deposition gauges

3.3.4.1 Monitoring locations and data availability

Forty or more sites have been used by CVO for DDGs since 1994. Eight gauges are currently in operation around the Cadia mine site (DG9A, DG5A, DG12A, DG15A, DG17, DG18, DG19, DG29A)[12]; and three gauges around the CVO dewatering site in Blayney (DG06, DG08, and DG09). The monitoring results from the DDGs in Blayney are not relevant to this report.

The locations of the DDGs around the Cadia mine site are shown in Figure 3-3. Cadia (2018) notes that the location of DG12A does not meet all of the criteria associated with Australian Standard /New Zealand Standard AS-NZS 3580.1.1.2007[13] for the location of monitoring equipment. It is not stated whether this means that this site has the potential to understate or overstate deposition rates.

The material collected in the dust deposition gauges is analysed for a range of components including total solids, total solubles, total insolubles, ash, and combustible matter. Heavy metals are also analysed, with only copper measured until July 2019 when a wider suite of heavy metals started to be tested on a routine basis.

Cadia (2018) and the AEMRs state that to determine the mine contribution of generated dust, CVO assesses compliance the ash content fraction of the measured insoluble solids. AEMR 2016 explains this stating that "*Combustible matter is the portion of the insoluble matter lost during combustion and the ash content is the material left after combustion. Due to the nature of the site operations, the handling of material (such as the removal and transportation of topsoil and overburden) is expected to be the largest contributor to deposited dust emissions. The ash content is an indication of the mineral content of the dust (often soil or rock particles) and is considered to be an accurate representation of dust deposition from Cadia's mining activities. The proportion of combustible matter indicates the amount of organic matter (such as insects, vegetation and algae) collected in the gauge and is not considered a meaningful measurement of dust contributions from Cadia*".

Therefore, only the ash content fraction is reported in the AEMRs for assessing compliance with the deposition criteria (for example, Table 6-6 of AEMR 2022, and Table 4.1 of Appendix 1 to AEMR 2023). This approach seems reasonable, based on the explanation above.

Jacobs also notes that the study reported in Serinus (2021) found that surface materials eroded from the TSFs may present as soluble solids in the DDGs (see Section 3.3.6.1), and therefore there may be some relevance in assessing soluble solids as well. However, it is unlikely that useful information for understanding impacts from the TSFs would be gained from this due to the long averaging period of one month necessary for deposition monitoring compared to the relatively short dust event durations (of a few hours) attributed to wind erosion from the TSFs.

Data that was provided to Jacobs by CVO includes the following for each DDG:

1. July 2014 – June 2017
    a. Ash, combustible matter, insoluble solids, soluble solids, and copper.
2. July 2017 – June 2019
    a. Monthly values for ash and total insoluble.
    b. No data for combustible matter, soluble solids, or copper.

[12] These eight locations are specified in the EPL.

[13] This standard was updated in 2016.

3. July 2019 – May 2023
    a. Ash, combustible matter, insoluble solids, soluble solids, copper.
    b. Additional heavy metals data for aluminium, antimony, arsenic, barium, beryllium, boron, cadmium, chromium, cobalt, iron, lead, manganese, mercury, molybdenum, nickel, selenium, silver, tin, uranium, zinc.
    c. Ash and insoluble solids data only for February 2020 and November 2020 (no heavy metals data).
    d. No heavy metals data except copper for March – April 2020, June – October 2020, December 2020 – February 2021, and April-July 2021.

3.3.4.2 Data relevance

The risk of amenity impacts from settling dust is traditionally assessed using dust deposition criteria expressed as the mass of dust settling over a unit area over a period of 30 days. However, problems with using monthly-averaged criteria for dust deposition are now widely recognised. The traditional dust deposition measurement methods require a long averaging period of a month so that experimental error in the test data is minimized, no reliable dust deposition measurement methods are available for shorter term measurements, and samples are easily compromised as discussed in the paragraph above. Whilst assessment of dust deposition against the monthly or annual average criteria provides evidence of long term trends in dust deposition, the data is available too slowly to be used as a reactive management tool. In addition, dust deposition can cause amenity impacts over much shorter timeframes than a month, even over a matter of hours, during events when elevated levels of TSP are emitted (such as high wind speeds).

The use of DDG data to validate a dispersion model is also fraught with uncertainty due to the emission rate assumptions that are necessary for dust emitting sources (as discussed in Section 0) and the need for site-specific particle size distribution in the suspended dust mass so that particle settling rates can be simulated (as discussed in Section 5.6).

3.3.4.3 Data analysis

The DDG data is reviewed annually and reported in the AEMRs. The contribution to deposited dust that is from the Cadia mine is calculated from the measured ash content minus a background deposition value. The method of determining the background deposition for any given month is described in multiple references including Appendix 7 of AEMR 2020, Appendix 1 of AEMR 2021 and Appendix 1 of AEMR 2023 as follows (paraphrased): "*The background deposition is taken to be the average level recorded by the monitors in the network which were upwind of CVO for more than 80% of the time during each monthly sampling period. The hourly wind direction data from the Cadia Valley Operations on-site weather station were used to calculate the period during which this occurred and would account for the range of different wind conditions experienced*". The explanation does not state which wind directions are considered to be "upwind of CVO" for each DDG site.

Due to the comprehensive analysis of the ash content and insoluble solids deposition results in the AEMRs and the TAS Reports, and the limited value of the DDG data to this report, Jacobs has not prepared an independent analysis of the ash content and insoluble solids deposition data. However, those reports do not routinely report heavy metals results, and therefore Jacobs has conducted a preliminary review of the heavy metal data.

Since heavy metal deposition results started to be reported in July 2019, most of the heavy metal results have returned concentrations less than or close to the limit of detection, with the exception of aluminium, copper, iron, manganese, and zinc. Of these, aluminium, iron, manganese and zinc are common elements in the earth's crust and the presence of these elements in the samples is expected. However, the solid particles containing elevated concentrations of copper could have originated from the Cadia mine site. Therefore, in this report heavy metal data is displayed only for copper. The monitoring results for all eight DDGs around the Cadia mine are shown in Figure 3-21 for the period July 2016 to May 2023, with a closer view of the data post July-2019 shown in Figure 3-22. Copper deposition rates appear to have been increasing over 2016-2017, but have reported lower deposition rates consistently since July 2019. There is no data available for July 2017 - June 2019. From Figure 3-22, in recent years the highest copper deposition rates tend to be reported from DDGs 9A, 12A and 18, which are all on the east side of the mine and relatively close to the mine dust sources.

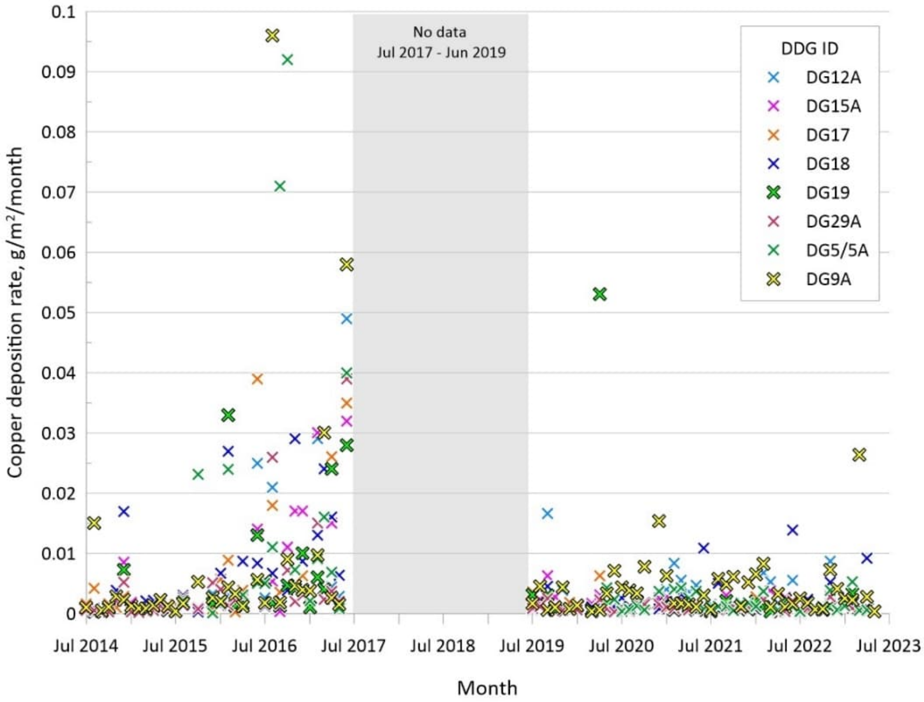

Figure 3-21. Copper deposition results from DDGs, July 2014 – May 2023.

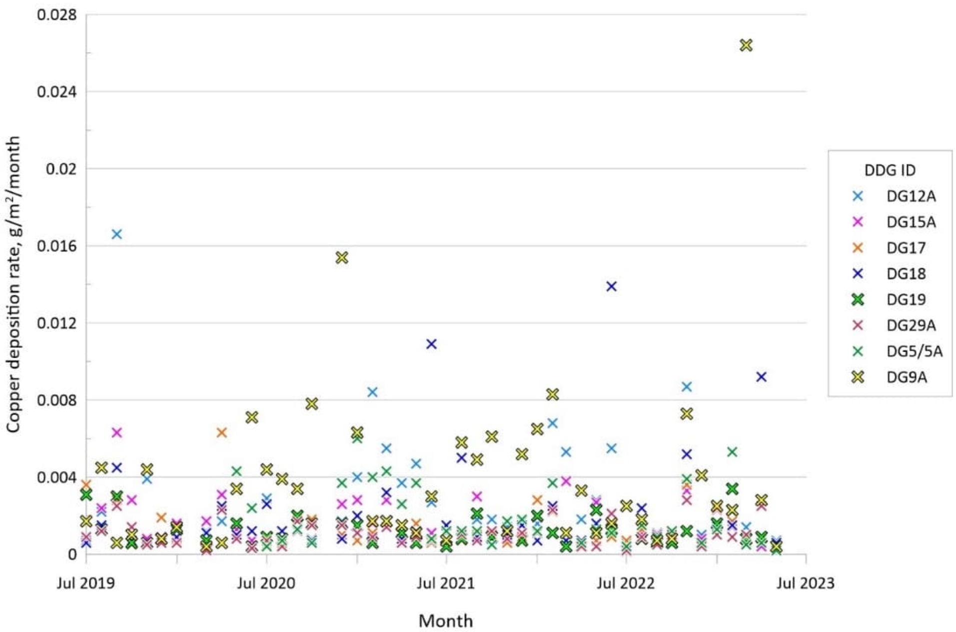

Figure 3-22. Copper deposition results from DDGs, July 2019 – May 2023.

3.3.5 Other test methods

3.3.5.1 HVAS

Newcrest (2023b) states that Cadia commenced sampling for TSP with HVAS equipment in April 2020. Newcrest (2023a) states that the HVAS "*measures and analyses Total Suspended Particulate Matter (TSP) in accordance with the guidelines specified in AS3580.9.3 Methods for the Sampling and Analysis of Ambient Air – Determination of Suspended Particular Matter – Total Suspended Particulate Matter (TSP) – High Volume Air Sampler Gravimetric Method*." These HVAS samplers are used in strategic locations in the monitoring network and are also able to collect sufficient material suitable for metals analysis over a 24-hour period (TAS, 2023a).

The HVAS data is not reported on the CVO website and in the monthly air quality monitoring reports by Advitech, nor is it reported in the AEMRs. Some heavy metals concentration data from the HVAS was provided by CVO for the preparation of this report, however the data was in the form of raw laboratory analyses, provided no sample locations, contained dates that did not match with the reported data in Serinus (2021), and was not able to be converted to meaningful ambient air quality results.

HVAS data from 2020 is tabulated in Serinus (2021), which reports 24-hour average PM_{10} (not TSP) and 19 heavy metal species at Bundarra, Flyers Creek, Triangle Flat, and Meribah. The samples were collected approximately fortnightly over the 2020 period.

HVAS data is analysed in TAS (2023) for the period January 2022 to February 2023. Graphs of PM_{10} concentrations and heavy metal concentrations for aluminium, barium, chromium, copper, lead, manganese, and zinc are provided in the report. TAS (2023) states that most of the other sampled metals; antimony, arsenic, beryllium, cadmium, cobalt, mercury, molybdenum, nickel, selenium, silver and tin were below the detection limit or only had a few samples near detectable levels, which is consistent with the findings from the DDGs (see Section 3.3.4.3).

It is not clear whether the HVAS measures only PM_{10} concentrations and the heavy metals in the PM_{10} fraction, or all TSP. However, Zephyr (2022) states that a HVAS monitor measuring TSP every six days was sighted at Meribah during the site visit.

TAS (2023) concludes that the average recorded PM_{10} and metal concentrations at each monitor were generally similar over the monitoring period, and that in general the recorded, detectable metal concentrations were found to be low compared to relevant assessment criteria. No comparison of PM_{10} or TSP concentrations from the HVAS instrument compared to the TEOM and BAM instruments is provided, but could be helpful to validate the assumption that PM_{10} is 39.1% of TSP (as per Section 3.3.1) and to inform ambient heavy metal concentrations.

3.3.5.2 LVAS

Serinus (2021) states that CVO acquired LVAS equipment, primarily to conduct monitoring for respirable crystalline silica. Discussion of respirable crystalline silica potential impacts is outside the scope of this report. However, since this monitoring involved collection of $PM_{2.5}$ samples, $PM_{2.5}$ particulate matter concentrations were also determined. Several LVAS samples were collected at Bundarra and Woodville over the period July -December 2020, over durations ranging from 24 hours to 1009 hours. Serinus (2021) also mentions collection of PM_4 samples by the LVAS, although it is not clear if this data was used for the assessment.

TAS (2020c) recommended the ongoing use of LVAS monitoring, co-located at two of the AQMS. Jacobs is not aware of whether this recommendation was implemented, as LVAS data is not reported on the CVO website and in the monthly air quality monitoring reports by Advitech, nor is it reported in the AEMRs. In addition, TAS (2023a) does not discuss nor analyse any LVAS data. However, Zephyr (2022) states that a LVAS monitor measuring PM_{10} (not $PM_{2.5}$) every six days was sighted at Meribah during the site visit.

3.3.5.3 DustTrak

Zephyr (2022) states that a DustTrak monitor measuring PM_{10} and $PM_{2.5}$ continously was sighted at Meribah during the site visit. DustTrak data is not reported on the CVO website and in the monthly air quality monitoring reports by Advitech, nor is it reported in the AEMRs. No information is available to Jacobs regarding how many DustTrak monitors are used, where these locations are, and what parameters are measured.

3.3.6 Other ambient air quality studies

3.3.6.1 Serinus (2021)

The study reported in Serinus (2021) was an environmental health assessment of the tailings dust to address community concerns about not fully understanding what is in the dust and what potential impacts the dust could have on community health and agricultural enterprises. Observations and conclusions from the study that may be relevant to this report include:

- Based on the data and information available and the ambient dust levels measured by the study, there is no current evidence to suggest that dust from the CVO tailings storage facilities or emissions from the mine ventilation system pose a health risk to the community.
- Metal concentrations in the tailings material were found to be very low, except for aluminium as aluminosilicate and iron, as iron-sulphur compounds.
- Secondary minerals are the most likely tailings component to become airborne, due to their location at the surface of the tailings storage facility and comparatively low density. They are expected to be the first to be mobilised as dust and/or travel the furthest if they become airborne during windy conditions. After deposition, they are also the most likely minerals to subsequently dissolve upon contact with water due to their high solubility.
- Approximately 10 to 20 wt% of deposited dust reporting to DDGs was in a soluble form, consistent with a theory that highly soluble efflorescent (surface) materials from the tailings would be the most likely to be mobilised as dust in windy conditions and travel the furthest. This suggests, at least to some extent, that deposited dust is influenced by tailings dust.

3.3.6.2 ANSTO (2023)

ANSTO (2023) reports on Stage 2 of a study undertaken by ANSTO to sample and characterise fine particulate matter ($PM_{2.5}$) for a 24-hour period twice each week at four sampling sites (selected in Stage 1) around Cadia Valley Operation (CVO) mine for a 12-month period from February 2022 to February 2023. Jacobs does not have access to the Stage 1 report.

The four monitoring sites were identified as Millthorpe, Mandurama, Panuara and Orange. With the exception of the Panuara site, the sites are all 8-16 km from the mine.

Sampling at each site was conducted for 24-hours each Sunday and Wednesday, therefore the monitoring covers two days out of every seven over the monitoring period. Each sample was analysed for $PM_{2.5}$ mass, black carbon, and the concentration of 23 chemical species that could be used to determine the likely source of particulate matter in the samples using a method known as “fingerprinting”.

Observations and conclusions from the study that may be relevant to this report include:

- The Panuara site was specifically chosen in Stage 1 for its proximity to the CVO mine to potentially collect a larger amount of CVO mine-related $PM_{2.5}$ mass during sampling – which was not observed in the results.
- "Soil" fingerprints, generally driven by key elements aluminium, silica, titanium, calcium and iron, represent soils blown in by dust storms, from agricultural or mining activities, or from retrained road dusts. The "soil" fingerprint was taken to represent the potential mine contribution to $PM_{2.5}$ in each sample.
- The analysis showed that the "soil" fingerprint was not the highest fingerprint contribution at any of the sites, and that overall the "soil" source contribution to the $PM_{2.5}$ mass was quite low. Only the "soil" fingerprints showed directionality towards the CVO mine when plotted with wind direction.
- Wind back-trajectory intersection analysis found no consistent pattern of elevated "soil" source days related to the mine location.

Overall, Jacobs concludes from this study that at the measured locations and based on the "two days in seven" sampling regime, $PM_{2.5}$ air quality appears to be good, and there is no strong evidence that contributions from the mine to $PM_{2.5}$ are higher than background, although it is possible that soil percentages and salts are higher nearer to the CVO site.

3.4 Complaints and dust incidents

Table 3-2 lists the TSF-related dust complaints for the calendar year 2022 and the first half of 2023, recorded in the AEMRs for 2022 and 2023. Dust lift-off events from 2022 are further assessed in Section 6.2.2.

Table 3-2. Summary of TSF Dust complaints in January – December 2022, from AEMR (2022) and (2023).

Date	Summary	Description provided in AEMR
5/1/22	Local residents reported dust lift-off from the Tailings Storage Facilities.	The incident was investigated by the Surface Operations team. Tailings dust lift-off was identified as coming from sections of the NTSF during a high wind event during the morning ahead of wet weather. The panther was operational, and all available water carts were working in the area.
1/3/22	Local residents reported dust lift-off from the Tailings Storage Facilities	The incident was reported to the Surface Operations team, who advised that there was tailings dust lift-off and they were actively managing it through water carts and spot spraying.
19/4/22	Several landowners raised concerns over dust from the tailings dam	The complaints were made regarding dust lifting from the Northern Tailings Storage Facility (NTSF) at approximately 10:00 am. Cadia had mobilised the panther at approximately 6.30 am as part of routine operations and prior to any dust lift-off. In accordance with normal procedure, the surface operations supervisor continued inspections of the area between 7:00 am and 7:30 am and noted no dust lift-off. At around 8:00 am, crews noticed dust starting to lift on the NTSF and the panther was re-deployed to target areas of concern. Wind speed at this time was approximately 43km/hr. By 1:00 pm, Cadia received reports that the dust had begun to significantly subside. Communication was provided to landholders.
13/10/22	Six residents contacted Cadia regarding	A formal response was provided on the steps undertaken to mitigate dust lift off, including deploying all available water carts, and recommissioning the panther following a break down.

	dust lifting from the TSFs.	
31/10/22	Several complaints from residents in the Errowanbang area relating to visible dust seen from the tailings dams.	Assessment of environmental monitoring sites outside the lease did not record any elevated dust readings of PM_{10} or $PM_{2.5}$.
3/11/22 (complaint was made on 5/11/22)	A resident from Forest Reefs, via phone, reported a dust complaint.	As the complaint was recorded after the fact, a visual assessment could not be completed. A review of environmental data showed that there were no elevated dust readings of PM_{10} or $PM_{2.5}$ at the time of the reported dust.
12/11/22	Three complaints were received via text message from residents in the Errowanbang area relating to dust from the TSF before major rain.	Dust was being actively managed during this time at site and the increased wind was at the front of a storm. Rain then developed about 30 minutes later and there was no further dust.
6/01/23 (2 complaints)	Two residents reported visible dust from the TSF	Complaints were acknowledged, and a formal response was provided advising of the dust mitigation efforts in the week leading up to the concern, and the direct actions taken.
11/01/23 (2 complaints)	Two local residents reported lift off of dust from the STSF	Complaints were acknowledged, and a formal response was provided advising of the dust mitigation efforts in the week leading up to the concern, and the direct actions taken.
12/01/23	A local resident reported lift-off of dust from the STSF	A formal response was provided advising of the dust mitigation efforts in the week leading up to the concern, and the direct actions taken.
5/03/23	A local resident reported lift-off of dust from the TSF	At the time of the complaint, all water carts and dust suppression equipment (Panther) were working.
12/03/23	A local resident reported lift-off of dust from the TSF	At the time of the complaint, all water carts and dust suppression equipment (Panther) were working.

20/03/23 (5 complaints)	A local resident reported lift-off of dust from the TSF	At the time of the complaint, all water carts and dust suppression equipment (Panther) were working.
28/04/23	A local resident reported lift-off of dust from the TSF	At the time of the complaint, all water carts and dust suppression equipment (Panther) were working.

Jacobs reviewed the hourly-average wind speeds measured at SLB and Ridgeway AWS on the dates listed in Table 3-2 where complaints of dust lift-off from the TSFs were reported. Dust lift-off events that generated complaints about dust from the TSFs generally occurred on days when wind speeds exceeded about 8 m/s as an hourly average in this period.

4. Emissions Inventory

4.1 The importance of the emission inventory

The complexity of dispersion models varies greatly from one project to the next depending on the number of different sources to consider. In the case of a power station for example, there might only be one stack source to consider. However, in the case of a mine site there are many different sources of particle emissions to account for. Sources of dust emissions from CVO include the following activities:

- Surface stockpiles
- Ore processing and crushing
- Bulldozer and grader operations
- Loading and handling of ore, waste rock, and construction materials
- Vent emissions from underground mining
- Dust generated by the wheels of vehicles travelling on haul roads and unsealed surfaces (collectively referred to as "vehicle-tracked dust").
- Wind erosion from Tailings Storage Facilities (TSFs) and other exposed surfaces including stockpiles and roads.

The collective list of these sources and the emission rates allocated to each source is called the "emissions inventory".

In a dispersion model, downwind concentrations predicted to be caused by an individual source vary in direct proportion with the emission rate – so if the emission rate from a source (such as ore crushing) is doubled, the downwind concentrations due to that source will also double. However, when a dispersion model has many sources, the combined effect of all the sources might mean that some sources emit a lot more particles than others, so some sources are relatively inconsequential to the overall concentrations outside the mine boundary. Other sources may be relatively dominant, and the model is said to be sensitive to those inputs.

Emission factor publications are published references which define typical dust emission rates from different types of mining activities as a function of the intensity of the activity and source-specific variables (such as how many tonnes of ore are handled by a conveyor per hour, or what the average silt content is of an unsealed road that a haul truck travels on).

For any mining operation, a large number of input variables are needed to define the emission factors (EFs) and build the emission inventory. Some of these input variables can be easily quantified, and others require assumptions. Any air quality assessment report that relies on an emission inventory for dispersion modelling should clearly define all inputs for developing that emission inventory, and identify any assumptions that the model may be sensitive to.

The dust sources at CVO and the emission factors relevant to each source are discussed in further detail in the following sections, along with a review of the input variables adopted in the TAS Reports.

4.2 Vent Monitoring

4.2.1 Available monitoring data

Monitoring of air flows and particle emissions from the vents is conducted by Ektimo. The test reports summarized in Table 4-1 were available to Jacobs. In addition to the pollutants measured, each test also reported flow conditions in the vents, including volumetric flow rates and gas temperature.

Table 4-1. Summary of Ektimo vent test reports provided to Jacobs

Report number	Date of testing	Vents included in testing	Pollutants reported
R011403a2	3-5 Nov 2021	VR5, VR8	Solid particles (total) PM_{10}, $PM_{2.5}$ Other particle sizes
R012219 [draft]	28 Feb – 3 Mar 2022	VR3A, VR5, VR7, VR8	Solid particles (total) PM_{10}, $PM_{2.5}$ Heavy metals Diesel particulate matter Crystalline silica
R015051r	24-25 May 2023	VR8	Solid particles (total) PM_{10}, $PM_{2.5}$ Heavy metals
R014793	28 Jun 2023	VR8	Solid particles (total) PM_{10}, $PM_{2.5}$ Heavy metals
R015420	10 Jul 2023	VR8	Solid particles (total) Heavy metals
R015421	21 Jul 2023	VR8	Solid particles (total) Heavy metals
R015453	1 Aug 2023	VR8	Solid particles (total) Heavy metals
R015549a [draft]	15 Aug 2023	VR8	Solid particles (total) Heavy metals
R015630p [preliminary]	29 Aug 2023	VR8	Solid particles (total)

4.2.2 Discharge characteristics

The dispersion of pollutants discharged from a stack can be sensitive to several characteristics of the discharge, including:

- Stack height
- Plume exit velocity
- Direction of exhaust flow (although in this case, all vents discharge vertically into the air)
- Temperature of exhaust air
- Whether building downwash is incorporated.

TAS (2023a) provides a summary of the discharge parameters, including the information in Plate 4-1, stating that these parameters were based on the most recent measurements conducted by Ektimo at the time of the modelling[14]. TAS (2023a) does not state whether building downwash is incorporated for VR8, and if so what input parameters were used to establish the downwash settings in the model.

Parameter	VR3A	VR5	VR7	VR8
Height (m)	5.6	5.6	5.6	15
Diameter (m)	5.0	5.4	6.2	10.2
Temperature (ºC)	23.3	24.5	23.5	22.5

Plate 4-1. Discharge characteristics for vent emissions stated in Table 5-3 of TAS (2023).

TAS modelled the emission from VR8 as one combined discharge point, rather than three individual vents. Combining multiple discharge points into one stack for the model inputs can reduce model running time, and will often have no more than a minor impact on the model results. However, it is necessary to maintain the same efflux velocity by setting the single stack to have a diameter which represents the same cross-sectional area as the areas of the stacks which are represented. In addition, a preliminary model run comparing separate stacks with a combined stack should be conducted to check that the model is not sensitive to combining the discharges.

In TAS (2023), the diameter of the combined VR8 stack is stated to be 10.2 m. This is a larger stack than would be calculated for the three individual vents, noting that the vents are square with side length of 4.7 m which gives a cross-sectional area for each vent of 22.09 m^2 or an equivalent diameter of 5.3 m per vent. The combined vent with the same cross-sectional area would have an equivalent diameter of 9.2 m, which is smaller than the diameter of 10.2 m stated in TAS (2023). The model results may be sensitive to this setting.

In TAS (2023), the flow rate from each vent was varied in accordance with the charts shown in Plate 4-2. The report does not state whether these are actual flow rates or flow rates referenced to standard conditions (dry gas, 0°C temperature and 1atm pressure). In this report Jacobs will use the convention Sm^3 to refer to a volume that has been corrected to standard conditions, and Am^3 to refer to a volume at operating conditions.

Jacobs does not have access to the data used to generate the charts shown in Plate 4-2, and therefore cannot replicate the hourly varying emission profile that was used by TAS (2023a). This data was requested from CPHL. In response, TAS (2023b) explained the source of the ventilation data, stating that "*this was provided to TAS by the mine. TAS understands that the data was not collected by direct measurement of flow rates and was not determined based on operating conditions … rather the flow rates were determined based on measured operational motor power consumption*" and "*there is no certain way to determine which or how many of the three ducts were operating at any one time, or at what flow rates and velocities the individual ducts were operating*".

[14] From the Ektimo report number R012219 referenced in TAS (2023); this is the Ektimo testing over 28 February – 2 March 2022.

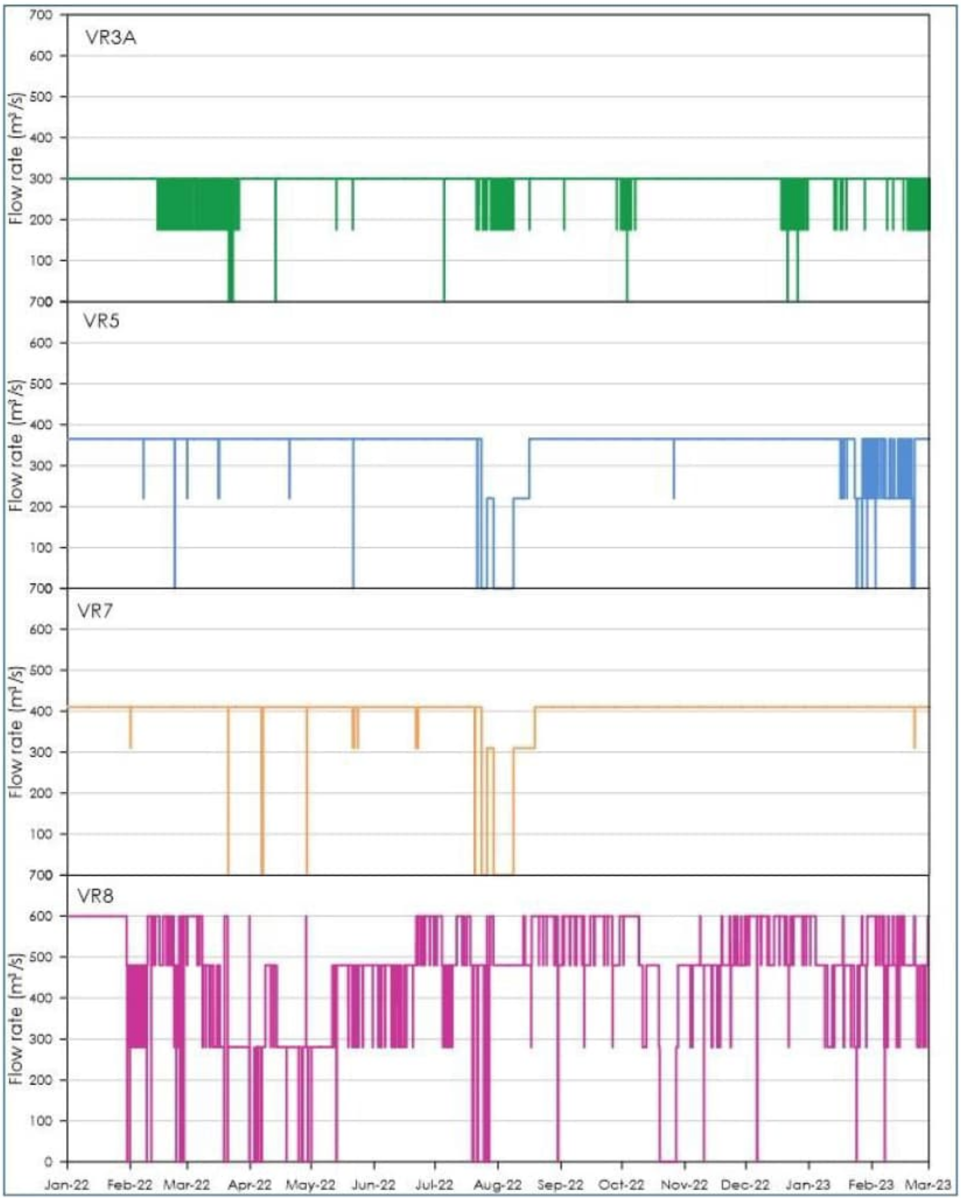

Plate 4-2. Modelled ventilation rates adopted for ventilation shafts shown in Figure 5-4 of TAS (2023).

From Plate 4-2, the vents appear to operate in step-change fashion between a range of setpoints – for VR8 for example these appear to be 280 m^3/s, 480 m^3/s and 600 m^3/s. If the flows in Plate 4-2 are referenced to standard gas conditions, then the setpoint of 480 Sm^3/s corresponds with the flow regime that was measured throughout the Ektimo testing in July – August 2023[15], where the operational status in each report is stated to be operation of two fans from VR8, with Fan 2 at 70-75% and Fan 3 at 80-81% with a total flow rate of 460-490 (average 478) Sm^3/s.

[15] Ektimo reports for testing on 10/7/23, 21/7/23, 1/8/23, and 15/8/23.

The following options are recommended for dispersion sensitivity testing:

1. Start by modelling a "base case" – stack arrangement and emission rates as TAS (2023a).
2. Sensitivity to vent dimensions for VR8
    a. Compare one combined vent at 10.2m (as TAS 2023a) with using two vents each discharging 50% of the flow.
3. Sensitivity to assumed discharge temperature:
    a. Compare dispersion from VR3A, VR5, VR7 and VR8 (as two vents) at TAS (2023a) input temperatures (base case), versus 290K.
4. Compare dispersion without building downwash (base case) with included building downwash:
    a. For VR8, using the following dimensions inferred from Figure 4-1:
        i. Height of horizontal vent – 5.4m.
        ii. Height of fan shed – 7.8m.
        iii. As these vents are very large, the vents should also be included as downwash elements.
    b. For VR3A, VR5 and VR7.
        i. For these vents, there are no buildings or structures close to the vents that could influence dispersion except for the vents themselves. As these vents are very large, the vents should be included as downwash elements.

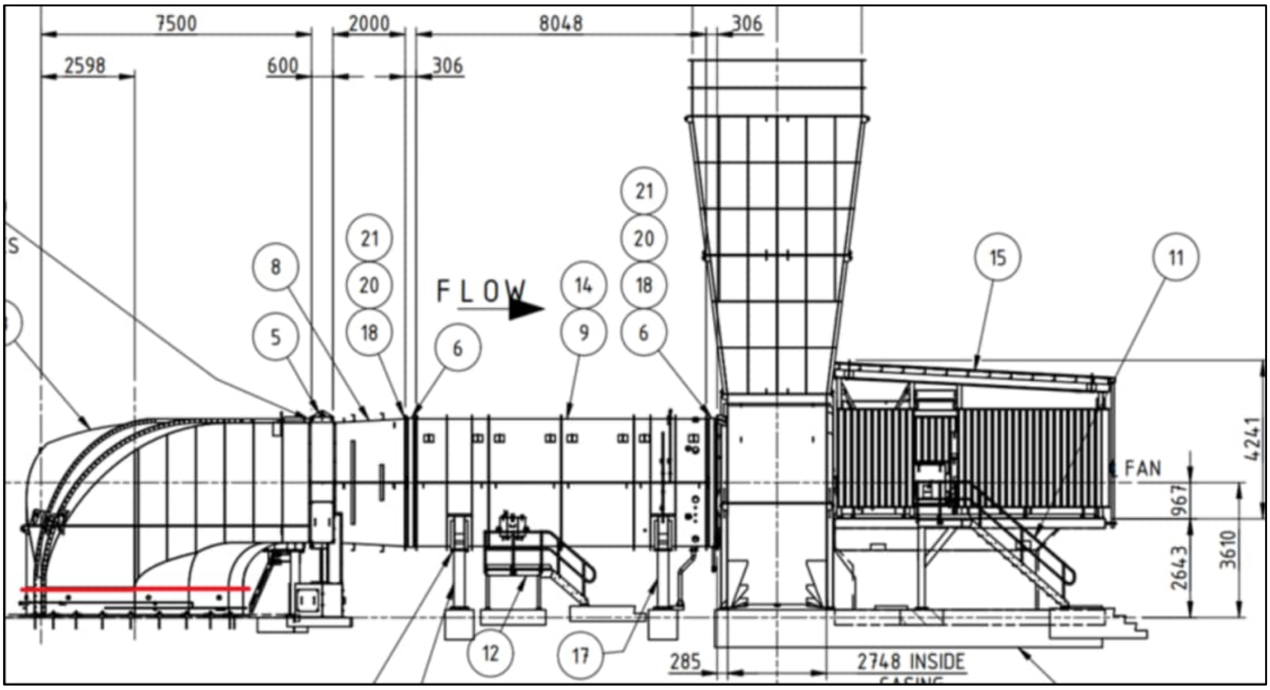

Figure 4-1. Dimensions of each surface fan infrastructure, VR8. From Ektimo (2022). Red line indicates the sampling plane for Ektimo testing.

4.2.3 Emission rates proposed for modelling

4.2.3.1 Emission rates for dispersion sensitivity tests

For the dispersion sensitivity tests, Jacobs applied the same emission concentrations for the modelling of PM_{10} and $PM_{2.5}$ emissions from the vents as those applied by TAS (2023a) (see Plate 4-3), which are in turn taken from Ektimo (2022). The reference conditions for the concentrations in Plate 4-3 are not stated in TAS (2023a); Jacobs assumes that standard conditions are applied, as this is consistent with the reporting convention in Ektimo (2022).

Pollutant	VR3A	VR5	VR7	VR8
Solid particles (TSP)	62	1.3	13	360
Fine particles (PM_{10})	49	0.69	9.3	220
Fine particles ($PM_{2.5}$)	19	0.24	2.7	74

Plate 4-3. Emission concentrations (mg/Sm³) for vent stacks stated in Table 5-6 of TAS (2023a).

The emission rates from the vents are calculated by multiplying the concentration by the flow rate. Jacobs adopted the following constant flow rates for the sensitivity testing:

- For VR3A, VR5 and VR7 – flow rates reported in Ektimo (2022).
- For VR8 – flow rate of 480 Sm³/s.

These applied concentrations and flows were the same for all of the sensitivity test runs, and are summarized in Table 4-2.

Table 4-2. Vent flow rates and emission rates for sensitivity test modelling

Vent	VR3A	VR5	VR7	VR8
Flow rate, Sm³/s	215	300	303	480
Flow rate, Am³/s	265	365	370	581
PM_{10} concentration, mg/Sm³	49	0.69	9.3	220
$PM_{2.5}$ concentration, mg/Sm³	19	0.24	2.7	74
PM_{10} emission rate, g/s	10.5	0.21	2.8	106
$PM_{2.5}$ emission rate, g/s	4.1	0.072	0.82	35.5

4.2.3.2 Emission rate scenarios requested by EPA

EPA requested a series of emission rate scenarios for the vents:

1. Historic scenario at emission rates reported in Ektimo (2022), as TAS (2023a) (same as base case).
2. Current scenario at 2023 emission rates following installation of controls on VR8, with VR8 as one stack at equivalent diameter calculated by Jacobs, and using the average emission rates from Ektimo (2023b, c, d, e, f and g).
3. Current emissions scenario with maximum flow rates (current average concentrations kept the same as scenario 2), splitting VR8 into three stacks.
4. Current vents, maximum flow rates, and “regulatory case” TSP concentration of 50 mg/Sm³ in all vents.

5. "MOD15 regulatory case" – including new vents proposed by MOD15 which are VR11, R-VR4 and R-VR6, at maximum flow rates and TSP concentration of 50 mg/Sm^3 in all vents. Jacobs was provided with the vent locations and discharge characteristic for these vents from Airen (2024).

Jacobs applied the following assumptions to define the emission characteristics for each of these scenarios:

- All discharge temperatures at 290K except for Scenario 1 where the temperatures measured in Ektimo (2022) and also used in TAS (2023a) were applied.
- For Scenarios 3, 4 and 5:
  - The ratio of 83% for Sm^3:Am^3 was applied, which was the average ratio of standard volumetric flow rate to actual volumetric flow rate measured in Ektimo (2023b, c, d, e, f and g) for operating temperatures of 287-291K.
  - For VR8 and the new MOD15 vents:
    - the ratio of PM_{10}:TSP was assumed to be 50%, which was the average ratio of PM_{10}:TSP measured in Ektimo (2023a and b).
    - the ratio of $PM_{2.5}$:TSP was assumed to be 13.1%, which was the average ratio of $PM_{2.5}$:TSP measured in Ektimo (2023a and b).
  - For VR3, 5 and 7:
    - The PM_{10} and $PM_{2.5}$ ratios to TSP were taken from the only testing available from these vents, in Ektimo (2022).

The emission characteristics applied for each vent and each Scenario are listed in Table 4-3 to Table 4-7.

Table 4-3. Vent flow rates and emission rates for emission modelling requested by EPA, Scenario 1 (base case)

Vent	VR3A	VR5	VR7	VR8
Flow rate, Sm^3/s	215	300	303	480
Flow rate, Am^3/s	265	365	370	581
TSP concentration*, mg/Sm^3	62	1.3	13	360
PM_{10} concentration, mg/Sm^3	49	0.69	9.3	220
$PM_{2.5}$ concentration, mg/Sm^3	19	0.24	2.7	74
PM_{10} emission rate, g/s	10.5	0.21	2.8	106
$PM_{2.5}$ emission rate, g/s	4.1	0.072	0.82	35.5
Discharge temperature, K	296.4	297.6	296.6	295.6
Number of vents	1	1	1	1
Diameter of (each) vent, m	5	5.4	6.2	10.2
Exit velocity, m/s	13.5	15.9	12.3	7.1

* Provided for information only, TSP emissions were not modelled.

Table 4-4. Vent flow rates and emission rates for emission modelling requested by EPA, Scenario 2

Vent	VR3A	VR5	VR7	VR8
Flow rate, Sm^3/s	215	300	303	480
Flow rate, Am^3/s	259	356	362	570
TSP concentration*, mg/Sm^3	62	1.3	13	33
PM_{10} concentration, mg/Sm^3	49	0.69	9.3	16.5
$PM_{2.5}$ concentration, mg/Sm^3	19	0.24	2.7	4.3
PM_{10} emission rate, g/s	10.5	0.21	2.8	7.9
$PM_{2.5}$ emission rate, g/s	4.1	0.072	0.82	2.1
Discharge temperature, K	290	290	290	290
Number of vents	1	1	1	1
Diameter of (each) vent, m	5	5.4	6.2	9.2
Exit velocity, m/s	13.2	15.5	12.0	8.6

* Provided for information only, TSP emissions were not modelled.

Table 4-5. Vent flow rates and emission rates for emission modelling requested by EPA, Scenario 3

Vent	VR3A	VR5	VR7	VR8
Flow rate, Sm^3/s	300	370	400	600
Flow rate, Am^3/s	363	448	484	727
TSP concentration*, mg/Sm^3	62	1.3	13	33
PM_{10} concentration, mg/Sm^3	49	0.69	9.3	16.5
$PM_{2.5}$ concentration, mg/Sm^3	19	0.24	2.7	4.3
PM_{10} emission rate, g/s	14.7	0.26	3.72	9.90 (total across 3 vents)
$PM_{2.5}$ emission rate, g/s	5.7	0.09	1.08	2.6 (total across 3 vents)
Discharge temperature, K	290	290	290	290
Number of vents	1	1	1	3
Diameter of (each) vent, m	5	5.4	6.2	5.3
Exit velocity, m/s	18.5	19.6	16.0	11.0

* Provided for information only, TSP emissions were not modelled.

Table 4-6. Vent flow rates and emission rates for emission modelling requested by EPA, Scenario 4

Vent	VR3A	VR5	VR7	VR8
Flow rate, Sm^3/s	300	370	400	600
Flow rate, Am^3/s	363	448	484	727
TSP concentration*, mg/Sm^3	50	50	50	50
PM_{10} percentage of TSP	79.0%	53.1%	71.5%	50.0%
$PM_{2.5}$ percentage of TSP	30.6%	18.5%	20.8%	13.1%
PM_{10} concentration, mg/Sm^3	39.5	26.5	35.8	25
$PM_{2.5}$ concentration, mg/Sm^3	15.3	9.2	10.4	6.5
PM_{10} emission rate, g/s	11.9	9.8	14.3	15.0 (total across 3 vents)
$PM_{2.5}$ emission rate, g/s	4.6	3.4	4.1	3.9 (total across 3 vents)
Discharge temperature, K	290	290	290	290
Number of vents	1	1	1	3
Diameter of (each) vent, m	5	5.4	6.2	5.3
Exit velocity, m/s	18.5	19.6	16.0	11.0

* Provided for information only, TSP emissions were not modelled.

Table 4-7. Vent flow rates and emission rates for emission modelling requested by EPA, Scenario 5

Vent	VR3A, VR5, VR7, and VR8	VR11	R-VR4	R-VR6
Flow rate, Sm^3/s	As Scenario 4	332	249	249
Flow rate, Am^3/s	As Scenario 4	400	300	300
TSP concentration*, mg/Sm^3	As Scenario 4	50	50	50
PM_{10} percentage of TSP	As Scenario 4	50.0%	50.0%	50.0%
$PM_{2.5}$ percentage of TSP	As Scenario 4	13.1%	13.1%	13.1%
PM_{10} concentration, mg/Sm^3	As Scenario 4	25	25	25
$PM_{2.5}$ concentration, mg/Sm^3	As Scenario 4	6.5	6.5	6.5
PM_{10} emission rate, g/s	As Scenario 4	8.30	6.23	6.23
$PM_{2.5}$ emission rate, g/s	As Scenario 4	2.17	1.63	1.63
Discharge temperature, K	As Scenario 4	290	290	290
Number of vents	As Scenario 4	1	1	1
Diameter of (each) vent, m	As Scenario 4	7	4.5	4.5
Exit velocity, m/s	As Scenario 4	10.4 (horizontal discharge)	18.9	18.9

* Provided for information only, TSP emissions were not modelled.

4.3 Emission Factors and Inventory

4.3.1 Emission factor basis

The TAS Reports refer to the United States Environmental Protection Agency (USEPA) Compilation of Air Pollutant Emissions Factors from Stationary Sources (AP-42), the Australian National Pollutant Inventory (NPI) emission estimation technique manuals, and Katestone (2011) as the basis for EF development. These references represent the state of knowledge for EF assumptions for mining operations, provided that the recommended EFs are applied in relevant context.

The TAS Reports provide a summary of the EF equations used and the variables adopted, for example as shown in Plate 4-4. However, no additional detail is provided in the reports to justify the selection of variables such as silt content, moisture content, and intensity rates.

EFs and relevant variables are discussed for each activity type in the following sections.

Table C-1: Emission factor equations

Activity	Emission factor equation		
	TSP	PM_{10}	$PM_{2.5}$
Loading / emplacing overburden	$EF = 0.74 \times 0.0016 \times \left(\frac{U}{2.2}^{1.3} \Big/ \frac{M}{2}^{1.4}\right) kg/tonne$	$EF = 0.35 \times 0.0016 \times \left(\frac{U}{2.2}^{1.3} \Big/ \frac{M}{2}^{1.4}\right) kg/tonne$	$EF = 0.053 \times 0.0016 \times \left(\frac{U}{2.2}^{1.3} \Big/ \frac{M}{2}^{1.4}\right) kg/tonne$
Hauling on unsealed surfaces	$EF = \left(\frac{0.4536}{1.6093}\right) \times 4.9 \times (s/12)^{0.7} \times (1.1023 \times M/3)^{0.45} kg/VKT$	$EF = \left(\frac{0.4536}{1.6093}\right) \times 1.5 \times (s/12)^{0.9} \times (1.1023 \times M/3)^{0.45} kg/VKT$	$EF = \left(\frac{0.4536}{1.6093}\right) \times 0.15 \times (s/12)^{0.9} \times (1.1023 \times M/3)^{0.45} kg/VKT$
Dozers on overburden	$EF = 2.6 \times s^{1.2} / M^{1.3}\ kg/hr$	$EF = (0.45 \times s^{1.5} / M^{1.4}) \times 0.75\ kg/hr$	$EF = (2.6 \times s^{1.2} / M^{1.3}) \times 0.105\ kg/hr$
Secondary ore crushing	$EF = (0.0027 + 0.0125)\ kg/t$	$EF = (0.0012 + 0.0043)\ kg/t$	$PM10 \times (0.00005/0.00027)\ kg/t$
Wind erosion on exposed areas, stockpiles	$EF = 3{,}504\ kg/ha/year$	$0.5 \times TSP$	$0.075 \times TSP$
Grading roads	$EF = 0.0034 \times (S)^{2.5}$	$EF = 0.0056 \times (S)^2 \times 0.6$	$EF = 0.0034 \times (S)^{2.5} \times 0.031$

EF = emission factor, U = wind speed (m/s), M = moisture content (%), s = silt content (%), W = average weight of vehicle (tonne), VKT = vehicle kilometres travelled (km), S = mean vehicle speed (kph).

Table C-2: Dust Emissions Inventory

Activity	TSP emission	PM10 emission	PM25 emission	Intensity	Units	EF - TSP	EF - PM10	EF - PM25	Units	Var. 1	Units	Var. 2	Units	Var. 3 (TSP / PM10 / PM25)	Units	Var. 4	Units	Var. 5	Units	Control	Units
CE - General constuction work	52,993	27,556	1,590	3,785	t/y	14	7.28	0.42	kg/h												
CE - Loading waste to trucks	1,332	630	95	1,296,296	t/y	0.00103	0.00049	0.00007	kg/t	2.17	ave. $(ws/2.2)^{1.3}$	3.85	M.C. %								
CE - Hauling waste to emplacement area	11,414	2,442	244	1,296,296	t/y	0.0587	0.0126	0.0013	kg/t	199	t/load	3.92	km/return	3.0 / 0.6 / 0.1	kg/VKT	2	S.C. %	244	Weight (t)	85	% Control
CE - Emplacing waste at dump	1,332	630	95	1,296,296	t/y	0.00103	0.00049	0.00007	kg/t	2.17	ave. $(ws/2.2)^{1.3}$	3.85	M.C. %								
CE - Dozers working on waste rock dumps	26,258	4,827	2,757	8,445	h/y	3.1	0.6	0.3	kg/h	5	S.C. %	3.85	M.C. %								
CE - Secondary ore crushing	106,400	38,500	3,311	35,000,000	t/y	0.03	0.01	0.0009	kg/t											90	% Control
CE - Loading crushed ore to storage pile from underground	35,962	17,009	2,576	35,000,000	t/y	0.00103	0.00049	0.00007	kg/t	2.17	ave. $(ws/2.2)^{1.3}$	3.85	M.C. %								
CE - Ore processing in mill (x5)	179,812	85,046	12,878	175,000,000	t/y	0.00103	0.00049	0.00007	kg/t	2.17	ave. $(ws/2.2)^{1.3}$	3.85	M.C. %								
WE - waste rock dumps	760,691	380,346	57,052	217	ha	3,504	1,752	263	kg/ha/y												
WE - pit tailing storage facility	406,341	203,170	30,476	116	ha	3,504	1,752	263	kg/ha/y												
WE - subsidence zone	166,087	83,044	12,457	47	ha	3,504	1,752	263	kg/ha/y												
WE - plant stockpiles and exposed areas	286,513	143,256	21,488	82	ha	3,504	1,752	263	kg/ha/y												
WE tailings storage facilities	2,816,236	1,408,118	211,218	804	ha	3,504	1,752	263	kg/ha/y												
Grading roads	23,935	8,363	742	38,889	km	0.62	0.22	0.02	kg/VKT	8	km/h										
Ventilation shaft emissions (x4)	205,131	80,001	9,600	8,760	h/y	23.4	9.1	1.1	kg/h	7,920,000	m3/h	2.96	mg/m3								
Conveyors and conveyor transfer points	10,789	5,103	773	35,000,000	t/y	0.00103	0.00049	0.00007	kg/t	2.170866	ave. $(ws/2.2)^{1.3}$	3.85	M.C. %							70	% Control
Stripping topsoil + dozer activity	38,130	7,010	4,004	12,264	h/y	3.1	0.6	0.3	kg/h	5	S.C. %	3.85	M.C. %								
Loading material to haul truck	989	468	71	962,448	t/y	0.00103	0.00049	0.00007	kg/t	2.17	ave. $(ws/2.2)^{1.3}$	3.85	M.C. %								
Hauling material to emplacement area	68,398	14,632	1,463	962,448	t/y	0.474	0.101	0.010	kg/t	52	t/load	14.6	km/return	1.7 / 0.4 / 0.04	kg/VKT	2.0	S.C. %	69	Weight (t)	85	% Control
Unloading material at emplacement area	989	468	71	962,448	t/y	0.00103	0.00049	0.00007	kg/t	2.17	ave. $(ws/2.2)^{1.3}$	3.85	M.C. %								
Rehandle material	198	94	14	192,490	t/y	0.00103	0.00049	0.00007	kg/t	2.17	ave. $(ws/2.2)^{1.3}$	3.85	M.C. %								
WE - tailings construction area	688,012	344,006	51,601	196.4	ha	3,504	1,752	263	kg/ha/y												
Total Emissions (kg/year)	**5,887,941**	**2,854,718**	**424,576**																		

Plate 4-4. Dust emissions inventory information supplied in TAS (2020a).

4.3.2 Surface stockpiles

There are several ore and waste stockpiles at the mine site. Ore is transported from underground via conveyor and delivered directly to the main stockpile (referred to by CVO as the main crushed ore stockpile, or COS) at the surface. Other stockpiles are also visible within the processing area on the Cadia aerial map associated with secondary crushing and subsequent processing steps. The locations of these stockpiles can be seen in Figure 4.2.

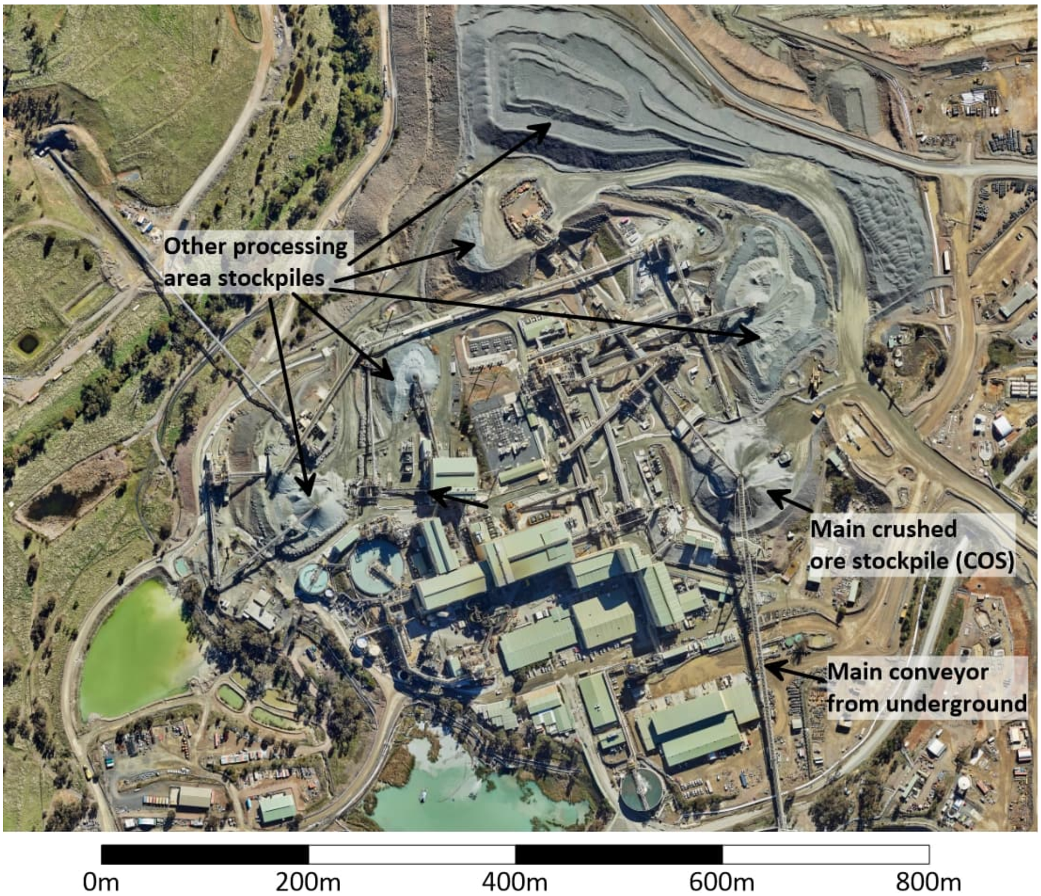

Figure 4.2: Aerial image of processing plant from Cadia aerial photograph supplied by CVO.

The operation of the main COS in the processing area is described in Section 5.1 of Zephyr (2022):

> *This stockpile is maintained as high as possible to minimise the drop height from the conveyor and also to maintain sufficient weight to effectively draw it down. It is reclaimed via three feeders underneath the stockpile and conveyed to the processing plant.*
>
> *If this main stockpile reaches capacity, material is removed via truck and transported to a smaller stockpile. This material then re-feeds the main stockpile as required.*

Zephyr (2022) also describes the dust control provisions for the main COS, including a photo showing the conveyor loading to the main COS with no evidence of dust evolution from the COS surface:

> *There are no water sprays on the external surfaces of the main stockpile. However, water sprays on the conveyor provide moisture to the raw material and the stockpile is constantly loaded to the top so little dust was observed to be generated by this source. Water carts are used to aid dust suppression on the unsealed roads between the main stockpile and the smaller stockpile when required.*
>
> *Conveyor transfer chutes are sealed and water mist spray installations have been designed for some transfer chutes, significantly reducing dust escaping from these locations. Dust is currently well managed from surface stockpiles and associated activities.*

During the Jacobs site visit, dust was observed to be consistently emitted from the COS surface during conveyor operation, contrary to the observations made by Zephyr – see Picture A-8 in Appendix A. Dust emissions of this type are addressed under the "loading and handling" activity in Section 4.3.5.

Dust was also observed to be generated by trucks on the short haul road between the COS and the smaller stockpile, although this was later rectified by the operation of water trucks (Pictures A-9 and A-10, Appendix A). Dust emissions of this type are addressed under the "vehicle-tracked dust" activity in Section 4.3.8.

Stockpiles also have the potential to emit dust during high wind speeds. Wind speeds were low on the day of the Jacobs site visit, so the potential for dust evolution from stockpile surfaces during high wind speeds could not be observed. Wind erosion from stockpiles is handled in the same manner as wind erosion from any other surface in the TAS Reports, and Jacobs agrees that this is an appropriate approach although the controls applied to stockpiles may be different to controls applied to other surface sources.

4.3.3 Ore processing

Ore processing involves a sequence of crushing, grinding and flotation steps through two concentrator lines, as shown in Figure 4.3. Most of these steps are carried out in buildings which reduces the potential for dust emissions although fugitive emissions from building openings are still possible. Dust controls for ore processing are described in Zephyr (2022), Chapter 5.2. The report notes that "*Much has already been done, or is being done, to reduce dust at the source for the processing plant, but there are also a number of notifications and work orders for additional improvements, investigative and corrective work*."

The TAS Reports include a specific EF for secondary and tertiary crushing activities. Dust emissions of this type are addressed under the "crushing" activity in Section 4.3.4.

The TAS Reports also include an EF for "ore processing in Mill" which is based on the same equation as conveyor handling emissions but with an intensity of five times the annual ore production rate and no controls. The basis for this assumption is unclear but Jacobs presumes that this is intended to account for various conveyor drop points on to stockpiles within the processing area, and possibly also to account for fugitive emissions from the various processing steps. However, if this is the case then the emission rate should be reduced due to controls that are present for these sources. Dust EFs for conveyor drop points, including from this activity, are addressed under the "loading and handling" activity in Section 4.3.5.

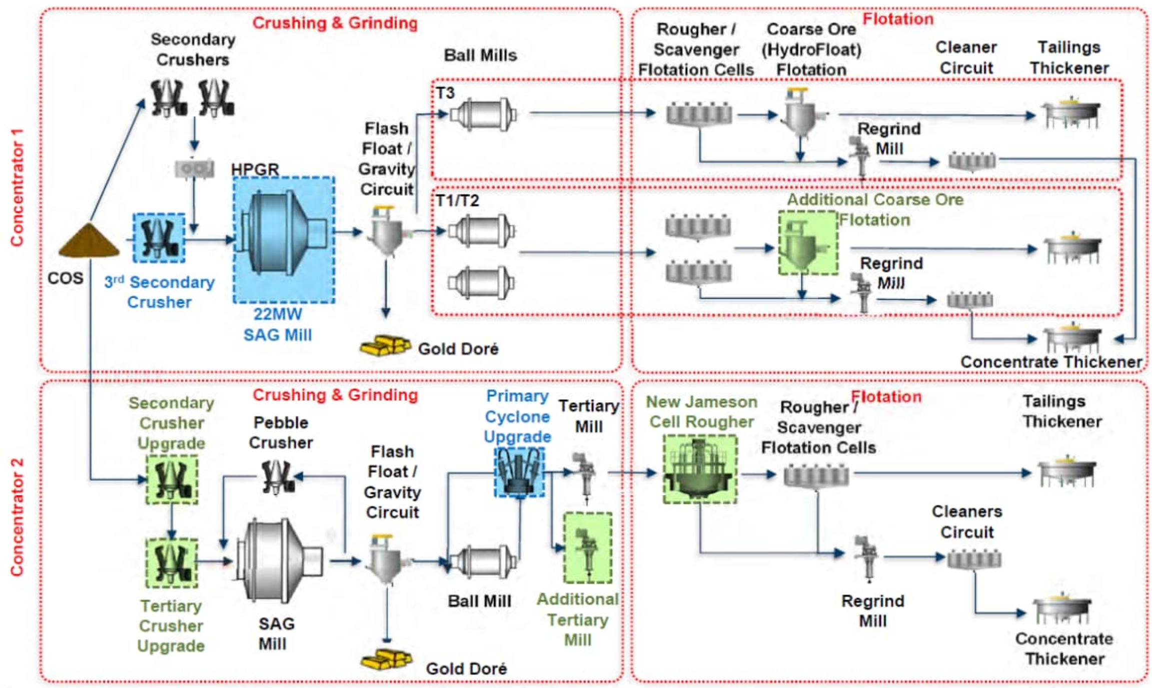

Figure 4.3: Ore processing steps at Cadia Mine, from Figure 17-1 of Newcrest (2020).

4.3.4 Crushing

4.3.4.1 Emissions basis

The TAS Reports include an EF for secondary and tertiary crushing which is dependent on the tonnes of material crushed. These EFs are taken from NPI (2012b) which recommends default EFs for crushing activities at metalliferous mines. Values are provided for both high-moisture and low-moisture content ores, with the definition of a high-moisture content ore being *"one that either naturally, or as a result of additional moisture at the primary crusher (usually), has a moisture content of more than 4% by weight"*. The EFs are summarized in Table 4.9.

CVO supplied data provided of "belt cut" moisture content analysis – monthly samples from July 2017 of moisture content in ore conveyed from underground. The average moisture content from these samples was 1.6%, indicating that the ore from Cadia East could be classified as a low moisture content ore. However, the values adopted in the TAS Reports are those for a high moisture content ore.

Table 4.8: Emission factors for crushing from NPI (2012b) Table 3

Activity	High moisture content ore		Low moisture content ore		EF Units
	TSP	PM_{10}	TSP	PM_{10}	
Secondary crushing	0.03	0.012	0.6	No value provided – Jacobs estimates 0.03 based on TSP:PM_{10} ratio for tertiary crushing	kg/T handled
Tertiary crushing	0.03	0.010	1.4	0.08	kg/T handled

The EFs adopted in the TAS Reports are summarized in Table 4.9, along with alternatives recommended by Jacobs. Jacobs also recommends that the sensitivity of the assumption of high moisture content ore be tested. The sensitivity options are discussed in Section 4.3.4.3.

Table 4.9: Recommended EFs for crushing

Pollutant	EF Units	TAS EF	Jacobs' recommended EF		Comments
			High moisture content ore	Low moisture content ore	
PM_{10}	kg/T processed	0.011	0.012	0.03	TAS EF is average of secondary and tertiary crushing EFs in NPI (2012b) for high moisture content ore of 0.012 and 0.010 kg/T respectively. As tertiary crushing is a minor aspect of the crushing process at Cadia, Jacobs recommends relying on the secondary crushing EF only.
$PM_{2.5}$	kg/T processed	0.0009	0.0012	0.003	TAS EF basis is not specified. Jacobs recommends using an EF which is 10% of the PM_{10} EF, based on the controlled EFs in AP42 11.19.2 for mineral products and stone crushing, for which on average the $PM_{2.5}$ EFs are about 10% of the PM_{10} EFs.

Newcrest (2020), Section 1.15, describes the process of crushing ore at Cadia. Figure 4.3 showed the two concentrator lines at Cadia from that reference. At the time of publication in of Newcrest (2020), Concentrator 1 processed 23 MT/a, and Concentrator 2 processed 7 MT/a. Since that time, it is understood that both concentrators may have been increased in capacity through debottlenecking projects (as these are described in Newcrest (2020) as future planned projects which may now have been completed). Concentrator 1 had one secondary crushing stage, and Concentrator 2 had three crushing stages (secondary, tertiary and pebble) although the pebble crushing did not handle the full throughput. Due to the double crushing steps in Concentrator 2, Jacobs considers that the tonnage throughput for emissions calculation should be increased by 7 MT/a.

The emission rate from crushing steps depends on the tonnage throughput. TAS (2020a) and HAS (2009) both used the total annual ore tonnage to calculate the crushing emission rate. TAS (2023a) used a much smaller percentage of the total annual ore tonnage, however no explanation for this change is provided.

Activity data for total ore extraction tonnage for each financial year ending June is provided in the AEMRs published by CVO:

- AEMR 2019 - 29,302,110 T/a
- AEMR 2020 - 29,345,770 T/a
- AEMR 2021 - 32,370,828 T/a
- AEMR 2022 - 25,861,109 T/a
- AEMR 2023 – 29,082,463 T/a.

A typical annual extraction tonnage of 30 MT/a is assumed by Jacobs for emission calculations. This is consistent with the “ore on conveyor” tonnage of 30,043,251 T/a used by TAS (2023). This figure of 30 MT/a is increased to 37 MT/a to account for the two crushing stages in Concentrator 2.

4.3.4.2 Controls

The crushing emission rates are reduced by 90% in both HAS (2009) and the TAS Reports to account for emission controls. The tables in Attachment EB of HAS (2009) state that this is an assumed reduction to account for covers and enclosure. However, the basis for this assumption is not defined. The sensitivity of this assumption should be checked by comparing the model results with a 90% reduction against a lesser control of 70% reduction which is specified in Katestone (2011) Table 96 for enclosed conveyor transfers.

4.3.4.3 Emission rates proposed for modelling

The following options are recommended for emission sensitivity testing:

1. Base case:
    a. Jacobs recommended EFs assuming a high moisture content ore
    b. Activity intensity of 37 MT/a
    c. Control efficiency 90%
2. Sensitivity test for EFs – as Option 1 but low moisture content ore basis
3. Sensitivity test for control efficiency – as Option 1 but with 70% control efficiency
4. Sensitivity test for both EF and control efficiency (combining options 2 and 3)

The EFs and rates assumed for crushing are summarized in Table 4.10.

Table 4.10: Emission Sensitivity Test Options for Crushing

Option	EF, kg/T		Activity intensity	Control efficiency	Total emission rate, kg/h	
	PM_{10}	$PM_{2.5}$			PM_{10}	$PM_{2.5}$
1. Base case	0.012	0.0012	37 MT/a	90%	5.07	0.51
2. Sensitivity test for EFs	0.03	0.003	37 MT/a	90%	12.7	1.27
3. Sensitivity test for control efficiency	0.012	0.0012	37 MT/a	70%	15.2	1.52
4. Sensitivity test for both EFs and control efficiency	0.03	0.003	37 MT/a	70%	38.0	3.80

4.3.5 Loading and handling

4.3.5.1 Emissions basis

The loading and handling category includes emissions from:

- Batch loading activities such as a loading trucks using excavators or front end loaders, trucks dumping loads, emplacing loads at storage locations, and general handling of material; and
- Continuous loading activities such as conveyors and conveyor transfer points.

The TAS reports apply the following equations for both batch and continuous loading and handling which are specified in both NPI (2012b) and USEPA (2006a) for handling overburden at coal mines:

$$EF = k \times 0.0016 \times \left| \frac{\left(\frac{U}{2.2}\right)^{1.3}}{\left(\frac{M}{2}\right)^{1.4}} \right| \ kg/tonne$$

where

k = 0.74 for TSP, 0.35 for PM_{10}, and 0.053 for $PM_{2.5}$
U = mean wind speed in m/s
M = moisture content of material being handled, in percent by weight in natural state (ie. prior to addition of water for dust control)

Equation 1

AP-42 states that Equation 1 is applicable for the following range of parameters:

- Wind speed 0.6-6.7 m/s
- Moisture content 0.25-4.8%
- Silt content 0.44-19%.

Whilst silt content is included, it does not appear as a factor in Equation 1. USEPA (2006a) states that while it is reasonable to expect that silt content and emission factors are interrelated, no significant correlation between the two was found during the derivation of the equation, probably because most tests with high silt contents were conducted under lower winds, and vice versa.

The averaging period for the mean wind speed is not specified in the references, and is commonly taken to be the annual mean wind speed. This approach appears to have been taken in the TAS Reports, but is not specifically stated. It is reasonable to assume that emission rates from handling operations would increase with wind speed, as this is usually readily observed on any work site. A sensitivity test using hour-by-hour varying wind speeds based on SLB AWS wind records was therefore included in the model runs.

In TAS (2023a), Equation 1 is used to calculate the emission rates for all loading and handling, assuming a moisture content of 3.85% and mean wind speed of 3.84 m/s[16]. The justification for this moisture content and wind speed is not provided.

Jacobs has calculated the mean annual wind speed for 2022 for SLB and Ridgeway to be 3.96 and 4.16 m/s respectively, from the hourly-average wind records supplied by CVO.

Figure 4.4 shows the PM_{10} EF for loading and handling using Equation 1, as a function of moisture content and mean wind speed. The calculated EF is quite sensitive to moisture contents less than about 4%. TSP and $PM_{2.5}$ emission rates vary similarly as the equations are the same except for a linear scaling factor.

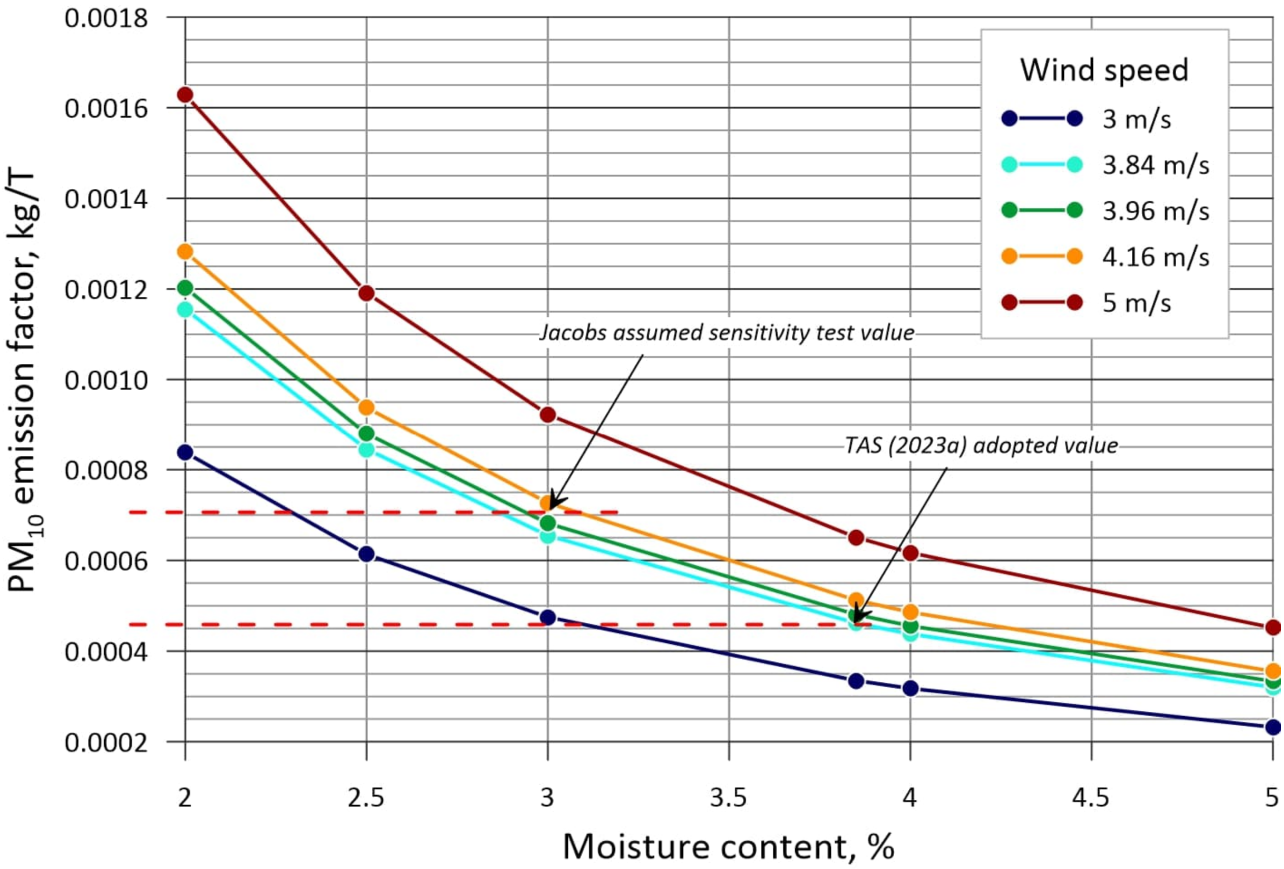

Figure 4.4: TSP EFs for loading and handling activities, calculated from Equation 1, as a function of mean wind speed and moisture content.

[16] Back-calculated by Jacobs based on the wind speed correction variable $(ws/2.2)^{1.3}$ value of 2.06 stated in TAS (2023a) Table A-2.

NPI (2012b) advises that Equation 1 provides estimates for batch loading that are unrealistically low for Australian conditions, and instead recommends the EFs summarized in Table 4.11 for handling of overburden at coal mines.

Table 4.11: Emission factors for loading and handling on overburden at coal mines

Activity	NPI (2012b) recommended EF		Jacobs calculated EF*	EF Units
	TSP	PM_{10}	$PM_{2.5}$	
Excavators/Shovels/Front-end loaders (on overburden).	0.025	0.012	0.00179	kg/T handled
Trucks (dumping overburden).	0.012	0.0043	0.00086	kg/T handled

* Assuming $PM_{2.5}$:TSP ratio from Equation 1

NPI (2012b) also recommends default emission factors for handling, transferring, and conveying operations at metalliferous mines, which are drawn from USEPA (1982) and shown in Table 4.12. Values are provided for both high-moisture and low-moisture content ores, with the definition of a high-moisture content ore being *"one that either naturally, or as a result of additional moisture at the primary crusher (usually), has a moisture content of more than 4% by weight"*. Based on the average belt-cut moisture content of 1.6% in the ore from Cadia East as introduced in Section 4.3.4.1, the ore at Cadia would be a low-moisture content ore.

Table 4.12: Emission Factors for Loading and Handling at Metalliferous Mines (from NPI (2012b) Table 3)

Activity	High moisture content ore		Low moisture content ore		EF Units
	TSP	PM_{10}	TSP	PM_{10}	
Handling, transferring, and conveying including wheel and bucket reclaimers (except bauxite)	0.005	0.002	0.06	0.03	kg/T handled

Table 4.13 summarises the various loading and handling operations and respective intensities applied in TAS (2023a), and the interpretation applied by Jacobs for EF testing.

Table 4.13: Emission rate activity basis for loading and handling activities

Activity	Activity intensity (T/a)	Control efficiency	Comments
Cadia East operations			
Loading waste to trucks	827,705	0%	Jacobs cannot verify this activity intensity, and assumes this is correct.
Emplacing waste at dump	827,705	0%	Jacobs cannot verify this activity intensity, and assumes this is correct.
Loading crushed ore to main COS from underground	4,145,282	0%	Jacobs assumes that this activity represents the dropping of ore from the conveyor onto the main COS. This activity rate in TAS (2023a) seems low, and Jacobs expects that the full extraction rate should be used which is consistent with TAS (2020a) and HAS (2009). Jacobs will apply the full extraction rate of 30,043,251 T/a as per the conveyor transfer points activity.

Conveyor transfer	30,043,251	70%	This is for just one transfer point, and is assumed to represent the first transfer point when the conveyor comes to the surface from underground. There are also multiple conveyor transfer points throughout the processing area. Jacobs assumes that the "ore processing" emission factor (see next row) is intended to account for these additional transfer point emissions. 70% control is applied in TAS (2023a) for enclosures, and appears reasonable.
Ore processing in mill	150,216,255	0%	As commented in row above, this activity is assumed to account for multiple transfer points within the processing area. The activity rate is defined in TAS (2023a) as "5x throughput rate", and no controls are applied.
Loading crushed ore into trucks to feed main COS from storage	4,959,288	0%	This activity is included in TAS (2023a) in the Jan-Feb 2023 inventory but not the Jan-Dec 2022 inventory. The activity intensity in column 2 is the equivalent annual rate based on the Jan-Feb 2023 activity intensity of 826,548 T. Jacobs cannot verify this activity intensity, and assumes this is correct.
Emplacing ore at storage location or main COS	9,411,486	0%	This activity is included in TAS (2023a) in the Jan-Feb 2023 inventory but not the Jan-Dec 2022 inventory. The activity intensity in column 2 is the equivalent annual rate based on the Jan-Feb 2023 activity intensity of 1,568,581 T. Jacobs cannot verify this activity intensity, and assumes this is correct.
Tailings construction work			
Loading material to haul truck	7,174,831	0%	Jacobs cannot verify this activity intensity, and assumes this is correct.
Unloading material at emplacement area	7,174,831	0%	Jacobs cannot verify this activity intensity, and assumes this is correct.
Rehandle material	1,434,966	0%	This activity is included in TAS (2023a) in the Jan-Dec 2022 inventory but not the Jan-Feb 2023 inventory. Jacobs cannot verify this activity intensity, and assumes this is correct.

4.3.5.2 Controls

No correction to the emission rates for loading and handling is applied in the TAS Reports for mitigation controls except for the conveyor transfer points which are partly enclosed and have a 70% emission reduction applied. However, this correction is not applied to the "ore processing" activity.

Other mitigation controls for loading and handling activities include minimizing drop heights (such as from loader bucket to truck bed, or from truck bed to ground), water application, and modifying activities in windy conditions[17]. Jacobs is not able to quantify the extent of use of these controls at Cadia nor whether it would be appropriate to apply a control factor to these activities.

4.3.5.3 Emission rates proposed for modelling

The TAS Reports do not say whether all the loading and handling activities are assumed to operate 24 hours per day, 7 days per week ("24/7"). Jacobs was advised by CVO at the site visit that the processing plant and short haul operations operate 24/7, but long haul and construction operations operate only in daylight hours. For modelling, Jacobs has assumed that the definition of daylight hours is constant for all days of the year, 7am to 6pm, 11 hours per day ("11/7"). Subtle changes to this operating assumption are unlikely to affect model results, because the shortest averaging periods predicted are 24-hours duration.

The following options are recommended for emission sensitivity testing:

1. Base case – as TAS (2023a) Jan-Dec 2022 emission inventory
2. Sensitivity test for EFs from Equation 1 assuming the following:
    a. Lower moisture content nominally assumed at 3.0%.
    b. Mean wind speed from average of SLB and Ridgeway annual wind speeds (4.06 m/s).
    c. Activity intensities from TAS (2023a) Jan-Dec 2022 emission inventory except for correction to loading rate to main COS from underground.
    d. Include activity of loading ore to and from main COS and storage location (this activity is included in TAS (2023a) for the Jan-Feb 2023 inventory, but not in the Jan-Dec 2022 inventory).
    e. 70% emission reduction due to controls on conveyors and conveyor transfers
    f. Excluding the ore processing activity.
    g. Assuming 24/7 operation of short haul activities and 11/7 operation of long haul activities.
3. Sensitivity test for EFs with assumptions from Option 2 and with NPI recommended emission factors for overburden batch loading operations from Table 4.11.
4. Sensitivity test for EFs with assumptions from Option 2 and with NPI recommended emission factors for low moisture content ores at metalliferous mines (from Table 4.12) for ore handling.
5. Sensitivity test for hour-by-hour variation of emission rate with wind speed, with moisture content and activity rates as Option 2.

The EFs and rates assumed for loading and handling are summarized in Table 4.10. The ore processing emission rate is very large relative to the other loading and handling activities. It is recommended that the basis for definition of this activity be requested from CVO. For the analysis of sensitivity tests by dispersion modelling, the ore processing emission rate will not be included.

[17] Katestone (2011) Table 90

Table 4.14: Emission Sensitivity Test Options for loading and handling

Activity	EF, kg/T		Activity intensity, T/a	Control efficiency	Assumed operating hours	Total emission rate, kg/h	
	PM_{10}	$PM_{2.5}$				PM_{10}	$PM_{2.5}$
Option 1 – Base case							
Loading waste to trucks	0.000462	0.000070	827,705	0%	24/7	0.0436	0.0066
Emplacing waste at dump	0.000462	0.000070	827,705	0%	24/7	0.0436	0.0066
Loading crushed ore to main COS from underground	0.000462	0.000070	4,145,282	0%	24/7	0.2185	0.0331
Conveyor transfer points	0.000462	0.000070	30,043,251	70%	24/7	0.4751	0.0720
Ore processing in mill	0.000462	0.000070	150,216,255	0%	24/7	7.91[&]	1.20[&]
Loading crushed ore into trucks to feed main COS from storage*	0.000462	0.000070	0	-	-	0	0
Emplacing ore at storage location or main COS*	0.000462	0.000070	0	-	-	0	0
Loading material to haul truck	0.000462	0.000070	7,174,831	0%	11/7	0.8253	0.1250
Unloading material at emplacement area	0.000462	0.000070	7,174,831	0%	11/7	0.8253	0.1250
Rehandle material	0.000462	0.000070	1,434,966	0%	11/7	0.1651	0.0250
Option 2 – Sensitivity test for EFs from Equation 1, include activity of loading ore to and from main COS and storage location							
Loading waste to trucks	0.000704	0.000107	827,705	0%	24/7	0.067	0.01
Emplacing waste at dump	0.000704	0.000107	827,705	0%	24/7	0.067	0.01
Loading crushed ore to main COS from underground	0.000704	0.000107	30,043,251	0%	24/7	2.415	0.37
Conveyor transfer points	0.000704	0.000107	30,043,251	70%	24/7	0.724	0.11
Ore processing in mill	0.000704	0.000107	150,216,255	0%	24/7	12.1&	1.83&
Loading crushed ore into trucks to feed main COS from storage*	0.000704	0.000107	4,959,288	0%	24/7	0.399	0.06
Emplacing ore at storage location or main COS*	0.000704	0.000107	9,411,486	0%	24/7	0.756	0.11
Loading material to haul truck	0.000704	0.000107	7,174,831	0%	11/7	1.258	0.19
Unloading material at emplacement area	0.000704	0.000107	7,174,831	0%	11/7	1.258	0.19
Rehandle material	0.000704	0.000107	1,434,966	0%	11/7	0.252	0.04

Option 3 – Sensitivity test for EFs with NPI (2012b) recommended values for batch loading operations on overburden, include activity of loading ore to and from main COS and storage location							
Loading waste to trucks	0.012	0.00179	827,705	0%	24/7	1.134	0.169
Emplacing waste at dump	0.0043	0.000859	827,705	0%	24/7	0.406	0.081
Loading crushed ore to main COS from underground	0.000704	0.000107	30,043,251	0%	24/7	2.415	0.366
Conveyor transfer points	0.000704	0.000107	30,043,251	70%	24/7	0.724	0.110
Ore processing in mill	0.000704	0.000107	150,216,255	0%	24/7	12.1&	1.83&
Loading crushed ore into trucks to feed main COS from storage*	0.012	0.00179	4,959,288	0%	24/7	6.79	1.01
Emplacing ore at storage location or main COS*	0.0043	0.000859	9,411,486	0%	24/7	4.62	0.923
Loading material to haul truck	0.012	0.00179	7,174,831	0%	11/7	21.4	3.20
Unloading material at emplacement area	0.0043	0.000859	7,174,831	0%	11/7	7.68	1.54
Rehandle material	0.012	0.00179	1,434,966	0%	11/7	4.29	0.64
Option 4 – Sensitivity test for EFs with NPI (2012b) recommended values for handling low moisture content ore from metalliferous mines, include activity of loading ore to and from main COS and storage location							
Loading waste to trucks	0.03	0.0043	827,705	0%	24/7	2.83	0.41
Emplacing waste at dump	0.03	0.0043	827,705	0%	24/7	2.83	0.41
Loading crushed ore to main COS from underground	0.03	0.0043	30,043,251	0%	24/7	103	14.7
Conveyor transfer points	0.03	0.0043	30,043,251	70%	24/7	30.9	4.42
Ore processing in mill	0.03	0.0043	150,216,255	0%	24/7	514[&]	74[&]
Loading crushed ore into trucks to feed main COS from storage*	0.03	0.0043	4,959,288	0%	24/7	17.0	2.43
Emplacing ore at storage location or main COS*	0.03	0.0043	9,411,486	0%	24/7	32.2	4.62
Loading material to haul truck	0.012	0.00179	7,174,831	0%	11/7	21.4	3.20
Unloading material at emplacement area	0.0043	0.000859	7,174,831	0%	11/7	7.68	1.54
Rehandle material	0.012	0.00179	1,434,966	0%	11/7	4.29	0.64

[&] Whilst emission rates for this source are provided in the table for comparison, this source will not be included in the sensitivity testing dispersion modelling for all loading and handling activities, because the basis for definition of this source is unclear and the emission rates are very large relative to the other loading and handling sources. However, the model results for this source will be presented as a separate activity.

4.3.6 Bulldozers

4.3.6.1 Emissions basis

The EFs for bulldozer activities applied in the TAS Reports are taken from NPI (2012b) and USEPA (1998):

$$EF_{TSP} = 2.6 \times s^{1.2} \times M^{-1.3}\ kg/h$$

$$EF_{PM_{10}} = 0.34 \times s^{1.5} \times M^{-1.4}\ kg/h$$

where s = silt content (%)
M = surface material moisture content

Equation 2

No equations are provided in either reference for $PM_{2.5}$, however Table 11.9-2 of USEPA (1998) recommends calculating the $PM_{2.5}$ emission rate by multiplying the TSP emission rate by a factor of 0.105.

Equation 2 is sensitive to the assumed silt and moisture content. Figure 4.5 shows the PM_{10} EF for loading and handling using Equation 2 as a function of moisture content and mean wind speed. The calculated EF is quite sensitive to moisture contents less than about 5%. The TAS reports assume a silt content of 5% and moisture content of 3.85%, however no justification is provided for these assumptions.

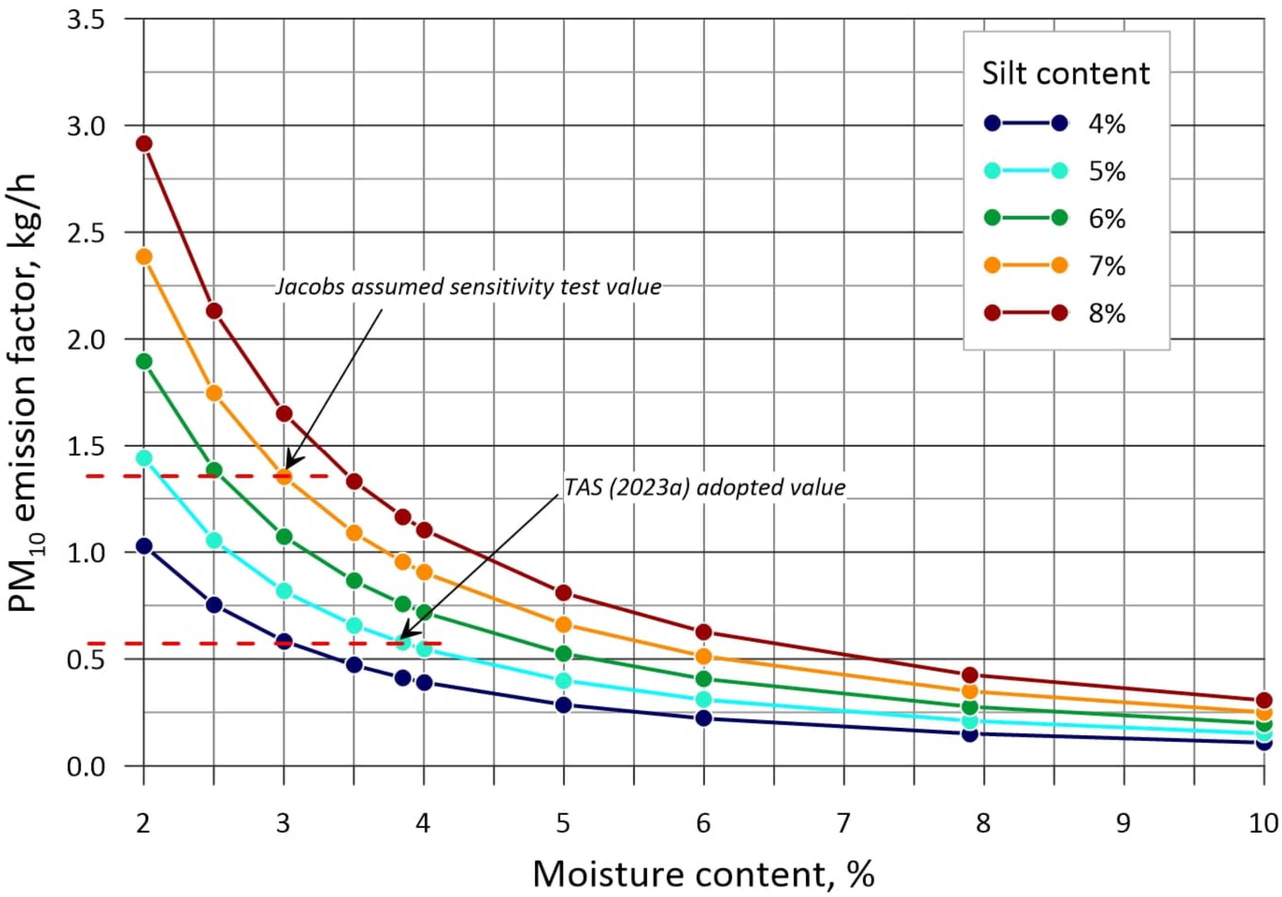

Figure 4.5: PM_{10} EFs for bulldozer activities, calculated from Equation 2, as a function of mean wind speed and moisture content.

Katestone (2011) explains that particulate matter emissions occur as a result of the bulldozer movement and the effect of the tracks finely grinding the soil or coal. Emissions of particulate matter are enhanced by the airflow generated by the bulldozer's cooling fans and diesel exhaust and if the bulldozer repeatedly traverses the same ground. The emission rate of particulate matter due to bulldozing is directly related to the number of hours of operation and is not a function of bulldozer speed or travel distance.

The emission rates for bulldozing activities used in HAS (2009), TAS (2020a) and TAS (2023a) have progressively increased, due to the assumed hours of bulldozer operation assumed in the reports:

- HAS (2009) - 6,515 h/a
- TAS (2020a) – 24,494 h/a
- TAS (2023a) – 410,301 h/a

The large increase in hours of bulldozer operation between TAS (2020a) and TAS (2023a) is due to use of bulldozers for TSF construction activities. The bulldozer activities are divided into three categories in TAS (2023a):

- Dozers working on waste rock dumps - 5,416 h/a
- General construction, and stripping topsoil - 404,885 h/a

4.3.6.2 Controls

No emissions reduction is applied in the TAS Reports for bulldozer activities. Katestone (2011) notes that there is very little information in the literature on minimising emissions of particulate matter from bulldozers, and that NPI states that there are no controls to reduce emissions from bulldozers working on coal or other materials. However, Katestone (2011) also comments that the NPI provides a 50% control factor for scrapers operating on topsoil when the soil is naturally or artificially moist and it is likely that a similar effect would be achieved for bulldozers if the working areas could be kept moist.

No controls are assumed for bulldozing activities in this report.

4.3.6.3 Emission rates proposed for modelling

The TAS Reports do not say whether all the bulldozing activities are assumed to operate 24/7. Jacobs has assumed that the bulldozers operate during daylight hours (11/7) in the same manner as applied to long haul loading and handling activities (Section 4.3.5.2).

The following options are recommended for emission sensitivity testing:

1. Base case – activity rates and emission factors as per TAS (2023a) Jan-Dec 2022 emission inventory, with 11/7 operation.
2. Sensitivity test for EFs from Equation 2 assuming the following:
   a. Lower moisture content, nominally assumed at 3.0%.
   b. Higher silt content, nominally assumed at 7.0%.
   c. Activity rates and operating hours same as Base case.

The EFs and rates assumed for bulldozing are summarized in Table 4.15.

Table 4.15: Emission Sensitivity Test Options for bulldozing

Activity	EF, kg/h		Activity intensity, h/a	Control efficiency	Assumed operating hours	Total emission rate, kg/h	
	PM_{10}	$PM_{2.5}$				PM_{10}	$PM_{2.5}$
Option 1 – Base case							
Waste dump area	0.576	0.326	5,416	0%	11/7	0.85	0.48
General and construction	0.576	0.326	404,885	0%	11/7	63.9	36.2
Option 2 – Sensitivity Test							
Waste dump area	1.073	0.562	5,416	0%	11/7	1.59	0.83
General and construction	1.073	0.562	404,885	0%	11/7	119.1	62.3

4.3.7 Graders

4.3.7.1 Emissions basis

The EFs for grader activities are a function of the kilometres travelled by the vehicles (vehicle-kilometres travelled, or VKT). The EFs applied in the TAS Reports are taken from NPI (2012b) and USEPA (1998):

$$EF_{TSP} = 0.0034 \times S^{2.5}\ kg/VKT$$

$$EF_{PM_{10}} = 0.0034 \times S^{2.0}\ kg/VKT$$

where S = vehicle speed (km/h)

Equation 3

No equations are provided in either reference for $PM_{2.5}$, however AP-42 (11.9, Table 11.9-2) recommends calculating the $PM_{2.5}$ emission rate by multiplying the TSP emission rate by a factor of 0.031.

Equation 3 is sensitive to the speed of grader operation, as shown in Figure 4-6. The TAS reports assume a grader speed of 8 km/h, however no justification is provided for this assumption.

AP-42 (Ch 11.9 Table 11.9-3) provides typical values for grader speeds of 8-19 km/h, with a geometric mean of 11.4 km/h. The value of 8 km/h assumed in the TAS reports is at the lowest end of this range.

The emission rates for grading activities used in HAS (2009), TAS (2020a) and TAS (2023a) have varied, due to the assumed kilometres travelled by graders in each emission inventory:

- HAS (2009) - 30,000 VKT/a
- TAS (2020a) – 38,889 VKT/a
- TAS (2023a) – 15,380 VKT/a

The reduction in kilometres travelled between the TAS (2020a) and TAS (2023a) inventories is not explained in the TAS Reports.

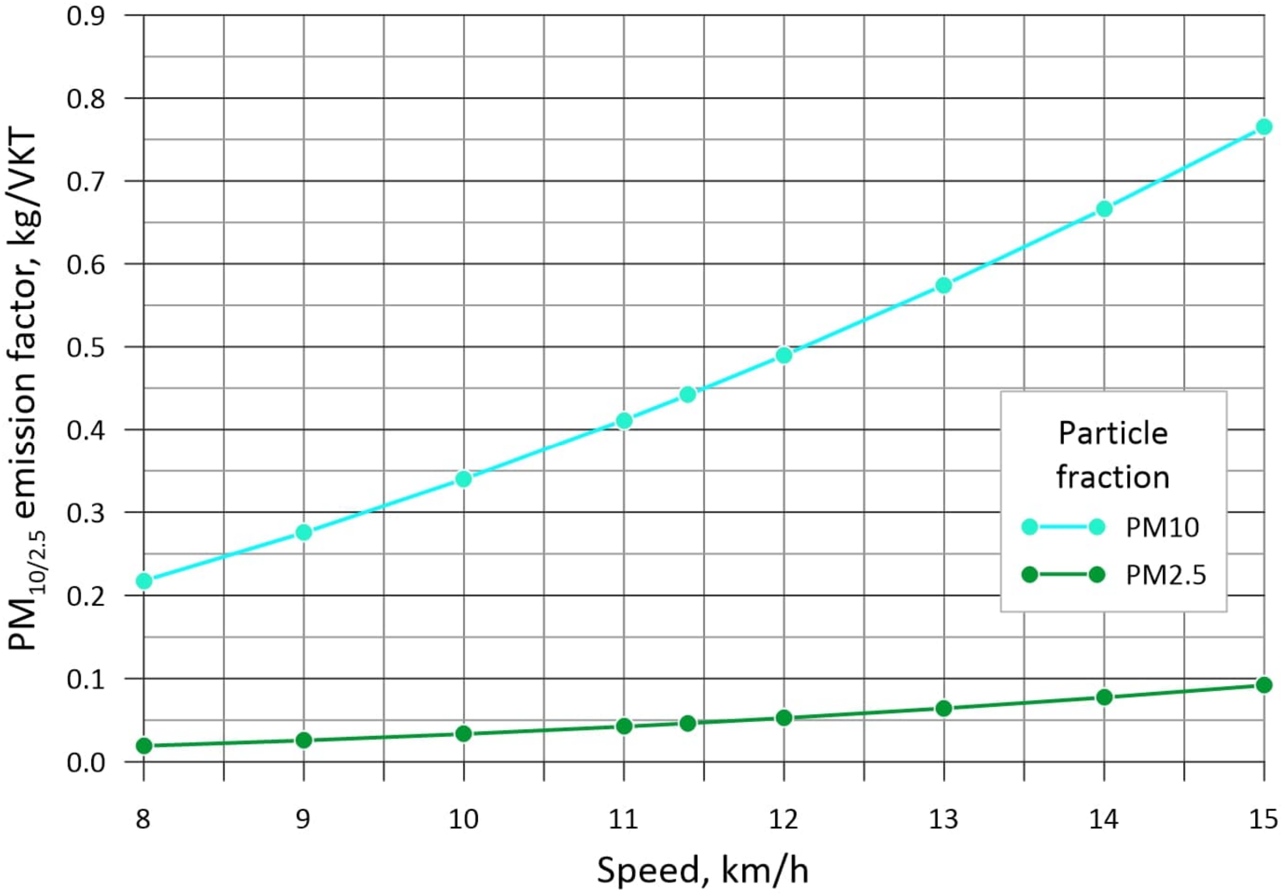

Figure 4-6. PM_{10} and $PM_{2.5}$ EFs for grader activities, calculated from Equation 3, as a function of vehicle speed.

4.3.7.2 Controls

No control efficiency is applied to grader emission rates in the TAS Reports. Jacobs has found no information in the literature on minimising emissions of particulate matter from graders, except for the obvious method of limiting vehicle speeds.

4.3.7.3 Emission rates proposed for modelling

The TAS Reports do not say whether all the grading activities are assumed to operate 24/7. Jacobs has assumed that the graders operate during daylight hours (11/7) in the same manner as applied to long haul loading and handling activities and bulldozers.

The following options are recommended for emission sensitivity testing:

1. Base case – activity rates and emission factors as per TAS (2023a) Jan-Dec 2022 emission inventory, with 11/7 operation.
2. Sensitivity test for EFs from Equation 3 assuming the following:
    a. Grader speed of 11.4 km/h (AP-42 geometric mean).
    b. Activity rates as per TAS (2020a).

The EFs and rates assumed for graders are summarized in Table 4-16.

Table 4-16. Emission sensitivity test options for graders

Activity	EF, kg/VKT		Activity intensity, VKT/a	Control efficiency	Assumed operating hours	Total emission rate, kg/h	
	PM_{10}	$PM_{2.5}$				PM_{10}	$PM_{2.5}$
Option 1 – Base Case	0.22	0.019	15380	0%	11/7	0.8	0.1
Option 2 – Sensitivity test	0.44	0.046	38889	0%	11/7	4.3	0.4

4.3.8 Vehicle-tracked dust emissions

4.3.8.1 Emissions basis

Emission rates from movement of vehicles on unsealed roads depend on the silt content of the road surface, the vehicle mass, and the number of kilometres travelled. The TAS Reports apply the EF formula from NPI (2012b) and USEPA (2006b), which is shown in Equation 4.

$$EF_{TSP} = \frac{0.4536}{1.6093} \times 4.9 \times \left(\frac{s}{12}\right)^{0.7} \times \left(\frac{W \times 1.1023}{3}\right)^{0.45} \; kg/VKT$$

$$EF_{PM_{10}} = \frac{0.4536}{1.6093} \times 1.5 \times \left(\frac{s}{12}\right)^{0.9} \times \left(\frac{W \times 1.1023}{3}\right)^{0.45} \; kg/VKT$$

where s = silt content of road surface material (%)
W = vehicle mass (tonnes)

For $PM_{2.5}$, for vehicle-tracked emissions the fraction recommended by USEPA (2006b) is 10% of PM_{10}.

Equation 4

The silt content assumed for Equation 4 has varied from 5% in HAS (2009), to 2% in TAS (2020a), and back to 5% in TAS (2023a). The rationale for the variations in assumed silt content is not provided in the TAS reports.

USEPA (2006b) provides a wide range of typical silt contents for unsealed industrial haul roads from less that 2% to more than 20%. Research conducted for the Australian Coal Association Research Program (ACARP, 2014) quoted data ranging from <2% to more than 9% (Figure 4-7) for surface samples collected from three mine sites in NSW. Samples were collected from uncontrolled and controlled (water application) surfaces, as well as permanent and temporary surfaces. ACARP (2014) states that a wide range of silt contents were measured, both when considering a single site, and across all sites. When the data were grouped by road type, there was no clear distinction between controlled or uncontrolled, permanent or temporary road surface. ACARP (2014) therefore recommended that site-specific silt data should be used as input to the emission equation.

The silt content of haul roads at the Cadia mine may vary across the site depending on the method of road construction and maintenance. Jacobs is not aware of any site-specific testing of haul road silt content at the Cadia mine.

Truck mass assumptions for the "W" variable as well as data for the distance travelled per year are also provided in the TAS Reports. The activity statistics for hauling from TAS (2023a) are provided in Table 4-17. Jacobs is not able to independently verify this data and assumes that this data is correct.

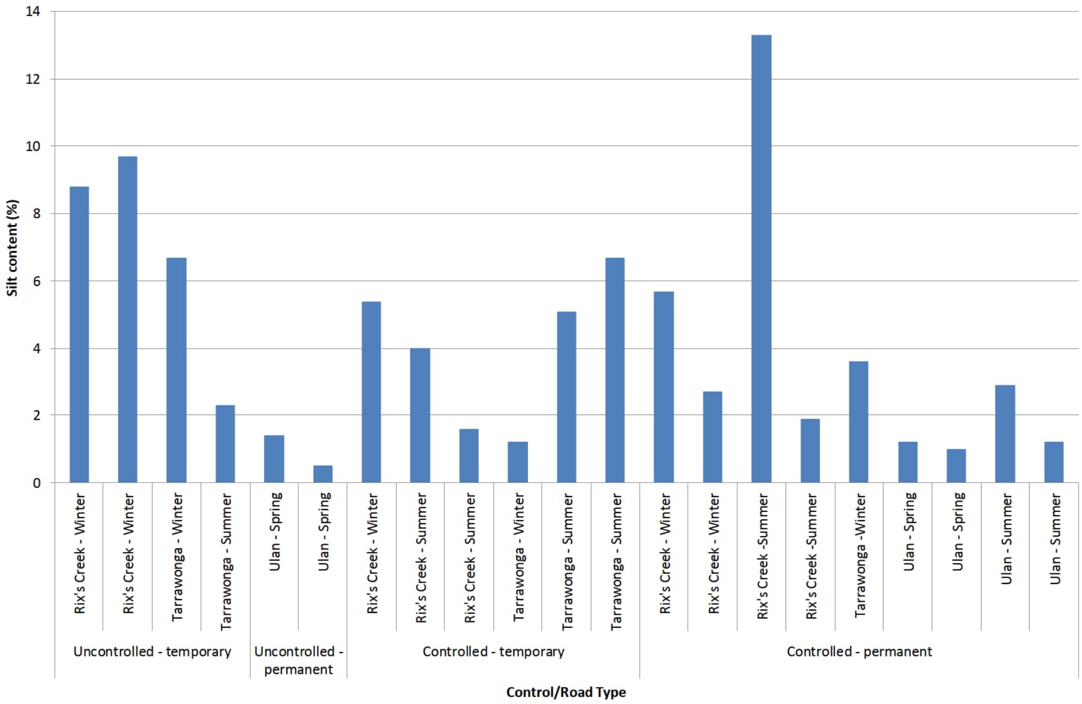

Figure 4-7. Silt content of roads sampled at NSW coal mines – from ACARP (2014).

Table 4-17. Activity data for hauling in TAS (2023a)

Road type	Mass carried per load	Loaded truck mass (average of loaded and unloaded journey leg)	Mass hauled per year	Journeys per year	Km travelled per load (return journey)	Total km travelled*
Long haul - Tailings contruction	199	244	7,174,831	36,054	17.4	627,347
Short haul to waste emplacement	199	244	827,705	4,159	3.92	16,305
Short haul stockpile to COS and return	157	225	9,411,486*	59,946	2.9	173,843

* Mass hauled over two-month period Jan-Feb 2023, multiplied by six to scale up to full year.

4.3.8.2 Controls

The TAS Reports assume an 85% control efficiency for vehicle-tracked emissions across the whole mine site. NPI (2012b) recommends the following controls for haul roads:

- 50% for level 1 watering (2 litres/m^2/h)
- 75% for level 2 watering (> 2 litres/m^2/h)
- 100% for sealed or salt-encrusted roads

Therefore, an assumption of 85% control is quite high and the rationale for applying this control level should be requested from CVO.

Jacobs observed the water trucks in operation at Cadia during the site visit, and the water application did appear to be quite successful at reducing visible dust emissions. However, during the site visit dust emissions were also observed from haul roads lacking water application (such as Picture A-9, Appendix A).

Since watering is the most effective method for control of haul road dust, it follows that emissions from vehicles travelling on unsealed roads would be lower after rainfall. To test for the effect of this, Jacobs recommends testing the effect on dispersion if emissions from haul roads are suppressed after rain. Whilst consideration of the amount and duration of rainfall required to reduce emissions and the influence of other factors such as temperature, humidity, and evaporation is outside the scope of this report, Jacobs has applied some nominal assumptions about rainfall in order to test whether the dispersion model is sensitive to this approach, and defines "rain days" as follows:

- Emission rates are reduced to zero for any given hour if there has been at least 2mm of rain in the last 24 hours, or 10mm of rain in the last 48 hours. Rainfall is determined based on hourly rainfall data from Ridgeway AQMS.

4.3.8.3 Emission rates proposed for modelling

The TAS Reports do not say whether all the hauling activities are assumed to operate 24/7. As with the loading and handling emission rates, Jacobs has assumed that short haul activities operate 24/7, and long haul activities operate 11/7.

The following options are recommended for emission sensitivity testing, and are also summarized in Table 4-18:

1. Base case – as TAS (2023a) Jan-Dec 2022 emission inventory:
   a. Silt content 5%
   b. No short haul activities between ore stockpile and COS
   c. Controls 85%
   d. No daytime weighting for short haul activities
2. Sensitivity test for daytime weighting – long haul activities 11/7, all other parameters as Option 1.
3. Sensitivity test for lower average silt content of 2%, all other parameters as Option 2.
4. Sensitivity test for higher average silt content of 6%, all other parameters as Option 2.
5. Sensitivity test for inclusion of short haul activities between ore stockpile and COS, all other parameters as Option 2.
6. As for Option 5, but sensitivity test for lower average control efficiency of 50%.
7. As for Option 6, but sensitivity test for exclusion of emissions on "rain days".

Table 4-18. Emission sensitivity test options for vehicle-tracked emissions

Option	Average silt content	Including short haul ore stockpile/COS route	Operating hours for long haul activities	Control efficiency
1. Base Case	5%	No	24/7	85%
2. Daytime weighting	5%	No	11/7	85%
3. Lower silt content	2%	No	11/7	85%
4. Higher silt content	6%	No	11/7	85%
5. Short haul ore included	5%	Yes	11/7	85%
6. Lower average control efficiency	5%	Yes	11/7	50%
7. Effect of excluding emissions on rain days[1]	5%	Yes	11/7	50%, + no emissions on rain days[1]

1. Emission rates are reduced to zero for any given hour if there has been at least 2mm of rain in the last 24 hours, or 10mm of rain in the last 48 hours. Rainfall is determined based on hourly rainfall data from Ridgeway AQMS.

4.3.9 Wind erosion

4.3.9.1 Emissions basis

Lift-off of particulate matter caused by wind erosion can develop in three stages as the surface wind speed increases (Katestone, 2011):

- Saltation: is the term adopted for the initial stage when particles begin to move on the surface prior to becoming airborne.
- Minor lift-off: refers to the stage where very fine particles become airborne.
- Major lift-off: refers to the stage where relatively large quantities of variable size particles become airborne.

The surface wind speeds that produce these stages of wind erosion depend on the nature of the erodible material. Materials that contain minimal amounts of finer particles or that have a large proportion of larger particles would tend to be more resistant to major lift-off as are materials that form a surface crust, whereas finer materials are characterised by relatively low surface wind speed thresholds for saltation, minor and major lift-off.

The threshold friction velocity is defined as the point at which wind erosion is initiated. The threshold friction velocity depends on the size distribution of surface particles, such that the larger the particles, the lower the potential for emissions. If the wind speed near the surface of the erodible materials is less than the threshold friction velocity, particulate emissions would not occur. Conversely, if the wind speed is greater than the threshold friction velocity particulate emissions would occur.

As the wind speed increases, particulate emissions increase rapidly, roughly in proportion with the cube of the wind speed increase (for example, if the wind speed increases 2-fold, the emission rate increases 8-fold) (Skidmore and Hagen, 1977).

4.3.9.1.1 Estimation Method 1

The EF equation for wind erosion in NPI (2012b) for active coal stockpiles is:

$$EF(TSP) = 1.9 \times (\frac{s}{1.5}) \times 365 \times (\frac{365 - p}{235}) \times (\frac{f}{15})\ kg/ha/y$$

where	s =	silt content (%)
	p =	number of days per year when rainfall is greater than 0.25 mm
	f =	percentage of time that wind speed is greater than 5.4 m/s at the mean height of the stockpile. WRAP (2006) advised that f should be calculated from short term averages such as a 2-minute wind gust

Equation 5

Equation 5 is derived from earlier editions of USEPA (2006a) up to 1988 but is not included in later versions of that reference.

NPI (2012b) also states that the same emission estimation equation can be used for characterizing emissions from other exposed areas, and recommends that the following default values be applied in the absence of other information:

- 0.4 kg/ha/h for TSP
- 0.2 kg/ha/h for PM_{10}.

AP-42 (Ch13.2.5) recommends applying 7.5% of TSP for the $PM_{2.5}$ EF from wind erosion.

The TAS Reports apply these default EFs for wind erosion at Cadia. However, the TAS Reports do not say if the hourly emission rates are weighted according to the wind speed (and if so, what weighting regime is used) or whether these EFs are applied constantly for each hour of the year.

4.3.9.1.2 Estimation Method 2

The default EF of 0.4 kg/ha/h in NPI (2012b) comes from SPCC (1983). SKM (2005) explains that the SPCC (1983) factor was not based on measurements, but is likely an estimate using Equation 5 and typical Hunter Valley values with a silt content of 7%, number of rain days (80) and with 13.4% of the wind greater than 5.4 m/s. Therefore, the default value is highly specific to a location and ore type.

Instead of applying the default Hunter Valley values, location-specific values for s, p and f can be substituted into Equation 5:

- s - the silt content will vary across the Cadia site depending on the type of surface. The potential silt content of haul roads was discussed in Section 4.3.8. The silt content of the TSFs is unknown, and is likely to be higher than from the haul roads.
- p – the days per year with rainfall above 0.25mm measured near Cadia is shown in Table 4-19. The lower rainfall during drought years 2017-2019 is clearly visible in the data. Based on this data, a value of p of about 70 would represent a dry year at Cadia, a value of about 100 would represent an average year, and a value of about 135 would represent a wet year.
- f - the frequency of wind speeds exceeding 5.4 m/s at the AWS near Cadia is shown in Table 4-20. A value of about 25-27% appears to be representative of the Cadia environment, based on the average SLB wind speeds. A value of 25% was adopted by Jacobs for the sensitivity tests.

The effect of s%, p and f% on the emission factor is shown in Figure 4-8. As the EF is linearly dependent on p, the EF calculated for a dry year (such as 2017-2019) with 70 days of rain per year is 1.9 times higher than the EF for a wet year such as 2022 with 135 days of rain per year.

The values of s, p, f and the resulting EF for this sensitivity test are summarized in Table 4-21.

Table 4-19: Rainfall measured near Cadia – days per year with rainfall greater than 0.25mm

Calendar year	AWS Location		
	Orange Airport	Ridgeway	SLB
2015	114		
2016	121		
2017	76	68	66
2018	78	73	67
2019	71	69	97
2020	105	96	103
2021	129	89	115
2022	139	135	131

Table 4-20: Frequency of wind speeds measured near Cadia exceeding 5.4 m/s

Calendar year	AWS Location			
	Orange Airport 1-hour average wind speeds	Ridgeway 1-hour average wind speeds	Ridgeway 10-minute average wind speeds	SLB 1-hour average wind speeds
2015	26%	23%	24%	n/d*
2016	31%	25%	26%	n/d*
2017	27%	23%	24%	26%
2018	29%	25%	25%	29%
2019	30%	24%	24%	28%
2020	29%	27%	28%	30%
2021	28%	24%	24%	24%
2022	28%	24%	24%	26%
Average, 2017-2022	28.6%	24.4%	24.8%	27.1%

* data not available

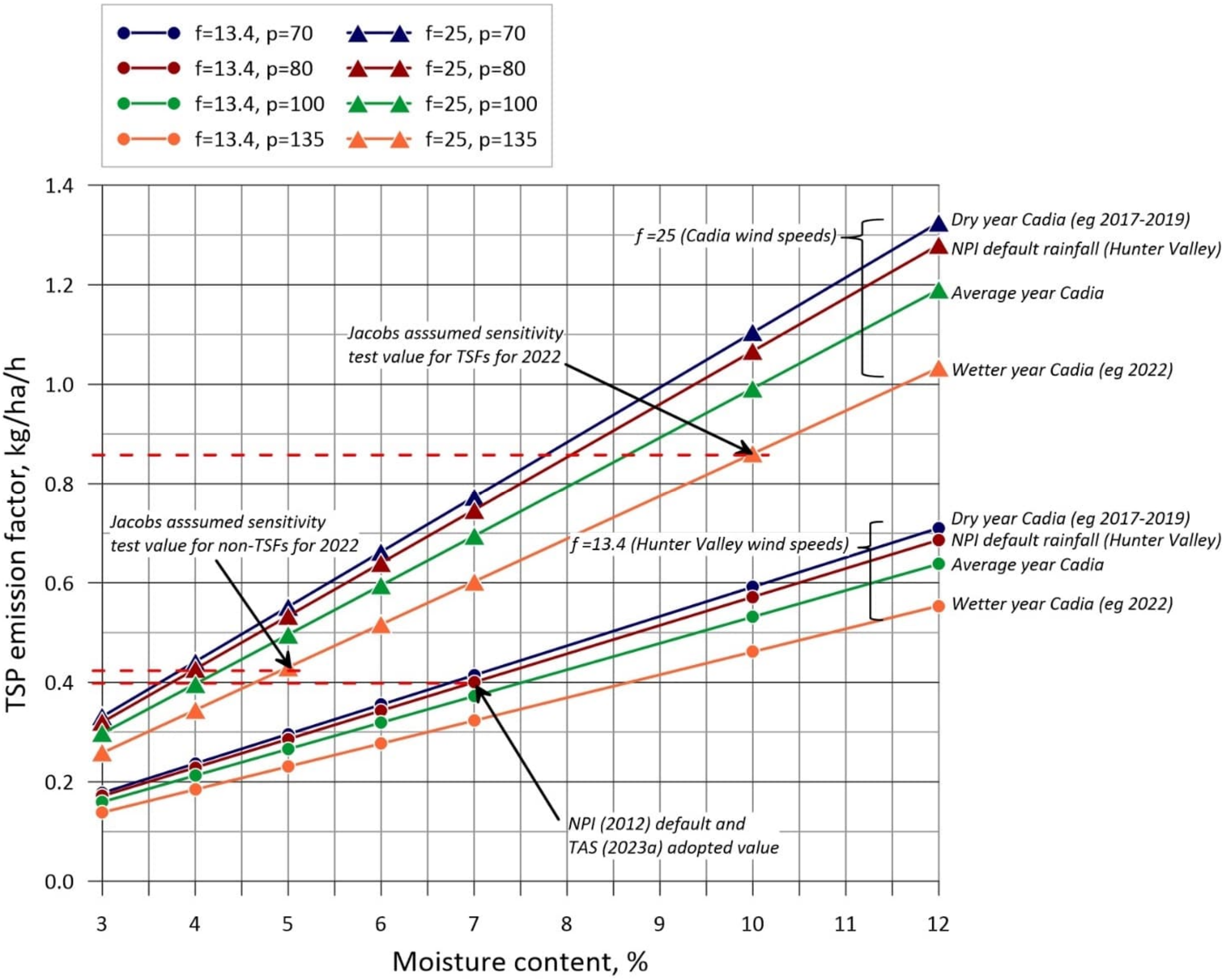

Figure 4-8. Effect of s%, p and f% on wind erosion EF.

Table 4-21. Summary of uncontrolled EFs calculated for Estimation Method 2.

Source type	Assumed parameters for Equation 5			Percentage of TSP that is PM_{10}	Uncontrolled EF (kg/ha/h)
	S(%)	p	f(%)		
TSFs	10	135*	25	50%	0.43
Non-TSFs	5	135*	25	50%	0.215
NPI (2012) default and TAS (2023) values	7	80	13.4	50%	0.20

* p value representing a “wetter” year applied, because the model is based on 2022 emissions.

4.3.9.1.3 Estimation Method 3

Equation 5 provides an annual EF as a function of rainfall days, but no recognition of whether the rainfall is seasonal or not. The original derivation of Equation 5 is discussed in Bohn et al (1978). The denominator of 235 in Equation 5 derives from the original measurement research, to adjust to an annual period for the number of wet days during the test period. "Wet days" is defined in that context as measurable rain, more than 0.01 inch or 0.25mm.

Bohn et al (1978) also suggests that p can be set to zero to give a dry emission factor. A control factor then needs to be applied if there has been sufficient rain to suppress wind erosion. Jacobs considers that using the "wet days" definition from the original Equation 5 may not be suitable, for several reasons:

- A small amount of rain (say, 0.5mm) is unlikely to control wind erosion for long in the Cadia environment, particularly if that rain occurred much earlier in the day.
- If the rain occurred late in the day then the controls should not apply to earlier hours.
- A large amount of rain on previous day(s) may continue to exert a control that would not be recognized by this "wet days" definition.

Therefore, Jacobs has tested the control factor for the sensitivity test with p=0 in Equation 5 by applying the "rain days" weighting introduced in Section 4.3.8.2. As noted in that section, this "rain days" weighting requires some nominal assumptions about rainfall and should only be considered as a test whether the dispersion model is sensitive to this approach and whether further investigation is warranted.

The values of s, p, f and the resulting EF for this sensitivity test are summarized in Table 4-22.

Table 4-22. Summary of uncontrolled EFs calculated for Estimation Method 3.

Source type	Assumed parameters for Equation 5			Percentage of TSP that is PM_{10}	Uncontrolled EF (kg/ha/h)
	S(%)	p	f(%)		
TSFs	10	0	25	50%	0.685
Non-TSFs	5	0	25	50%	0.342

4.3.9.1.4 Estimation Method 4

The final emission estimation method tested for wind erosion uses the friction velocity equation from NPI (2012b) shown in Equation 6. This estimation method was only tested for the TSFs, due to the large dust emission risk associated specifically with that source.

This method recognizes that mean atmospheric wind speeds are not sufficient to sustain wind erosion from flat surfaces, and estimated emissions should be related to wind gusts of highest magnitude. If wind speeds are below the threshold friction velocity, then emissions are set to zero.

$$P = 58\,(u^* - u_t)^2 + 25(u^* - u_t) \text{ for } u^* \geq u_t$$

$$P = 0 \text{ for } u^* \leq u_t$$

where p = erosion potential, g/m^2
$u^* = 0.053\, u_{10+}$
u_{10+} = fastest mile of reference anemometer of period between disturbances (m/s)

Equation 6

Collating discussion from WRAP (2006), USEPA (2006a), SKM (2005), and NPI (2012a) the wind speed for u_{10+} in this equation should be calculated from the 2-minute wind guest, or 1.18-1.27 times the hourly wind speed in the absence of any gust data.

Jacobs does not have gust data available for the SLB AWS, but does have gust data for Ridgeway AWS for February 2022 to September 2023 and gust data and 2-minute average data for Orange Airport for January 2019 – September 2023. Analysis of available gust, 2-minute average, 10-minute average and 60-minute average data for Orange Airport and Ridgeway AWS with a focus on hourly-average wind speeds exceeding 8 m/s revealed that:

- Ratio of 2-min max speed:60-min average speed at Orange Airport) is a factor of about 1.25.
- Ratios of gust to 10-min and 60-min speeds at Ridgeway are about 1.125x higher than at Airport.
- Therefore, it is inferred that the ratio of 2-min max speeds:60-min average speeds at Ridgeway and SLB might also be about 1.125x higher than at Airport.
- Overall therefore, the ratio of 2-min speed to 60-min speed at Ridgeway and SLB is assumed to be about 1.4 (=1.25 x 1.125).

Therefore, in Equation 6 u_{10+}, the highest 2-minute average wind speed in the hour, was taken to be 1.4x the hourly average wind speed.

Figure 4-9 shows the calculation of the EF using Equation 6 and assumed values for u_t of 0.4 to 0.8.

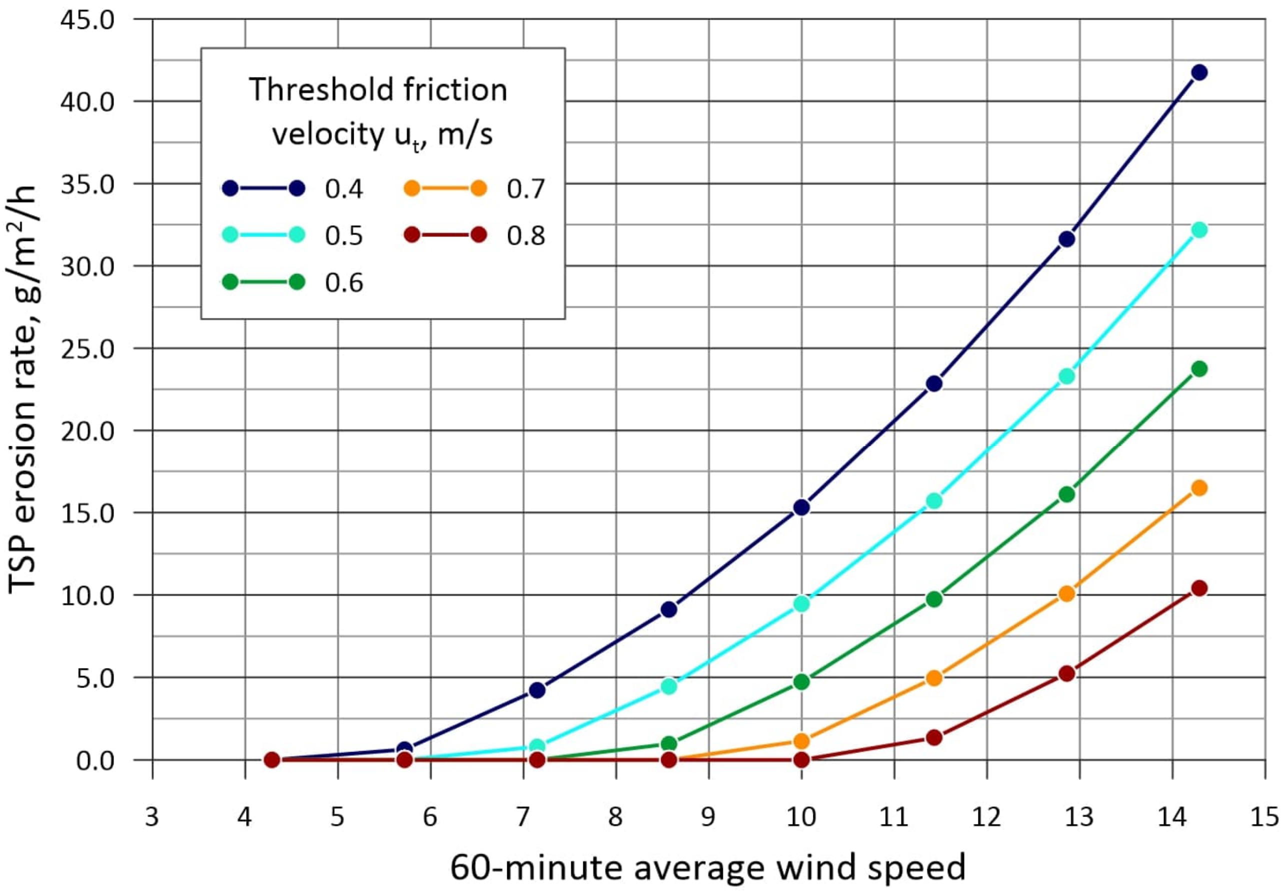

Figure 4-9. Emission factors calculated using friction velocity equation for various wind speeds and assumed values of threshold friction velocity.

The threshold friction velocity parameter, u_t, was tested for three different values of 0.4, 0.5 and 0.6 to test how the model simulates a dust event during high wind speeds. Higher values of u_t shown in Figure 4-9 were not tested as these predict low levels of dust emissions during 60-minute average wind speeds of 8-10 m/s which does not correlate with observed trends as discussed in Section 3.4.

4.3.9.2 Controls

The potential for dust emissions from wind erosion can be reduced through applying water and/or chemical suppressants to the exposed surface, stabilizing the surface with covers, grass, or large-diameter aggregate, land rehabilitation, or by providing shelter to reduce localized wind speeds. These measures are all applied at Cadia with varying effectiveness depending on the type and location of the exposed surface.

NPI (Fugitive Dust, 2012b) provides reduction factors for a variety of control measures for open area wind erosion (replicated in Table 4-23), although the reference recommends that once a control strategy is implemented on-site, dust monitoring should be performed to determine the actual reduction in emissions.

Table 4-23. Percentage reduction to emission factors for open area wind erosion with control systems, from Table 6 of NPI (2012b).

Control method	Factor reduction (%)
Apply dust suppressants to stabilize disturbed area after cessation of disturbance	84
Apply gravel to stabilize open areas	84
Primary rehabilitation	30
Vegetation established but not demonstrated to be self-sustaining – weed control and grazing control	40
Secondary rehabilitation	60
Revegetation	90

TAS (2021) assumed the following for dust control from the TSFs:

- With normal operation of the TSFs the potential dust emissions from the surface would be approximately half due to the moisture of the material and when not in operation (i.e. dry) would likely generate the full amount of dust emissions.
- To account for the application of dust suppressant applied to the TSF surface, it was a assumed the potential dust emissions would be reduced by approximately a third (a factor of 30% reduction appears to have been used).

TAS (2023a) applied a slightly different approach, stating that *"The dust mitigation measures implemented by [CVO] to reduce potential dust emissions on the TSF surfaces have been considered in this assessment (which included mitigation of 50%)"*. However, no controls are stated in the emission inventory data in Table A-2 of TAS (2023a), and the annual TSP, PM_{10} and $PM_{2.5}$ emission loads due to wind erosion from the TSFs in Table 5-4 of TAS (2023a) do not account for any controls. Therefore, it is not clear if any controls were applied in TAS (2023a) or not.

4.3.9.3 Emission rates proposed for modelling

Jacobs modelled wind erosion from three categories of open areas:

1. TSFs, excluding wet areas of TSFs.
2. Dry areas around TSFs

3. Processing and other areas

Stockpiles were treated in the same manner as flat open areas.

The areas allocated to each of these source types are shown in Figure 4-10. These areas were drawn by Jacobs off the Cadia mine georeferenced aerial image provided by CVO and shape files provided by Cadia showing the locations of different site activities.

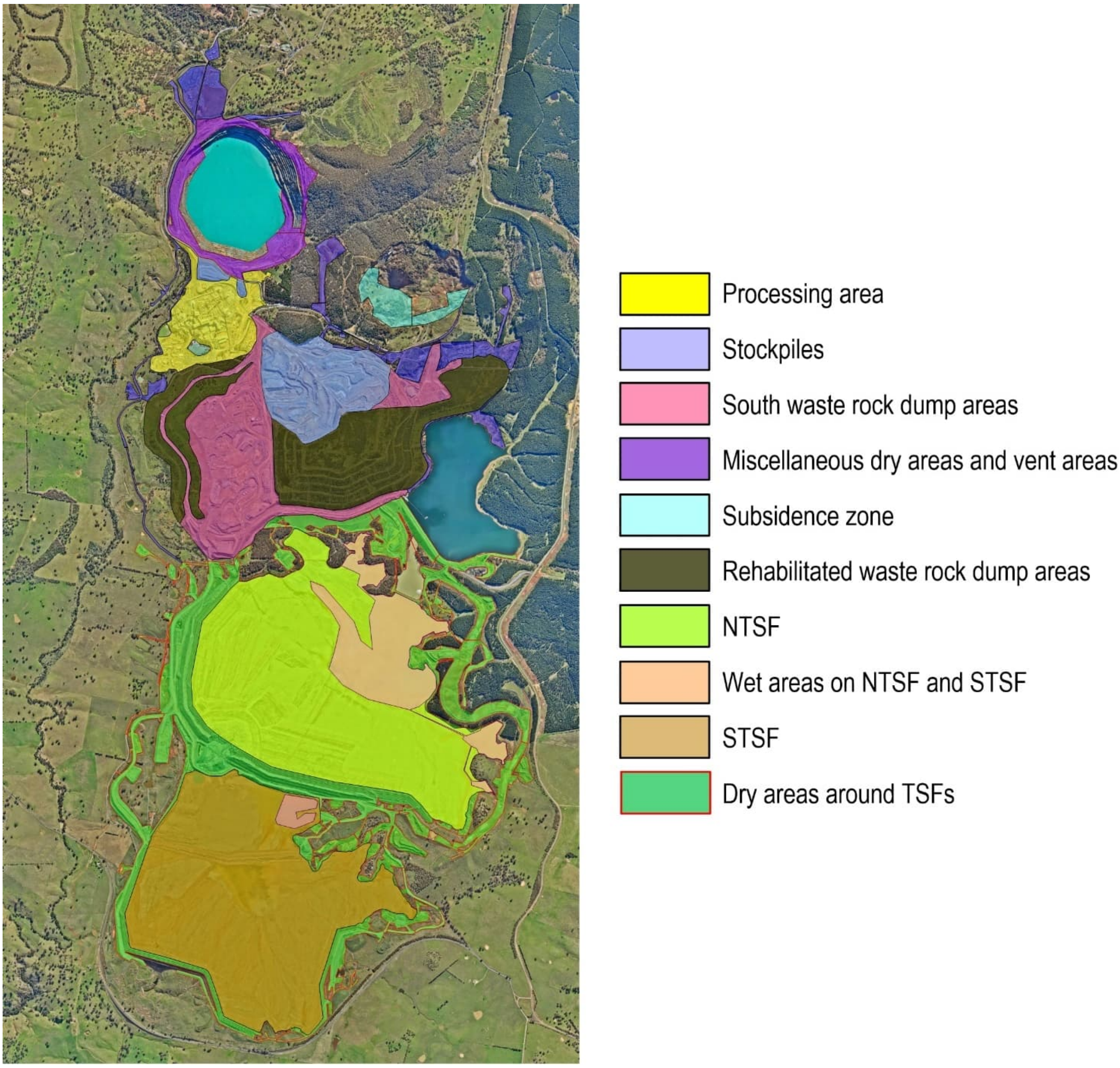

Figure 4-10. Open area wind erosion sources.

The dimensions of each area type defined in TAS (2023a) and measured by Jacobs are listed in Table 4-24. Jacobs applied the areas measured by Jacobs in the emission inventory and dispersion model set-up for wind erosion sources.

Table 4-24. Source areas for wind erosion.

Area description in TAS (2023a)	Surface area of source (ha) used in TAS (2023a)	Area measured by Jacobs (ha)	Jacobs comments
Waste rock dumps	262	156	Assume rehabilitated rock dumps have no dust erosion. The two areas of active waste rock dumps total 156 ha.
Pit tailing storage facility	64	48	Full pit surface area is 151 ha including the water surface. 48 ha is the estimated dust potential area.
Subsidence zone	96	22	Subsidence zone dust potential area appears to be about 22 ha, and total about 50 ha. Unknown whether TAS (2023a) included any other subsidence zones.
Plant stockpiles and exposed areas	249	233	Processing area is 65 ha. Other stockpiles 92 ha. Other miscellaneous exposed areas 76 ha.
Tailings storage facilities	827	707	Area of NTSF and STSF = 441 + 370 = 811 ha, if include wet areas. Wet areas = 104 ha. Total dust potential area therefore is 707 ha
Tailings construction area	211	311	Unclear what this area is defined as in TAS Reports. Jacobs measured dry area fully around TSFs = 1122 ha incl TSFs, = 311 ha without TSFs
TOTAL	**1709**	**1477**	

The following options are recommended for emission sensitivity testing, also summarized in Table 4-25:

1. Base case
   a. All sources emitting PM_{10} at 0.2 kg/ha/h, constant 24/7
   b. No wind speed weighting
   c. No controls
2. Sensitivity test for wind speed weighting:
   a. As Option 1, except that the annual mass emission of PM_{10} is distributed across the full hours of the year in proportion with the cube of the 60-minute average wind speed measured at SLB AWS.
3. Sensitivity test for adding controls to Option 2, using the following assumed control efficiency representing the combined effect of water or chemical application, surface treatments, land rehabilitation and sheltering:
   a. TSFs, 50%
   b. Dry areas around TSFs, 70%
   c. Processing and other dry areas, 70%.
4. Sensitivity test for rain days, using Option 3 with the addition of emissions being omitted on “rain days” as defined in Section 4.3.8.2.
5. Sensitivity test for Estimation Method 2 - applying site-specific values of s, p and f in Equation 5, using the same assumed control efficiency as Option 3.

6. Sensitivity test for Estimation Method 3 - assumption of p=0 with same assumed control efficiency as Option 3 plus no emissions on "rain days".

7. Sensitivity test for Estimation Method 4 –friction velocity approach using Equation 6. Only tested using TSFs areas, and no controls assumed as the purpose of the test is to trial whether the dispersion model will simulate a dust event similar to observed events over 2018-2021.

    a. Option 7(a) - u_t assumed to be 0.4 m/s for Equation 6.

    b. Option 7(b) - u_t assumed to be 0.5 m/s for Equation 6.

    c. Option 7(c) - u_t assumed to be 0.6 m/s for Equation 6.

Table 4-25. Emission sensitivity test options for open area wind erosion

Option	Emission Estimation Method	Cubed wind speed weighting applied?	Controls applied for watering, surface treatments, shelter?	"Rain days" [2] control applied?
1. Base Case	1	No	No	No
2. Wind speed weighting	1	Yes	No	No
3. Controls	1	Yes	Yes	No
4. Rain days assumption	1	Yes	Yes	Yes
5. Site-specific values of s, p and f	2	Yes	Yes	No
6. Assume p=0	3	Yes	Yes	Yes
7a. Friction velocity equation	4 u_t = 0.4m/s	No[1]	No[1]	No[1]
7b. Friction velocity equation	4 u_t = 0.5m/s	No[1]	No[1]	No[1]
7c. Friction velocity equation	4 u_t = 0.6m/s	No[1]	No[1]	No[1]

1. Wind speed weighting is inherent in calculation approach. Only TSFs modelled for these options, with no controls applied.

2. Emission rates are reduced to zero for any given hour if there has been at least 2mm of rain in the last 24 hours, or 10mm of rain in the last 48 hours. Rainfall is determined based on hourly rainfall data from Ridgeway AQMS.

5. Modelling Methodology

5.1 Introduction

Dispersion modeling uses mathematical formulations to characterize the atmospheric processes that disperse a pollutant emitted by a source. Based on emissions and meteorological inputs, a dispersion model can be used to predict concentrations at selected downwind receptor locations.

Advanced dispersion models such as the CALPUFF model used for CVO allow meteorological conditions to vary across the modelling domain and up through the atmosphere. This is a complex situation that requires complex and realistic meteorological data inputs, usually over a 12-month period or multiple years if required by the regulator. Approved Methods requires “at least one year of site-specific meteorological data” for a “Level 2” impact assessment which is the type of assessment used for CVO.

Because meteorological sites do not provide the relevant data at every point in the modelling domain, a meteorological model is used to predict and provide the meteorological variables at sites where information is not available. The CALPUFF dispersion model then uses this pre-processed meteorological data for analysis.

In the following sections the preparation of the meteorological data, which is processed by a model called CALMET, is described separately to the CALPUFF dispersion model inputs.

Guidance on running CALMET and CALPUFF for modelling applications in New South Wales was prepared for the NSW EPA by TRC Environmental Corporation (OEH, 2011). Since its publication, the guidance in OEH (2011) has become widely adopted by consultants in Australia and New Zealand as a best practice guideline for CALMET and CALPUFF modelling. The guidance in that document was followed in the preparation of CALMET and CALPUFF in this report.

5.2 Methodology in TAS Reports

5.2.1 TAS (2020a)

The following methodology was adopted for the model inputs in TAS (2020a):

1. CALMET
    a. 2017 calendar year was used based on an analysis of data trends in meteorological data recorded and appropriate monitoring data for the area.
    b. Hybrid approach for meteorological inputs to CALMET, using the TAPM prognostic model plus surface observations
    c. TAPM grids of 30km 10km 3km and 1km, and 35 vertical grid levels
    d. CALMET single domain of 30x30km with 0.3 km grid resolution
    e. Surface observations incorporated from SLB AWS, Ridgeway AWS, Orange Airport AWS, and Bathurst AWS although the Bathurst AWS would have had no influence on model results due to its long distance from CVO.
    f. TERRAD (terrain radius of influence weighting) 10 km
    g. R1 and R2 (surface and upper air observations relative weighting factor) 8 and 8 km
    h. RMAX1 and RMAX2 (surface and upper air observations radius of influence) 10 and 10 km

2. CALPUFF
    a. Emission sources simulated as volume sources
    b. No information provided on volume source dimensions
    c. No information provided about whether any CALPUFF dispersion parameters were varied from default settings.
    d. Annual average background concentrations assumed to be the difference between a measured concentration at TEOM location, and the predicted model concentration at that location. Methodology not clear as to how 24-hour background concentrations were subsequently estimated.
3. Assumed controls on emission sources:
    a. Both NTSF and STSF conservatively modelled as unmitigated emission (whole surface available as a wind erosion source with no controls)
    b. The effect of the precipitation rate (rainfall) in reducing dust emissions was not considered
    c. One operating scenario considered – representing the Modification 14 application including production rate increase and construction works on the NTSF and STSF
    d. "Reasonable best practice dust mitigation" assumed applied where feasible.

5.2.2 TAS (2021)

1. CALMET
    a. 2017 – mid 2021 period modelled.
    b. All other inputs same as TAS (2020a)
2. CALPUFF
    a. Emission sources and extent of information supplied same as TAS (2020a).

5.2.3 TAS (2023a)

1. CALMET
    a. January 2022 to February 2023 period modelled.
    b. All other inputs same as TAS (2020a)
2. CALPUFF
    a. Emission sources and extent of information supplied same as TAS (2020a).
    b. Included four ventilation shafts (VR3A, VR5, VR7, and VR8) as point sources.
    c. Background concentrations calculated by a new method, see Section 5.7.
3. Assumed controls on emission sources:
    a. Both NTSF and STSF modelled with 50% emission reduction assumed due to controls
    b. The effect of the precipitation rate (rainfall) in reducing dust emissions was not considered
    c. One operating scenario considered – representing the Modification 14 application including production rate increase and construction works on the NTSF and STSF
    d. "Reasonable best practice dust mitigation" assumed applied where feasible.

In September 2023 NSW EPA requested that the model input files created by TAS for the modelling in TAS (2023a) be provided, as there are many model input settings that were not stated in the report (see also Section 5.3). However TAS (2023b) stated that "*TAS policy is to immediately delete modelling files due to size and to protect its intellectual property. The requested files cannot be provided as they do not exist*". This is surprising, as in Jacobs' experience it is normal practice for modelling files prepared as part of a regulatory application to be supplied on request for review to confirm the inputs into the model. This is also a requirement in Approved Methods.

Whilst it is correct that some modelling files are very large, the input files are actually quite small. This is an extreme and unusual approach that restricts the potential for quality control and retrospective checking of model inputs, and is contrary to the requirements in Approved Methods. The approach is not supported by Jacobs.

5.3 CALMET

5.3.1 Settings

The CALMET model was run in "hybrid mode", using a combination of surface observations and upper air simulations from The Air Pollution Model (TAPM) (Hurley, 2008).

TAPM predicts three-dimensional meteorology, including terrain-induced circulations. TAPM is a prognostic meteorological model that uses databases of terrain, vegetation and soil type, leaf area index, sea-surface temperature, and synoptic-scale meteorology analyses for various regions around the world. TAPM is used to predict meteorology parameters at both ground level and at heights of up to 8000 m above the surface.

A summary of settings applied for TAPM is provided in Table 5-1. The settings used by Jacobs for TAPM appear to be the same as those used in the TAS Reports, however some of the input settings listed in Table 5-1 are not stated by TAS.

The settings applied for CALMET are provided in Table 5.6, including the comparative settings used in TAS (2023a), where such information is available.

In Table 5.6, only some of the settings used by Jacobs and TAS can be compared due to the limited information provided by TAS. For the parameters that can be compared, the settings used by Jacobs and TAS for CALMET are the same for some parameters, but vary for others.

Table 5-1. Summary of input settings for TAPM

Parameter	Description
Model version	4.0.5
Number of grids (spacing)	4 nested grids, grid spacings 30000m, 10000m, 3000m, 1000m
Number of grid nodes in each grid	35 in both N-S and E-W directions, and 30 vertical levels.
Simulation period	25 Dec 2021 to 31 Dec 2022 (only data from 1 January 2022 used in CALMET)
Terrain information	AUSLIG 9 second (TAPM default database)
Centre of analysis	Centre co-ordinate 33° 29'S, 149° 0'E
Local data assimilation	Not included
Advanced options	All retained at default settings

Table 5-2. Summary of input settings for CALMET

Parameter	Settings used by Jacobs	Settings used by TAS (2023a)
Model version	6.5.0	Not stated
Graphical user interface	Lakes Environmental CALPUFF View	Not stated
Grid size and resolution	100 x 100 grid cells, cell size 300m	Same as Jacobs
Time Step	3600 seconds	Not stated
Vertical levels	10 levels 0, 20, 40, 80, 160, 320, 640, 1200, 2000, 3000, 4000m	Not stated
Terrain information	Imported from global SRTM1 database supplied with CALPUFF View package (approximately 30m resolution)	Not stated
Land use data	Determined in CALPUFF View based on land use codes drawn directly over an aerial map.	Not stated
TERRAD	4 km	10 km
Wind field settings ▪ R1, R2 ▪ RMAX1, RMAX2	 10, 10 km 12, 12 km Varying radius of influence = True	 8, 8 km 10, 10 km Not stated
Surface station inputs	▪ Wind speed and direction – Ridgeway, SLB, Orange Airport ▪ Temperature, humidity and station pressure - Ridgeway, SLB, Orange Airport ▪ Cloud cover – Orange Airport ▪ Relative humidity, cloud used from surface data rather than prognostic	▪ Ridgeway, SLB, Orange Airport, Bathurst ▪ Ridgeway, SLB, Orange Airport, Bathurst (except no pressure for Bathurst) ▪ Orange Airport ▪ Not stated
Wind direction averaging	▪ 1-hour averages for Ridgeway calculated using vector method in USEPA (2000) from 10-minute as-received raw data ▪ 1-hour averages for SLB used as-received, filtered to remove anomalies derived from potential issue with averaging method (as described in Section 3.2.2.2) ▪ 1-hour averages for Orange Airport calculated using vector method in USEPA (2000) from 1-minute as-received raw data	Not stated
Surface wind vertical extrapolation	IEXTRP = -4	Same as Jacobs

Layer-dependent surface and upper air station bias	Zero at all levels (default setting)	-1, -0.5, -0.25, 0, 0, 0, 0, 0
Use of prognostic data	As initial guess field	Not stated
Other advanced options	All retained at default settings	Not stated

OEH (2011) notes that when using CALMET with observational data, there are seven critical parameters which must be carefully assessed and which are unique to every application. These parameters are TERRAD, RMAX1, RMAX2, R1, R2, IEXTRP and BIAS.

Jacobs and TAS have applied similar values for RMAX1, RMAX2, R1, and R2, and the same setting for IEXTRP. Different values have been assumed for TERRAD, and for BIAS.

The BIAS setting is a vertical layer-dependent weighting factor of surface vs. upper air wind observations in defining the Initial Guess Field (IGF) winds. The IGF is the initial guess of the wind vector at each grid point in the model domain and at each vertical level, which is then adjusted at each point for terrain influences (according to the TERRAD setting) and observation influences (according to the R1, R2, RMAX1 and RMAX2 settings). In this application, the IGF winds have been defined by the TAPM prognostic outputs, and there are no upper air wind observations. Jacobs prepared preliminary CALMET models to compare CALMET outputs for the default BIAS settings (used by Jacobs) versus the settings used by TAS (2023a), and found that the model was insensitive to the BIAS settings applied.

The TERRAD setting is the "terrain radius of influence", or the distance that CALMET "looks" from any given grid point to decide whether terrain influences the wind at that particular grid point. TERRAD should not be too small otherwise nearby valley walls which contribute to the slope flow will not be seen. On the other hand TERRAD must not be so large that hills more than one valley away is seen. Guidance provided in OEH (2011) indicates that TERRAD can be estimated as the typical ridge-to-ridge distance divided by two, and usually rounded up. OEH (2011) also notes that typical values of TERRAD are between 5-15 km with an upper limit of about 20 km, however this does depend on grid resolution and the particular site being modelled. In modelling situations with complex terrain and sensitive receptors, Jacobs has found it beneficial to use values of TERRAD at the low end of this range, relying on the TAPM IGF to incorporate the larger scale terrain effects.

Jacobs selected a TERRAD value of 4 km, noting that many of the valleys around CVO that may influence the behaviour of the wind field between CVO and the sensitive receptors are about 7-10 km across (Figure 5-1). A TERRAD value of 10 km, as used in the TAS Reports, which is equivalent to a ridge-to-ridge distance of 20 km on Figure 5-1, may miss the influence of these smaller terrain variations. Given the lack of meteorological observations in the southeast quadrant of the model domain, the CALMET model (and therefore also the CALPUFF dispersion model) may be sensitive to the choice of TERRAD value.

Jacobs prepared preliminary CALMET models to compare CALMET outputs for these different TERRAD settings, and found that the model was slightly sensitive to the TERRAD settings, particularly in the south and southeast of the domain.

The grid resolution needs to be sufficiently fine to create data that is adequate for the application and to appropriately characterize the wind flows within the model domain, whilst balancing this against the run times and file sizes. In this case, both Jacobs and TAS selected a 300 m grid resolution. Jacobs compared the CALMET model outputs for 300 m and 200 m grids, and concluded that the meteorological outputs were very similar and did not warrant the much longer running times and file sizes implicit in the use of a 200 m grid.

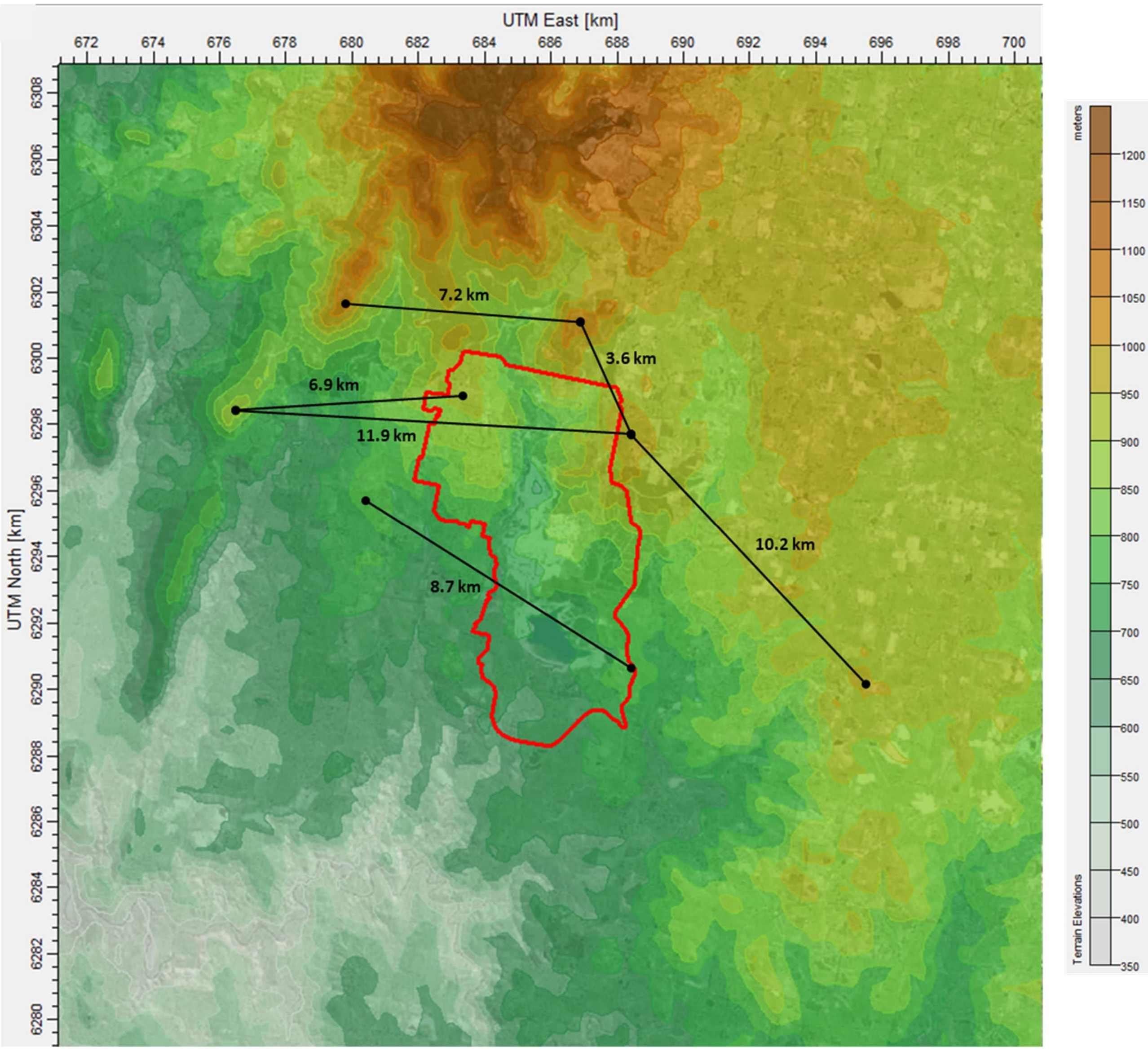

Figure 5-1. Ridge to ridge distances in valleys around CVO, used by Jacobs to determine appropriate value of TERRAD for CALMET.

5.3.2 Outputs

Jacobs has extracted wind field data from the CALMET model for the same specifications as provided in TAS (2023a) to allow comparison of the models. The wind field for 5 June 2022 00:00 local time which is provided in TAS (2023a) Figure 5-1 is shown in Figure 5-2 alongside the extraction from Jacobs' CALMET model for the same hour. The wind field is largely very similar, with some differences at the outer reaches of the model domain which are likely to be due in large part of the slightly different values of R1 and RMAX1, and TERRAD. To illustrate this, Jacobs also ran a CALMET model with the same TAPM and surface observation inputs, and the same settings of BIAS, TERRAD, R1, R2, RMAX1 and RMAX2 as used in the TAS Reports. This wind field in shown in Figure 5-3 for the same extracted hour of 5 June 2022 00:00. The wind field appears almost identical to the TAS (2023a) wind field.

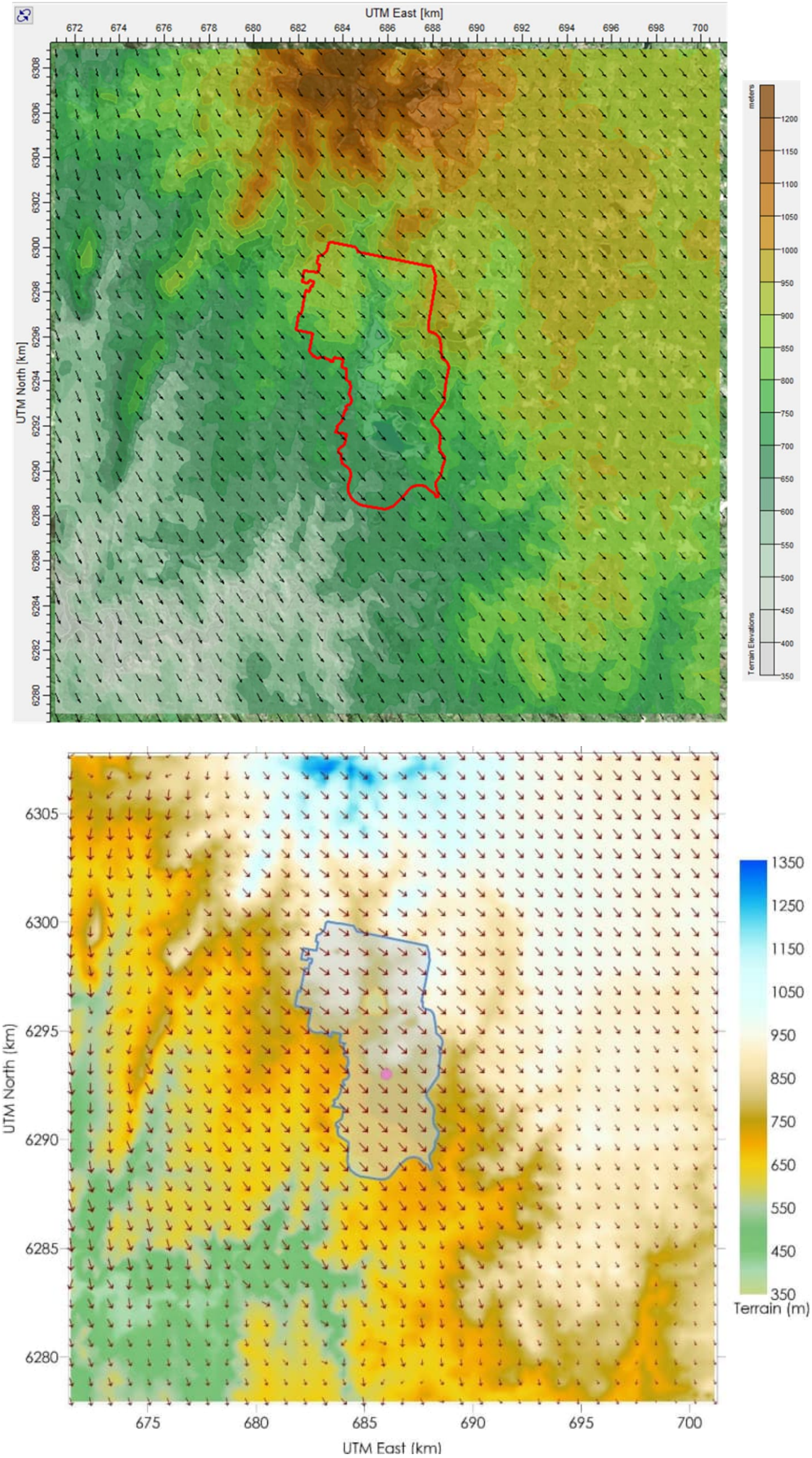

Figure 5-2. Comparison of wind field at surface predicted by Jacobs CALMET (above) and TAS (2023a) CALMET (below) for 5 June 2023 00:00.

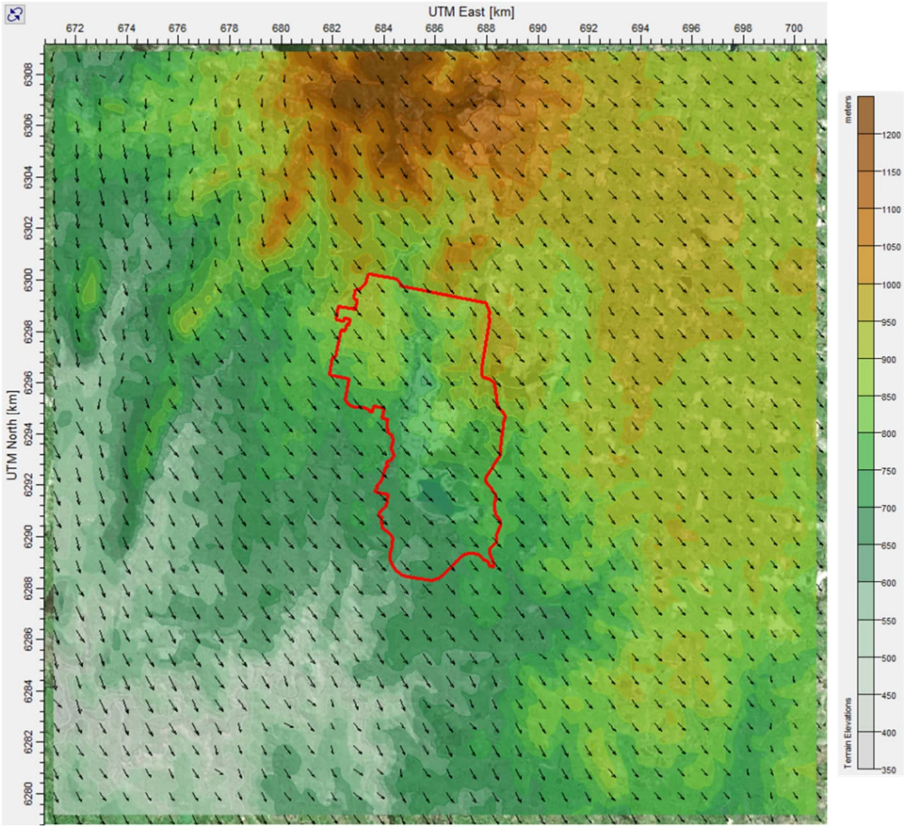

Figure 5-3. Comparison of wind field at surface predicted by Jacobs CALMET using TAS settings for 5 June 2023 00:00.

Lastly, Figure 5-4 compares the windroses extracted from CALMET at the centre point of the grid (at the pink dot in the lower image in Figure 5-2), for the CALMET run with Jacobs' recommended settings, and the CALMET run by Jacobs with TAS input settings. The two windroses are almost identical, highlighting that at this location the choice of settings is less important than the observation data inputs. Given that this location is 4.9 km from the Ridgeway AWS and 2.8 km from the SLB AWS, this is logical.

In Figure 5-4, the windrose extracted at this point provided in TAS (2023a) is also shown. It is noted that this windrose is for a slightly longer data period, with two additional months compared with the CALMET runs by Jacobs, however this will only cause a small difference to the windrose. Notwithstanding the different time periods, there are some differences in the windroses between those prepared from the Jacobs data, and that shown in TAS (2023a). These differences are consistent with the differences in the SLB meteorological data shown in Figure 5-4 and highlight the dependence of this location on SLB data.

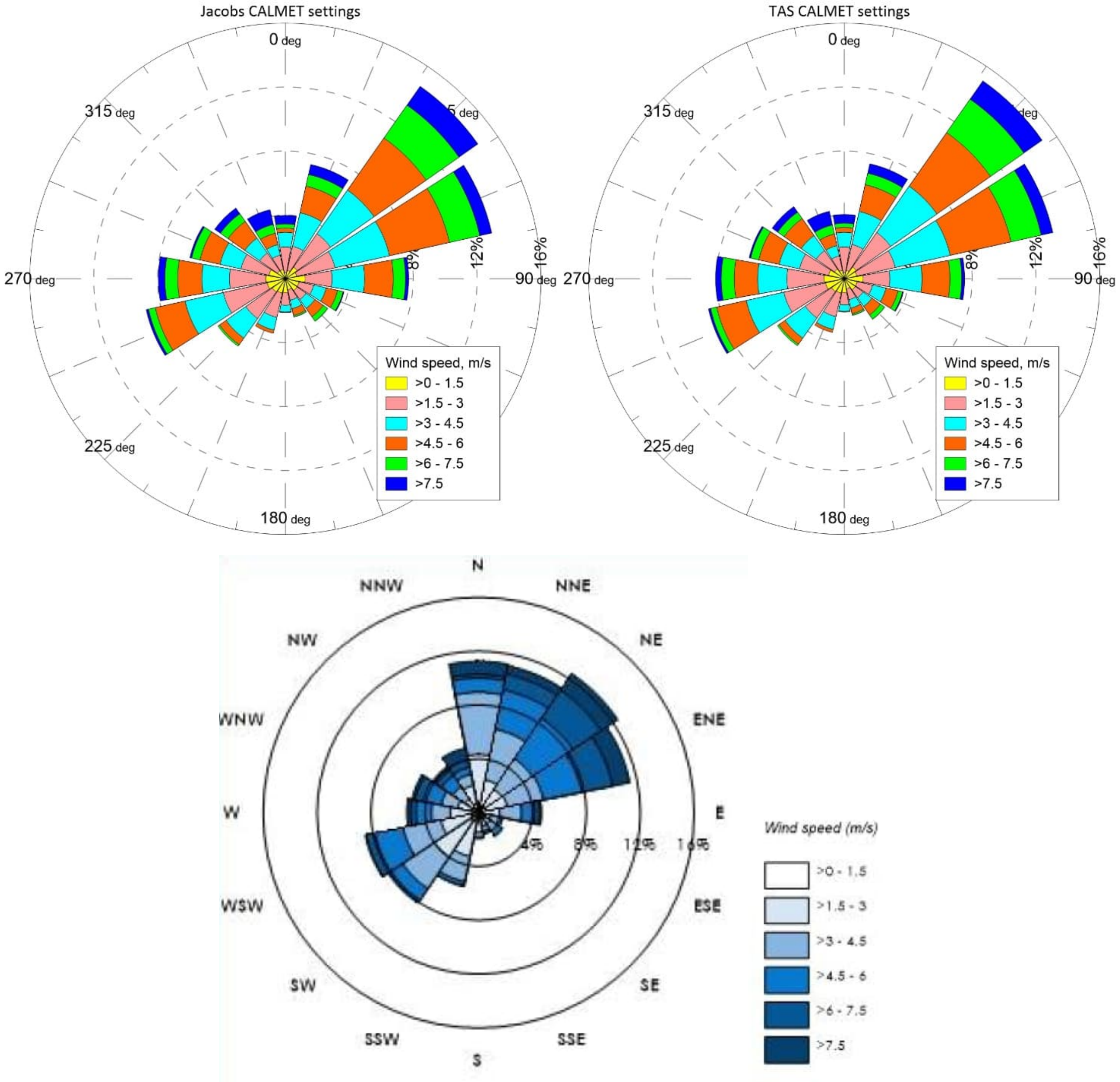

Figure 5-4. Windroses comparing 1-hour average wind speed and direction for January – December 2022 at domain centre point, comparing Jacobs' recommended CALMET settings (top left) with Jacobs' replication of TAS (2023a) CALMET settings (top right). Bottom: Windrose for same grid point for January 2022 – February 2023 (slightly longer data period) in TAS (2023a).

Whilst the windrose analysis for the grid centre point has been provided to allow comparison with TAS (2023a), this data point has no special significance. It would be more relevant to consider how the wind fields differ between the various combinations of settings in the east and southeast of the model domain further away from the observation sites and close to the most dense clusters of sensitive receivers. However, there is no wind observation data in that part of the domain to compare the CALMET model results against to validate the most appropriate selections of model settings.

The gap in local meteorological information in the southeast part of the modelling domain means that CALMET must make estimates of likely wind patterns in that part of the model domain, which are much more dependent on user settings for R1 and RMAX1 and the underlying prognostic IGF than at locations closer to the Ridgeway and SLB AWS.

Confidence in future modelling results in this part of the domain could be increased if the meteorological modelling was supported by additional wind observations in the southeast part of the domain, somewhere in the area represented by the Triangle Flat and Meribah BAM locations. Jacobs recommends that an additional AWS be installed in this area. The site would not need to host a full range of meteorological monitoring instruments, as the priority would be to collect wind speed and direction data.

5.4 CALPUFF

The settings applied for CALPUFF are provided in Table 5-3, including the comparative settings used in TAS (2023a), where such information is available.

Table 5-3. Summary of input settings for CALPUFF

Parameter	Settings used by Jacobs	Settings used by TAS (2023a)
Model version	6.5.0	Not stated
Graphical user interface	Lakes Environmental CALPUFF View	Not stated
Grid size	Same grid extent as shown in the model contour plots in TAS (2023a).	Not stated, but inferred to be the same as Jacobs from the model contour plots.
Time Step	3600 seconds	Not stated
Sampling grid resolution	300m uniform grid, plus discrete receptors representing house locations	Not stated
Wet removal modelled	Yes	Not stated
Dry deposition modelled	Yes	Yes (mentioned only briefly)
Method used to compute dispersion coefficients (MDISP)	MDISP = 2: dispersion coefficients from internally calculated sigma v, sigma w using micrometeorological variables	Not stated
Building downwash algorithm (for point sources only)	PRIME	Not stated
Minimum turbulence velocity sigma-v over land	Default setting of 0.5m/s for all stability classes	Not stated
Minimum wind speed allowed for non-calm conditions	Default setting of 0.5 m/s	Not stated

5.5 Area-type versus volume-type source characterisation

In CALPUFF, sources can be generally characterised as point (such as from a stack), area (such as from an open exposed flat area of ground or water), or volume (such as a stirred-up cloud of dust from a building or vehicle). The TAS Reports use volume sources to represent all emissions at CVO except for the vents which are modelled as point sources. Hypothetically, the open areas at CVO such as the TSFs should be modelled as area sources, however Jacobs tested the sensitivity of the dispersion model to this assumption and found that using the source split up into 20 volume sources or 20 area sources made very little difference to the model results. This is because of the long dispersion distances involved at CVO. The effect of choice of source type for simulating a constant emission rate from the STSF is shown in Figure 5-5. Therefore, the model is insensitive to the choice of source type, provided that the large sources such as the TSFs are divided up into a sufficient number of smaller sources such as appears to have been done by TAS (2023a).

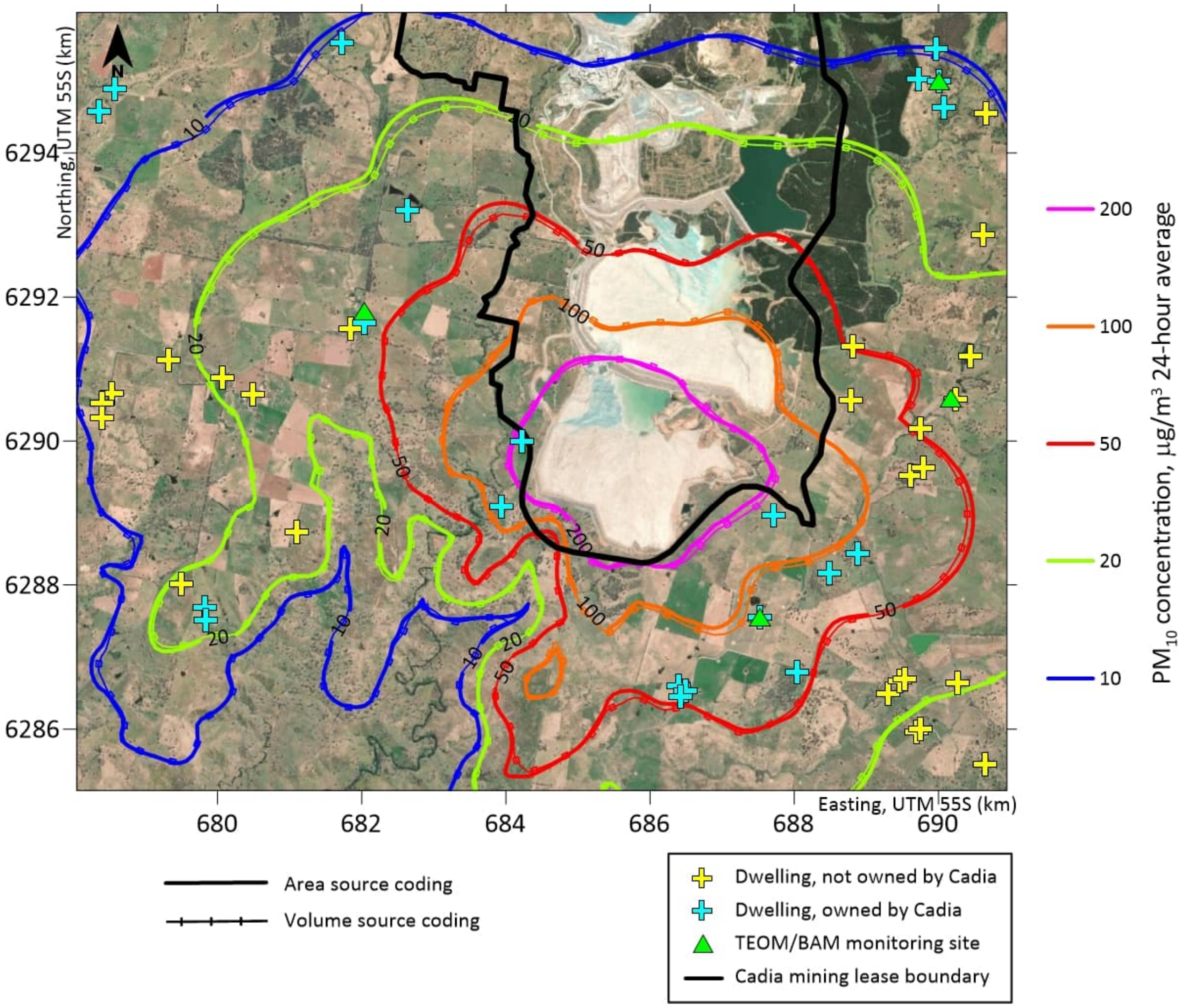

Figure 5-5. Comparison of dispersion result for 24-hour average concentrations of PM_{10}, for coding emissions from STSF as area or volume source type. Constant emission rate.

Other specialist source characterization options are also available in CALPUFF, such as the "haul roads" option, which breaks a haul road route up into a sequence of volume sources and distributes the emission rate along the travel route in proportion with the length of the route. Jacobs compared the haul road option with an equivalent area source option (see Section 6.1.5), and found that the dispersion results were very similar, with the haul road volume sources option generating slightly higher concentrations. The haul road volume sources option was also easier to set up and change emission rates, although it required longer running times. Due to the significant model speed penalty of the haul road option due to the number of volume sources that are generated, Jacobs only used the haul road option for bulldozers rather than for all vehicle movements.

5.6 Use of Deposition

"Dry deposition" is an option in the CALPUFF model that simulates the settling of particles in the air as they travel downwind. The larger the aerodynamic diameter of the particles the faster they settle. CALPUFF requires user input for the size distribution of the particles that are being dispersed. Whilst default values for particle size distribution are provided by CALPUFF for PM_{10}, the default values are too small for dust dispersion where the PM_{10} fraction is a lot bigger than the $PM_{2.5}$ fraction as is found in mining applications.

The input information required by CALPUFF for simulating particle settling and scavenging is as follows:

- Geometric mass mean diameter
- Geometric standard deviation

This assumes that particles in the PM_{10} size range will vary in size according to a normal distribution that can be expressed as a mean diameter and standard deviation. It is not appropriate to set the geometric mass mean diameter to 10 µm, as this means CALPUFF will assume that larger particles than 10 µm are included in the mass and will overestimate the settling rate.

TAS (2023a) indicates that dry deposition was used in the modelling, but does not state what size distribution settings were assumed either for PM_{10} or for larger particles. Jacobs focused on the dispersion of PM_{10} due to the relevance of this pollutant to health-based assessment criteria.

Ideally, particle size distribution data for PM_{10} would be available for each source. However, such data would rarely be available. Instead, a reasonable assumption of mean diameter and standard deviation must be made. TAS (2023a) does not state what assumptions were included in the CALPUFF model to simulate settling and deposition. Jacobs adopted a nominal geometric mass mean diameter of 4 µm, and geometric standard deviation of 2 µm. The particle settling settings are summarized in Table 5-4.

Table 5-4. Particle deposition settings for CALPUFF

Data source	Geometric mean diameter, µm	Geometric standard deviation, µm
CALPUFF default	0.48	2
Assumed by Jacobs	4	2
Assumed in TAS (2023a)	Not stated	Not stated

Jacobs tested the model sensitivity to using dry deposition (at the settings assumed by Jacobs shown in Table 5-4), compared to not using dry deposition using a constant emission rate off the STSF as a demonstration. The comparison of model results is shown in Figure 5-6. The model appears to be moderately sensitive to the use of deposition, with deposition causing the dispersion to occur more quickly with lower ground level concentrations predicted at sensitive receptors.

Jacobs has not investigated the model sensitivity to different assumptions about geometric mean diameter and standard deviation, and is not aware of what assumptions were applied by TAS (2023a).

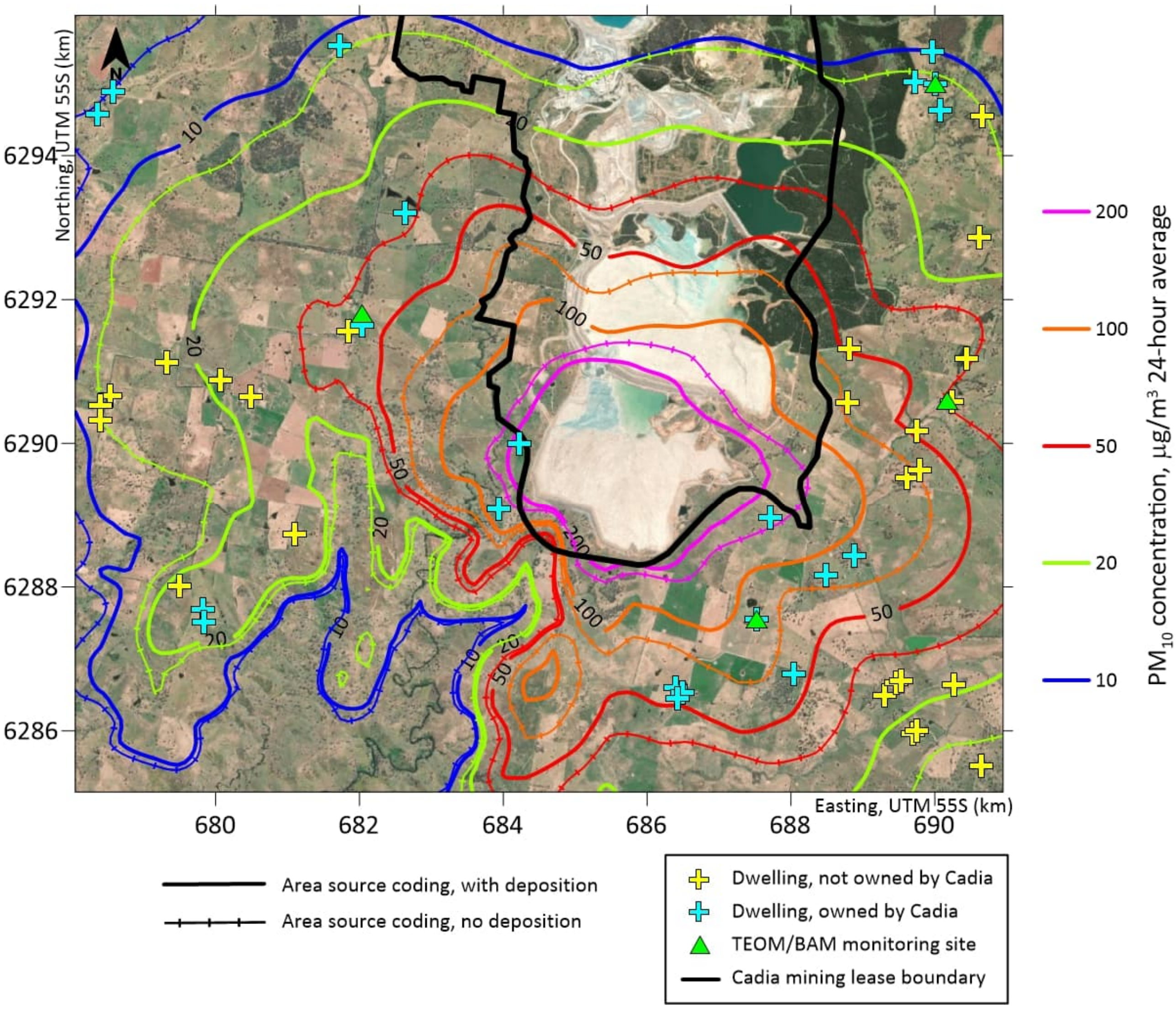

Figure 5-6. Comparison of dispersion result for 24-hour average concentrations of PM_{10}, with or without deposition, for emissions from STSF as area source type. Constant emission rate.

5.7 Background

Background concentrations refer to the concentrations of a pollutant, in this case PM_{10} or $PM_{2.5}$, that are already in the air due to other local or regional emission sources excluding Cadia. For example, these background sources could be smoke from chimneys, vehicle exhausts, dust lift-off from dry paddocks, or even much more distant sources such as bushfires or dust storms.

Dispersion models can predict either incremental or cumulative concentrations:

- Incremental concentrations refer to just the part of the total concentration in ambient air which is contributed by an individual source, in this case operations at the mine site.
- Cumulative concentrations refer to the total concentration of a pollutant in ambient air, combined from all emission and background sources. The cumulative concentration is the total exposure to a pollutant at a sensitive receptor and is the most appropriate parameter for health-based risk assessments.

In the Approved Methods, the impact assessment criteria applies to cumulative concentrations, requiring the incremental concentrations from a specific source to be combined with background concentrations from all other sources before comparison with the relevant impact assessment criteria.

Background concentrations can be calculated in various ways, depending on data availability. In TAS (2023), ambient monitoring data for the TEOM and BAM monitoring locations surrounding CVO were used to calculate the background level. The downwind angle range shown in Plate 5-1 for each of the monitors was applied to determine when the monitor was either downwind or upwind of CVO. Jacobs agrees with these downwind angle ranges, except for Meribah where a downwind angle range of 285-10° is considered more appropriate.

Monitor	Downwind angle range
Bundarra	30° - 135°
Flyers Creek	205° - 320°
Triangle Flat	240° - 340°
Meribah	305 °- 10°
Woodville	200 °- 310°

Plate 5-1. Downwind angle range used to calculation background concentrations, stated in Table 2 of TAS (2023b).

TAS (2023b) does not state whether the SLB or Ridgeway AWS data was used to calculate whether each monitoring location was downwind of Cadia on an hour-by-hour basis. Jacobs replicated the calculation of background concentrations using both Ridgeway hourly average data calculated from 10-minute averages, and the amended SLB 1-hour averages with corrected wind direction anomalies discussed in Section 3.2.2.2.

Jacobs also replicated the calculation of background concentrations using both the Meribah wind angle from TAS (2023b) of 305-10°, and Jacobs' recommended wind angle of 285-10°. Jacobs found that the 24-hour average background concentration was often slightly higher when calculated with the Meribah downwind angle of 305-10° versus the 285-10° angle, although this difference only exceeded 1 $\mu g/m^3$ on four days in 2022 for PM_{10}, and only exceeded 0.5 $\mu g/m^3$ on two days in 2022 for $PM_{2.5}$. Therefore, the difference was not sufficiently significant to warrant further consideration.

In comparing 24-hour averaged calculated by Jacobs with those tabulated for 2022 in Table 3 of TAS (2023b), Jacobs found that there were a number of days whether either or both the PM_{10} and/or $PM_{2.5}$ background concentration was considerably higher in the TAS dataset than calculated by Jacobs, with no raw data in the 1-hour average dataset for all BAM/TEOM locations to indicate why the concentration calculated by TAS was so much higher. Examples of these anomalies are shown in Table 5.5. Overall, the 24-hour concentrations from TAS (2023b) were at least 2.0 $\mu g/m^3$ higher than calculated by Jacobs on 20% of the days in 2022 for PM_{10}, and at least 0.5 $\mu g/m^3$ higher for $PM_{2.5}$.

The calculated annual average background PM_{10} and $PM_{2.5}$ is shown in Table 5.6. The annual average for PM_{10} is slightly higher based on the TAS (2023b) data, compared to that calculated by Jacobs. However, the $PM_{2.5}$ annual averages are the same.

The calculation of background concentrations is relevant to the dispersion modelling as it affects the calculation of cumulative concentrations and the comparison of those predicted concentrations with measured data.

Table 5.5: Examples of anomalies in comparison of background 24-hour average PM_{10} concentrations calculated by Jacobs, versus values tabulated in TAS (2023b).

Date	TAS (2023b) stated 24-hour average PM_{10} concentration, µg/m^3	24-hour average PM_{10} concentration calculated by Jacobs, µg/m^3	
		Based on SLB directions	Based on Ridgeway directions
24/6/22	7.6	2.8	3.5
20/8/24	15.3	4.7	4.8
31/10/24	10.9	3.3	3.6
1/12/22	18.1	13.3	13.4

Table 5.6: Comparison of background annual average PM_{10} and $PM_{2.5}$ concentrations.

Pollutant	Calculated from TAS (2023b) tabulated data, µg/m^3	Calculated by Jacobs, µg/m^3	
		Based on SLB directions	Based on Ridgeway directions
PM_{10}	8.8	7.7	7.8
$PM_{2.5}$	3.7	3.7	3.6

6. Model Results

6.1 Emission Sensitivity Studies

For the sensitivity test runs, each source discussed in Sections 4.2 and 4.3 was modelled individually which the model results focusing on 24-hour average PM_{10} concentrations for the various discharge and emission factor sensitivity options. The annual average PM_{10} concentrations were also compared for some activity groups where wind speed or rain is an input factor.

The sensitivity test models were run with a reduced domain extent for faster model run times.

Details of the model runs and results are provided in Appendices B to P. Conclusions from the sensitivity tests are summarized below.

6.1.1 Vents

The model results show the following:

1. Dispersion from all vents is moderately sensitive to the discharge temperature, with lower temperatures producing higher ground-level concentrations.
2. Dispersion from VR8 is slightly sensitive to inclusion of building downwash, with options using building downwash producing higher ground-level concentrations, but vents VR3A, VR5 and VR7 are insensitive to building downwash.
3. Dispersion from VR8 is slightly sensitive to defining the discharge as being from two vents, versus one vent with the diameter applied in TAS (2023a). Options using two vents produce higher ground-level concentrations than with one vent.

6.1.2 Crushing

The model results are moderately sensitive to the EFs and assumed control efficiency, with the predicted maximum 24-hour average PM_{10} at Woodville varying between 1.5 and 10 μg/m^3, and varying between 0.3 and 2.5 μg/m^{3}at Meribah.

6.1.3 Loading and Handling

This activity group includes both batch loading activities and continuous loading activities as described in Section 4.3.5. For the sensitivity testing, the "ore processing in mill" activity is excluded from the loading and handling emission inventory because the basis for definition of this source is unclear and the emission rates are very large relative to the other loading and handling sources. The model results for that source alone are provided in the following section instead.

The model results show the following:

1. Applying the NPI emission factors for handling low moisture content ore from metalliferous mines results in high PM_{10} concentrations at the Cadia monitoring sites that are not reflected in the monitoring data, therefore is it likely that these emission factors are too high for the Cadia ore.
2. The calculation of emissions from loading and handling requires several assumptions about activity rates, hours of operation, and emission factors. The model results outside the mining lease boundary are highly sensitive to these assumptions.

3. Concentrations predicted by the model are reduced when wind speed dependence is taken into account, and this may be an improvement over using a constant emission rate. However, this wind speed dependence can only apply to sources where Equation 1 is relevant; for example if the NPI-recommended factors for batch loading from Run 3 are applied, that emission factor is not wind speed-dependent.

6.1.4 Ore Processing

The model results show the following:

1. As found with the loading and handling sources, applying the NPI emission factors for handling low moisture content ore from metalliferous mines results in high PM_{10} concentrations at the Cadia monitoring sites that are not reflected in the monitoring data, therefore is it likely that these emission factors are too high for the Cadia ore.
2. The model results outside the mining lease boundary in the vicinity of sensitive receptors are not particularly sensitive to the other EF assumptions.

6.1.5 Bulldozers

To model emissions from the bulldozer activity, it was necessary to assume what proportion of the total annual bulldozer activity would be attributed to each part of the mine site (such as construction to the east of NTSF or construction to the west of NTSF or construction to the southwest of STSF), and then assume that those activities are distributed along the full haul road route even across the full year. However, with a mobile source like bulldozing where activity might be focused in just one area for a period of time and gradually move from week to week, modelling with constant assumed proportion of bulldozer activity in different parts of the mine may not be representative of reality. This is particularly significant for bulldozer emissions, because the emission factor is highly dependent on the running hours.

Notwithstanding, the model results show that ambient air quality concentrations of PM_{10} are moderately sensitive to the emission factor for bulldozing,.

6.1.6 Graders

The model results for the grader emissions indicate low concentrations beyond the mining lease boundary, to the extent that the results are insensitive to the selection of emission factors.

6.1.7 Vehicle-Tracked Dust

This activity group includes:

- Long-haul route for tailings construction
- Short-haul route to waste emplacement
- Short-haul route for transferring ore to and from COS stockpiles

The model results are moderately sensitive to each of the variables of daytime weighting, lower silt content, assumed average control efficiency, and whether short haul ore routes are included. Overall, combinations of variations to these factors can make a large difference to the model results.

For the options that tested the effect of excluding emissions on “rain days”, there were very minor differences between the model results for the 24-hour average, but slightly reduced concentrations in the annual averages when “rain days” are accounted for.

However, the definition of "rain days" in this report is nominal to test whether the dispersion model is sensitive to this approach, and would require site specific validation before being introduced as a feature of the modelling approach for Cadia.

6.1.8 Wind Erosion

The model results show the following:

1. Distributing the emissions as a function of the cube of the wind speed has a very significant impact on model results both at the 24-hour and annual average.
2. Allowing for control efficiency has a very significant impact on model results, and would be sensitive to the amount of control that is assumed; noting that this may vary for different open area types.
3. Eliminating wind erosion emissions on rain days (essentially assuming 100% control effectiveness after a rain event) has a moderate impact on model results in some parts of the domain, and a minor impact in other areas; however the extent of impact would also depend on the control efficiency assumed on non-rain days. The change in impact is more noticeable at the 24-hour average than the annual average.
4. Applying site-specific values for s, p and f in the wind erosion equation causes the concentrations from the TSFs to approximately double for both the 24-hour and annual average, but the concentrations resulting from the other open area sources are only slightly higher. The change in concentrations for the TSFs is due to the assumed higher silt content, and would need to be verified for actual site conditions.

   The concentrations from the other open areas are largely unaffected because although the value for f has increased, the values for s and p have decreased compared to the default equation.

   It is also noted that a value of p representing a "wetter year" was applied, because the modelled year was 2022. In a dry year, such as 2018, the concentrations arising from wind erosion off all the open areas predicted by the model would have been higher.
5. The model is sensitive to the approach of assuming p=0 in the wind erosion equation and eliminating wind erosion emissions on "rain days", particularly for the TSFs.

Overall, whilst there is considerable variation in model results between the options, the comparison is constrained by the uncertainty in the input assumptions for silt content of the various surfaces, and the efficiency of controls. The lower the silt content and the better the control efficiency, the less significant the variations in model results between the options. Therefore, site-specific validation of the silt content and control efficiency off the various open area types would refine the comparison of emission estimation methods.

Regardless, it is clear that the TSFs represent a potentially dominant source of wind erosion emissions. Anecdotal observations suggest that wind-generated emissions from the TSFs may only be noticeable during higher wind speeds, and therefore the threshold friction velocity calculation method may be more relevant so as to not overstate contributions from the TSFs under lower wind speeds. Model results for the TSFs using the threshold friction velocity method are provided in the following section.

6.1.9 Summary

Table 6.1 provides a summary of the degree of sensitivity to input parameters for each of the source types, based on Jacobs' qualitative assessment of the extent of variation between the options tested for each source. The sources that are most sensitive to inputs are loading and handling, vehicle-tracked dust, and wind erosion.

Table 6.1: Summary of sensitivity of each source to input parameters.

Source	Parameters subject to sensitivity testing	Insensitive *	Slightly sensitive[1]	Moderately sensitive[1]	Highly sensitive[1]
Vents	Discharge temperature			✓	
	Inclusion of building downwash		✓		
Crushing	Emission factors			✓	
Loading and handling	Emission factors				✓
	Wind speed dependence			✓+[2]	
Ore processing	Emission factors		✓		
Bulldozers	Emission factors			✓	
Graders	Emission factors	✓			
Vehicle-tracked dust	Emission factors				✓
	Adjustment for "rain days"		✓+[3]		
Wind erosion	Emission factor definition				✓
	Wind speed dependence				✓
	Adjustment for "rain days"			✓	

1 Sensitivity rating based on change in model results and qualitative judgement of the potential for this change to influence cumulative concentrations at sensitive receptors:

- **Insensitive** – Minimal change to incremental concentrations, and/or predicted incremental concentrations outside mine boundary are so low that selection of emission parameter is insignificant.
- **Slightly sensitive** – Less than approximately 10% increase in incremental concentrations outside mine boundary, and unlikely to cause an increase in total number of receptors that exceed air quality objectives in Approved Methods when combined with all mine emissions.
- **Moderately sensitive** – More than approximately 10% increase in incremental concentrations outside mine boundary at some sensitive receptors, and/or changes to locations where elevated impacts are predicted to occur; and unlikely to cause an increase in total number of receptors that exceed air quality objectives in Approved Methods when combined with all mine emissions.
- **Highly sensitive** – More than approximately 100% increase in incremental concentrations outside mine boundary at some sensitive receptors, and/or increases the total number of receptors that could exceed air quality objectives in Approved Methods when combined with all mine emissions.

2 Change implied is positive, ie. reduces the predicted concentrations.

3 Change implied is slightly positive for annual average PM_{10}, and insignificant for 24-hour average PM_{10}.

6.2 Threshold Friction Velocity Method for Wind Erosion

6.2.1 Emission rate simulations

Figure 6-1 shows the emission rate calculated from a 250,000 m^2 area of TSFs (representing a 500m x 500m patch of TSF surface) for the three tested u_t values of 0.4, 0.5 and 0.6 m/s. The SLB wind speed, which is critical to the calculated emission rate for any given hour, is also shown on the graph. The graph shows that as the value of u_t increases, the emission rates decrease and so does the number of peak emission events in the year.

Based on this graph, and in the absence of rainfall or other effective controls, there would have been the potential for visible dust events from the TSFs on several days in 2022 as listed in Table 6-2. Some of these events may have been of short duration and/or occurring overnight, and therefore not observed as significant visible dust events. Dates in the table where the risk of dust lift off may have been reduced due to rainfall (based on hourly rainfall records at SLB and Ridgeway AWS) are marked with a raindrop symbol.

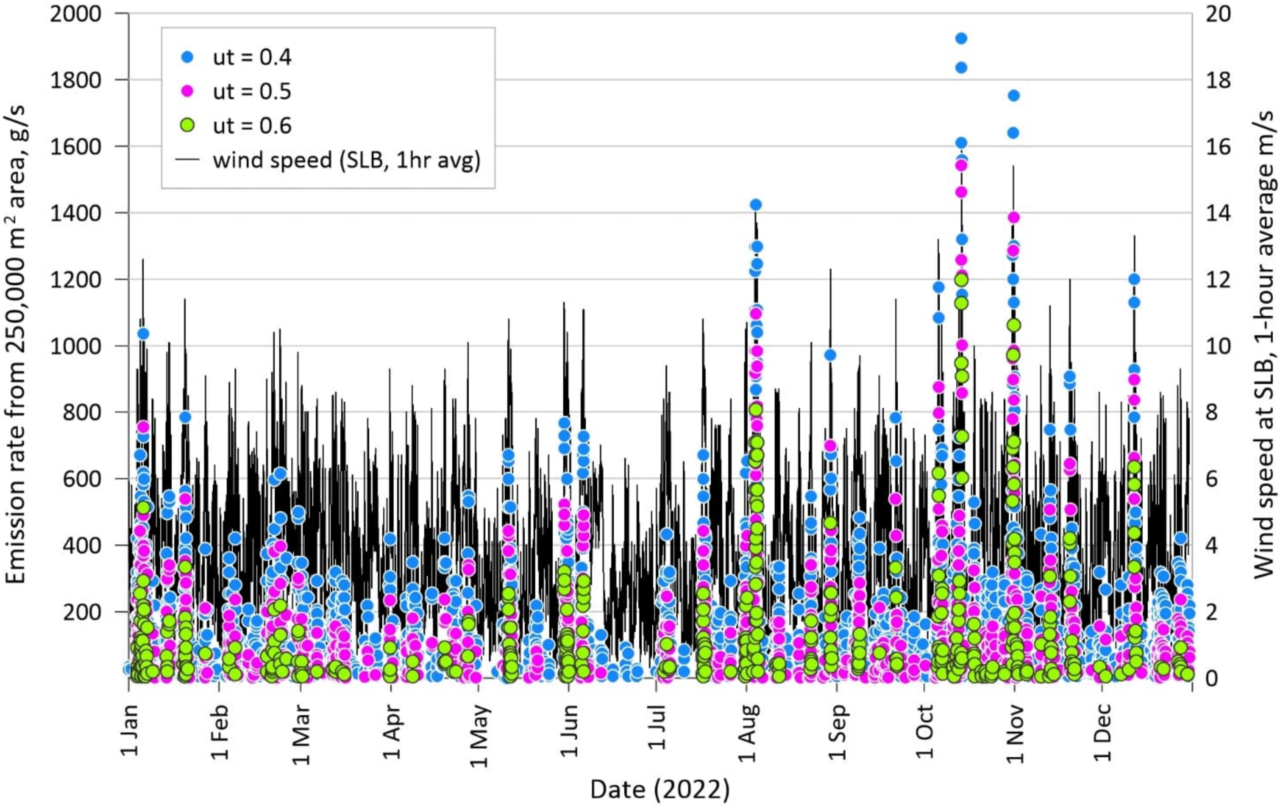

Figure 6-1. Wind erosion rates for a 250,000 m^2 area source (representing a 500m x 500m square patch of TSF surface) based on the threshold friction velocity calculation method – full 2022 year.

Table 6-2. Periods of elevated wind erosion risk from TSFs in 2022 based on Figure 6-1.

Event with multiple hours duration during daytime	Event overnight but extended duration (minimum 4 hours)	Event of short duration and overnight	Daytime event of 1-3 hour duration
20 January💧	4-5 January	14 January	7 January💧

11 May	**5-6 January*** ☹	19, 22♦ February	6 February
30♦ and 31♦ May	5-6 June♦	28 February (☹ on 1Mar)	31 March♦
17 July	29-30 August♦	12 May♦	19 April♦ ☹
3-4 August* ♦(part)	**5-6 October*** ♦	1♦, 23♦ August	27 April♦
13 October* ☹	12-13 October	21 September	4♦ and 31♦ July
31 October* ♦ ☹	**13 November** ♦ ☹	6-7 October	3 August♦
	19-20 November♦	10 November	8 September♦
	11-12 December* ☹	27 December	7 October

* (bold font) Period of higher risk of dust emissions from TSFs based on wind speeds and/or duration of event

☹ Recorded as a complaint incident in AEMR (2022) or (2023)

♦ Risk of dust emissions may have been reduced due to rainfall

The dates in 2022 which appear to have the highest potential for TSF dust emissions from wind erosion are identified in Table 6-2 in bold and with an asterisk. These dates have the highest emission rates and the longest duration of emission events. The events where dust complaints due to the TSFs were reported by CVO are also marked in the table.

Figures in Appendix J show the emission rate profile data for periods covering 4-6 January, 3-4 August, 5-6 October, 13 October, 31 October, 12-13 November, and 11-12 December. Concurrent rainfall measured at SLB or Ridgeway is also shown on the graphs. The following observations apply to each of these event dates:

- **4-6 January 2022**: As shown in Table 3-2, dust complaints relating to the TSFs were received on 5 January. CVO's response states that "there was a high wind event during the morning ahead of wet weather". Figure J-1 shows that high wind speed events were recorded on the mornings of both 5 and 6 January, and rainfall was registered after about 9pm on 6 January which may have helped to suppress dust emissions after that time. On both 4-5 and 5-6 January, the peak emission rates (and coinciding wind speeds) occur overnight, and therefore the full extent of dust lift-off may not have been visible.
- **3-4 August 2022**: Figure J-2 shows that wind speeds were high on 4 August, reaching an hourly average of 13 m/s overnight and during the afternoon. Rainfall was also recorded during the day on 4 August, however there are no records of dust lift-off observations or complaints on 3-4 August to indicate whether the rainfall was sufficient to control the dust emissions.
- **5-6 October 2022**: There are no reports of a dust lift-off event on these days. Figure J-3 shows that wind speeds were high on the evening of 5 October, and also 6 October. The full extent of the dust lift-off event may not have been visible due to night-time hours which may have contributed to the lack of dust lift-off reports. However, rain falling earlier on 5 October may have helped to suppress dust emissions.
- **13 October 2022**: Six residents contacted Cadia regarding dust lifting from the TSFs on this day. CVO acknowledged a dust lift-off event occurring on this day, although the hours of the event are not recorded in AEMR (2023). Figure J-4 shows that the recorded wind speeds exceeded 8 m/s and were likely sufficient to increase the risk of dust lift-off overnight on 12-13 October, and then in particular from about 6pm on 13 October until the onset of rain at about midnight which coincided with a rapid drop in wind speed.
- **31 October 2022**: Several complaints about visible dust were received on this day. CVO acknowledged a dust lift-off event occurring on this day. Figure J-5 shows that wind speeds were very high, ranging from 8 m/s to nearly 18 m/s for most of the day. Rainfall was recorded between 9am and 1pm, and then after 6pm at Ridgeway and SLB. As the hours of the dust lift-off event are not recorded in AEMR (2023), the effect of rainfall on reducing dust lift off cannot be assessed based on the available data.

- **12-13 November 2022:** AEMR (2023) states that three complaints about dust from the TSFs were received on 12 November. While 12 November is not identified as a high-risk day for dust lift off based on the threshold friction velocity calculation, early hours of 13 November (2am to 7am period) show an elevated period of emissions prior to the onset of rain (see Figure J-6). The response provided by CVO for this event (see Section 3.4) states that "Dust was being actively managed during this time at site and the increased wind was at the front of a storm. Rain then developed about 30 minutes later and there was no further dust." Therefore, whilst the date of the event is recorded as 12 November, the event is assumed to relate to the wind early on 13 November.
- **11-12 December 2022**: CVO acknowledged a dust lift-off event on 11 December in Section 8.2.1 of AEMR (2023), however there are no complaints reported in Table 18-3 of AEMR (2023) for December. Figure J-7 shows that hourly-average wind speeds ranged from 8 m/s to 13 m/s across the period from 10pm on 11 December to 5am on 12 December, implying an increased risk of dust lift-off during this time. However, this would have mainly occurred during night-time hours and therefore the full extent of the dust lift-off event may not have been visible. AEMR (2023) does not state when the dust lift-off event occurred, nor how the event was observed.

6.2.2 Dispersion event simulations

Figures illustrating the predicted sequence of hourly plume movement for the main dust lift-off events described above and for u_t values of 0.4, 0.5 and 0.6 m/s are provided in the Appendices K to P. The plume sequence for 5-6 October is not provided because there were no complaints recorded on these days and it is likely that rain reduced the risk of dust emissions. The concentration scale for all plume screenshots in Appendices K to P is shown at the start of Appendix K.

Unsurprisingly, these figures demonstrate that higher values of u_t correspond with smaller dust plume extents, lower suspended PM_{10} concentrations, and shorter duration events.

The events all correspond with winds blowing from the north, north-northeast or north-northwest. The Meribah AQMS may have been partially downwind of the TSFs for some of the hours during the dust lift-off events, but for the majority of the time during these events there were no air quality monitoring stations downwind of the TSFs under these wind directions. The operational monitoring sites B1-B6 on Figure 3-3 may have recorded useful data to validate these dust event simulations if they were operating at the time, but Jacobs does not have access to this data.

AEMR 2023 states that dust lift off was observed on 13 and 31 October, 12 November, and 11 December 2022, but that compliance criteria was not exceeded at any of the monitoring points as a result of these dust lift off events. This is also unsurprising, given the wind directions at the time of these events and the locations of the BAM monitoring sites.

These simulations demonstrate a potential alternative way of modelling emissions from the TSFs under high wind events. However, the simulations cannot be calibrated to the CVO site because of the lack of available operational monitoring data close to the TSFs.

6.3 Vent Model Runs

Figures Q-1 to Q-5 in Appendix Q show the vent model results for Scenarios 1-5 requested by the EPA as summarized in Table 6-3. The figures show incremental model results (with no background air quality or other mine sources included) so the relative contributions of the various vents or groups of vents can be visualized. Cumulative model results for each of these runs are presented and discussed in Section 6.6.

Table 6-3: Model runs for vent scenarios requested by EPA (see Section 4.2.3.2 for details)

Run name	Source group	Incremental results figure
Scenario 1 – As TAS (2023a) – 2022 measured flow rates and emission rates	VR3A, VR5 and VR7 VR8 (as one vent) All vents	Figure Q-1(a) Figure Q-1(b) Figure Q-1(c)
Scenario 2 – Post controls 2023, average emission rates and flow rates	VR3A, VR5 and VR7 VR8 (as two vents) All vents	Figure Q-2(a) Figure Q-2(b) Figure Q-1(c)
Scenario 3 – Post controls 2023, average emission concentrations, maximum flow rates	VR3A, VR5 and VR7 VR8 (as three vents) All vents	Figure Q-3(a) Figure Q-3(b) Figure Q-3(c)
Scenario 4 – Regulatory concentrations, maximum flow rates	VR3A, VR5, VR7 VR8 (as 3 vents) All vents	Figure Q-4(a) Figure Q-4(b) Figure Q-4(c)
Scenario 5 - Regulatory concentrations, maximum flow rates, including MOD15 vents	VR3A, VR5, VR7, VR8 (as three vents) VR11, R-VR4, R-VR6 All vents	Figure Q-5(a) Figure Q-5(b) Figure Q-5(c)

Figure 6-2 to Figure 6-4 compare Scenarios 2 and 3, Scenarios 2 and 4, and Scenarios 4 and 5 respectively.

Overall, the model results show that the predicted concentrations beyond the mine site boundary increase as the emission rates increase through Scenarios 2, 3, 4, and 5, however the degree of increase in concentration depends on the location on the model domain.

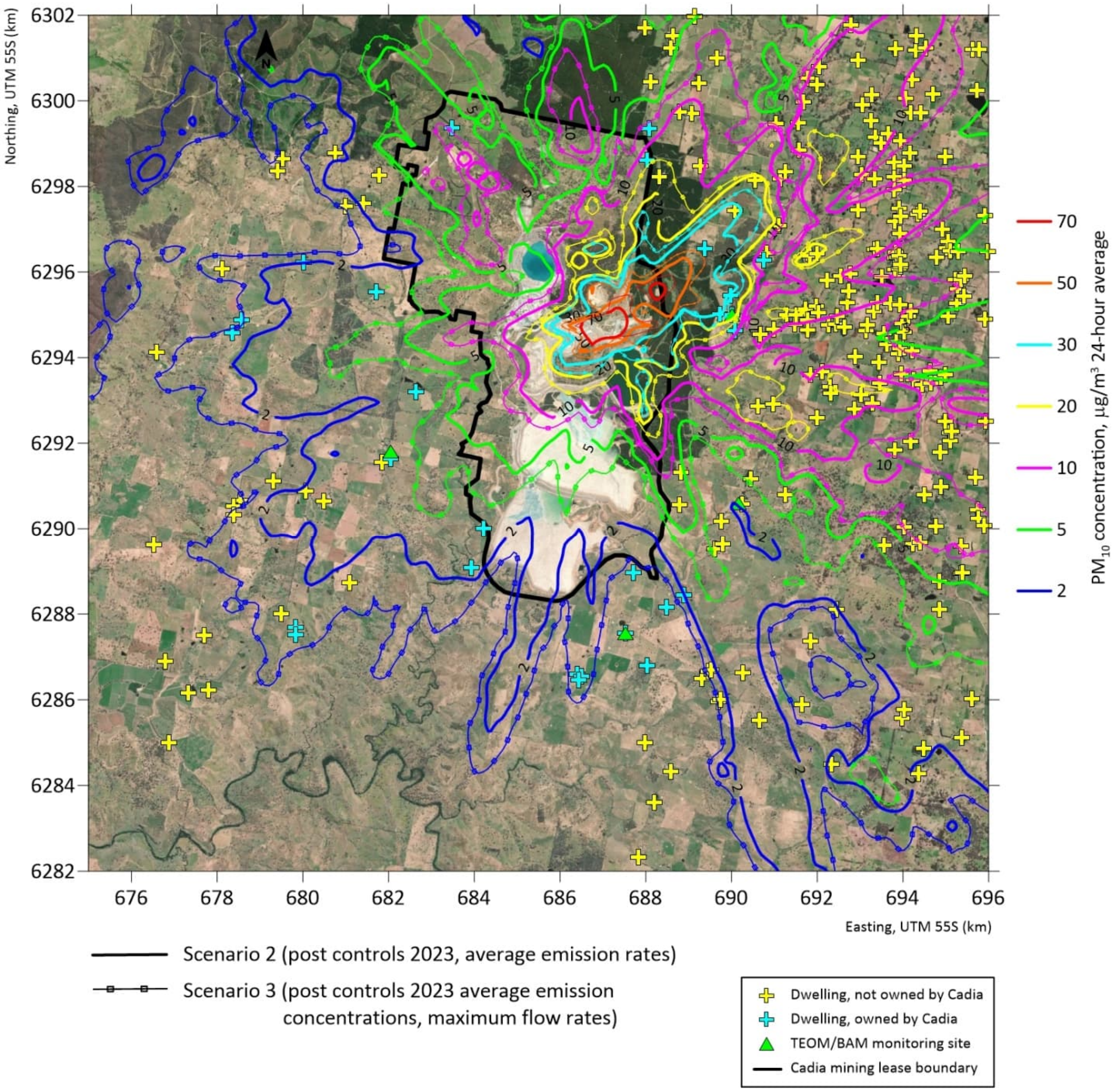

Figure 6-2. Comparison of Scenarios 2 and 3 for vent emissions requested by EPA – 24-hour average PM_{10} (comparing average flow rates with maximum flow rates).

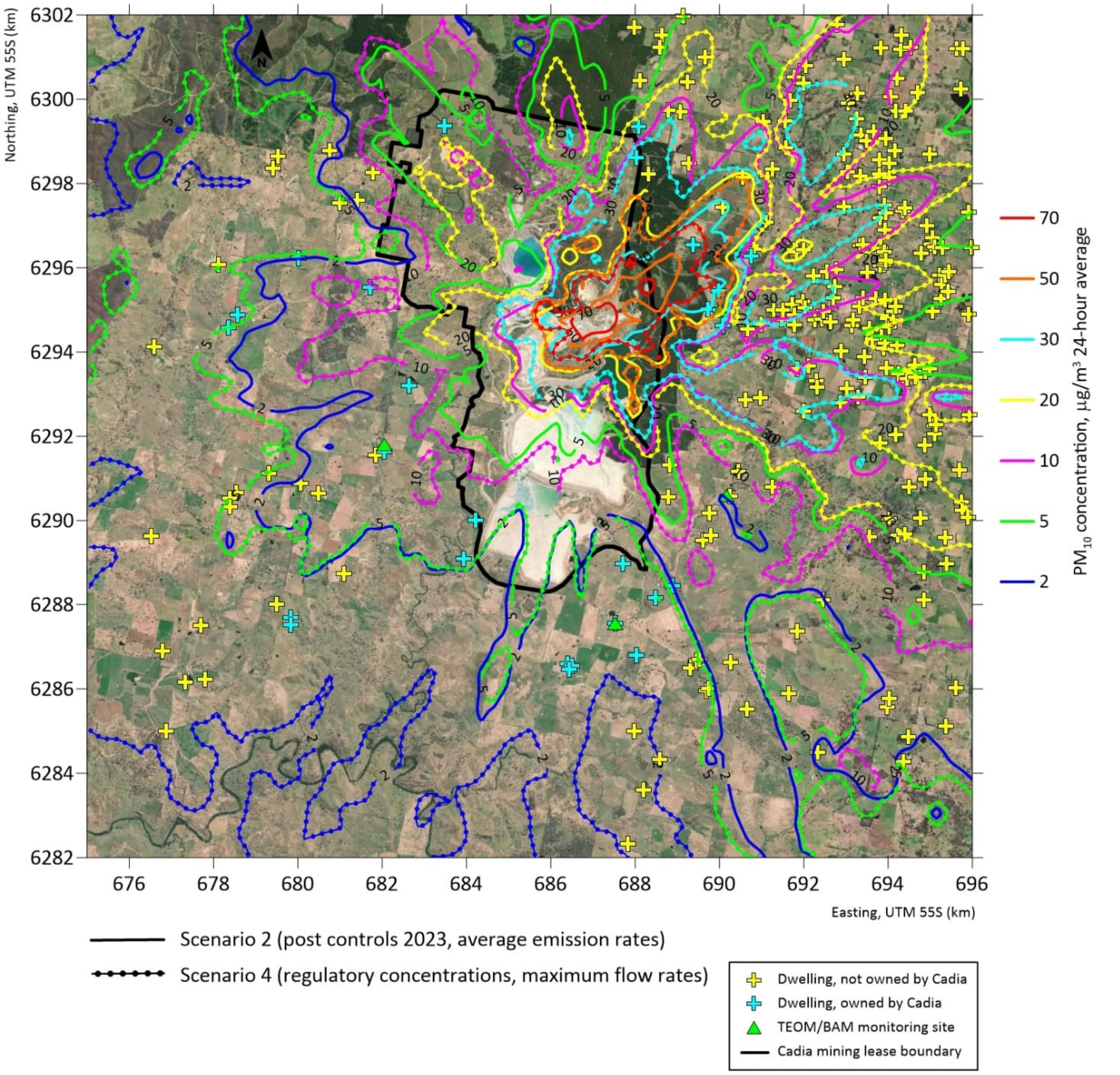

Figure 6-3. Comparison of Scenarios 2 and 4 for vent emissions requested by EPA – 24-hour average PM_{10} (comparing 2023 average emission rates with regulatory maximum emission rates).

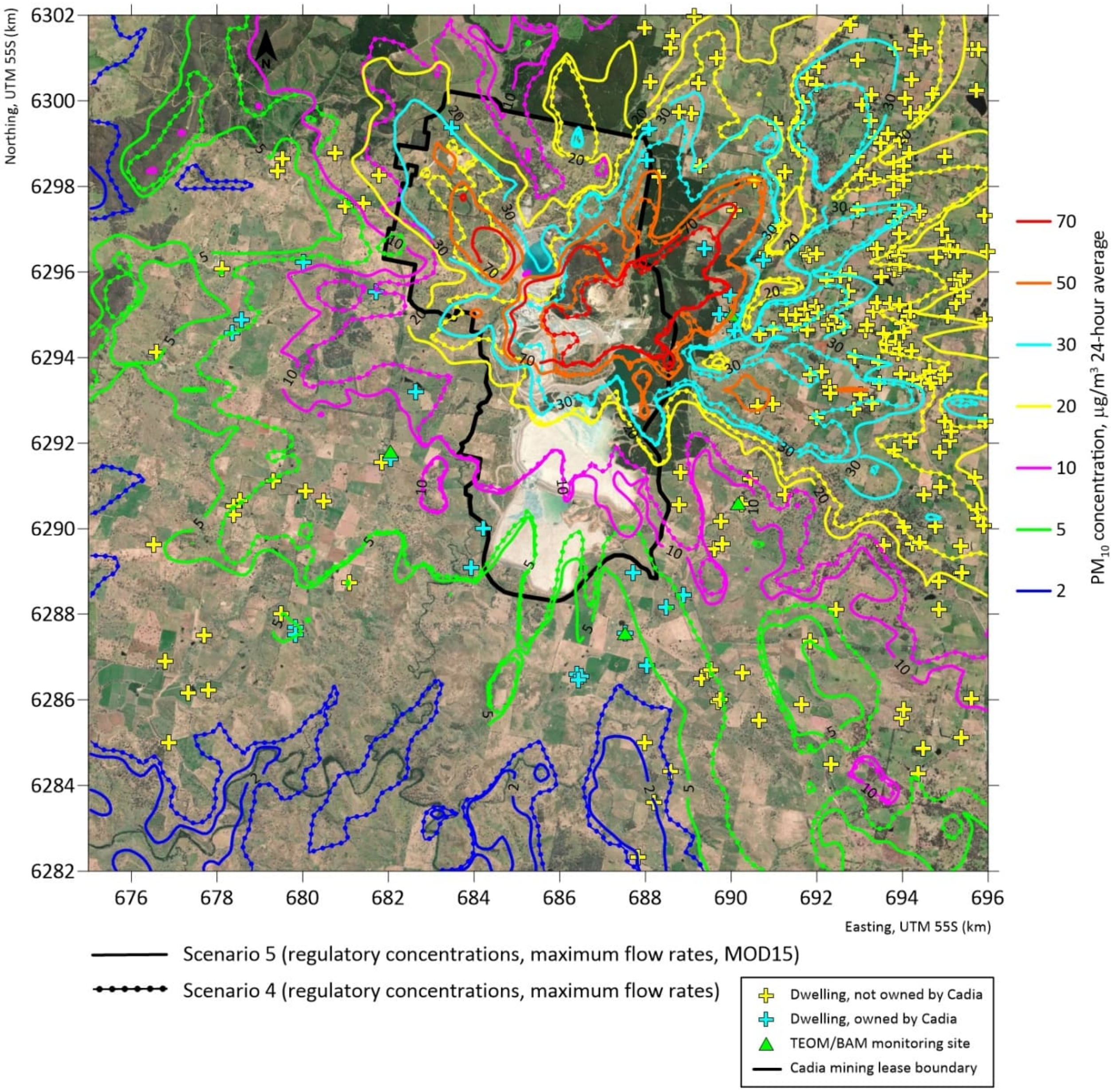

Figure 6-4. Comparison of Scenarios 4 and 5 for vent emissions requested by EPA – 24-hour average PM_{10} (effect of adding MOD15 stacks, all vents at regulatory maximum emission rates)

6.4 Comparison of Model Results with TAS (2023a)

6.4.1 Contour plot comparisons

Jacobs' model results for incremental PM_{10} and $PM_{2.5}$ using the closest possible replication of the TAS (2023a) emission inventory are presented in Figure 6-5 to Figure 6-8. The model results are expressed using the same conventions as in TAS (2023a) and overlaid on the equivalent figures from TAS (2023a) for direct comparison.

The emission inventory used by Jacobs for this purpose included the following assumptions:

- Emissions from crusher, dozers, graders, handling, and vehicles all as the "base case" emission inventories described in Section 4.
- For loading and handling, activity of loading ore to and from main COS and storage location was not included.
- Discharge characteristics and emission rates from vents 3A, 5 and 7 as "Scenario 1" (Table 4-3).
- Discharge characteristics from vent 8 as "Scenario 1" (Table 4-3), however PM_{10} emission rate reduced by 90%, and emission rate reduced by 50% for $PM_{2.5}$.
- Wind erosion sources as "Option 2" (Table 4-25), with all sources emission rates varying by cube of wind speed. In addition, all emission rates reduced by 50% for controls.
- Ore processing source as TAS (2023a) emission inventory with no controls.

The PM_{10} model results compare well in most parts of the domain for both the 24-hour and annual average periods. Notwithstanding, there are notable differences in the 24-hour average results from Figure 6-5:

1. The Jacobs model underpredicts concentrations compared to TAS (2023a) in the south part of the domain, but predicts higher concentrations in the northwest part of the domain.
2. The Jacobs model predicts a different footprint shape for contour lines in the northeast part of the domain; this is probably reflecting the emissions from VR8 as discussed further in the following section.
3. The Jacobs model predicts lower concentrations at Woodville and Meribah AQMS than TAS (2023a), but similar concentrations at Bundarra and Triangle Flat.

Similar observations are noted for the PM_{10} annual average, but these are fairly small incremental differences between the models that may not be noticeable in actual monitoring data.

The $PM_{2.5}$ model results do not compare as well for 24-hour averages. Notable differences in the 24-hour average results from Figure 6-7 include:

1. The Jacobs model underpredicts the maximum incremental concentrations compared to TAS (2023a) in the south part of the domain, but predicts higher concentrations in the northwest, north, northeast and east parts of the domain. This is particularly noticeable in the northeast quadrant where, like with PM_{10}, a different contour footprint shape is seen compared to the TAS model. In this Jacobs model, the concentrations predicted in this area are driven by the $PM_{2.5}$ emission rate from the VR8 vent. However, this should be the same emission rate in both models so the compared difference cannot be explained.
2. The Jacobs model predicts lower maximum incremental concentrations at the Triangle Flat and Meribah AQMS than TAS (2023a), about the same at Bundarra, and higher concentrations at Woodville.

Similar observations are noted for the $PM_{2.5}$ annual average, however these are fairly small incremental differences between the models that may not be noticeable in monitoring data.

In locations where 24-hour average incremental concentrations of PM_{10} are less than 20 µg/m^3, or 24-hour average incremental concentrations of $PM_{2.5}$ are less than 10 µg/m^3, it is unlikely that cumulative concentrations (after background is added) would exceed the air quality objectives in Approved Methods. Similar comment applies for annual-average incremental concentrations of PM_{10} and $PM_{2.5}$ of 10 and 3 µg/m^3 respectively. These concentrations are considered the indicator threshold for potential cumulative impacts in the following discussion.

Considering Figure 6-5 to Figure 6-8 for the “existing” 2022 emission inventory, at many sensitive receptors across the modelling domain the difference in concentrations predicted by the two models is of low consequence, because the indicator threshold concentration for potential cumulative impacts is not exceeded for either. This applies to all of the off-site annual average incremental concentrations of PM_{10} and $PM_{2.5}$, and most of the receptors for 24-hour average concentrations.

At some receptors for the 24-hour averages, the indicator threshold is exceeded with both models suggesting that the cumulative impacts may exceed the Approved Methods air quality objectives, although the number of exceedance per year at a given receptor could be different depending on the model used.

However, there are some sensitive receptors where 24-hour average incremental concentrations exceed the indicator threshold values in the Jacobs model but not the TAS model, particularly to the northwest of the Cadia boundary. As the indicator threshold concentrations only provide a preliminary screening test for the risk of cumulative concentrations exceeding the air quality objectives in Approved Methods, further analysis of cumulative concentration predictions is required to assess this risk, as discussed in Section 6.5.

The differences noticed between the two models may be due to any or all the different approaches used to define the emission rates, how the dust is released from each emission source, and/or model setup. Without full access to the SLB wind data and model input files used by TAS (2023a), Jacobs cannot further isolate the causes of these differences.

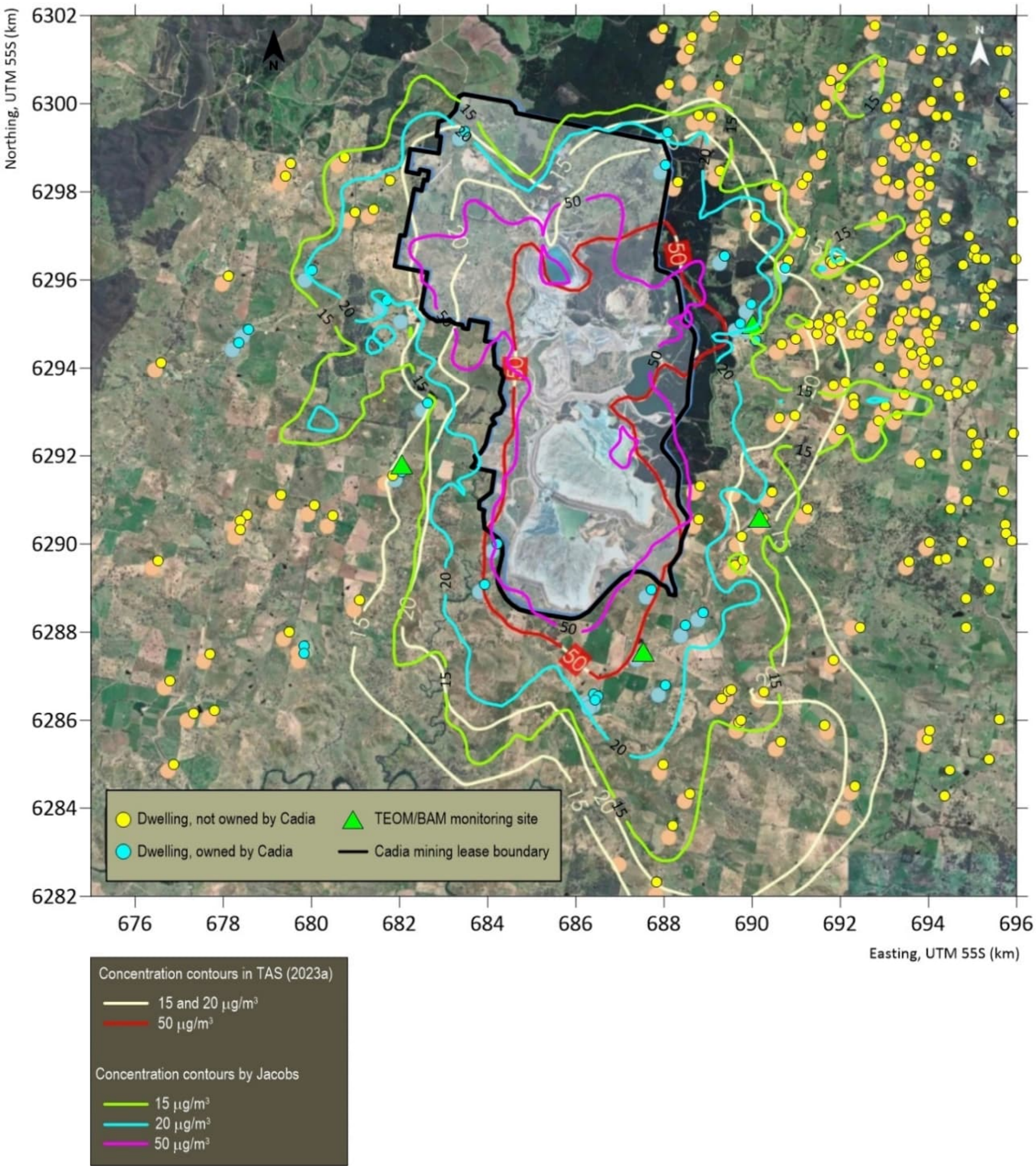

Figure 6-5. Comparison of TAS (2023a) incremental model results for CVO with Jacobs closest replicate of TAS emission inventory – PM_{10} 24-hour average.

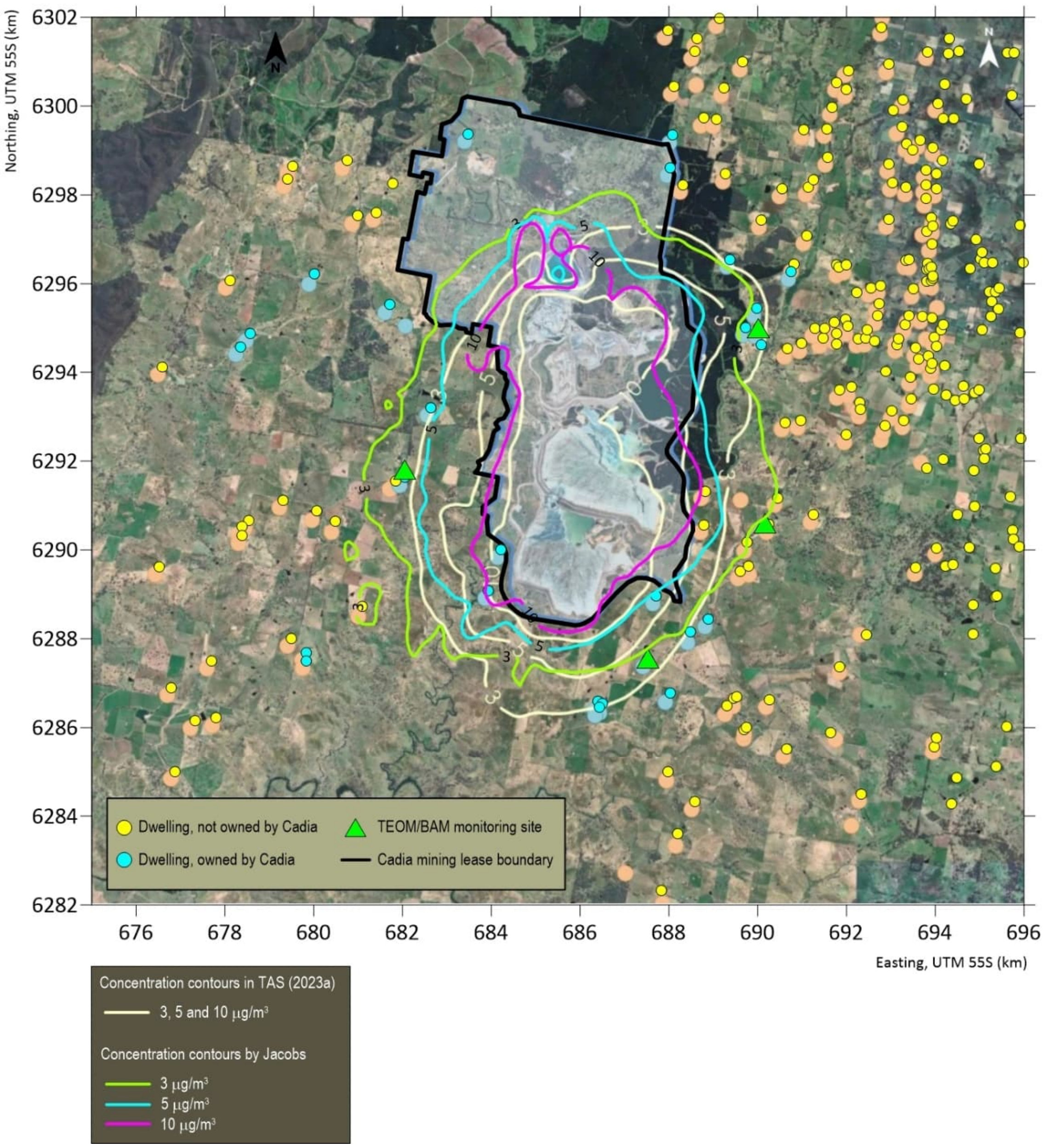

Figure 6-6. Comparison of TAS (2023a) incremental model results for CVO with Jacobs closest replicate of TAS emission inventory – PM_{10} annual average.

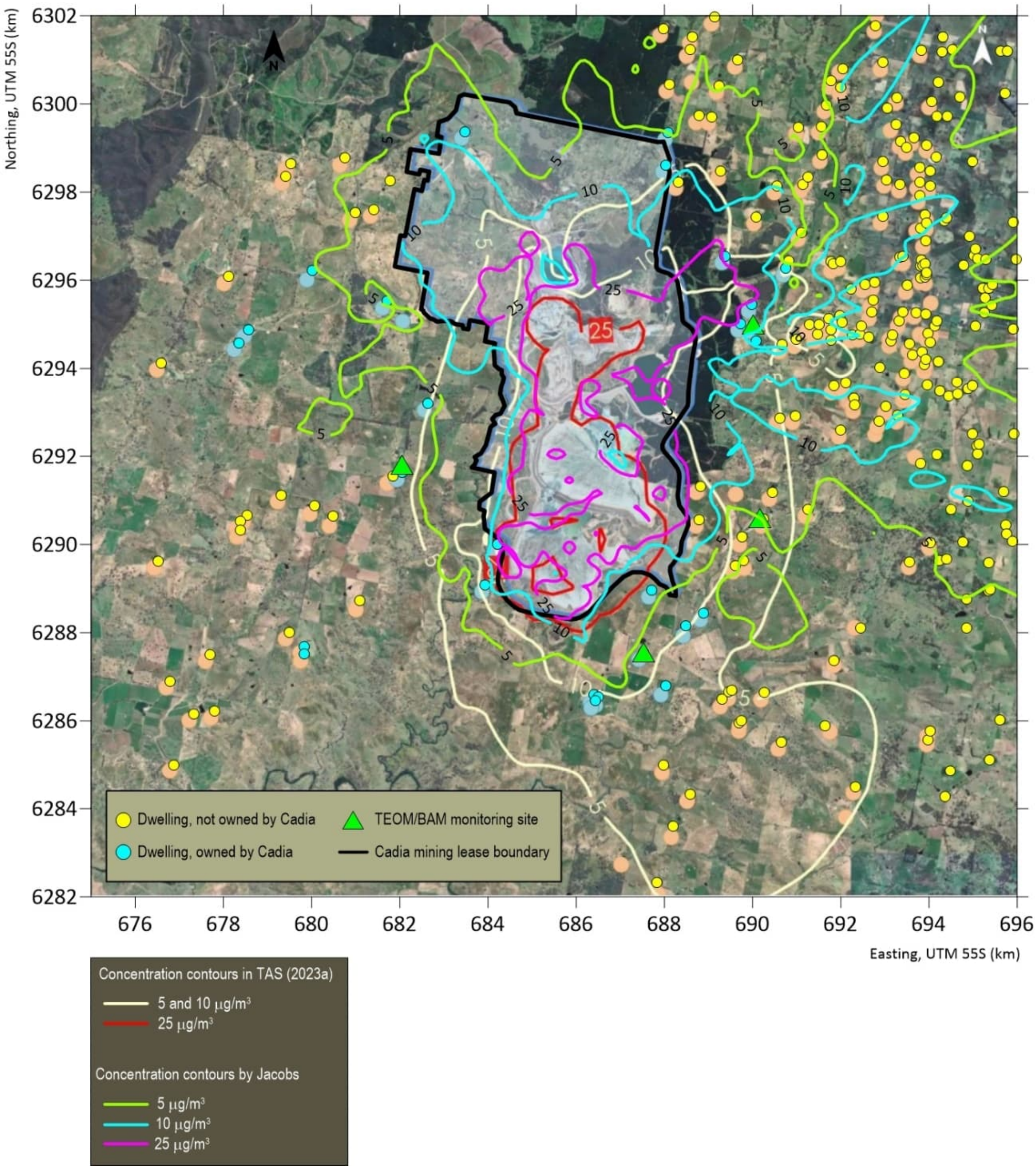

Figure 6-7. Comparison of TAS (2023a) incremental model results for CVO with Jacobs closest replicate of TAS emission inventory – $PM_{2.5}$ 24-hour average.

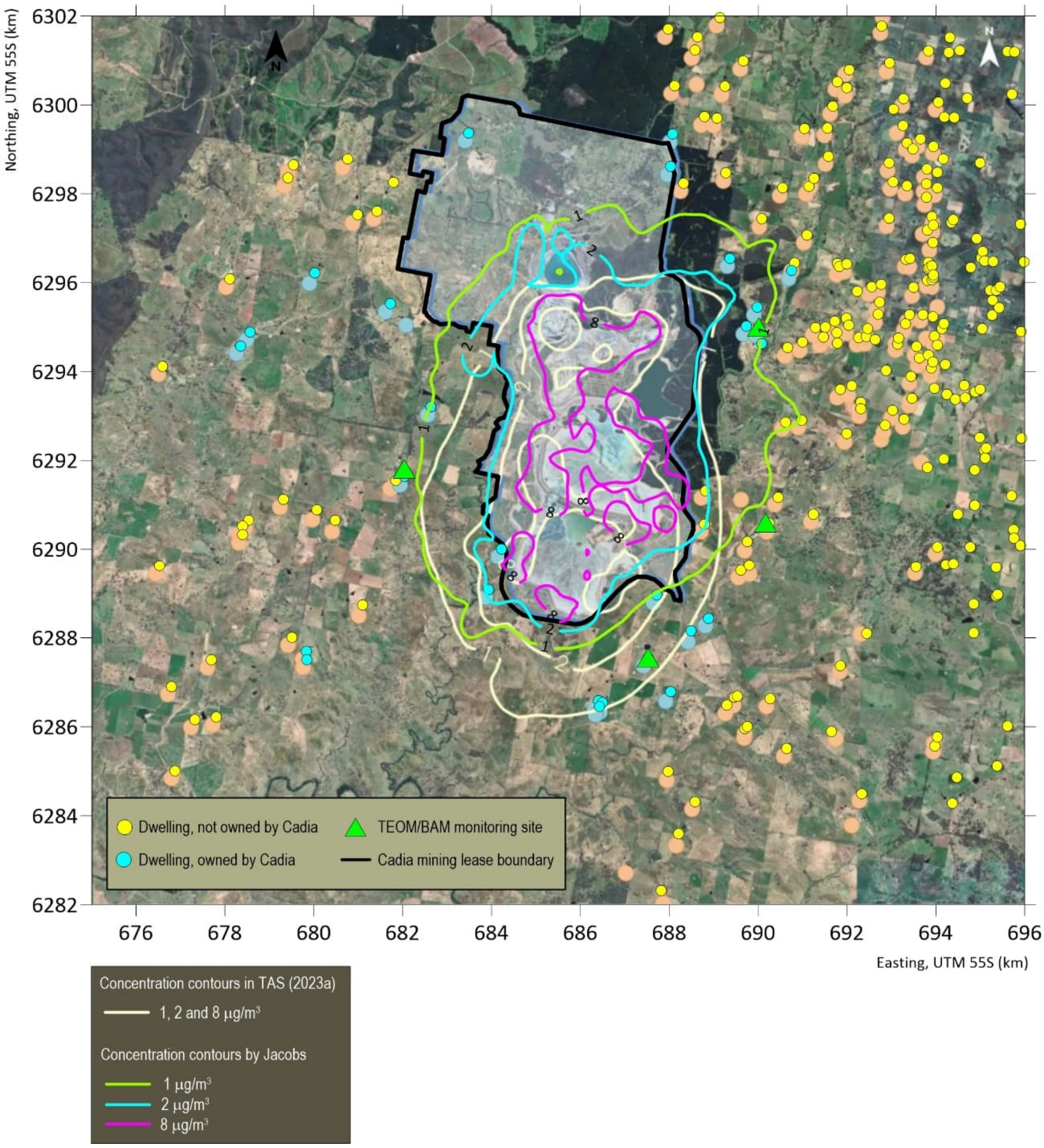

Figure 6-8. Comparison of TAS (2023a) incremental model results for CVO with Jacobs closest replicate of TAS emission inventory – $PM_{2.5}$ annual average.

6.4.2 Comparison of Jacobs model against monitoring data

Jacobs prepared cumulative model results for the "as TAS 2023a" scenario by adding contemporaneous background concentrations on an hour-by-hour basis as outlined in Section 5.7. The cumulative model results were then extracted for each hour at the locations of the four BAM AQMS. Quantile-quantile (or Q-Q) plots comparing the statistical distribution of measured versus modelled concentrations are shown in Figure 6-9 for PM_{10} and Figure 6-10 for $PM_{2.5}$. Only the time period when BAM data was measured was used to create the Q-Q plots, so maximum concentrations shown on the graphs may not be the same as reported elsewhere for the full 2022 year.

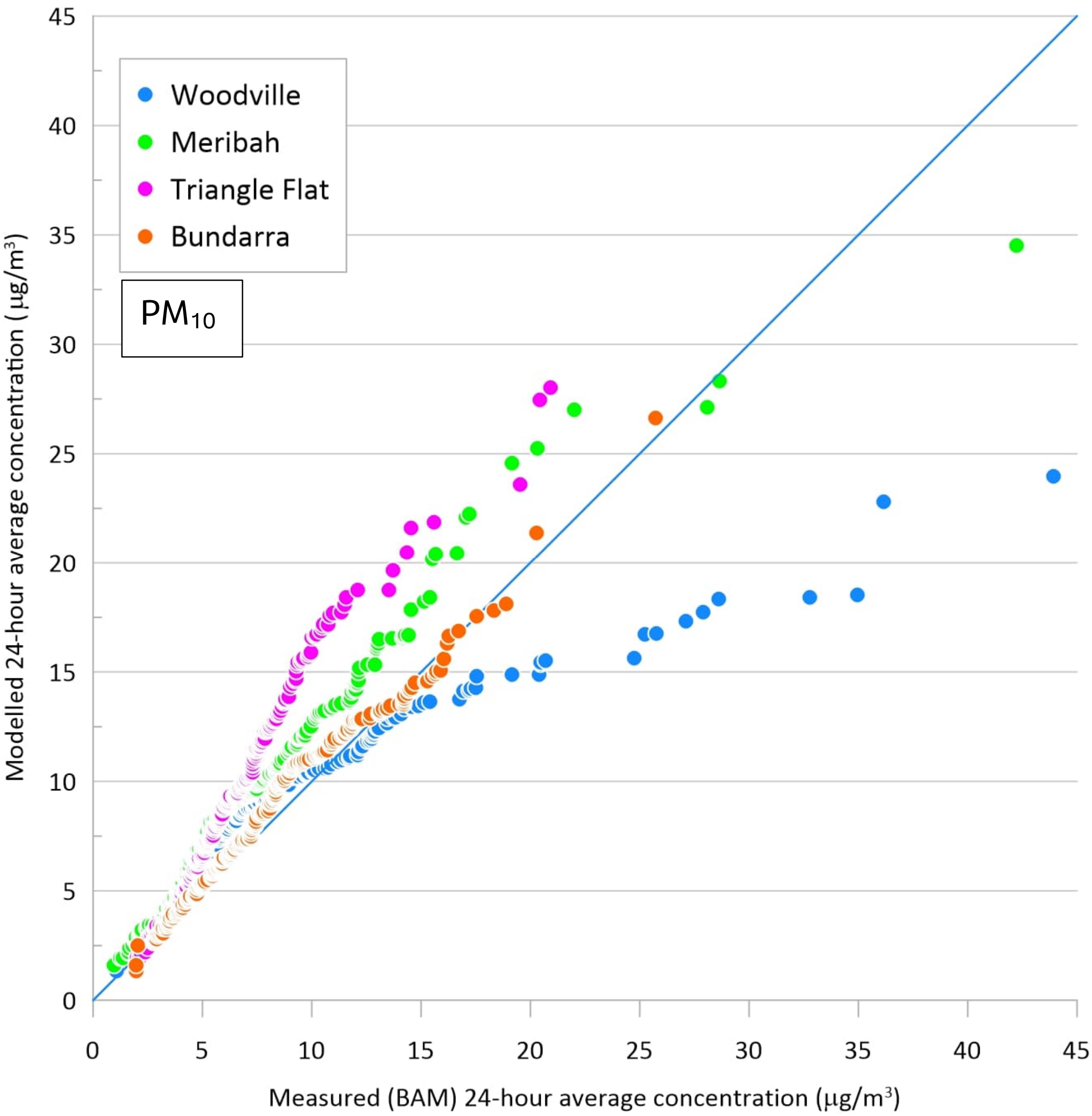

Figure 6-9. Quantile-quantile plots comparing Jacobs cumulative model results for CVO (closest replicate to TAS (2023a) emission inventory) with measured data from BAMs, 2022. PM_{10} 24-hour average.

For PM_{10}, the Q-Q plots show good agreement for Bundarra, Triangle Flat and Meribah, although Meribah may be slightly underpredicting measured data at high end concentrations. However, Woodville is showing considerable underprediction of measured concentrations.

For $PM_{2.5}$, the Q-Q plots also show good agreement for Bundarra and Triangle Flat, but a more pronounced underprediction of measured data at higher concentrations for Meribah, and a similar degree of underprediction for Woodville.

The underpredictions seen at Meribah may be due to the uncertainty in wind vector predictions in this part of the domain, and resulting differences in the Jacobs and TAS CALMET models.

The underpredictions seen at Woodville may be due to the assumptions about reduction in emission rates from VR8. However, the differences could also be due in part to other factors such as the meteorological model setup and dispersion settings, or even the differences in calculation of background concentrations as discussed in Section 5.7. The causes of the different model results cannot be further investigated without additional information and data relating to the TAS model setup as identified throughout this report.

With the Jacobs model setup, the TAS (2023a) conclusion that at 2022 emission rates, PM_{10} emission rates from VR8 should be reduced by 90% and $PM_{2.5}$ emission rates by 50% seems unrealistic.

With any comparison of modelled versus measured data, it is always a tough ask for a model to replicate the top measured predictions, particularly when background concentrations are a large component of the cumulative concentration, and when there is a limited duration to the dataset like that investigated. Other factors that affect the predicted maximum and high-percentile concentrations are:

- With point sources (such as the vents) in complex terrain, it is difficult to precisely predict ground level impacts in both time and space simultaneously.
- The cumulative concentration is the sum of the incremental concentration and the assumed background at the time, so is subject the assumed representative background at any given hour.
- The actual background at the modelled location might also be subject to local interferences that increase the measured concentrations and that aren't accounted for in the background concentration - for example, nearby wood smoke emissions.

These comments are general limitations of the Q-Q plot approach to validate a model for PM_{10} and $PM_{2.5}$, which apply not only to the Q-Q figures in this report but also to the Q-Q validation rationale used by TAS (2023a).

Given that the emission scenario modelled in TAS (2023a) was the 2022 emission inventory prior to the installation of controls on VR8, further efforts to validate the CVO dispersion model would be better focused on the existing post-controls emission scenario. Jacobs' recommended model for that scenario is discussed in the following section, however validation against ambient monitoring data has not been carried out due to the lack of availability of measured data for the relevant time period.

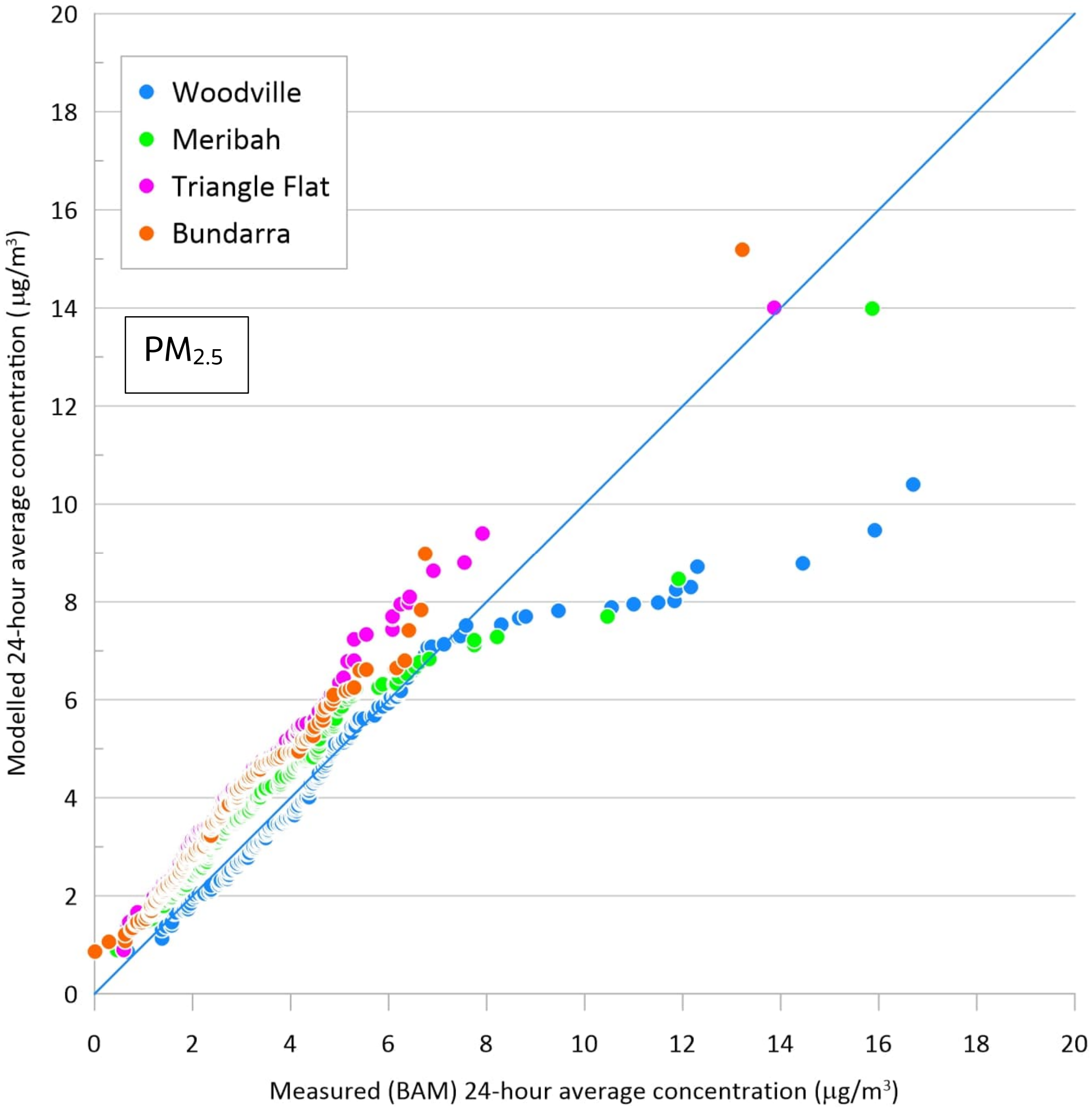

Figure 6-10. Quantile-quantile plots comparing Jacobs cumulative model results for CVO (closest replicate to TAS (2023a) emission inventory) with measured data from BAMs, 2022. $PM_{2.5}$ 24-hour average.

6.5 Cumulative Emission Models

6.5.1 Options Tested

Jacobs compared three options for the total cumulative emissions from current CVO operations (after VR8 controls installed) including background air quality, based on the review of emission factors, activity intensity data, and the sensitivity analyses presented in earlier sections of this report. The basis for emissions adopted for each source type in the model are summarized in Table 6-4. The models were run using the 2022 meteorological data.

Table 6-4. Sources included in Jacobs' model for current CVO operations

Source Type	Emission option adopted for the Lower Bound model	Emission option adopted for the Moderate Bound model	Emission option adopted for the Upper Bound model	Cross-reference
Crusher	Base case	Option 3	Option 3	Table 4.10
Ore processing	Base case, plus 90% reduction for controls	As lower bound	Base case, plus 70% reduction for controls	Option 1, Table 4.14
Bulldozers	Base case	As lower bound	Option 2	Table 4.15
Graders	Base case with TAS (2020a) activity intensity	As lower bound	Option 2	Table 4-16
Loading and handling	Option 5 (Option 2 with wind speed weighting)	As lower bound	Option 3 (plus no wind speed weighting)	Table 4.14
Vehicle-tracked emissions	Option 7 with 85% control	Option 7 with 75% control	Option 7 with 50% control	Table 4-18
Dry areas, non TSFs	Option 5 with 70% control	As lower bound	Option 6 with 70% control	Table 4-25
TSFs	Option 3 with 70% control	As lower bound	Option 3 with 50% control	Table 4-25
Vents VR3A, 5 and 7	Scenario 2	As lower bound	Scenario 3	Table 4-4 Table 4-5
Vent VR8	Scenario 2	As lower bound	Scenario 3	Table 4-4 Table 4-5

The results for each of the models were extracted for each hour at the locations of the four BAM AQMS. Quantile-quantile (or Q-Q) plots comparing the statistical distribution of measured versus modelled concentrations are shown in Appendix R. Only the time period when BAM data was measured was used to create the Q-Q plots.

Overall, the Upper Bound model predicts higher concentrations at each AQMS than were measured in 2022, and the Lower Bound model predicts equivalent or slightly lower concentrations. High-quantile measured concentrations at Woodville are higher than the predicted concentrations, but this may be due to either emissions from VR8 or local background emissions.

The Moderate Bound model appears to be a reasonable overall match with the AQMS, predicting slightly higher than measured data which is appropriate for regulatory modelling. Therefore, based on the comparison to 2022 measured data, the emission scenario represented by the Moderate Bound model is recommended by Jacobs as a suitable cumulative model for emissions from CVO operations.

6.5.2 Recommended Model

The contour plot figures for the Jacobs recommended model (ie. the Moderate Bound model) are shown in Figures S-1 to S-8 in Appendix S. Both incremental (CVO operations only, Figures S-1 to S-4) and cumulative (including background air quality, Figures S-5 to S-8) model results are shown.

Model results for individual houses close to the mine boundary and within the 40 µg/m^3 contour for cumulative 24-hour average PM_{10} (Figure S-5), as well as the four AQMS locations, are listed in Table 6-5. The locations of these receptors are shown in Figure 6-11. Cumulative 24-hour average PM_{10} concentrations are predicted to exceed the Approved Methods air quality objective at three privately owned dwellings – R1, R2 and R8.

Table 6-5. Discrete receptor model results for cumulative 24-hour and annual average PM_{10} and $PM_{2.5}$, Jacobs recommended model for 2022 emission inventory.

Receptor ID (Figure 6-11)	Cumulative 24-hour average, µg/m^3		Cumulative annual average, µg/m^3		Receptor type
	PM_{10}	$PM_{2.5}$	PM_{10}	$PM_{2.5}$	
Approved Methods air quality objective	50	25	25	8	
R1	57.2	16.4	9.9	3.9	Private-owned dwelling
R2	56.2	17.3	9.6	3.9	Private-owned dwelling
R3	46.0	15.0	8.9	3.7	Private-owned dwelling
R4	40.1	14.8	9.0	3.7	Private-owned dwelling
R5	32.6	14.8	9.2	3.7	Private-owned dwelling
R6	40.3	14.9	10.0	4.1	Private-owned dwelling
R7	46.5	19.7	12.9	5.2	Private-owned dwelling
R8	54.9	24.8	12.6	5.1	Private-owned dwelling
R9	39.2	14.1	8.2	3.4	Private-owned dwelling
R10	45.1	14.1	8.3	3.5	Private-owned dwelling
R11	39.1	14.1	8.2	3.5	Private-owned dwelling
R12	51.6	15.6	10.0	4.0	CHPL-owned dwelling
R13	74.1	22.7	10.9	4.3	CHPL-owned dwelling
R14	55.5	15.8	10.7	4.2	CHPL-owned dwelling
R15	47.2	16.0	10.9	4.3	CHPL-owned dwelling
R16 Woodville	42.2	15.6	10.3	4.1	AQMS
R17 Meribah	26.9	14.1	8.9	3.6	AQMS
R18 Triangle Flat	28.7	14.1	9.4	3.8	AQMS
R19 Bundarra	28.1	15.6	10.2	3.9	AQMS

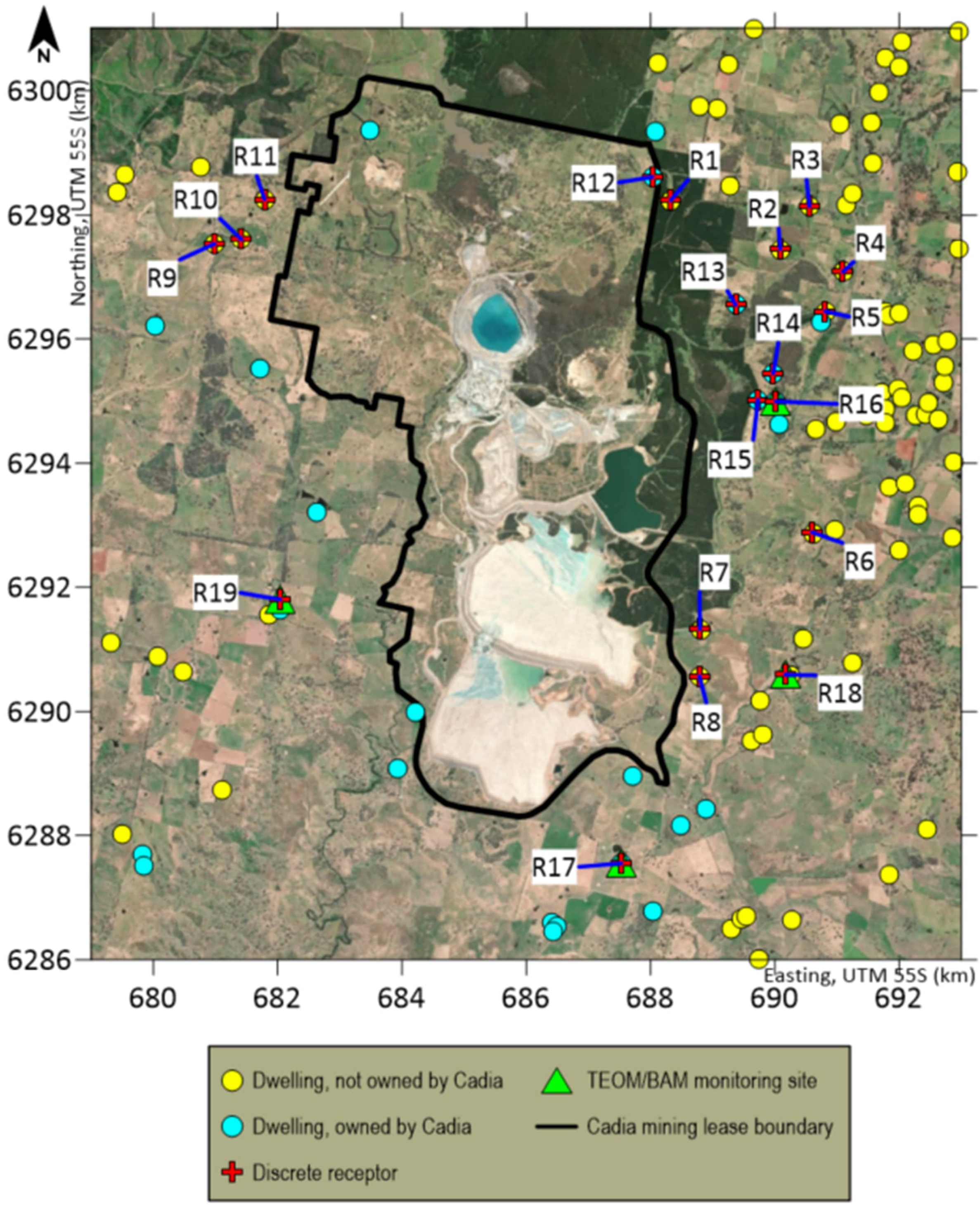

Figure 6-11. Discrete receptor locations.

The model, which is based on the 2022 emission inventory, indicates a risk of several privately-owned houses and CPHL-owned houses being exposed to 24-hour average cumulative PM_{10} or $PM_{2.5}$ concentrations approaching or exceeding the Approved Methods objectives.

It is also noted that the locations of the existing AQMS may not be suitable to capture the highest PM_{10} and $PM_{2.5}$ concentrations predicted by the model at residences.

6.6 Vent Emission Scenario Cumulative Models

The vent emission scenarios identified in Section 4.2.3.2 were added to the Jacobs recommended model whilst retaining all other emission sources and background air quality.

The cumulative model results for the five vent scenarios are shown as contour plots in Appendix T. Tables comparing the 24-hour and annual average PM_{10} and $PM_{2.5}$ results for each scenario at each discrete receptor from Figure 6-11 are shown in Table 6-6 to Table 6-9. The tables list both incremental and cumulative concentrations and, for 24-hour averages, the number of exceedances of the Approved Methods ambient air quality criteria (if any).

Scenario 1 represents the measured 2022 emission rates from VR8 prior to the installation of controls and without any adjustment of emission rates to account for particle entrainment in droplets. The model results are significantly higher than in the other scenarios, and are not realistic of future emissions from Cadia.

Summary contour plots comparing a single cumulative concentration contour for Scenarios 2, 3, 4 and 5 are provided in Figure 6-12 to Figure 6-15. Scenario 1 is not shown on these plots because it is considered to be unrealistic. Scenario 2 is the same as the Jacobs “moderate bound” model presented in the previous section.

The plots show increasing predicted concentrations beyond the site boundary at the regulatory limits and with the inclusion of MOD15.

Table 6-6. Discrete receptor model results for cumulative 24-hour average PM_{10}, Jacobs recommended model for 2022 emission inventory plus Vent Scenarios.

Receptor ID (Figure 6-11)	24-hour average PM_{10}, µg/m^3 *															Receptor type
	Vent Scenario 1			Vent Scenario 2			Vent Scenario 3			Vent Scenario 4			Vent Scenario 5			
	Incr.	Cum.	Excd.	Incr.	Cum.	Excd.	Incr.	Cum.	Excd.	Incr.	Cum.	Excd.	Incr.	Cum.	Excd.	
Approved Methods air quality objective		50			50			50			50			50		
R1	55	76	3	51	57	1	57	63	1	77	83	2	83	89	3	Private-owned dwelling
R2	82	91	3	47	56	1	49	59	1	75	84	2	86	95	4	Private-owned dwelling
R3	49	58	2	37	46		39	49		60	69	2	69	79	2	Private-owned dwelling
R4	25	47		19	40		20	37		28	44		33	46		Private-owned dwelling
R5	26	39		21	33		22	36		26	40		27	42		Private-owned dwelling
R6	67	73	3	23	40		29	47		52	65	4	58	68	4	Private-owned dwelling
R7	47	56	1	42	47		42	47		42	49		42	49		Private-owned dwelling
R8	52	57	2	50	55	2	50	55	2	50	55	2	50	55	2	Private-owned dwelling
R9	36	42		32	39		33	39		35	40		40	47		Private-owned dwelling
R10	47	51	1	42	45		42	46		45	48		46	51	1	Private-owned dwelling
R11	41	44		36	39		36	40		38	42		50	55	1	Private-owned dwelling
R12	44	57	1	46	52	1	51	57	1	68	74	2	78	84	3	CHPL-owned dwelling
R13	122	132	9	65	74	2	67	76	2	97	106	6	104	113	7	CHPL-owned dwelling
R14	114	136	10	34	56	1	37	57	1	62	80	9	65	82	9	CHPL-owned dwelling
R15	125	138	6	34	47		41	52	1	68	81	8	72	84	10	CHPL-owned dwelling
R16 Woodville	98	111	2	29	42		33	45		53	66	3	56	69	5	AQMS
R17 Meribah	19	27		19	27		19	27		20	27		21	29		AQMS
R18 Triangle Flat	19	29		19	29		19	29		19	29		19	29		AQMS
R19 Bundarra	16	29		10	28		10	28		12	29		13	30		AQMS

* Incr. = incremental concentration Cum. = cumulative concentration Excd. = number of exceedances of Approved Methods criteria (blank = none).
Cumulative concentrations exceeding Approved Methods air quality objective shown in brown font.

Table 6-7. Discrete receptor model results for cumulative 24-hour average $PM_{2.5}$, Jacobs recommended model for 2022 emission inventory plus Vent Scenarios.

Receptor ID (Figure 6-11)	24-hour average $PM_{2.5}$, µg/m^3 *															Receptor type
	Vent Scenario 1			Vent Scenario 2			Vent Scenario 3			Vent Scenario 4			Vent Scenario 5			
	Incr.	Cum.	Excd.	Incr.	Cum.	Excd.	Incr.	Cum.	Excd.	Incr.	Cum.	Excd.	Incr.	Cum.	Excd.	
Approved Methods air quality objective		25			25			25			25			25		
R1	19	33	1	15	16		17	18		23	24		24	26	1	Private-owned dwelling
R2	27	29	2	14	16		15	17		23	25		26	28	1	Private-owned dwelling
R3	16	18		11	15		12	15		18	20		21	23		Private-owned dwelling
R4	8	16		6	15		5	15		8	15		9	16		Private-owned dwelling
R5	8	16		5	15		6	15		8	15		8	16		Private-owned dwelling
R6	23	25	1	7	15		9	16		16	21		18	22		Private-owned dwelling
R7	19	23		15	20		15	20		16	20		16	20		Private-owned dwelling
R8	20	25		20	25		20	25		20	25		20	25		Private-owned dwelling
R9	10	15		9	14		9	14		9	14		11	15		Private-owned dwelling
R10	12	15		10	14		11	14		11	14		12	16		Private-owned dwelling
R11	11	15		9	14		9	14		10	14		13	17		Private-owned dwelling
R12	13	26	1	13	16		15	17		20	22		23	24		CHPL-owned dwelling
R13	40	42	4	19	21		20	22		29	31	2	30	33	2	CHPL-owned dwelling
R14	39	43	5	11	16		11	16		19	22		20	23		CHPL-owned dwelling
R15	43	47	2	11	16		13	16		21	25		22	25	1	CHPL-owned dwelling
R16 Woodville	34	37	1	9	15		10	15		16	20		17	20		AQMS
R17 Meribah	4	14		3	14		3	14		3	14		4	14		AQMS
R18 Triangle Flat	6	14		6	14		6	14		6	14		6	14		AQMS
R19 Bundarra	4	16		2	16		2	16		3	16		4	16		AQMS

* Incr. = incremental concentration Cum. = cumulative concentration Excd. = number of exceedances of Approved Methods criteria (blank = none).
Cumulative concentrations exceeding Approved Methods air quality objective shown in brown font.

Table 6-8. Discrete receptor model results for cumulative annual average PM_{10}, Jacobs recommended model for 2022 emission inventory plus Vent Scenarios.

Receptor ID (Figure 6-11)	Cumulative annual average PM_{10}, µg/m³ *										Receptor type
	Vent Scenario 1		Vent Scenario 2		Vent Scenario 3		Vent Scenario 4		Vent Scenario 5		
	Incr.	Cum.	Incr.	Cum.	Incr.	Cum.	Incr.	Cum.	Incr.	Cum.	
Approved Methods air quality objective		25		25		25		25		25	
R1	4	11	3	10	3	10	4	11	5	12	Private-owned dwelling
R2	4	11	2	10	3	10	4	11	5	12	Private-owned dwelling
R3	3	10	2	9	2	9	3	10	3	11	Private-owned dwelling
R4	3	10	2	9	2	9	3	10	3	10	Private-owned dwelling
R5	4	11	2	9	2	9	3	10	3	10	Private-owned dwelling
R6	5	12	3	10	3	10	4	11	5	12	Private-owned dwelling
R7	7	14	6	13	6	13	6	13	6	14	Private-owned dwelling
R8	6	13	6	13	6	13	6	13	6	13	Private-owned dwelling
R9	1	8	1	8	1	8	1	8	2	9	Private-owned dwelling
R10	1	9	1	8	1	8	1	9	2	9	Private-owned dwelling
R11	1	9	1	8	1	8	1	8	2	9	Private-owned dwelling
R12	4	11	3	10	3	10	4	11	5	12	CHPL-owned dwelling
R13	7	14	4	11	4	11	6	13	7	14	CHPL-owned dwelling
R14	8	15	4	11	4	11	6	13	6	14	CHPL-owned dwelling
R15	7	14	4	11	4	11	6	13	6	14	CHPL-owned dwelling
R16 Woodville	6	13	3	10	4	11	5	12	5	12	AQMS
R17 Meribah	2	9	2	9	2	9	2	9	2	9	AQMS
R18 Triangle Flat	3	10	2	9	2	9	3	10	3	10	AQMS
R19 Bundarra	4	11	3	10	3	10	4	11	4	11	AQMS

* Incr. = incremental concentration Cum. = cumulative concentration

Table 6-9. Discrete receptor model results for cumulative annual average $PM_{2.5}$, Jacobs recommended model for 2022 emission inventory plus Vent Scenarios.

Receptor ID (Figure 6-11)	Cumulative annual average $PM_{2.5}$, μg/m^3 *										Receptor type
	Vent Scenario 1		Vent Scenario 2		Vent Scenario 3		Vent Scenario 4		Vent Scenario 5		
	Incr.	Cum.	Incr.	Cum.	Incr.	Cum.	Incr.	Cum.	Incr.	Cum.	
Approved Methods air quality objective		8		8		8		8		8	
R1	1	4	1	4	1	4	1	4	1	5	Private-owned dwelling
R2	1	5	1	4	1	4	1	4	1	4	Private-owned dwelling
R3	1	4	1	4	1	4	1	4	1	4	Private-owned dwelling
R4	1	4	1	4	1	4	1	4	1	4	Private-owned dwelling
R5	1	4	1	4	1	4	1	4	1	4	Private-owned dwelling
R6	1	5	1	4	1	4	1	4	1	5	Private-owned dwelling
R7	2	6	2	5	2	5	2	5	2	5	Private-owned dwelling
R8	2	5	2	5	2	5	2	5	2	5	Private-owned dwelling
R9	0	4	0	3	0	3	0	3	0	4	Private-owned dwelling
R10	0	4	0	3	0	3	0	4	1	4	Private-owned dwelling
R11	0	4	0	3	0	3	0	4	1	4	Private-owned dwelling
R12	1	4	1	4	1	4	1	4	1	5	CHPL-owned dwelling
R13	2	5	1	4	1	4	2	5	2	5	CHPL-owned dwelling
R14	2	6	1	4	1	4	2	5	2	5	CHPL-owned dwelling
R15	2	5	1	4	1	4	2	5	2	5	CHPL-owned dwelling
R16 Woodville	2	5	1	4	1	4	1	5	1	5	AQMS
R17 Meribah	0	4	0	4	0	4	0	4	0	4	AQMS
R18 Triangle Flat	1	4	1	4	1	4	1	4	1	4	AQMS
R19 Bundarra	1	4	1	4	1	4	1	4	1	4	AQMS

* Incr. = incremental concentration Cum. = cumulative concentration

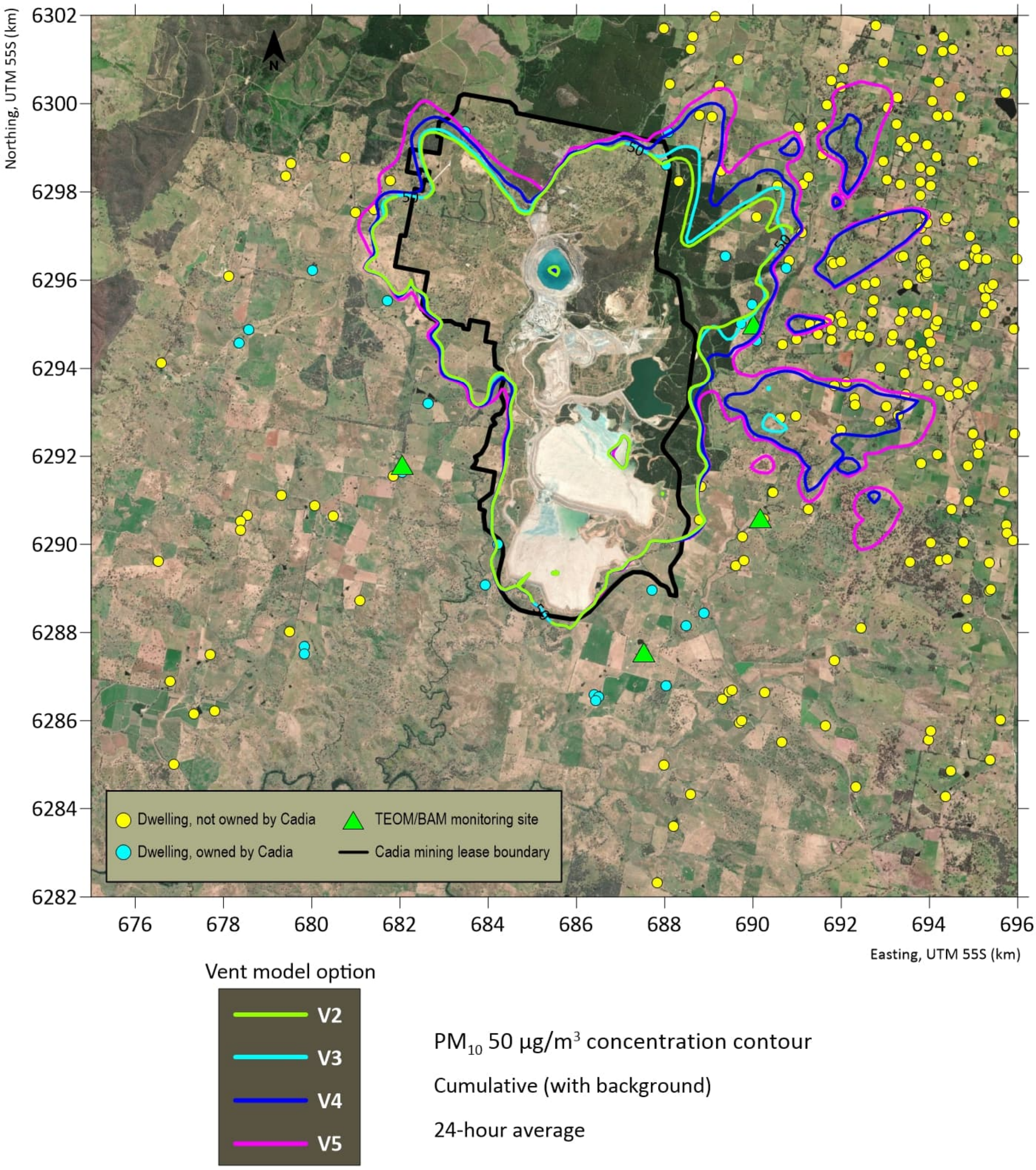

Figure 6-12. Comparison of vent scenarios 2, 3, 4 and 5 for cumulative 24-hour average PM_{10}.

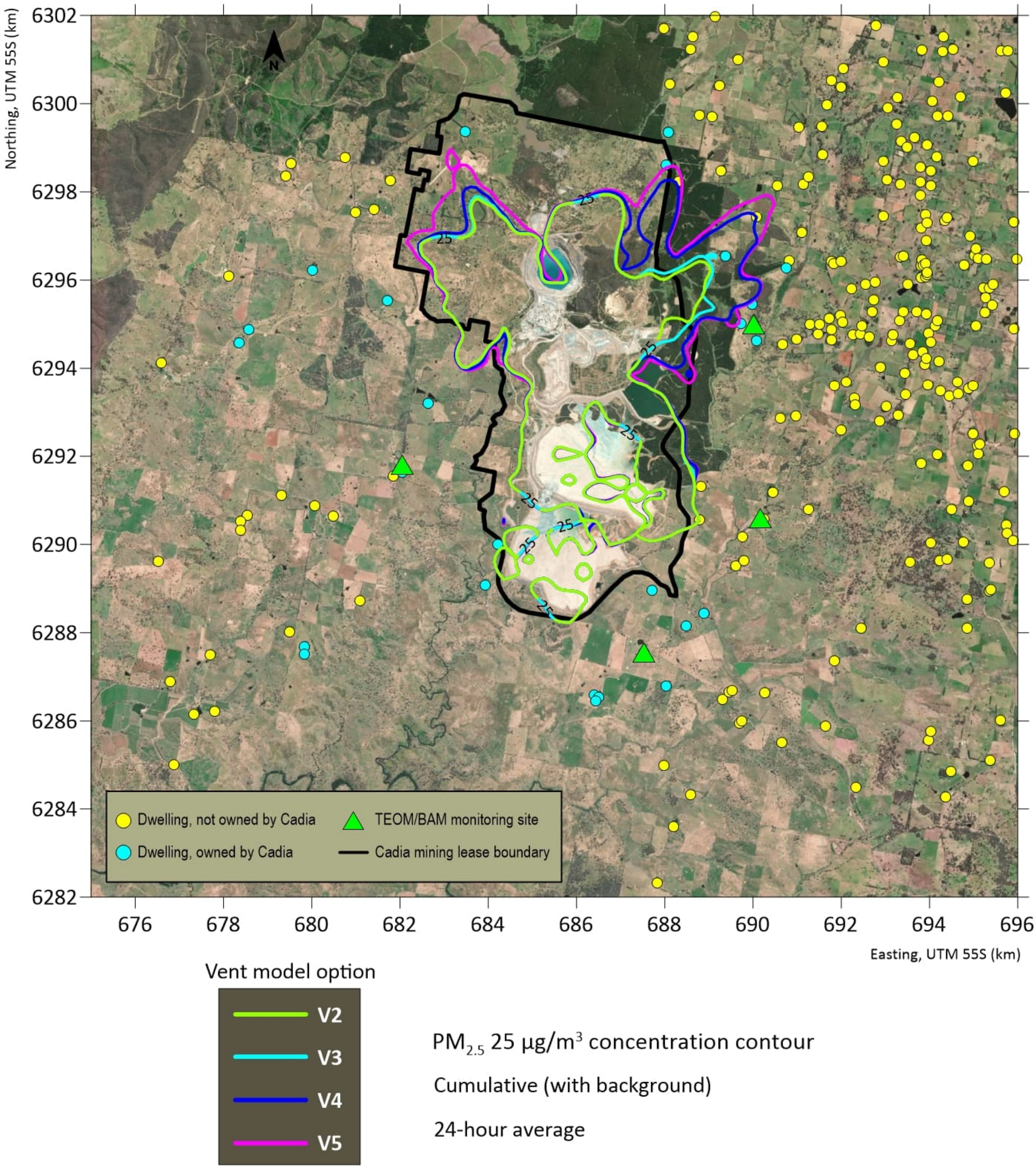

Figure 6-13. Comparison of vent scenarios 2, 3, 4 and 5 for cumulative 24-hour average $PM_{2.5}$.

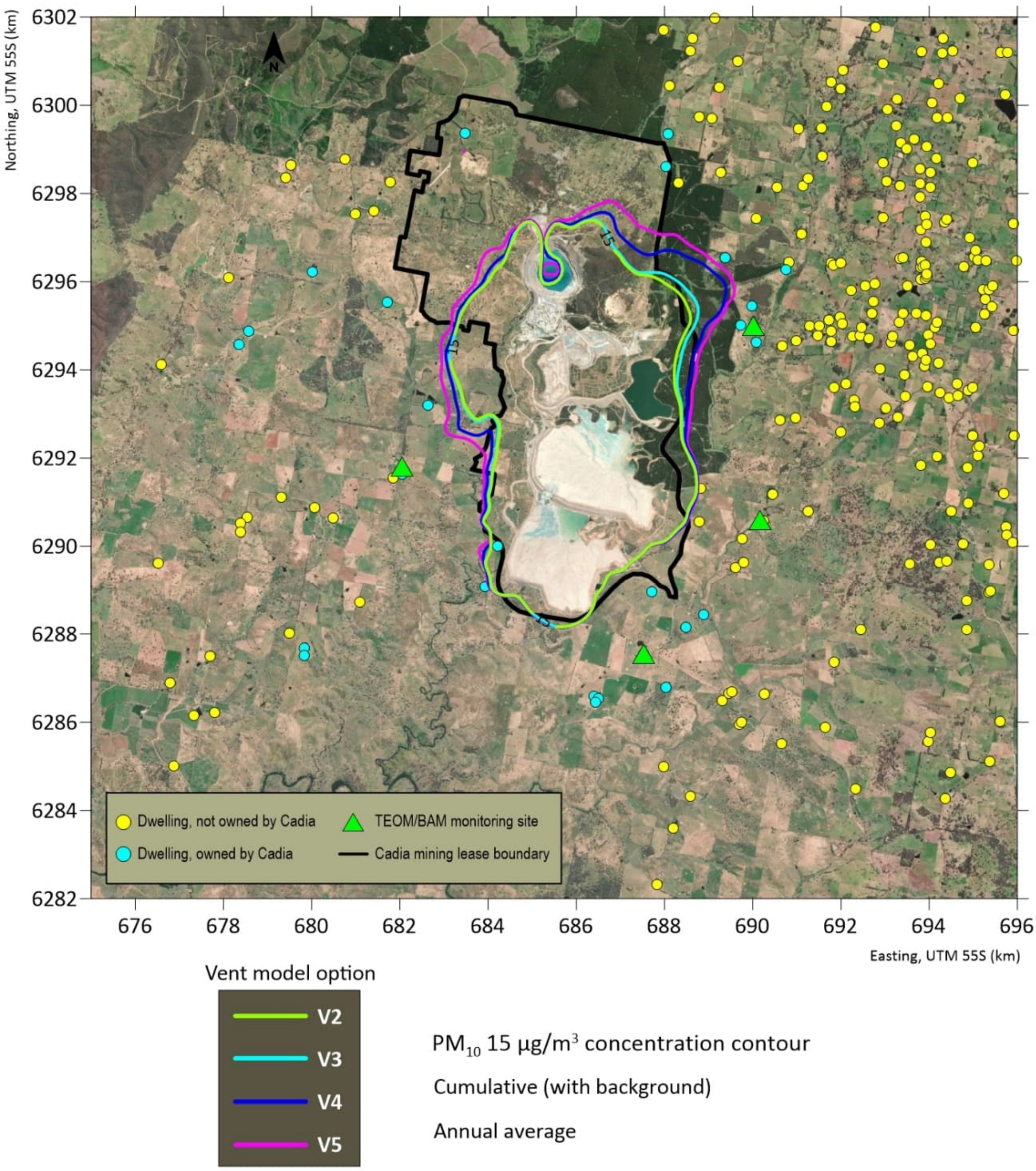

Figure 6-14. Comparison of vent scenarios 2, 3, 4 and 5 for cumulative annual average PM_{10}.

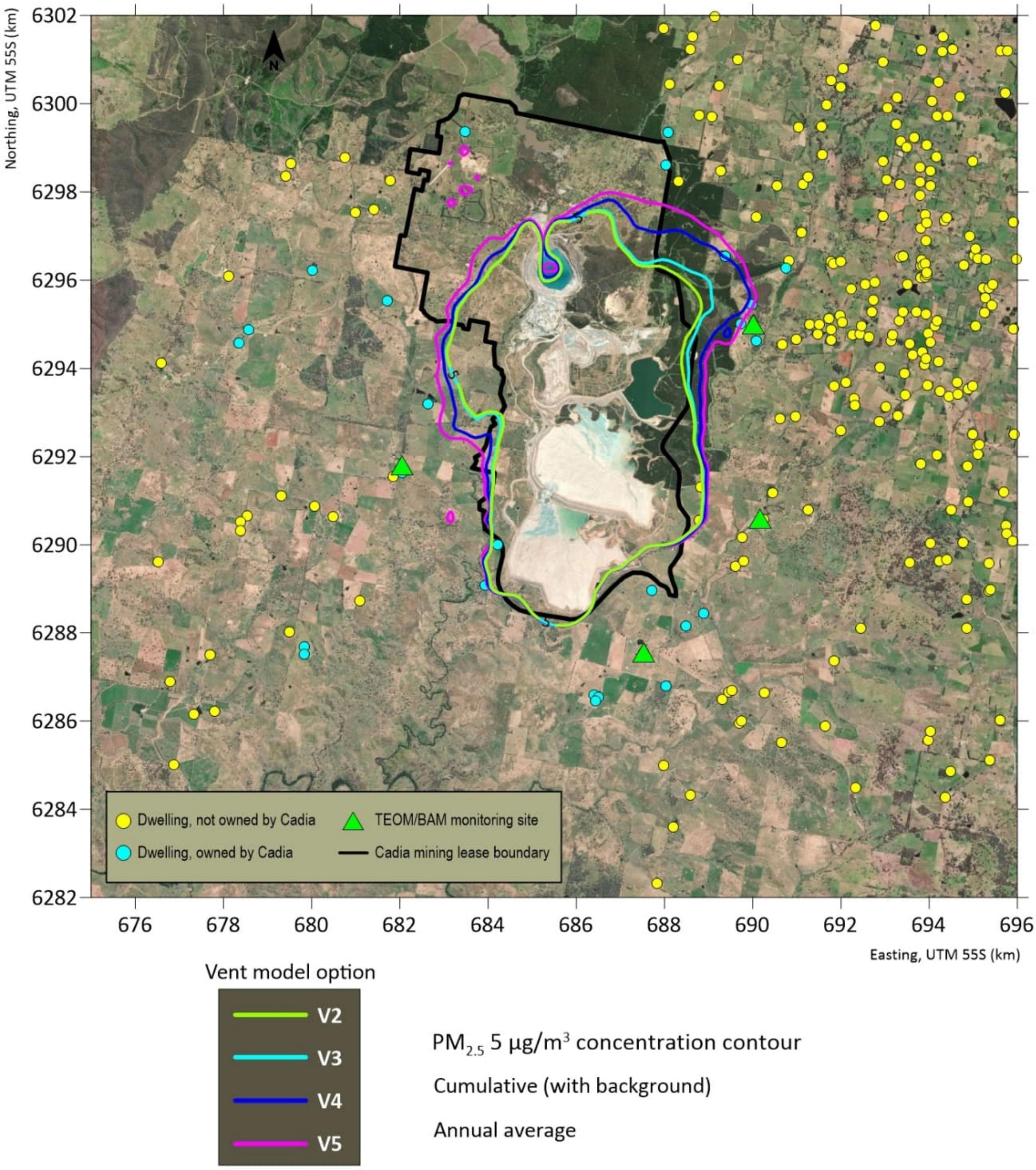

Figure 6-15. Comparison of vent scenarios 2, 3, 4 and 5 for cumulative annual average $PM_{2.5}$.

7. Recommendations

The recommendations listed below are raised for the purposes of allowing more transparent independent verification of monitoring data and potential air quality impacts in the future, and also to improve any future modelling assessment.

7.1 Recommendations arising from Existing Conditions review

1. AEMR reporting
    a. For reporting of annual average PM_{10} and $PM_{2.5}$ in the AEMRs, each AEMR should clearly state if any data during extraordinary events has been removed from the dataset, including an explanation for this and a list of the dates that were excluded.
2. Monitoring sites
    a. A new dust monitor should be established downwind of the TSFs under northeasterly winds, that collects data that is appropriate to report externally to EPA and the public and can be used to demonstrate the effectiveness of the TSF mitigation plan.
    b. Review Woodville site location for the representativeness of the Woodville site and potential influences from wood smoke. Consider alternative sites that do not have the same potential for influence by non-mine sources.
3. Meteorological data
    a. Include 1-hour average wind speeds and directions for SLB AWS calculated from 10-minute average meteorological data in any future revisions to the Cadia model prepared as part of this report.
    b. Whenever wind speed and direction data records for Ridgeway and/or SLB are requested from CPHL, the data should be requested in both 10-minute averages and at shorter intervals, such as 1-minute average recordings, so that calculated averages can be independently verified. If this data is not being recorded, it is recommended that CPHL commence recording of this data as soon as possible.
4. Vent emissions
    a. For VR3A, VR5 and VR7, the discharge parameters and emission rates are based on only one round of testing in 2022 and it is recommended that the longer term representativeness of these inputs could be refined through additional testing.
    b. Jacobs is not aware of whether the emissions from vents VR3A, VR5 and VR7 suffer from the same measurement difficulties as VR8, however further clarification on this could be beneficial to understanding the potential impact from these sources

7.2 Recommendations for Future Reports

5. Future air quality assessment reports prepared by, or on behalf of CPHL should include the following:
    a. Crushing emissions basis
        i. Confirm the current crushing stages and design throughput for each Concentrator.
        ii. Assumption basis for total annual ore throughput in crushing stages.
        iii. Justify the assumption of 90% control for each crushing stage and/or alternative representative control efficiency.
    b. Loading and handling emissions basis

        i. Validation of assumed moisture content of 3.85%.
        ii. Confirm basis for definition of "ore processing" activity intensity, which is nominally 5x the annual throughput rate with no controls.
        iii. Provide validation of all assumed activity intensities for loading and handling from CVO.
    c. Bulldozers emissions basis
        i. Justification of the assumed silt and moisture content for bulldozer activities, including providing a likely range for these parameters.
        ii. Review whether it would be appropriate to apply a control factor to bulldozer activities, depending on the practicality of keeping handled material moist.
    d. Graders emission basis
        i. Confirm the basis for estimating annual VKT for graders
        ii. Confirm the basis for assuming grader speed of 8 km/h and how this is controlled at CVO.
    e. Vehicle-tracked dust emissions basis
        i. Justify site specific average silt content values
        ii. Detail operating hours of short and long haulage and how that is incorporated into the model
        iii. Justify adopted control efficiency for watering activity
    f. Wind erosion emissions basis
        i. Provide details of the method of applying the EF to open area wind erosion – either constant or varying with wind speed (if the latter, specifying the weighting regime that was used).
        ii. Provide maps showing the areas assigned to each area source.
        iii. Justify control efficiencies for the TSFs now that mitigation trials are well progressed; including whether some portions of the surface are regarded as having a higher control efficiency than other areas.

6. Non-constant source emissions
    a. Detail which sources are subject to wind-dependent emissions, and how this wind-dependence is applied.
    b. Detail which sources are subject to time-dependent emissions, such as activities which operate for less than 24 hours per day.

7. Background concentrations
    a. Detail methods of calculating representative background concentrations.

8. Supply of modelling files to EPA
    a. All model input files should be stored by the consultant or CPHL, and made available to EPA on request. This would include any meteorological data files, and supplementary emission rate input files used in the modelling.

9. Local meteorological data observations
    a. An additional AWS should be installed in the area represented by the Triangle Flat and Meribah BAM locations. The site would not need to host a full range of meteorological monitoring instruments, as the priority would be to collect wind speed and direction data to provided improved confidence in future modelling results in this part of the domain.

8. Conclusions

This report provides an independent technical review of air quality impact assessments that have been prepared generally over the 2020-2023 period for CVO, and presents an independent atmospheric dispersion model that simulates the dispersion of particulate emissions from the mine.

During the review, the following key findings were noted:

1. There is a potential issue with the method of calculating 1-hour average wind directions in the meteorological data provided by CPHL, which can lead to errors such as a wind direction being recorded as southerly when it was in fact a northerly. This could be problematic if CPHL relies on this data (for example, comparing dates and times of complaint reports with wind direction records) or provides this data to external stakeholders. This issue appears to have been corrected in the modelling conducted by TAS (2023a). However, the problem may also be present in the 10-minute data averages provided by CPHL, which are also calculated values. The quality and methods of averaging all raw meteorological data collected by, or on behalf of CPHL should be reviewed.

2. The mine site is favorably positioned for dispersion of dust during strong winds from the north-northeast to north directions, due to the absence of privately-owned dwellings close to the CPHL boundary downwind of the TSFs under those winds. Jacobs recommends that a new dust monitor be established downwind of the TSFs under northeasterly winds, that collects data that is appropriate to report externally to EPA and the public and can be used to demonstrate the effectiveness of the TSF mitigation plan and calibrate the dispersion model under high wind speeds.

3. The complexity of dispersion models varies greatly from one project to the next depending on the number of different sources to consider. In the case of a mine site there are many different sources of particle emissions to account for. Emission factor references are used to build the emission inventory that is a key input to the dispersion model. Any air quality assessment report that relies on an emission inventory for dispersion modelling should clearly define all inputs for developing that emission inventory, and identify any assumptions that the model may be sensitive to. Similarly, the input settings used to set up the sources and dispersion parameters within the models should be clearly stated. Jacobs reviewed whether this information is provided in the TAS Reports, and particularly in TAS (2023a). Some data is clearly stated, but other assumptions are not stated or the adopted values are not justified. Recommendations are provided where further information could be supplied in future modelling assessments.

4. There is a gap in local meteorological information to the southeast of CVO which means that the meteorological modelling needed to inform the dispersion model must make estimates of likely wind patterns in that part of the model domain which are much more dependent on user settings than at locations closer to the CVO wind observation sites at Ridgeway and SLB. Confidence in future modelling results in this part of the domain could be increased if the meteorological modelling was supported by additional wind observations to the southeast of CVO, somewhere in the area represented by the Triangle Flat and Meribah BAM locations.

5. Jacobs prepared a dispersion model using the closest possible replication of the TAS (2023a) emission inventory to compare model results with TAS (2023a). The incremental model results compared well in some parts of the domain, particularly the west and southwest. However, there were some considerable differences in other parts of the domain, particularly for the 24-hour averaging period. In many respects, the differences in concentrations predicted by the models are of low consequence for the “existing” 2022 emission inventory, because even adding background concentrations is unlikely to increase the cumulative concentrations to the extent that additional sensitive receptors are potentially exposed to concentrations that exceed the air quality objectives in Approved Methods. However, there are some sensitive receptors where 24-hour average incremental concentrations are quite a lot higher in the

Jacobs model. Further analysis of cumulative concentration predictions was therefore conducted to assess the risk of air quality exceeding the air quality objectives in Approved Methods at these locations (see item 8 below).

6. The differences between the models also could be relevant for future assessment of the effects of proposed development or mitigation scenarios. These differences may be due to any or all the different approaches used to define the emission inventory, or model setup as discussed in this report. Without full access to the SLB wind data and model input files used by TAS (2023a), Jacobs cannot further refine the causes of these differences.

7. TAS (2023a) concluded that at 2022 emission rates, PM_{10} emissions from VR8 should be reduced by 90% and $PM_{2.5}$ emissions by 50%. With the Jacobs model setup, this conclusion seems unrealistic as the model is underpredicting measured concentrations at Woodville. However, with any comparison of modelled versus measured data, it is difficult for a model to replicate the top measured predictions at a precise location, particularly when background concentrations are a large component of the cumulative concentration, there is a risk of local interferences contributing to the measured concentrations, and when there is a limited duration to the dataset like that investigated here. Given that the emission scenario modelled in TAS (2023a) was the 2022 emission inventory prior to the installation of controls on VR8, further efforts to validate the CVO dispersion model would be better focused on the existing post-controls emission scenario.

8. Jacobs compiled models for current CVO operations (after VR8 controls installed) based on the review of emission factors, activity intensity data, and the sensitivity analyses presented in earlier sections of this report. Three options were compiled and compared against measured ambient air quality data at the four AQMS operated by CPHL. A recommended model arose from this comparison, for the option that best matched the AQMS data. The recommended model, which is based on the 2022 emission inventory, indicates a risk of several privately-owned houses and CPHL-owned houses being exposed to 24-hour average cumulative PM_{10} or $PM_{2.5}$ concentrations approaching or exceeding the Approved Methods objectives. It is also noted that the locations of the existing AQMS may not be suitable to capture the highest PM_{10} and $PM_{2.5}$ concentrations predicted by the model at residences.

The reviews conducted in this report have been more complex because of the lack of availability of model input files prepared by TAS on behalf of CPHL. The reasons for differences in model outputs between TAS (2023a) and Jacobs cannot be pinpointed and resolved without this information. Jacobs recommends that all model input files should be retained by the consultant or CPHL in future and be able to be provided to EPA if requested. Without this transparency, any model validation presented on behalf of Cadia cannot be fully independently reviewed.

9. References

Advitech (2023). Cadia Air Quality Monitoring Report, March 2023. Prepared for Newcrest Mining Ltd, Rev1 (Final) 7 July 2023.

Airen (2024). Supplementary Air Quality Impact Assessment, Cadia Valley Operations Modification 15. Report prepared for CHPL by Airen Consulting, Rev 0, 11 April 2024.

Australian Coal Association Research Program (ACARP) (2014). Mobile Sampling of Dust Emissions from Unsealed Roads, Stage Two. Report prepared for Australian Coal Research Limited by Pacific Environment Limited.

Australian Nuclear Science and Technology Organisation (ANSTO) (2023). Stage 2 – 12-month Final Report: Cadia Valley Operations PM2.5 Study. Report dated June 2023.

Bohn, R. et al (1978). Fugitive Emissions from Integrated Iron and Steel Plants. Report prepared by Midwest Research Institute, Missouri for USEPA reference EPA-600/2-78-050, March 1978.

CPHL (2016), Cadia Valley Operations Annual Environmental Management Report 2015/2016, submitted to DPE on 28 October 2016

CPHL (2019), Cadia Valley Operations Annual Environmental Management Report 2018/2019, submitted to DPE on 29 October 2019

CPHL (2020), Cadia Valley Operations Annual Environmental Management Report 2019/2020, submitted to DPE on 27 October 2020

CPHL (2021), Cadia Valley Operations Annual Environmental Management Report 2020/2021, submitted to DPE on 29 October 2021

CPHL (2022), Cadia Valley Operations Annual Environmental Management Report 2021/2022, submitted to DPE on 31 October 2022

CPHL (2023), Cadia Valley Operations Annual Environmental Management Report 2022/2023, submitted to DPE on 31 October 2023

Ektimo (2021), Emission Testing Report Return (Exhaust) Air Sampling Newcrest Mining Limited Orange. Report Number R011403a2. Prepared by Ektimo Pty Ltd, issued 17 December 2021.

Ektimo (2022), Mine Vent Emission Study Report Number R012219[Draft 2]. Prepared by Ektimo Pty Ltd, issued 24 May 2022.

Ektimo (2023a), VR8 Post Scrubber Sampling, Report Number R015051r. Prepared by Ektimo Pty Ltd, issued 24 July 2023.

Ektimo (2023b), VR8 – Fortnightly Testing (Round 1). Report Number R014793. Prepared by Ektimo Pty Ltd, issued 25 July 2023.

Ektimo (2023c), VR8 – Fortnightly Testing (Round 2). Report Number R015420. Prepared by Ektimo Pty Ltd, issued 4 August 2023.

Ektimo (2023d), VR8 – Fortnightly Testing (Round 3). Report Number R015421. Prepared by Ektimo Pty Ltd, issued 17 August 2023.

Ektimo (2023e), VR8 – Fortnightly Testing (Round 4). Report Number R015453. Prepared by Ektimo Pty Ltd, issued 29 August 2023.

Ektimo (2023f), VR8 – Fortnightly Testing (Round 5). Report Number R015549a[DRAFT]. Prepared by Ektimo Pty Ltd, issued 12 September 2023.

Ektimo (2023g), Preliminary Report on testing conducted 29 August 2023. Report number R015630p. Prepared by Ektimo Pty Ltd, issued 1 September 2023.

Holmes Air Sciences (2009). Air Quality Impact Assessment: Cadia East Project. Report prepared for Cadia Holdings Pty Ltd, April 2009. As attached to Cadia East Project Environmental Assessment 2009, Appendix E.

Hurley P.J. (2008). TAPM V4. Part 1: Technical Description. CSIRO Marine and Atmospheric Research Paper No. 25.

Katestone Environmental Pty Ltd (2011). NSW Coal Mining Benchmarking Study: International Best Practice Measures to Prevent and/or Minimise Emissions of Particulate Matter from Coal Mining. Final report prepared for Office of Environment and Heritage, reference KE1006953, June 2011.

National Environment Protection Council (NEPC) (2021). National Environment Protection (Ambient Air Quality) Measure, as amended, May 2021.

Newcrest (2018). Cadia Valley Operations Air Quality Monitoring Program, version 4 June 2018.

Newcrest (2020). Cadia Operations, NI 43-101 Technical Report. Report prepared for Newcrest Mining Ltd by Kevin Gleeson, Geoffrey Newcombe, Paul Griffin, and Philip Stephenson. Report effective date 30 June 2020.

Newcrest (2023a). Cadia TSF Dust Suppression Management and monitoring Plan, 710-000-EN-PLA-0027. Revision 1, 2 June 2023.

Newcrest (2023b). Letter to EPA from Newcrest Mining Ltd dated 7 July 2023, regarding Cadia Holdings Pty Ltd - Notice to Provide Information 3505650.

Newcrest (2023c). Letter to EPA from Newcrest Mining Ltd dated 6 October 2023, regarding Cadia Holdings Pty Ltd - Notice to Provide Information 3506856.

Newmont (2023). Modification 15 Tailings Storage Facility Embankment Buttressing. Modification Report, undated.

Newmont (2024). Cadia Air Quality and Greenhouse Gas Management Plan, 710-005-EN-PLA-0029. Rev2 issued 9/02/2024.

NPI (2006). Emission Estimation Technique Manual for Gold Ore Processing, Version 2.0. December 2006.

NPI (2012a). Emission Estimation Technique Manual for Fugitive Emissions, Version 2.0. January 2012.

NPI (2012b). Emission Estimation Technique Manual for Mining, Version 3.1. January 2012.

NSW EPA (2022). Approved Methods for the Modelling and Assessment of Air Pollutants in New South Wales.

NSW Government (2023). New South Wales Annual Compliance Report 2021, National Environment Protection (Ambient Air Quality) Measure. Report prepared by Department of Planning and Environment, June 2023. https://www.environment.nsw.gov.au/-/media/OEH/Corporate-Site/Documents/Air/national-environment-protection-measure-ambient-air-quality-nsw-compliance-report-2021-230223.pdf

NSW Minerals Council (2001). Particulate Matter and Mining; A NSW Minerals Council Technical Paper. Interim Report prepared by NSW Minerals Council with assistance from Holmes Air Sciences, 2 February 2001.

Office of Environment and Heritage (2011). "Generic Guidance and Optimum Model Settings for the CALPUFF Modelling System for Inclusion into the 'Approved Methods for the Modelling and Assessments of Air Pollutants in NSW, Australia'." Prepared for NSW Office of Environment and Heritage by TRC Environmental Corporation. March 2011.

SAGE Environmental Services (2023). Cadia Valley Operations Human Health Risk Assessment. Report prepared for Cadia Holdings Pty Ltd, 1 September 2023.

Serinus (2021), Tailings dust environmental health assessment and monitoring study review. Prepared by Serinus for Newcrest Mining Limited Cadia Valley Operations – 2 July 2021.

Skidmore, E.L. and Hagen L.J. (1977). Reducing Wind Erosion with Barriers. Transactions of the American Society of Agricultural Engineers (Vol. 20, No. 5, 1977).

SKM (2005). Improvement of NPI Fugitive Particulate Matter Emission Estimation Techniques. Final report prepared for WA Department of Environment, May 2005.

State Pollution Control Commission (SPCC) (1983). Air Pollution from Coal Mining and Related Developments. ISBN 0 7240 5936 9.

TAS (2020a). Air Quality Impact and Greenhouse Gas Assessment Cadia Valley Operations Processing Rate Modification. Report prepared by Todoroski Air Sciences for Cadia Holdings Pty Ltd, 1 December 2020. Report accessed from NSW Government Major Projects Planning Portal - https://majorprojects.planningportal.nsw.gov.au/prweb/PRRestService/mp/01/getContent?AttachRef=MP06_0295-MOD-14%2120201210T102623.722%20GMT.

TAS (2020b), Cadia Valley Operations – Ventilation shaft air modelling. Letter from Todoroski Air Sciences to Cadia Valley Operations Environmental Specialist dated 26 May 2020 (Appendix C of Serinus, 2021)

TAS (2020c), Air Quality Monitoring Plan Cadia Valley Operations – Tailings Storage Facility. Report prepared by Todoroski Air Sciences on 9 June 2020 (Appendix C of Serinus, 2021)

TAS (2021), Air Dispersion Modelling Cadia Valley Operations Tailings Storage Facilities. Prepared by Todoroski Air Sciences, issued 8 October 2021 to address EPL Condition U1.3

TAS (2023a). Cadia Valley Operations Air Dispersion Model 2022. Report prepared for Cadia Valley Operations, 4 July 2023.

TAS (2023b). Letter to Newcrest regarding "Response to EPA review of 2022 Air Quality Dispersion Modelling Report", 26 October 2023.

TAS (2023c). Air Quality Impact and Greenhouse Gas Assessment Cadia Valley Operations Modification 15. Report prepared by Todoroski Air Sciences for Cadia Holdings Pty Ltd, 15 November 2023. Report accessed from NSW Government Major Projects Planning Portal - https://www.planningportal.nsw.gov.au/major-projects/projects/mod-15-various-including-tailings-dam-embankment-upgrade.

USEPA (1982). AP-42 Chapter 11.24 Metallic Minerals Processing. August 1982 (reformatted January 1995).

USEPA (1998). AP-42 Chapter 11.9 Western Surface Coal Mining. November 2006.

USEPA (2006a). AP-42 Chapter 13.2.4 Aggregate Handling and Storage Piles. November 2006.

USEPA (2006b). AP-42 Chapter 13.2.2 Unpaved Roads. November 2006.

USEPA (2006c). AP-42 Chapter 13.2.5 Industrial Wind Erosion. November 2006.

Western Region Air Partnership (WRAP, 2006). Fugitive Dust Handbook. Prepared by Countess Environmental for Western Governors' Association, 7 September 2006.

Zephyr Environmental (2022). Cadia Valley Operations Independent Air Quality Audit, 11 August 2022.